# University of Southampton

Faculty of Engineering and Physical Sciences

Transportation Research Group

**A Comparative Assessment of Intercity Transport Technologies,**

**with a Saudi Arabian Case Study**

by

**Hamad Almujibah**

A dissertation submitted in partial fulfilment of the requirements for the degree of

Doctor of Philosophy in Transportation

December 2020

**University of Southampton**

# ABSTRACT

Faculty of Engineering and Physical Sciences
Transportation Research Group

Thesis for the degree of

DOCTOR OF PHILOSOPHY

**A Comparative Assessment of Intercity Transport Technologies, with a Saudi Arabian Case Study**

Hamad Almujibah

With increasing urbanization worldwide, passenger demand for inter-urban travel has grown and the development of new transport technologies is needed, such as High-Speed Rail (HSR), Magnetic Levitation (Maglev) and Hyperloop. This thesis undertakes a comparative assessment of these three intercity transport technologies in terms of their service characteristics. The aim is to identify the most suitable transport mode with the lowest average social and operator cost for an identified corridor under the level of demand that is forecast.

The comparative assessment method comprises four models. The first is the Total Social Cost Model (TSCM), which focuses on calculating the social and financial costs according to the vehicle characteristics and unit costs of each of the transport technologies studied. It includes operator cost, user cost, external cost and, hence, social cost and average social cost. Second, a Demand Forecast Model (DFM) is developed to forecast travel demand for HSR flows. This model includes parameters such as the population along the corridor, Gross Domestic Product (GDP) per capita, generalized journey time, percentage of unemployment and number of years since the lines opened. The third model is a Stated Preference Model (SPM) to examine the choice of Hyperloop over other modes of transport and to gain an understanding of how decisions are made when people are faced with several transport alternatives. The fourth is the Elasticity of Demand Model (EDM) to determine existing mode flows in terms of generalized journey time, including by conventional rail, air, car and bus.

The Riyadh–Dammam corridor in Saudi Arabia is used as a case study to apply the comparative assessment method proposed by this thesis to examine High Speed Ground Transportation (HSGT). The aims are to determine the most suitable transport modes in terms of level of service and total social and operator costs, and to forecast passenger demand. In this case study, Hyperloop appears to be the best next-generation HSGT, since it has the lowest average social cost (ASC) of €67.70 per passenger in 2030, compared to €103.30 for HSR and €100.20 for Maglev due to its lower capacity, which leads to a high hourly service frequency.

# TABLE OF CONTENTS

**ABSTRACT**

**TABLE OF CONTENTS** ..... i

**LIST OF TABLES** ..... vii

**LIST OF FIGURES** ..... xiv

**DECLARATION OF AUTHORSHIP** ..... xvii

**ACKNOWLEDGEMENTS** ..... xix

**ABBREVIATIONS** ..... xxi

**PUBLICATIONS** ..... xxiii

**CHAPTER 1. INTRODUCTION ..... 1**

1.1 HIGH-SPEED GROUND TRANSPORTATION TECHNOLOGIES ..... 1

1.1.1 High-Speed Rail technology ..... 1

1.1.2 Magnetic levitation technology ..... 2

1.1.3 Hyperloop technology ..... 3

1.2 COMPARATIVE ASSESSMENT STRUCTURE ..... 4

1.2.1 Knowledge gap ..... 4

1.2.2 Interaction between the different models ..... 5

1.3 RESEARCH OBJECTIVES ..... 7

1.4 THESIS STRUCTURE ..... 9

**CHAPTER 2. LITERATURE REVIEW OF HIGH-SPEED GROUND TRANSPORTATION TECHNOLOGIES ..... 13**

2.1 INTRODUCTION ..... 13

2.2 DEVELOPMENT OF HIGH-SPEED RAIL TECHNOLOGY ..... 13

2.2.1 High-Speed Rail in various countries ..... 17

2.2.1.1 Japan ..... 17

2.2.1.2 France ..... 18

2.2.1.3 Germany ..... 19

2.2.1.4 Spain ..... 21

2.2.1.5 Italy ..... 22

2.2.1.6 United Kingdom ..... 24

2.2.1.7 China ..... 26

2.2.1.8 Saudi Arabia ..... 27

2.2.2 Advantages and disadvantages of High-Speed Rail ..... 29

2.3 DEVELOPMENT OF MAGNETIC LEVITATION TECHNOLOGY ..... 31

2.3.1 Main principles of Maglev system ..... 32
2.3.1.1 Levitation ..... 33
2.3.1.2 Propulsion ..... 36
2.3.1.3 Guidance ..... 37
2.3.2 Magnetic levitation in various countries ..... 39
2.3.2.1 Chinese Shanghai Maglev line ..... 40
2.3.2.2 Chinese Changsha Maglev line ..... 41
2.3.2.3 South Korean Incheon Airport Maglev ..... 42
2.3.2.4 Japanese MLX-JR-Maglev ..... 43
2.3.2.5 Japanese Linimo Maglev line ..... 44
2.3.2.6 United Kingdom ..... 45
2.3.3 Advantages and disadvantages of Maglev ..... 46
2.4 Development of Hyperloop Technology ..... 50
2.4.1 Feasibility of Hyperloop ..... 50
2.4.2 Main components of Hyperloop system ..... 51
2.4.2.1 Propulsion system ..... 52
2.4.2.2 Levitation system ..... 53
2.4.3 Main parts of Hyperloop ..... 54
2.4.3.1 Capsule ..... 55
2.4.3.2 Tube ..... 57
2.4.3.3 Pillars ..... 58
2.4.3.4 Station ..... 58
2.4.4 Proposed Hyperloop routes worldwide ..... 60
2.4.5 Advantages and disadvantages of Hyperloop ..... 63
2.5 Summary ..... 65
2.6 Rail and Equity ..... 66
2.7 Conclusion ..... 67
**CHAPTER 3. METHODOLOGICAL REVIEW ..... 69**
3.1 Introduction ..... 69
3.2 Review of Total Social Cost Models ..... 69
3.3 Review of Forecasting Demand Model ..... 73
3.3.1 Review of models to forecast travel demand ..... 74
3.3.2 Overview of forecasting demand case studies ..... 78
3.4 Review of Elasticity of Demand Models ..... 89
3.4.1 Review of models of demand elasticity ..... 90
3.4.2 Overview of elasticity of demand studies ..... 94
3.5 Review of Stated Preference Methods ..... 98
3.5.1 Review of the Stated Preference Model ..... 99

3.5.2 Overview of stated preference case studies ..... 102
3.6 Overall Integrated Model ..... 105
3.7 Conclusion ..... 107
**CHAPTER 4. APPLICATION OF THE TOTAL SOCIAL COST MODEL ..... 110**
4.1 Introduction ..... 110
4.2 High-Speed Rail Technology ..... 110
4.2.1 Operator cost of High-Speed Rail ..... 110
4.2.2 User cost of High-Speed Rail ..... 113
4.2.3 External cost of High-Speed Rail ..... 114
4.3 Magnetic Levitation Technology ..... 119
4.3.1 Operator cost of Maglev ..... 119
4.3.2 User cost of Maglev ..... 120
4.3.3 External cost of Maglev ..... 121
4.4 Hyperloop Technology ..... 125
4.4.1 Operator cost of Hyperloop ..... 125
4.4.2 User cost of Hyperloop ..... 129
4.4.3 External cost of Hyperloop ..... 130
4.5 Background to the Case Study ..... 132
4.6 Existing Transport Modes Along Riyadh–Dammam Corridor ..... 134
4.6.1 Conventional train ..... 135
4.6.2 Bus ..... 135
*4.6.3* Car ..... 136
4.6.4 Air transport ..... 137
4.7 Conclusion ..... 138
**CHAPTER 5. DEVELOPING THE DIRECT DEMAND MODEL ..... 141**
5.1 Introduction ..... 141
5.2 Direct Demand Model ..... 141
5.2.1 Historical data of demand ..... 142
5.2.2 Selecting the Covariates ..... 146
5.2.2.1 Population ..... 147
5.2.2.2 Mean GDP per capita ..... 149
5.2.2.3 Mean service frequency ..... 151
5.2.2.4 Mean speed ..... 152
5.2.2.5 Mean fares ..... 153
5.2.3 Years since opening ..... 154

5.2.4 Direct demand regression model ..... 155
5.2.4.2 Log-linear model ..... 156
5.2.5 Regression analysis output ..... 157
5.2.5.1 Descriptive analysis ..... 157
5.2.5.2 Model coefficients ..... 158
5.2.5.3 Model correlation ..... 160
5.2.5.4 Model regression statistics ..... 162
5.2.5.5 Model ANOVA ..... 163
5.2.5.6 Model elasticity ..... 164
5.2.6 Residual analysis ..... 165
5.2.7 Causes of error ..... 167
5.2.7.1 Autocorrelation ..... 167
5.2.7.2 Multicollinearity ..... 167
5.2.7.3 Heteroscedasticity ..... 169
5.2.8 Box-Cox test ..... 169
5.3 Elasticity of Demand Model ..... 170
5.4 Conclusion ..... 173
**CHAPTER 6. DEVELOPING A STATED PREFERENCE MODEL 175**
6.1 Introduction ..... 175
6.2 Model Process ..... 175
6.3 Design of Experimental Choice ..... 178
6.3.1 Alternatives and attributes ..... 179
6.3.2 Variables ..... 179
6.3.3 Attribute levels ..... 180
6.4 Design of Fractional Factorial ..... 183
6.5 Design of Questionnaire ..... 185
6.5.1 Pilot survey ..... 185
6.5.2 Selecting respondents ..... 186
6.5.3 Ethical approval ..... 186
6.5.4 Sample size ..... 186
6.6 Data Collection ..... 187
6.6.1 Survey distribution ..... 187
6.6.2 Survey observations ..... 188
6.7 Conclusion ..... 190
**CHAPTER 7. APPLICATION OF DEMAND MODELS ..... 193**
7.1 Introduction ..... 193
7.2 Direct Demand (HSR) ..... 193

7.3 Demand Elasticity (Maglev) ..... 195
7.4 Stated Preference (Hyperloop) ..... 197
7.4.1 Multinomial logit model ..... 197
7.4.1.1 Calibration results ..... 198
7.4.2 Nested logit model ..... 210
7.5 Demand Forecast ..... 215
7.5.1 Impact of HSR on existing transport modes ..... 215
7.5.2 Evolution of HSR traffic ..... 219
7.5.3 Forecasting Hyperloop demand ..... 220
7.6 Conclusion ..... 236
**CHAPTER 8. COMPARATIVE ASSESSMENT OF TOTAL SOCIAL COST MODEL ..... 238**
8.1 Introduction ..... 238
8.2 Total Social Cost Model ..... 238
8.2.1 Operator cost ..... 239
8.2.1.1 Infrastructure cost ..... 239
8.2.1.2 Rolling stock/capsule cost ..... 242
8.2.2 Total operator cost ..... 245
8.2.3 User cost ..... 246
8.2.3.1 Access/egress time ..... 246
8.2.3.2 Waiting time ..... 247
8.2.3.3 In-vehicle time ..... 247
8.2.4 Total user cost ..... 248
8.2.5 External environmental cost ..... 249
8.3 Results and Discussion ..... 251
8.3.1 Total operator costs ..... 252
8.3.2 Total user costs ..... 258
8.3.3 Total external environmental costs ..... 260
8.4 Comparative Assessments ..... 262
8.5 Conclusion ..... 265
**CHAPTER 9. CONCLUSIONS ..... 266**
9.1 Introduction ..... 266
9.2 Research Summary ..... 266
9.2.1 Research tasks ..... 268
9.2.2 Contribution to knowledge ..... 270
9.3 Future Work ..... 271

9.3.1 Combinations of high-speed ground transport services.....272
9.3.2 Evaluation of passenger demand level.....272
9.3.3 A substantial database for high-speed ground transport systems .272
9.3.4 Policy implications of equity issues.....272
9.3.5 Limitations of the research.....273
**REFERENCES.....275**
**APPENDICES**
Appendix A: Spreadsheet cost model interface ……293
Appendix B: Public Transport Authority's Approval letter ……..297
Appendix C: Approval Letter by Faculty Ethics Committee ……...298
Appendix D: Questionnaires of Experiment 1 ……..299
Appendix E: Questionnaires of Experiment 2……...309
Appendix F: Stata Outcomes with Service Frequency for Experiment 1……..321
Appendix G: Stata Outcomes with Service Frequency for Experiment 2.……322
Appendix H: Nested Logit Model Using Stata for Experiment 1……323
Appendix I: Nested Logit Model Using Stata for Experiment 2……..…..325

## LIST OF TABLES

Table 2-1*:* Overview of HSR network by country in January 2020. (Source: UIC, 2020a)..... 14

Table 2-2: High-speed traffic in the world in January 2020 (billions of passenger-km). (Source: UIC, 2020b) ..... 16

Table 2-3: Germany's High-Speed Rail passenger traffic. (Source: UIC, 2010c).. 20

Table 2-4: Spain's High-Speed Rail passenger traffic. (Source: UIC, 2010f)..... 22

Table 2-5: Italian HSR: NTV and Trenitalia's market shares. (Source: UIC, 2020b) ..... 24

Table 2-6: Italy's High-Speed Rail passenger traffic. (Source: UIC, 2010d) ..... 24

Table 2-7: Overview of existing Maglev network by country. (Source: Schonig, 2019) ..... 32

Table 2-8: Characteristics of EMS and EDS systems. (Source: Sharma *et al.*, 2014) ..... 36

Table 2-9: Guideway structures and suspension systems. (Source: Yaghoubi, Barazi and Aoliaei, 2012)..... 36

Table 2-10: 10 Winners of Hyperloop One Global Challenge. (Source: Simon and Choi, 2017) ..... 60

Table 2-11: Travel time of transport modes, including Hyperloop, San Francisco to Los Angeles. (Source: Virgin Hyperloop One, 2018) ..... 63

Table 3-1: Annual 2010 HSR ridership and distance. (Source: Levinson *et al.,* 1997) ..... 78

Table 3-2: Total intercity ridership in 2020 by source for funding scenario. (Source: Charles River Associates Incorporated, 2000)..... 80

Table 3-3: Total intercity ridership in 2020 by source for funding scenario. (Source: Charles River Associates Incorporated, 2000) ..... 81

Table 3-4: Taxonomy of impacts on HSR demand. (Source: Cascetta and Coppola, 2011) ..... 84

Table 3-5: Examples of exogenous and endogenous factors. (Source: 'Guidance note', 2019) ..... 85

Table 3-6: Evidence of HSR demand worldwide with a mean value. (Source: Preston, 2013) ..... 88

Table 3-7: Elasticity values for HSR. (Source: Roman, Espino and Martín, 2010) 95

Table 3-8: Summary of short-run aggregate values of public transport direct elasticity. (Source: Wallis, 2003) ..... 97

Table 4-1: Construction costs of new high-speed lines per route-km. (Source: Preston, 2013) ..... 111

Table 4-2: Estimated costs of a 500 km HSR line in Europe, at 2004 prices. (Source: Nash, 2010) ..... 112

Table 4-3: Average time to access HSR stations in Madrid and Barcelona, by mode. (Source: Pagliara, Vassallo and Román, 2012) ..... 113

Table 4-4: Main characteristics of fatal High-Speed Rail accidents. (Source: Janić, 2017) ..... 118

Table 4-5: Total costs of Maglev projects. (Source: Dona and Singh, 2017) ..... 119

Table 4-6*:* Land consumption of the Maglev system. (Source: Ziemke, 2010) .... 123

Table 4-7: Maglev noise levels at different speeds. (Source: Levinson *et al.*, 1996) ..... 124

Table 4-8: Investment and annual capital costs for Hyperloop infrastructure and vehicles at 2015 prices. (Source: Van Goeverden *et al.*, 2018) ..... 126

Table 4-9: Estimated cost of Hyperloop tube at 2015 prices. (Source: Taylor, Hyde and Barr, 2016) ..... 127

Table 4-10: Estimated annual costs of Hyperloop system at 2015 prices. (Source: Van Goeverden *et al.*, 2018) ..... 128

Table 4-11: Estimated annual costs of Hyperloop capsule at 2015 prices. (Source: Musk, 2013) ..... 128

Table 4-12: Capacity of different Hyperloop sizes. (Source: Walker, 2018) ..... 130

Table 4-13: Population of Saudi Arabia (2015–2019). (Source: GMI, 2020) ..... 133

Table 4-14: GDP of Saudi Arabia (2013–2018). (Source: World Bank, 2020b) .. 133

Table 4-15: Nos. of international tourists visiting Saudi Arabia per year. (Source: World Bank, 2020a) ..... 134

Table 5-1: Collated demand of the Riyadh–Dammam conventional rail line 2011–2018 ..... 144

Table 5-2: Collected demand of the North–South conventional rail line 2017–2018 ..... 145

Table 5-3: Population of cities along the Riyadh–Dammam included corridor (2011–2018) ..... 147

Table 5-4: Population of the cities along the North–South included corridor (2017-2018) ..... 148

Table 5-5: GDP per capita of cities along Riyadh–Dammam included corridor (2011–2018) ..... 149

Table 5-6: GDP per capita of cities along the North–South rail corridor (2017–2018) ..... 150

Table 5-7: Number of trains serving the Riyadh–Dammam Railway included corridor (2011–2018) ..... 152

Table 5-8: Number of trains per week serving the North–South railway included corridor (2017–2018) ..... 152

Table 5-9: Ticket price for economy class on Riyadh–Dammam corridor (Riyals) ..... 153

Table 5-10: Ticket prices for business class on Riyadh–Dammam corridor (Riyals) ..... 153

Table 5-11: Ticket prices for economy class on North–South corridor (Riyals) ... 153

Table 5-12: Ticket prices for business class on North–South corridor (Riyals) ... 154

Table 5-13: Estimated time from planning to operation of selected HSR lines. (Source: European Court of Auditors, 2018) ..... 154

Table 5-14: Years since opening the Riyadh–Dammam HSR line ..... 154

Table 5-15: Monthly dummy variables for the proposed Riyadh–Dammam HSR line ..... 155

Table 5-16: Descriptive statistics. Analysed by SPSS ..... 157

Table 5-17: Regression analysis output. Analysed by SPSS ..... 159

Table 5-18: Regression coefficients ..... 161

Table 5-19: Pearson’s correlation between only the independent variables ..... 162

Table 5-20: Regression analysis output. Analysed by SPSS ..... 163

Table 5-21: Model ANOVA regression analysis output. Analysed by SPSS ..... 164

Table 5-22: Elasticity of independent variables with respect to demand ..... 165

Table 5-23: Test of normality for residual, based on Shapiro-Wilk test. Analysed by SPSS ..... 166

Table 5-24: Autocorrelation using Durbin-Watson test. Analysed by SPSS ..... 167

Table 5-25: Collinearity statistics. Analysed by SPSS ..... 168

Table 5-26: Breusch-Pagan/Cook-Weisberg (heteroscedasticity test). Analysed by Stata ..... 169

Table 5-27: Residual sum of squares values. Analysed by Stata ..... 170

Table 5-28: Interchange penalties. (Source: Rail Delivery Group, 2011) ..... 172

Table 5-29: Service interval penalties (mins). (Source: Rail Delivery Group, 2011) ..... 172

Table 6-1: Combination of attributes and transport alternatives in first experiment ..... 179

Table 6-2: Combination of attributes and transport alternatives in second experiment ..... 179

Table 6-3: Nos. of variables for first experiment..... 180

Table 6-4: Nos. of variables for second experiment..... 180

Table 6-5: Index of experimental plan for first experiment ..... 181

Table 6-6: Attribute levels for nos. of alternatives in first experiment ..... 182

Table 6-7: Index of experimental plan for the second experiment..... 182

Table 6-8: Attribute levels for number of alternatives in the second experiment . 183

Table 6-9: Master plan for first experiment ..... 184

Table 6-10: Master plan for second experiment..... 185

Table 6-11: Total number of participants in each station or on train ..... 188

Table 6-12: Survey observations sample and percentages ..... 189

Table 6-13: Observations and percentages in choosing transport mode ..... 190

Table 7-1: Forecasting travel demand of proposed HSR line ..... 194

Table 7-2: Forecast demand for HSR in 2030, 2040 and 2050..... 195

Table 7-3: Average service interval penalties (in mins). (Source: Rail Delivery Group, 2011) ..... 196

Table 7-4: Forecasting service frequency changes ..... 196

Table 7-5: Forecasting travel demand of proposed Maglev line ..... 197

Table 7-6: Overall goodness of fit measure for first experiment ..... 199

7-7: Output results of using Stata for second experiment ..... 200

7-8: Result of likelihood ratio and the pseudo R-squared for first experiment ..... 201

7-9: Result of likelihood ratio and the pseudo R-squared for second experiment 202

7-10: Variance of value of time for combined gender in first experiment ..... 203

Table 7-11: Variance of value of time for combined gender in second experiment ..... 204

Table 7-12: Utility of transport modes in first experiment (No Car Available) ..... 205

Table 7-13: Utility of transport modes in second experiment (Car Available) ..... 206

Table 7-14: Probability of transport modes included in first experiment (mean value) ..... 207

Table 7-15: Probability of transport modes included in second experiment (mean value) ..... 208

Table 7-16: Values of alternative-specific constant for possible split between the two experiments ..... 209

Table 7-17: Utility and probability of transport modes included in the model ..... 210

Table 7-18: Outcome of nested logit analysis of first experiment ..... 211

Table 7-19: Outcome of nested analysis for second experiment ..... 214

Table 7-20: Diversion factors resulting from introduction of HSR. (Source: Preston, 2013) ..... 216

Table 7-21: Modal market share before and after introduction of HSR system. (Source: de Rus, 2009) ..... 216

Table 7-22: Trip distribution for intercity transportation before and after HSR operation in Taiwan. (Source: Cheng, 2010) ..... 217

Table 7-23: Evolution of HSR traffic in different countries (2010–2018). (Source: UIC, 2020b) ..... 219

Table 7-24: Nos. of passengers travelling on planes, buses, cars and classic rail along Riyadh–Dammam corridor in 2018 ..... 220

Table 7-25: Nos. of passengers who have access/no access to a car in 2018 ... 221

Table 7-26: Alternative-specific constants and utilities of included transport systems ..... 223

Table 7-27: Probability of existing transport modes before and after introducing HSR and Hyperloop for no car available ..... 224

Table 7-28: Probability of existing transport modes before and after introducing HSR for car available ..... 224

Table 7-29: Total demand for transport modes from the SP model after introducing HSR to both experiments ..... 225

Table 7-30: Total demand for transport modes from the SP model after introducing Hyperloop to both experiments ..... 226

Table 7-31: Estimated result of demand for each included transport mode when car is available or non-available in 2018 (NB Figures have been rounded) ..... 227

Table 7-32: Estimated demand of classic rail in 2030, 2040 and 2050 ..... 228

Table 7-33: Estimated demand for bus, car and air transport in 2030, 2040 and 2050 ..... 229

Table 7-34: Total new demand for travel in the corridor in 2018 ..... 230

Table 7-35: Logsum before and after adding HSR and Hyperloop for car and no car available ..... 232

Table 7-36: Determining the increased size of the market ..... 233

Table 7-37: Total abstracted demand for Hyperloop in 2018, 2030, 2040 and 2050 ..... 233

Table 7-38: Total Hyperloop demand in 2018 ..... 234

Table 7-39 Forecast demand for Hyperloop in 2030, 2040 and 2050 ..... 235

Table 8-1: Discount rates over different periods. (Source: Department for Transport, 2018) ..... 241

Table 8-2: Final endogenous demand levels for the initial year of operation (2030) ..... 252

Table 8-3: Basic input parameters of the characteristics of HSR, Maglev and Hyperloop systems ..... 253

Table 8-4: Unit costs of HSR, Maglev and Hyperloop at 2017 prices. ..... 254

Table 8-5: Conversion between years using consumer price index ..... 254

Table 8-6: Total infrastructure construction and maintenance costs (€/year) ..... 255

Table 8-7: Service frequency per hour ..... 256

Table 8-8: No. of acquired trains/capsules ..... 256

Table 8-9: Rolling stock/capsule acquisition cost (€/year) ..... 257

Table 8-10: Rolling stock/capsule operating cost (€/year) ..... 257

Table 8-11: Rolling stock/capsule maintenance cost (€/year) ..... 258

Table 8-12: Total annual passenger access/egress time (hours) ..... 259

Table 8-13: Total annual passenger waiting time (hours) ..... 260

Table 8-14: Total annual passenger in-vehicle time (hours) ..... 260

Table 8-15: Average cost of air pollution, noise pollution, climate change and accidents..... 261

Table 8-16: Rolling stock/capsule total operator costs (€/year) ..... 262

Table 8-17: Rolling stock/capsule total user costs (€/year)..... 263

Table 8-18: Total external costs of HSR, Maglev and Hyperloop (€/year) ..... 264

Table 8-19: Total social costs of HSR, Maglev and Hyperloop (€/year)..... 264

**LIST OF FIGURES**

Figure 1-1: Haramain High-Speed Rail. (Source: (Argaam, 2019) ..... 2

Figure 1-2: Shanghai Transrapid Maglev. (Source: Holmer, 2003) ..... 3

Figure 1-3: Hyperloop transport system. (Source: Schonig, 2019) ..... 4

Figure 1-4: Interaction between the models ..... 5

Figure 2-1: High-speed degrees of separation. (Source: Rutzen and Walton, 2011; de Rus, 2012a, 2012b) ..... 15

Figure 2-2: Map of HSR lines in Japan. (Source: UIC, 2020c) ..... 18

Figure 2-3: Map of HSR lines in France. (Source: UIC, 2020c) ..... 19

Figure 2-4: Map of HSR lines in Germany. (Source: UIC, 2020c) ..... 20

Figure 2-5: Map of HSR lines in Spain. (Source: UIC, 2020c) ..... 21

Figure 2-6: Map of HSR lines in Italy. (Source: UIC, 2020c) ..... 22

Figure 2-7: Map of HSR lines in the United Kingdom. (Source: UIC, 2020c) ..... 25

Figure 2-8: Map of HSR lines in China. (Source: UIC, 2020c) ..... 26

Figure 2-9: Map of HSR lines in Saudi Arabia. (Source: UIC, 2020c) ..... 28

Figure 2-10: Basic principles of magnetic levitation. (Source: Shaik, 2018) ..... 33

Figure 2-11: Electromagnetic suspension. (Source: Rose, Peterson and Leung, 2008) ..... 34

Figure 2-12: Electro-dynamic suspension. (Source: Rose, Peterson and Leung, 2008) ..... 35

Figure 2-13: Magnetic repulsion force. (Source: Sharma *et al.*, 2014) ..... 38

Figure 2-14: Magnetic-attractive force. (Source: Sharma *et al.*, 2014) ..... 39

Figure 2-15: Shanghai Maglev train. (Source: Edwin, 2015) ..... 40

Figure 2-16: Changsha Maglev line. (Source: Railway Pro, 2017)..... 41

Figure 2-17: Shanghai–Hangzhou Maglev line. (Source: Tracy, 2020)..... 42

Figure 2-18: Incheon International Airport Maglev. (Source: Rail Travel Station, 2019)..... 43

Figure 2-19: Japanese MLX Maglev train. (Source: Bonsor and Chandler, 2019) 44

Figure 2-20: Linimo Maglev train. (Source: Gizmo Highway, 2011)..... 45

Figure 2-21: Birmingham International Maglev shuttle. (Source: BBC News, 1999) ..... 46

Figure 2-22: Maglev enables higher average speed. (Source: Holmer, 2011)..... 47

Figure 2-23: Switching system on the Linimo line in Nagoya, Japan. (Source: Thorstrand, 2020) ..... 49

Figure 2-24: Artist’s impression of Hyperloop from Los Angeles to San Francisco. (Source: Davies, 2015) ..... 50

Figure 2-25: Hyperloop transport technology. (Source: Looveren, 2017) ..... 52

Figure 2-26: Hyperloop propulsion system. (Source: Mathur, 2017)..... 53

Figure 2-27: Hyperloop levitation system. (Source: ESTECO Academy, 2018).... 54

Figure 2-28: Main parts of Hyperloop system. (Source: RF Wireless World, 2015) ..... 55

Figure 2-29: Hyperloop passenger capsule. (Source: Anthony, 2013)..... 56

Figure 2-30: Hyperloop passenger tube. (Source: Coelho, 2016)..... 57

Figure 2-31: Hyperloop pillars. (Source: Musk, 2013)..... 58

Figure 2-32: Hyperloop passenger station. (Source: Sergeroux, 2016)..... 59

Figure 2-33: Saudi-Virgin Hyperloop One's Vision 2030 passenger pod. (Source: Lavars, 2018)..... 61

Figure 2-34: First Hyperloop planned for China. (Source: Wong, 2018) ..... 62

Figure 2-35: Canadian corridor between Toronto and Montreal. (Source: Janzen, 2016) ..... 62

Figure 2-36: Energy cost per passenger for modes of transport, San Francisco to Los Angeles. (Source: Musk, 2013) ..... 64

Figure 2-37: Cutaway of the passenger capsule. (Source: Ramachandran, 2013) ..... 65

Figure 3-1: Map of California High-Speed Rail line (CAHSR). (Source: Taylor, 2014) ..... 79

Figure 3-2: High-Speed Rail network of Italy. (Source: Ben-Akiva *et al.*, 2010) .... 82

Figure 4-1: Direct environmental airborne noise from HSR. (Source: Temple-ERM, 2013) ..... 116

Figure 4-2: Transrapid Maglev train. (Source: Transrapid International, 2002) ... 122

Figure 4-3: Elevated guideway. (Source: Transrapid International, 2002) ..... 122

Figure 4-4: At-grade guideway. (Source: Transrapid International, 2002) ..... 123

Figure 4-5: Fire in Shanghai's Maglev. (Source: Xinhua, 2006) ..... 125

Figure 4-6: Map of Saudi Arabia. (Source: Einstein, 2007) ..... 132

Figure 4-7 Riyadh–Dammam corridor, using different transport modes. (Source: Google Maps) ..... 135

Figure 4-8: Driving to/from Riyadh SAPTCO station and to/from Dammam SAPTCO station. (Source: Google Maps) ..... 136

Figure 4-9: Driving on main road between Riyadh and Dammam and via Hofuf. (Source: Google Maps) ..... 137

Figure 4-10: Driving to/from Riyadh King Khalid Airport and Dammam King Fahd Airport. (Source: Google Maps) ..... 138

Figure 5-1: Combined existing Riyadh–Dammam and North–South conventional lines ..... 143

Figure 5-2: Passenger demand for existing Riyadh–Dammam conventional rail 145

Figure 5-3: Passenger demand for existing North–South conventional rail ..... 146

Figure 5-4: Population of cities along the existing Riyadh–Dammam rail route .. 148

Figure 5-5: Population of cities along the existing North–South rail route (2017–2018)..... 149

Figure 5-6: GDP per capita in cities along the existing Riyadh–Dammam rail route ..... 150

Figure 5-7: GDP per capita of cities along the existing North–South rail route ... 151

Figure 6-1: Flowchart of mode-choice model..... 177

Figure 6-2: Framework of the design of choice experiment ..... 178

Figure 6-3: Conventional rail corridor of Riyadh–Dammam via Hofuf and Bqaiq. (Source: Google Maps)..... 187

Figure 7-1: Multinomial logit structure between the two experiments..... 208

Figure 7-2: Two-level nested structure for first experiment..... 211

Figure 7-3: Three-level nested structure of second experiment..... 213

Figure 7-4: Estimated demand for bus, car, air transport and classic rail in 2030, 2040 and 2050..... 229

## RESEARCH THESIS: DECLARATION OF AUTHORSHIP

Print name: **Hamad Almujibah**

Title of thesis: **A Comparative Assessment of Intercity Transport Technologies, with a Saudi Arabian Case Study**

I declare that this thesis and the work presented in it are my own and has been generated by me as the result of my original research.

I confirm that:

- This work was done wholly or mainly while in candidature for a research degree at this University;
- Where any part of this thesis has previously been submitted for a degree or any other qualification at this University or any other institution, this has been clearly stated;
- Where I have consulted the published work of others, this is always clearly attributed;
- Where I have quoted from the work of others, the source is always given. With the exception of such quotations, this thesis is entirely my own work;
- I have acknowledged all main sources of help;
- Where the thesis is based on work done by myself jointly with others, I have made clear exactly what was done by others and what I have contributed myself;

- Part of this work have been published as:

Almujibah, H. and Preston, J., 2018. The total social costs of constructing and operating a Maglev line using a case study of the Riyadh–Dammam corridor, Saudi Arabia. *Transportation Systems and Technology,* 4(3s1), 298-327.

Almujibah, H. and Preston, J., 2019. The total social costs of constructing and operating a high-speed rail line using a case study of the Riyadh–Dammam corridor, Saudi Arabia. *Frontiers in Built Environment*, 5, 79.

Signed:

Date: 10/12/2021

**ACKNOWLEDGEMENTS**

Foremost, I thank God for offering me the chance, the strength, ability and patience to carry out this study at the Faculty of Engineering and Physical Sciences, University of Southampton, which has provided me with a great environment to complete my studies. Extended thanks go to Taif University, Kingdom of Saudi Arabia, the Saudi Embassy and Cultural Bureau in London and the Saudi Public Transport Authority for sponsoring and supporting me to undertake my PhD degree.

I should like to express my deep and sincere sense of gratitude to my main supervisor, Professor John Preston, for his continuous support, patience, enthusiasm, motivation, guidance, recommendations, friendship and immense knowledge.

I should like to extend my gratitude to my co-supervisor Dr Simon Blainey and research fellow Dr James Pritchard, as well as to the rest of the Transportation Research Group's members at the University of Southampton. Their help, suggestions and comments have played an important role in my work.

I wish to extend my heartiest thanks to my lovely parents, my father Mr Raja Almujibah and my mother Mrs Norah Almujibah, for their unforgettable help and guidance in shaping my life with passion and positivity. I should also like to thank my beloved wife, Mrs Sarah Alwalah, for her great support that has enabled me to complete my studies successfully, and to my sons, Yousef and Younes, for their encouragement.

## ABBREVIATIONS

| | |
|---|---|
| ADIF | Administrador de Infraestructuras Ferroviarias |
| ARTC | Aichi Rapid Transit Company |
| ATC | Automatic Train Control |
| AVE | Alta Velocidad Espanola |
| CAHSR | California High-Speed Rail |
| CHSR | Chinese High-Speed Rail |
| CMS | Chuo Maglev Shinkansen |
| DFM | Demand Forecast Model |
| DB | Deutsche Bahn |
| EDM | Elasticity of Demand Model |
| EDS | Electro-Dynamic Suspension |
| EMS | Electromagnetic Suspension |
| EMF | Electro-Motive Force |
| EU | European Union |
| SNCF | French National Railway |
| GDP | Gross Domestic Product |
| GHGs | Greenhouse Gases |
| GTX | Great Train Express |
| HHSR | Haramain High-Speed Rail |
| HSR | High-Speed Rail |
| HSGT | High-Speed Ground Transportation |
| HS1 | High-Speed 1 |
| HS2 | High-Speed 2 |
| HSST | High-Speed Surface Transport |
| HTT | Hyperloop Transportation Technologies |
| IAM | Incheon Airport Maglev |
| ICE | Intercity Express |
| JNR | Japan National Railway |
| KAEC | King Abdullah Economic City |
| KIMM | Korea Institute of Machinery and Materials |
| LIM | Linear Induction Motor |
| LSM | Linear Synchronous Motor |
| Maglev | Magnetic Levitation |
| MoR | Ministry of Railways |
| SRMP | Saudi Railway Master Plan |
| SMTDCSP | Shanghai Maglev Transportation Development Company |
| SPM | Stated Preference Model |
| TEST | Tool for Evaluating Strategically Integrated Public Transport) |
| TGV | Train à Grande Vitesse |
| TSCM | Total Social Cost Model |
| UTM | Urban Transit Maglev |

## PUBLICATIONS

*Journal articles:*

Almujibah, H. and Preston, J., 2018. 'The total social costs of constructing and operating a Maglev line using a case study of the Riyadh–Dammam corridor, Saudi Arabia'. *Transportation Systems and Technology*, 4(3s1), 298-327.

Almujibah, H. and Preston, J., 2019. 'The total social costs of constructing and operating a High-Speed Rail line using a case study of the Riyadh–Dammam corridor, Saudi Arabia'. *Frontiers in Built Environment,* 5, 79.

*Conference proceedings:*

Almujibah, H.R. and Preston, J. 'Modelling of intercity transport mode-choice behaviour: Case study of Riyadh–Dammam corridor, Saudi Arabia'. Paper presented at *Railway Engineering 2019*, Edinburgh, United Kingdom.

Almujibah, H.R. and Preston, J. 'High-speed rail forecasting demand model, using Riyadh–Dammam corridor, Saudi Arabia as a case study'. Paper presented at *The Universities' Transport Study Group - 51st Annual Conference*, Leeds, United Kingdom.

# Chapter 1. Introduction

## 1.1 High-Speed Ground Transportation Technologies

In the past few decades, High-Speed Ground Transportation Technology **(**HSGT) has been adopted by several countries (Stiles, 1998). This involves upgrading existing rail infrastructure to support the transportation of passengers at speeds of over 200 km/h or developing new infrastructure with speeds in excess of 250 km/h. HSGT is designed to compete with existing modes of transport, such as cars, buses and conventional rail; moreover, it provides an alternative to air travel between heavily populated cities around 100 to 500 km apart (Stiles, 1998), or even further for very high-speed systems. HSGT is a less congested mode of travel than cars, buses and conventional rail as, despite their advantage of lower cost for In Saudi Arabia, it seems that classic rail involves some congestion. Together with the increasing price of petrol, this is the motivation for considering new HSGT systems.

Three forms of HSGT – HSR, Maglev and Hyperloop – have attracted much attention from operators and decision-makers worldwide. Governments, too, have acknowledged the benefits (Stansfield, 2018). A brief introduction to each system is presented separately, as follows.

### 1.1.1 High-Speed Rail technology

HSR is a technical and complex field. It comprises multiple technical elements: its infrastructure (new lines are designed to run at ‘a maximum speed of 250 km/h or more’) (UIC, 2020b); its rolling stock (specially designed train sets); and its operational regulations, maintenance systems, and so on, all using highly sophisticated technology.

Figure 1-1: Haramain High-Speed Rail. (Source: Argaam, 2019)

HSR has three main characteristics that attract both passengers and society: safety; capacity; and sustainability (Angoori, 2010). In addition, it represents a major technological achievement, as seen in Figure 1-1, and as a mode of travel for the twenty-first century it is a symbol of efficiency (Campos, de Rus and Barron, 2007b).

### 1.1.2 Magnetic levitation technology

Magnetic levitation (Maglev) is a form of transportation technology that is guided and ground-based. It was initially conceived in the 1960s and scaled-up in the 1980s and 1990s, and consists of a vehicle being lifted and propelled along a guideway (SANDAG, 2006). Rather than a mechanical system with bearings, axles and wheels, this highly advanced technology uses powerful magnets to propel the vehicles without any contact with the ground, as shown in Figure 1-2 (Yadav *et al.*, 2013).

Maglev can refer to a system in which the vehicles are raised by electromagnetic forces acting between coils at ground level and superconducting magnets on board (Pandey, Kumar and Tiwari, 2016). In this case, they vehicles can be propelled at high speeds with only moderate noise and energy (SANDAG, 2006).

Figure 1-2: Shanghai Transrapid Maglev. (Source: Holmer, 2003)

The technology can use electromagnetic force both to suspend and to propel the vehicles. The term ‘Maglev’ refers to both the vehicles and the guidance system, while ‘levitation’ refers to the technology that allows the vehicles to be propelled by magnets rather than wheels (Yadav *et al.*, 2013; Chopade, 2017a).

Maglev is an innovative technology, using magnetism to create a gap between the guideway and the vehicles, which then move along the magnetic fields that are established (Yaghoubi, Barazi and Aoliaei, 2012). Able to travel at up to 430 km/h, the Maglev Transrapid train was designed and built by Germany’s Transrapid International, a consortium of Siemens and ThyssenKrupp. Maglev also refers to a number of systems developed in Japan and Germany (DW, 2016).

### 1.1.3 Hyperloop technology

The term ‘Hyperloop’ refers to the concept described in the Hyperloop Alpha article published in 2013 by Tesla chief executive Elon Musk (see Figure 1-3). A Hyperloop consists of capsules travelling through a frictionless vacuum tube at high speed, floating on a cushion of air created by air compressors and linear induction motors (LIMs) (Krausz, 2016; Kale *et al.*, 2019).


Figure 1-3: Hyperloop transport system. (Source: Schonig, 2019)

This technology is still in its early stages, and it is attracting the attention of academia, engineers and supporters as there is obvious uncertainty about whether or not it will perform. It is generally believed that construction of any HSR, Maglev and Hyperloop system is beset with economic, management, legal and technical risks (DaTian *et al.*, 2015).

## 1.2 Comparative Assessment Structure

Much work has been undertaken on comparative assessments of urban public transport systems, as discussed in reputable articles on transport economics. These have attempted to assess the impacts on and benefits for both operators and users (Meyer, Kain and Wohl, 1965; Jansson, 1984; Meyer and Miller, 2001; Brand and Preston, 2003; Vuchic, 2005; Li and Preston, 2015; White, 2016). There have been rather fewer comparative assessments of inter-urban public transport systems (Levinson *et al.*, 1996; Campos, de Rus and Barron, 2007a).

### 1.2.1 Knowledge gap

In this study, a knowledge gap has been identified: how to determine the most appropriate HSGT system for a particular inter-urban corridor. A solution is provided through the development of a comparative assessment approach that forecasts the level of demand and calculaes the total social cost. There has been little development of methods to compare a range of HSGT systems strategically so that

the information may be applied to further cases considering new intercity transportation technologies, including new forms of transport. Moreover, demand for public transport is partly endogenous, since it depends on its speed, service frequency, and so on. This is why an examination of several models and approaches to determine demand is needed for assessment of HSGT.

A case study of the conventional rail lines of the Riyadh–Dammam and North–South corridors in Saudi Arabia forms part of this thesis. For the Riyadh–Dammam corridor, the Stated Preference (SP) method is employed to assess demand for a new transport mode that uses Hyperloop, while the Elasticity of Demand Model (EDM) is used to assess demand for a Maglev system. Demand for HSR is determined by a combination of the DFM and SP models.

### 1.2.2 Interaction between the different models

The comparative assessment involves four models, as shown in Figure 1-4: the Demand Forecast Model (DFM); the Total Social Cost Model (TSCM); the Stated Preference Model (SPM); and the Elasticity of Demand Model (EDM). These interact closely to analyse the performance of the three HSGT technologies under consideration and thus identify the most appropriate intercity passenger transport system. The TSCM is the main model used in this study, and it is a function of the service characteristics based on exogenous demand for the HSR, Maglev and Hyperloop systems.

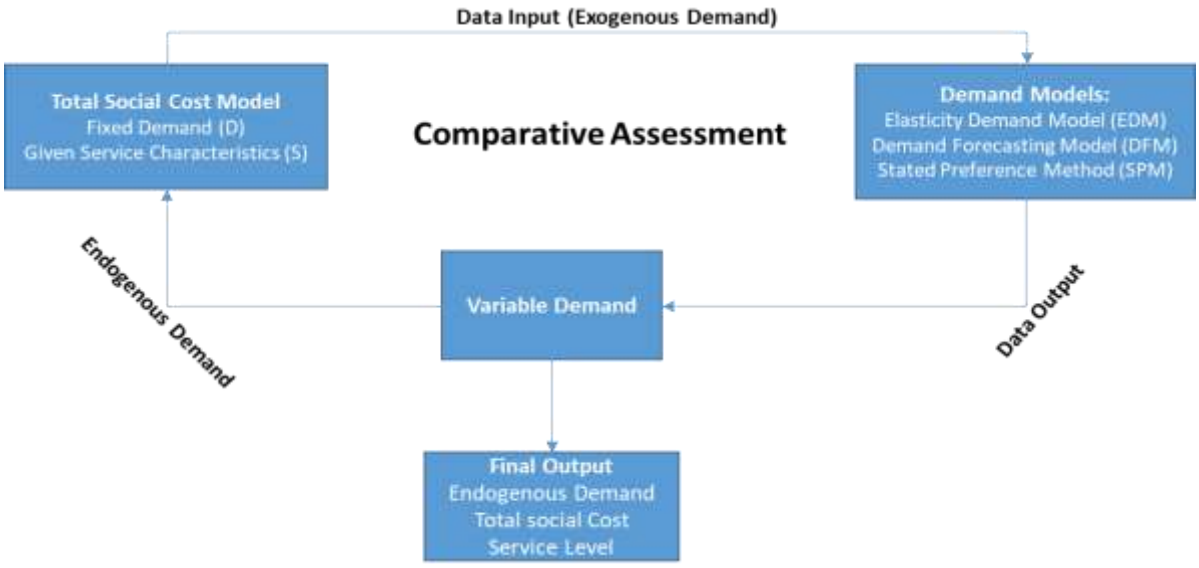


Figure 1-4: Interaction between the models

To undertake a comparative assessment of the various HSGT options, it is necessary to:

- Construct a model to forecast demand for travel by HSR technology, using the gravity model and secondary data input (exogenous demand) to achieve the base HSR flows.
- Estimate demand for Maglev, using the elasticity of generalized journey time in conjunction with data on generalized journey time for HSR and Maglev.
- Determine the base demand for Hyperloop, using the SP method with primary data resulting from a survey.
- Construct a TSCM to compare operator cost, user cost and external cost of the transport technologies under consideration. The strategy is to use Microsoft Excel to analyse the total social cost of daily passenger travel by HSR, Hyperloop and Maglev at various levels of demand, meaning that the results are based on endogenous demand.
- Use the EDM to determine current and future passenger flows by conventional rail, air, bus and car travel, using generalized journey times and data on population and income.

Figure 1.4 shows that a pragmatic modelling structure attempts to maximize the use of local data. The EDM is used in conjunction with the SPM to gain an idea of the extent of the generated and abstracted demand. The SPM indicates how much demand is diverted from other modes, while the logsum model shows the extent to which Hyperloop may generate additional demand. As a result, the logsum elasticity model was chosen, in contrast to the choice of the EDM to determine demand for Maglev. In the SP model, the two types used were the discrete-choice model and the logsum elasticity model.

The development of this generic comparative assessment tool is regarded as a contribution to knowledge, and it can be applied to an intercity transport corridor through a combination of techniques. It allows a suite of demand models to interact with respect to the total social cost model for high-speed modes of ground transport. In this case, a combination of a gravity demand, an elasticity and an SP model was

developed to forecast demand for HSR, Maglev and Hyperloop, respectively. The total social cost model was then developed by calculating the operator cost, user cost and external cost of various intercity HSGT systems such as HSR, Maglev and Hyperloop, given these demand forecasts. The choice of Saudi Arabia as a case study is justified by the fact that the country is looking to invest in HSGT currently, with a focus on classic and high-speed rail but also considering other options such as Maglev and Hyperloop.

## 1.3 Research Objectives

In this study, the main aim is to undertake a comparative assessment to analyse the feasibility of high-speed intercity public transport alternatives along the same corridor and in the same operating environment. The financial and social costs of various HSGTs are compared in a sequence of cost function, demand mode-choice and regression models. The three new technologies for intercity travel in this thesis were chosen because Saudi Arabia is already committed to HSR (e.g. Haramain High-Speed Rail) and is also considering its two main contenders, Maglev and Hyperloop. Of course, there are further possible technologies, such as autonomous road-based vehicles. Essentially, in terms of the development of rail technologies, Saudi Arabia is currently and somewhat uniquely developing a rail-based intercity network. This is not only the Haramain high-speed line but the recently developed North–South rail line, which makes Saudi Arabia an interesting case study.

In terms of the mode-choice model, the assessment offers valuable financial data for decision-makers dealing with the options for an operational network of HSGT technologies such as HSR, Maglev and Hyperloop. This study focuses on comparing and modelling these technologies to meet the following objectives:

- To determine the demand for intercity travel upon the introduction of a new transport mode, such as HSR, Maglev or Hyperloop. This is covered in Chapters 5, 6 and 7.
- To determine intercity travel's total social cost upon the introduction of a new transport mode, such as HSR, Hyperloop or Maglev. This is covered in Chapter 8.

- To analyse the benefits of HSGT options after applying the models to a case study rail corridor, later to be applied to corridors worldwide. This is covered in Chapter 8.

To achieve the above objectives, the following tasks were performed:

1) Undertake a contextual review (Chapters 2 and 5):

- Review current travel demand for HSR lines worldwide.
- Review current modes of transport in the Riyadh–Dammam corridor of Saudi Arabia with respect to cost, price, level of service and demand.
- Review the impact of various modes of travel, for instance air, conventional rail and road transport.
- Review the impact of introducing HSR, Maglev or Hyperloop technologies on the current transport system.

2) Undertake a methodological review (Chapters 3 and 4):

- Review current models for forecasting demand, including the direct demand model (DDM), EDM and SPM.
- Review current models of total social cost.
- Review appraisal frameworks.
- Collect data.
- Determine the data requirements and availability.
- Collate relevant existing data.
- Devise a questionnaire to gather data on the SP of passengers along the case study corridor in terms of journey time, cost, frequency, and so on.
- Collect background information on passengers' socioeconomic characteristics, attitudes and travel preferences along the case-study corridor, and quantify their impact on the demand for HSR and Hyperloop; the demand for Maglev is assumed.
- Collect data through an SP survey of a case-study corridor.

- Using Stata software, analyse the data collected.
- Calibrate and validate the models to assess demand for both current and alternative modes of travel.
- Undertake a comparative assessment taking the total social cost approach, in which demand is treated endogenously.

The typical approach to appraising intercity transport investments is to use cost–benefit analysis for various HSR (high speed rail) lines (e.g. HS2 in the United Kingdom). However, this requires detailed data and analysis, particularly in terms of forecasting demand, revenue and user benefits. This is appropriate at the detailed planning stage, but at the feasibility stage a more strategic approach is needed. This is provided by an assessment framework that combines three demand models with the total social cost model to achieve the main aim of this research: determining the most cost-effective HSGT system by comparing the average social cost of the three selected transport modes of HSR, Maglev and Hyperloop. One of the simplifications is to treat prices as transfers so that they can be ignored in the assessment, although they still need to be considered in the forecasting models (Preston, 2021).

## 1.4 Thesis Structure

To present the study in a logical sequence, this thesis is divided into 9 chapters. A brief description of each follows:

Chapter 1: Introduction

This covers the definition of HSGT technologies. It describes the research aim, objectives, tasks, and structure of the comparative assessment of the models and presents an outline of the whole thesis.

Chapter 2: Literature Review of High-Speed Ground Transportation Technologies

This theoretical stage reviews the background of HSGT technologies, including the development of HSR, Maglev and Hyperloop. It gives an overview of each HSGT in terms of global extent, advantages and disadvantages. The main principles behind Maglev and Hyperloop are included, and the main elements of Hyperloop.

Chapter 3: Methodological Review

This reviews the methodology of the total social cost models used in the past for each mode of HSGT in terms of operator cost, user cost and external environmental cost. It presents a brief explanation of each and results of projects in specific countries. A brief literature review of forecasting and elasticity of demand models is also provided, as well as that of the SP method, introducing each by means of its definition. Using each model, it reviews and discusses previous case studies.

Chapter 4: Application of the Total Social Cost Model

This reviews the operator cost of HSR technology, using estimated costs for existing infrastructure construction in Europe. An overview of operator cost of Maglev is presented for existing and proposed Maglev projects. The operator cost of Hyperloop technology is reviewed, based on proposed projects worldwide. User cost is expressed in terms of access/egress time, waiting time and in-vehicle travel time, as well as the external environmental cost. This also presents a brief description of the case study conducted in this research, starting with its location, population, GDP, economy and tourism. It covers the transport modes currently serving the corridor in question: conventional rail, car, bus and air.

Chapter 5: Developing Direct Demand Models

The chapter presents the models devised to forecast the travel demand, including the direct demand model (DDM) and elasticity of demand model (EDM). The first was developed to forecast travel demand for HSR and is based on independent socioeconomic variables for the cities along the proposed route, such as their population, mean GDP per capita, number of trains per day, mean speed and a dummy variable for the month. By contrast, the elasticity of demand approach was developed to forecast travel demand for Maglev, mainly on the basis of the relationship between the proposed HSR and Maglev lines in terms of numbers of trips and generalized journey times.

Chapter 6: Developing Stated Preference Models

The SP method was developed to determine the demand for Hyperloop by collecting data. It is based on a passenger survey along the case study's conventional rail corridor, establishing preferences and behaviour regarding travel by conventional rail, air, bus and car as well as by HSR and Hyperloop. The attributes of travel time, travel cost and service frequency are assessed.

Chapter 7: Application of Demand Models

The chapter presents the application of each demand model in detail, based on an analysis of the levels of demand forecast for 2030, 2040 and 2050 for the HSGT technologies considered in this research. It starts by determining demand for HSR, using the log-linear DDM, then forecasts demand for Maglev on the basis of the generalized journey times suggested by HSR's forecasted level of demand. It includes a section on assessing demand for Hyperloop by testing both nested logit and multinomial logit models in order to choose which achieves statistically significant results.

Chapter 8: Comparative Assessment of Total Social Cost Model

The chapter presents the application of the proposed comparative assessment. Modelling the introduction of the HSGT technologies of HSR, Maglev and Hyperloop in the Riyadh–Dammam corridor, Saudi Arabia, serves as a case study. The TSCM that is developed is explained using an Excel spreadsheet. This incorporates operator cost, consisting of the infrastructure's construction and maintenance costs, together with the costs for the acquisition, operation and maintenance of the rolling stock. It also covers user cost, which comprises passengers' access/egress, waiting and in-vehicle time. The external environmental cost is also an input, involving the costs associated with air pollution, noise, accidents and climate change. In order to calculate total user cost, the value of time is quantified.

Chapter 9: Conclusion and Future Work

The final chapter summarizes the whole study's findings and discusses its main achievements against the objectives specified in the first chapter. It describes the thesis' contribution to knowledge, its limitations and potential work in future.

# Chapter 2. Literature Review of High-Speed Ground Transportation Technologies

## 2.1 Introduction

This chapter investigates the three high-speed transport technologies considered in this study. Section 2.2 reviews the development of HSR technology through examining countries' networks and defining four models of exploitation. Section 2.3 presents the development of Maglev technology by means of definitions, a review of Maglev networks worldwide and its main three principles: levitation; propulsion; and lateral guidance. An overview of Hyperloop technology is presented in section 2.4, including its feasibility and main components, as well as the capsules, tubes, pillars and stations. The advantages and disadvantages of each HSGT are identified, while section 2.5 summarizes the chapter and draws conclusions.

## 2.2 Development of High-Speed Rail Technology

HSR is expanding rapidly across the world's continents, offering fast and efficient mobility in numerous nations. Currently, HSR is in operation in more than 21 countries, including Japan, France, Germany, Spain, Belgium, United Kingdom, South Korea, Italy, Taiwan, China, Saudi Arabia, the Netherlands, the United States and Morocco, and it is under construction in Iran, Switzerland, Mexico and elsewhere (UIC, 2020a) (see Table 2-1). As of January 2020, the total length of HSR networks in operation worldwide was 51,581 km, divided between six Asian countries, 12 European countries and two others. Table 2-1 shows those countries with an HSR either in operation or under construction, with the total length of their network. China has the world's most extensive network of HS services.

In HSR projects, heavy investment may be a measure to encourage passengers to shift to rail from other modes of transport, such as road or air transport, to balance the modal split and decrease the negative environmental impact (Gorlewski, 2011). In this case, construction of HSR could represent a valuable investment for some markets, offering faster, cleaner, safer and more reliable, more comfortable and more convenient travel between cities, as well as improving the economy and mobility of the system itself.

| Country | In operation (km) | Under construction (km) | Total network (km) |
|---|---|---|---|
| China | 35,048 | 5,250 | 40,298 |
| Spain | 2,827 | 795 | 3,622 |
| Japan | 3,041 | 402 | 3,443 |
| France | 2,734 | 0 | 2,734 |
| Germany | 1,571 | 147 | 1,718 |
| Turkey | 594 | 1,652 | 2,246 |
| Italy | 921 | 327 | 1,248 |
| South Korea | 893 | 0 | 893 |
| United States | 735 | 763 | 1,498 |
| Saudi Arabia | 449 | 0 | 449 |
| Iran | 0 | 1,336 | 1,336 |
| Taiwan | 354 | 0 | 354 |
| Belgium | 209 | 0 | 209 |
| Morocco | 200 | 0 | 200 |
| Switzerland | 144 | 15 | 159 |
| Netherlands | 90 | 0 | 90 |
| United Kingdom | 113 | 230 | 343 |
| Austria | 254 | 281 | 535 |
| Finland | 1,120 | 0 | 1,120 |
| Poland | 224 | 0 | 224 |
| Denmark | 60 | 0 | 60 |
| **Total** | **51,581** | **11,198** | **62,779** |

Table 2-1*:* Overview of HSR network by country in January 2020. (Source: UIC, 2020a)

Building a high-speed line may involve more costly investment than a conventional rail line, and when it comes to journey times the change in generalized travel cost should always be considered (Gorlewski, 2011). Moreover, the construction, operation and maintenance of HSR lines are significant aspects of a country's development plan for both its transport sector and policies. In Europe, three types of line are developed for high-speed infrastructure: new high-speed lines; upgrades to existing conventional lines for speeds of 200 km/h; and upgrades to conventional lines for a speed adapted to each case. The last represents the fully mixed model, as in Germany. Four exploitation models have been identified, as shown in Figure 2-1.

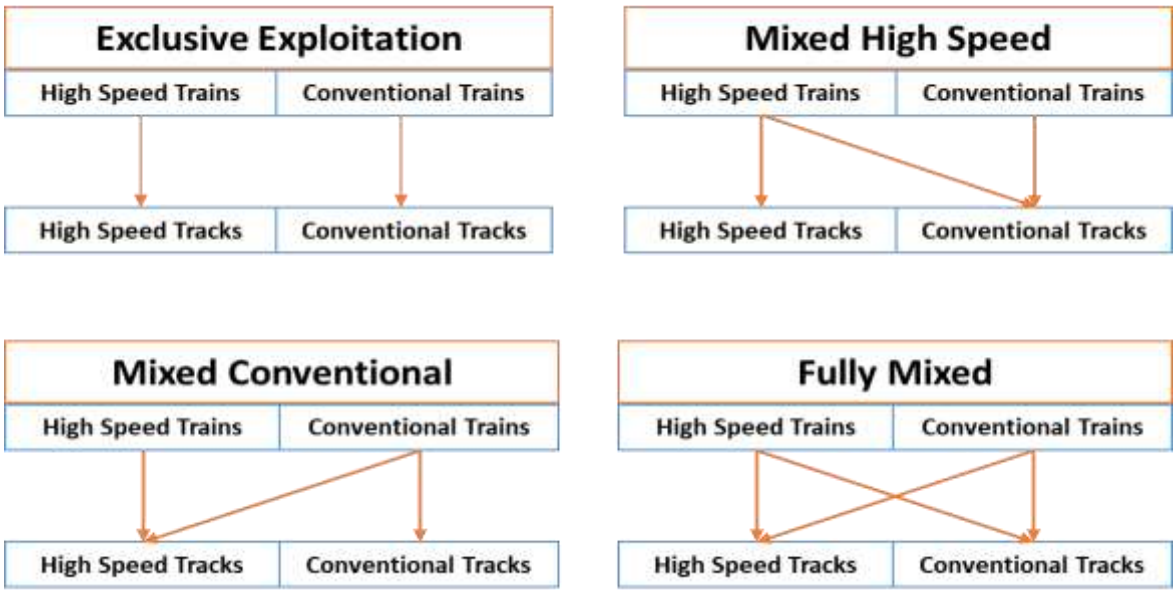


Figure 2-1: High-speed degrees of separation. (Source: Rutzen and Walton, 2011; de Rus, 2012a, 2012b)

First, the Japanese Shinkansen model is an example of infrastructure being fully shared between HSR and conventional rail services. Shinkansen lines adopted this model in 1964 due to capacity constraints on Japan's classic rail lines, which had been constructed in narrow gauge (1067 mm) due to the country's geology and geography. Japan National Railways (JNR) decided to design and build the new high-speed lines in standard gauge (1435 mm) and to market the HSR and conventional rail services completely independently (Campos, de Rus and Barron, 2006).

France is a good example of the second model, the mixed high-speed model, operated by TGV (Train à Grande Vitesse) since 1981, where HS trains run either on newly constructed lines or, at lower speeds, on upgraded conventional lines (Campos, de Rus and Barron, 2006). In this case, passengers will tend to switch from conventional trains as HSR serves a wider network and has more stations. A similar model lies behind the operation of the latest HSR line between Frankfurt and Cologne in Germany. In this model, the HS trains can use the conventional lines on only the few miles of track connecting stations in city centres to the newly constructed HS line. The HS trains run exclusively on HSR tracks for the major part of their journey, where no other types of trains operate (Ziemke, 2010).

Third, the mixed conventional model has been adopted in Spain, whereby some conventional trains can use high-speed tracks. This model is operated by Spain's

AVE (Alta Velocidad Espanola), some of whose conventional trains were constructed in broad gauge (1,676 mm). For example, Talgo 200 trains have been designed specifically as rolling stock to accelerate the interoperability of worldwide services and use the HSR infrastructure for higher speeds (de Rus, 2012a). Between 1992 and 2008, the technology was developed to allow trains to move between rail gauges: the new rolling stock can transfer from conventional to high-speed lines without stopping. This has extended the mixed HSR service to further places, especially to cities where HSR infrastructure has not yet been built (de Ureña, 2016). The main advantage is savings in the acquisition and maintenance of rolling stock while providing flexible high-speed services on existing lines.

Lastly, a fully mixed model has been adopted in Germany and Italy for maximum flexibility. HS trains can run on upgraded conventional lines, while lower-speed trains can run on HS lines over significant portions of the network (Ziemke, 2010; de Rus, 2012a).

| **Year** | **2010** | **2011** | **2012** | **2013** | **2014** | **2015** | **2016** | **2017** | **2018** |
|---|---|---|---|---|---|---|---|---|---|
| China (China Railway) | 46.3 | 105.8 | 144.6 | 214.1 | 282.5 | 386.3 | 464.1 | 557.6 | 680.5 |
| Japan (JR Group) | 76.9 | 79.6 | 84.2 | 78.4 | 89.2 | 97.4 | 99.6 | 101.4 | 103.6 |
| France (SNCF) | 51.9 | 52.0 | 51.1 | 50.8 | 50.7 | 50.0 | 50.5 | 58.3 | 56.8 |
| Germany (DB AG) | 23.9 | 23.3 | 24.8 | 25.2 | 24.3 | 25.3 | 27.2 | 28.5 | 31.1 |
| South Korea | 11.0 | 13.6 | 14.1 | 14.5 | 14.4 | 15.1 | 16.3 | 14.9 | 15.3 |
| Spain (Renfe Operadora) | 11.7 | 11.2 | 11.2 | 12.7 | 12.8 | 14.1 | 15.1 | 15.5 | 16.1 |
| Italy (Trenitalia) | 8.0 | 8.3 | 9.6 | 11.6 | 11.7 | 13.6 | 14.3 | 15.1 | 15.1 |
| Taiwan High-Speed Rail | 7.5 | 8.1 | 8.6 | 8.6 | 8.6 | 9.7 | 10.5 | 11.1 | 11.6 |
| Other companies | 7.3 | 10.5 | 14.8 | 15.2 | 18.2 | 20.0 | 22.6 | 24.5 | 26.0 |
| **Total** | **244.5** | **312.4** | **363.0** | **431.1** | **512.4** | **631.5** | **720.2** | **826.9** | **956.1** |

Table 2-2: High-speed traffic in the world in January 2020 (billions of passenger-km). (Source: UIC, 2020b)

As shown in Table 2-2, China's HSR network reached 680.5 billion passengers-kilometres in 2018, representing the world's highest demand, while Taiwan's HSR had the lowest demand, at 11.6 billion passenger-kilometres (UIC, 2020b).

### 2.2.1 High-Speed Rail in various countries

#### 2.2.1.1 Japan

Japan is a densely populated country of approximately 380,000 square km and in 2015 a total population of 128 million (Statistics Bureau, 2016), and it has large cities. In 2015, it was the third largest economy in the world, having a GDP of €3.69[1] trillion and GDP per capita of €27,879 (UIC, 2017). In terms of building HSR, Japan is a pioneering inventor. The decision to develop the HSR network, known as Shinkansen, was made after conventional lines for both passenger and freight had become extremely congested so that greater capacity was needed. The first line in its network came into service in October 1964, with a length of 515 km, linking two largest cities, Tokyo and Osaka, with an operating a speed of 210 km/h (UIC, 2017).

ATC (Automatic train control) is used as a safety mechanism system along the entire network of the Tokaido Shinkansen to display to the driver the maximum permitted speed (JR-Central, 2017). It automatically applies the brakes if this is exceeded, slowing the train to an allowable speed (JR-Central, 2017). Shinkansen has no record of a fatal accident on any train over the fifty years and longer since it commenced operation. It has achieved 95% punctuality, with an average delay of just 0.2 mins per train. For example, the Tokaido Shinkansen line links Tokyo, the capital, with Osaka via Nagoya with a high-frequency service of 358 trains per day (10 trains at peak hours from Tokyo), carrying around 445,000 passengers daily in 2016, compared to 61,000 in 1964 (JR-Central, 2017). Currently, the Japanese

[1] Conversion rates are €1 = $1.22 and £1 = €1.13.

Shinkansen has nine high-speed lines, as shown in Figure 2-2, with a total network of 3,041 km in operation and 402 km under construction (UIC, 2020a).

Figure 2-2: Map of HSR lines in Japan. (Source: UIC, 2020c)

Due to the high frequency of earthquakes in Japan, to reduce the risk of natural disasters slope protection, seismic reinforcement, wind barriers and avalanche fences were used for the HSR infrastructure construction, involving tunnelling and technical challenges (Palacin *et al.*, 2014).

#### 2.2.1.2 France

France is in Western Europe and, with a GDP of €1.815 trillion, it is the tenth largest economy in the world. Its GDP per capita was €28,688 in 2015. In terms of the development of HSR system, the French National Railway (SNCF) has had to provide extra capacity on the mainline service connecting two largest cities, Paris and Lyons. Offering faster services was also considered, and France decided to adopt the Japanese Shinkansen approach and build the HSR line on a new alignment (Amos, Bullock and Sondhi, 2010; UIC, 2010b). In 1981, it became the first country in Europe to provide an HSR service. This opened between Paris and Lyons, known as TGV Sud-Est, covering a distance of 419 km in about 2 hours, and it was followed by other lines (TGV Atlantique, TGV Mediterranée, TGV Rhone-Alpes, TGV Nord and TGV Est) (Amos, Bullock and Sondhi, 2010; UIC, 2010b).

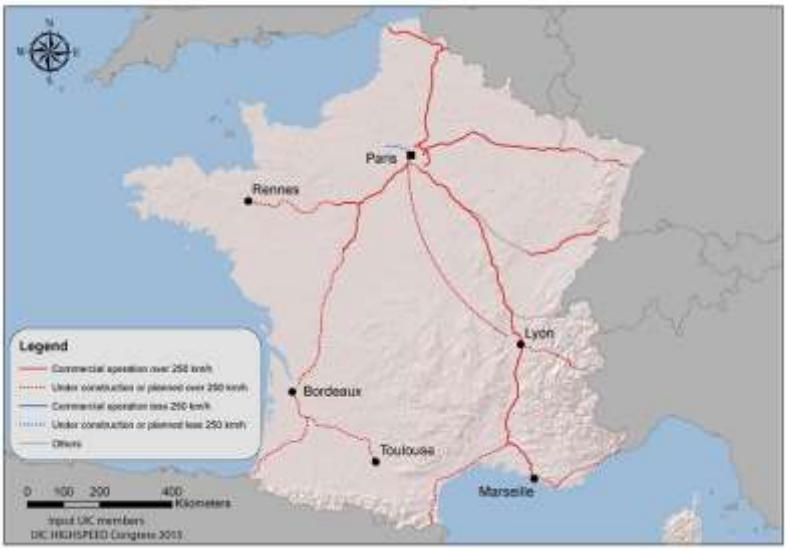


Figure 2-3: Map of HSR lines in France. (Source: UIC, 2020c)

The population of France is more distributed than in Japan, so the HSR service has longer corridors, as shown in Figure 2-3, serving small cities with lower demand. The three defining concepts of the first HSR line in France were to have a dedicated line for passenger traffic and a high-frequency operation with short travel times, and to integrate of HSR with the existing railway network, representing the lowest construction cost per kilometre. Traffic growth contributed to the HSR system's increasing profitability, achieving high operating speeds, reducing the cost of construction, operation and maintenance of new HSR lines and rolling stock and optimizing its capacity. For example, compared to the cost of the first TGV Sud-East line at just €3.28 million/km, the TGV Mediterranée, with seven long viaducts and tunnels of 17 km and 13 km, cost €12.29 million/km (Arduin and Ni, 2005).

#### 2.2.1.3 Germany

Germany is in Central Europe and has the largest economy in Europe, with a GDP of €2.53 trillion and €31,065 of GDP per capita per year. From the outset, the German Ministry of Transport consulted the Centre of Railway Management on whether the construction of new lines should follow the Japanese and French model and be dedicated to passenger traffic or, alternatively, should mix passenger and freight (Ebeling, 2005). HSR lines were developed by German federal transport at the beginning of 1970 to ease congestion on the conventional rail network and enable rail to compete with other transport modes. The first HSR line was

constructed to support the classic rail service, cutting travel time by running at a speed of 200 km/h, while newer lines run at speeds of up to 300 km/h (UIC, 2010c).


Figure 2-4: Map of HSR lines in Germany. (Source: UIC, 2020c)

The HSR Intercity Express (ICE) has a total of 1,571 km in operation and 147 km under construction, as shown in Figure 2-4 (UIC, 2020a). In Germany, Deutsche Bahn (DB) Holdings manages the operation of passenger and freight rail. It was founded in 1994 and also operates ICE trains outside of Germany. The finance for the construction of HSR lines is from federal government, as well as from local and state governments. ICE is designed to connect markets to major cities both within and outside Germany, and it already serves major European cities such as Paris, Brussels and Amsterdam (UIC, 2010c). As seen in Table 2-3, Germany's ICE system has seen steady growth, carrying about 74 million passengers in 2009 compared to just five million in its first year of operation (1991).

| Year | Passengers (thousand) | Passenger-km (million) |
|---|---|---|
| 1991 | 5,100 | 2,000 |
| 1997 | 30,947 | 10,073 |
| 2001 | 46,668 | 15,515 |
| 2009 | 73,709 | 22,561 |

Table 2-3: Germany's High-Speed Rail passenger traffic. (Source: UIC, 2010c)

Germany had the world's worst HSR accident in 1998 near the village of Eschede, when an HS train derailed and crashed into a road bridge. There were 101 fatalities and 88 injuries (Janić, 2017).

#### 2.2.1.4 Spain

Spain is in south-western Europe, with a GDP per capita of €25,966 in 2016 and 3% average annual growth (Ortega-Hortelano, Almujibah and Preston, 2018). The first HSR line opened in 1992, the year that Seville hosted the Universal Exposition, and it connects Madrid, Cordoba and Seville. It stretches from the centre of the country to the south of the Iberian Peninsula over a distance of 471 km. After opening its first HSR line, Spain rapidly expanded its high-speed network. The HSR service is known as AVE and is operated by Renfe Operadora, the state-owned railway company, while the infrastructure is managed by the state-owned company ADIF. As shown in Figure 2-5, Spain's HSR has a network of 2,827 km in operation and 795 km under construction, making it the longest in Europe. It operates at a maximum speed of 310 km/h (UIC, 2020a).


Figure 2-5: Map of HSR lines in Spain. (Source: UIC, 2020c)

After joining the European Union (EU) in 1986, Spain took advantage of European funds to develop its HSR network, and the network has been largely financed by EU and government sources. The first HSR line was based on the technical standards of the TGV network, with a standard gauge of 1,435 mm (Ortega-Hortelano et al., 2016). In 2013, there was an HS accident on the Madrid–Ferrol route due to a train

travelling at twice the allowed speed of 80 km/h upon entering a bend. This took place about 4 km outside the station of Santiago, in the northwest of Spain, and caused 79 fatalities and 139 injuries (Janić, 2017).

| Year | Passengers (thousand) | Passenger-km (million) |
|---|---|---|
| 1992 | 1,314 | 400 |
| 1997 | 4,032 | 1,266 |
| 2001 | 6,998 | 2,409 |
| 2009 | 28,751 | 10,490 |

Table 2-4: Spain's High-Speed Rail passenger traffic. (Source: UIC, 2010f)

Table 2-4 shows that Spain's AVE system has seen steady growth, carrying about 28,751 million passengers in 2009, compared to 1,314 million in its first year (1992) (UIC, 2010f).

#### 2.2.1.5 Italy

Italy is in Southern Europe and borders France, Austria, Switzerland and Slovenia. It has a GDP of €1.68 trillion and €27,798 of GDP per capita per year (UIC, 2010d). Currently, it has a total of 921 km of HSR lines and an additional 327 km under construction, as in Table 2-1 (UIC, 2020a).

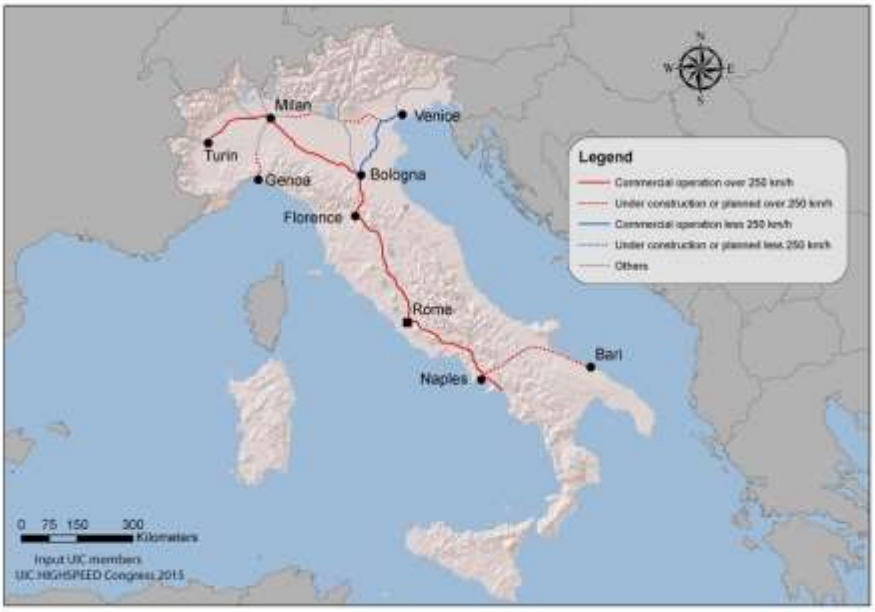


Figure 2-6: Map of HSR lines in Italy. (Source: UIC, 2020c)

Italy has a long history of transporting people around the country over its conventional rail network, as shown in Figure 2-6. The first HSR line was the Direttissima, which opened in 1978, connecting Rome with Florence at an average speed of 200 km/h, giving an end-to-end journey time of about 90 mins. In Italy, both passenger and freight rail operations were first controlled by the Italian State Railway, Ferrovie dello Stato (FS), then the country followed the European Union (EU) directive and separated the ownership of the infrastructure and the operation of the rail service (UIC, 2010d). As a result, the FS was retained as a holding company, owned by government, and three subsidiaries were established: Rete Ferroviária (RFI) for rail infrastructure and management; Treno Alta Velocita (TAV) for the planning and construction of high-speed lines; and Trenitalia to operate both passenger and freight trains. In 1991, a concession was awarded to TAV to construct and operate HSR lines between Turin and Venice, and between Milan and Naples, as TAV was 60% owned by private interests. After private shareholders became disinterested in 1998, 60% was acquired by FS to provide the capital required for the development of HSR, and TAV became a full subsidiary of FS (UIC, 2010d).

Trenitalia, the stated-owned rail-operating company in Italy, runs three HSR services: Frecciarossa for the latest service between Salerno and Turin, at operational speeds of up to 300 km/h; Frecciargento for the tilting trains running at up to 250 km/h on both the conventional rail and the HSR networks; and Frecciabianca to operate trains on conventional rail lines at speeds below 200 km/h to connect those destinations not covered by the two high-speed services. Besides Trenitalia, Nuovo Transporto Viaggiatori (NTV), a new private HDR operating company, started providing HSR services to the major Italian cities in 2012 with its Italo service (UIC, 2010d). NTV continues to attract new passengers. Its target market share has been achieved, as the number of passengers increased by 4.4% from 25.1 million in 2012 to 26.2 million in 2013, as shown in Table 2-5.

| | 2011 | 2012 | 2013 | 2014 | 2015 |
|---|---|---|---|---|---|
| **Annual Passengers (million)** | | | | | |
| Trenitalia | 23.4 | 25.1 | 26.2 | 29.1 | 31.2 |
| NTV | 0.0 | 2.0 | 6.2 | 6.5 | 9.1 |
| **Share of passengers** | | | | | |
| Trenitalia | 100.0% | 92.4% | 80.9% | 81.6% | 77.4% |
| NTV | 0.0% | 7.6% | 19.1% | 18.4% | 22.7% |

Table 2-5: Italian HSR: NTV and Trenitalia's market shares. (Source: UIC, 2020b)

Italy's HSR network has gradually increased its passengers from an annual 15.5 million in 2000, as shown in Table 2-6.

| Year | Passengers (thousand) | Passenger-km (million) |
|---|---|---|
| 2000 | 15,510 | 5,086 |
| 2001 | 18,785 | 6,763 |
| 2002 | 18,010 | 7,078 |
| 2003 | 19,092 | 7,431 |
| 2004 | 20,712 | 7,925 |
| 2005 | 21,906 | 8,550 |
| 2006 | 23,236 | 8,912 |
| 2007 | 23,430 | 8,818 |
| 2008 | 23,882 | 8,878 |
| 2009 | 33,377 | 10,746 |

Table 2-6: Italy's High-Speed Rail passenger traffic. (Source: UIC, 2010d)

In 2009, the system carried more than 33.4 million passengers, an increase of 40% from 23.9 million in 2008 (UIC, 2010d).

#### 2.2.1.6 United Kingdom

The United Kingdom is in Western Europe, and it has a GDP of €1.84 trillion and of GDP per capita of €29,426 per year. The idea for an HSR service was planned in 1998 as a single project, but due to financial difficulties it was divided into two phases. In 2003, the first UK HSR line opened between the Channel Tunnel and London, known as HS1, providing a direct international service to Paris and Brussels (UIC, 2010g).

The first section from the Channel Tunnel to Fawkham Junction runs over a distance of 75 km at an operating speed of 300 km/h. This section cost €2.16 billion and was opened to the public in 2003, both on time and on budget. By contrast, the second section, connecting Southfleet Junction to central London's St Pancras Station, opened in 2007 at a cost of €3.75 billion (UIC, 2010g). This line is the world's most

expensive HSR line ever built due to lengthy tunnelling to avoid environmental objections (Nash, 2010). Upon the opening of the HS1, travel times were mostly reduced, and it now takes just over two hours from London to Paris and less than two hours from London to Brussels and Lille (UIC, 2010g). In this case, the length of the HS1 line between St Pancras International in London and the Channel Tunnel is 108 km. The regular HS1 international passenger service began on 14 November 2007, with London–Paris in 2 hours 15 minutes, London–Brussels in 1 hour 51 minutes and London–Lille in just 1 hour 20 minutes. As London–Paris previously took around 2 hours 55 minutes, HS1 offered time savings of around 40 minutes (BBC News, 2003).


Figure 2-7: Map of HSR lines in the United Kingdom. (Source: UIC, 2020c)

In 2009, the Department of Transport developed plans for HS2, a new HSR network connecting London and Birmingham over a distance of 205 km in the first section. Another two sections are shown in Figure 2-7, one from London to Manchester and the other to Leeds, some 335 km, at an operating speed of 360 km/h across the whole HS2 network (UIC, 2010g). HS2 will be used separately by high-speed passenger trains, making it possible to run 18 trains per hour, each with capacity for 1,100 passengers. The cost for the first section of the HS2 route is between €17.9

billion and €19.8 billion, while the second section would cost a total of about €34.1 billion at 2009 prices. In this second section, which is to connect London to Manchester and Leeds, the unit rates per kilometre are: over undulating terrain, €19.9 million; over flat terrain, €18.5 million; in tunnels, €90.8 million; and through urban areas, €28.4 million) (Preston, 2010).

#### 2.2.1.7 China

China is in Asia, and is the world's fourth largest in terms of geographical extent. In terms of its economy, it has a GDP of €9.25 trillion and €6,885 GDP per capita per year. The Chinese HSR network is owned, developed and operated by the Ministry of Railways (MoR), and the first line was opened in 2003 between Qinhuangdao and Shenyang over a distance of 405 km and at an operating speed of 250 km/h (UIC, 2010a). China has the world's largest HSR network, with a total of 35,048 km in operation and 5,250 km under construction, due to strong support from the Chinese government and regular investment (UIC, 2020a). This rapidly growing HSR network is larger than the combined HSR networks of 17 European countries (8,948 km) as shown in Figure 2-8, and accounts for nearly 65% of the world's HSR lines (UIC, 2017). In many Chinese cities, it has been necessary to build multiple network stations due to the extremely high passenger demand (Chen, Tang and Zhang, 2014).


Figure 2-8: Map of HSR lines in China. (Source: UIC, 2020c)

As China is the world's most populous country, one of the main reasons for developing Chinese HSR (CHSR) is to reduce the disparity between the railway network's limited capacity and the strong demand for social transportation, especially during holidays. On the other hand, the cost of constructing a high-speed line with operational speeds of 300 km/h is about three times higher than that of a conventional rail line: investment in the actual total infrastructure for the intercity Beijing–Tianjin high-speed line was €2.63 billion for 118 km, and total investment in the Wuhan–Guangzhou high-speed line was €3.44 billion for 1,079 km (Chen, Tang and Zhang, 2014).

#### 2.2.1.8 Saudi Arabia

The Kingdom of Saudi Arabia (KSA) is one of the world's richest developing countries, primarily due to revenues from oil, which changed the Kingdom from a pre-industrial to a modern industrial country (Al-Ahmadi, 2006). It is in the Middle East on the Arabian Peninsula between the Red Sea and the Persian Gulf and is the world's thirteenth largest country in terms of area (2.15 million square km). The Saudi Railway Master Plan (SRMP) for the development of rail projects has three phases of development, the first covering 2010 to 2025; the second 2026 to 2033; and the third 2034 to 2040 (UIC, 2010e).

The first HSR project in Saudi Arabia, Haramain High-Speed Rail (HHSR), was a high priority. It now links the two holy cities of Mecca and Medina via Jeddah and King Abdullah Economic City (KAEC) in Rabigh, covering a distance of about 449 km, as shown in Figure 2-9, at a maximum operating speed of 300 km/h (Ferran, 2017).


Figure 2-9: Map of HSR lines in Saudi Arabia. (Source: UIC, 2020c)

Each train has a total length of 215 m, formed of 13 cars with 417 seats, and two-power units that generate a combined output of 8 MW, operating at a maximum speed of 330 km/h (Ferran, 2017).

The total construction costs of HHSR were about €13.5 billion, including civil works, the construction of stations, railway systems and rolling stock, and project management (ArabNews, 2017). One of the main reasons that led the Saudi government to build the HHSR is the growing number of annual pilgrims, Umrah[2] visitors and residents who travel to Mecca and Medina. Another is to relieve the congestion and reduce the air pollution from vehicles' exhaust on roads between these cities. The HHSR will reduce travel time between Jeddah and Mecca to 30 mins and between Mecca and Medina to two hours.

[2] Umrah is shorter version of the annual Hajj gathering, and can be performed at any time.

Many European rail infrastructure companies and rolling stock manufacturers have been involved in this project to transport approximately 11 million pilgrims plus visitors between the two holy cities (Railway Technology, Saudi Arabia, 2008). It links the city centres, boosting local business and tourism along the line. The HHSR has 35 Talgo 350 high-speed trains, designed and manufactured by Spanish Talgo with the most advanced safety systems, with the option for 20 more. On 25 September 2018, Saudi Arabia's King Salman officially launched the initial HHSR service of eight trips per day in both directions with a fleet of 35 trains. The first train ran on 4 October 2018 from Mecca to Medina via Jeddah Center Station and KAEC, and the service to Jeddah Airport began in late March 2019 (Aldroubi, 2018).

### 2.2.2 Advantages and disadvantages of High-Speed Rail

According to Rutzen and Walton (2011), for passengers there are direct social advantages of HSR systems, such as time savings, fewer accidents, greater comfort, fewer delays and less congestion than with air and road travel, and causing less smaller environmental impact.

Time saving is a major factor in the competition between transport modes. The perceived value of HSR's benefits depends on several elements, including whether the trip is for work or leisure and the specific mode of travel used to access the HSR station. Furthermore, the time saving relates to the mean journey length, the value placed on saving travel time and the relative door-to-door speeds. The proportion of HSR travellers who are business users and the number of trips that they generate have been identified as important variables (Preston, 2009).

For passengers, the value of time is the dominant factor, and convenience appears to be a greater influence on business travel than on regular commuting. However, the neighbourhoods near the major urban centres served by HSR enjoy the benefits of access to HSR, transferring to and from conventional rail services readily, while the places further along a HSR line have only limited access (Brunello, 2011). For example, in Spain HSR makes cities such as Madrid, Cordoba, Toledo, Seville and Barcelona more accessible to tourists (Loukaitou-Sideris and Peters, 2015). The greatest switch in passengers' transport mode is made from conventional rail and air travel since, despite the shorter journey times, with HSR travel a passenger still needs to allow time for access/egress, waiting and in-vehicle time. These need to

be considered, but generally they are shorter than at airports (Albalate and Bel, 2017). For example, around 42% of the main social benefit of HSR is its time saving, and most of the diverted passenger traffic has switched from conventional rail services along the Madrid–Barcelona corridor (1998), Madrid–Seville (1987), Madrid–East Coast (2003) and Madrid–North (2002) (Albalate and Bel, 2017).

The second key benefit of HSR is safety. Although there have been accidents, only a few have involved deaths: in terms of passenger fatalities per billion passenger-kilometres, HSR has proved to be the safest intercity transport mode for medium or long journeys. It accounts effectively for zero passenger fatalities per billion passenger-km overall, compared to 5.9 deaths by car travel and 0.4 by air and coach or bus travel (Rutzen and Walton, 2011). Japan is the clear leader, with no fatalities since HSR services began, while France has had only two fatalities, both due to accidents at stations where there were also conventional lines at stations for TGV trains. In general, HSR is far safer than road transport and compares favourably with air transport (Amos, Bullock and Sondhi, 2010).

A third key benefit of HSR is the greater comfort compared to conventional rail, road or air travel. Factors affecting comfort include noise, space, acceleration and the services that can be provided, such as catering, unlimited use of electronic devices or even a nursery for children, in some cases.

The congestion and delays experienced on the roads and at airports can also be avoided by using HSR. HSR offers a huge capacity, with up to 400,000 passengers per day on Tokaido Shinkansen (Tokyo–Osaka, 515 km) (Angoori, 2010; Rutzen and Walton, 2011).

When it comes to environmental impact, although the amount of polluting gases used by HSR includes those emissions produced to generate the electricity that it consumes, it is regarded as a less polluting mode of travel. It also has social benefits, mostly reducing accident rates through attracting passengers away from road traffic (Pourreza, 2011; Albalate and Bel, 2017). Further indirect benefits relate to economic development. For example, Shinkansen increased the employment rate in Kakogawa, a city 230 km from Tokyo, by 8% (Pourreza, 2011).

Increasing the capacity along routes has been behind construction of the world's major HSR lines, such as the first Shinkansen and TGV lines. In the United Kingdom in the 1970s and 1980s, the country's existing capacity was one of the main reasons why HSR development was not considered when other European countries, such as Italy, were building their HSR lines (Givoni, 2006). However, another reason is to attract economic activities to the major regional cities connected by HSR, at the same time helping to contain urban sprawl and promote a more logical territorial structure (Rutzen and Walton, 2011).

The key factor in the successful development of HSR is the identification of priority corridors, measured in terms of passenger demand, revenue and economic development. For example, the development of the Shinkansen HSR network since its launch in 1964 has brought benefits to both the regional and national economy, so local communities may contribute to funding (Rutzen and Walton, 2011).

On the other hand, HSR also involves economic, social and environmental disadvantages. First are the land requirements and environmental damage, as in order to avoid experiencing excessive centrifugal forces on bends when travelling at high speeds HSR requires greater curve radii. Consequently, constructing the infrastructure impinges on many land-use types, such as residential areas, forest, farmland, and so on, to maintain straight lines. HSR involves locating a high proportion of the track on structures (viaducts, bridges, embankments) and in tunnels and cuttings. This leads to problems of visual intrusion, severance and ecological disturbance. Second, huge investment is necessary due to 'the high maintenance costs and the low demand in many corridors', making HRS. lines difficult to justify from a socioeconomic point of view (Lusvter, 2015). Third, the high fares mean that its users are largely from high-income groups, leading to concerns of social exclusion: most low-income riders continue to use conventional train or road transport (Chen, Tang and Zhang, 2014).

## 2.3 Development of Magnetic Levitation Technology

Maglev trains move more smoothly and quietly, with less friction than wheeled mass transit systems. Only a small percentage of the overall energy consumption is for levitation, and most goes on overcoming air resistance. The vehicle levitation is kept

to a constant 10 mm above its guideway by an electronic control system (Yadav *et al.*, 2013). Recently, Maglev systems have become regarded as a transport solution thanks to their speed and the mechanical air gap between vehicles and track (Cassat and Bourquin, 2011). The Maglev system is now operational across South Korea, Japan and China, as shown in Table 2-7, with a total length of 73.3 km.

| **Maglev line** | **Location** | **Running since** | **Maximum speed (km/h)** | **Track length (km)** |
|---|---|---|---|---|
| Daejeon Expo Maglev | South Korea | 1993 | 100 | 1.0 |
| Incheon Airport Maglev | | 2016 | 110 | 6.1 |
| Linimo | Japan | 2005 | 100 | 8.9 |
| Shanghai Maglev Train | China | 2002 | 431 | 30.5 |
| Changsha Maglev Express | | 2016 | 100 | 18.55 |
| Beijing S1 Line | | 2017 | 110 | 8.25 |
| **Total** | | | | **73.3** |

Table 2-7: Overview of existing Maglev network by country. (Source: Schonig, 2019)

Maglev uses electromagnets located on the underside of each train to raise it to the ferromagnetic stators on the track, creating the current to levitate it, while the magnets on the sides keep it from moving laterally. To keep the train precisely 1 cm from the track, a computer adjusts the electrical current (Chopade, 2017a). Contactless transfer (e.g. linear generators, inductive power transfer, transformer action and gas turbine generators), created by flux harmonics induced in wires inserted in each motor pole, is used by high-speed Maglev to get the energy to the vehicles. The chosen technology for low-speed Maglev is the catenary, with a 1,500 VDC (Cassat and Bourquin, 2011).

### 2.3.1 Main principles of Maglev system

As shown in Figure 2-10, a Maglev system involves three major principles: levitation; propulsion; and lateral guidance. Levitation force provides the upward lift to the vehicle, while propulsion moves it forwards (Rose, Peterson and Leung, 2008).

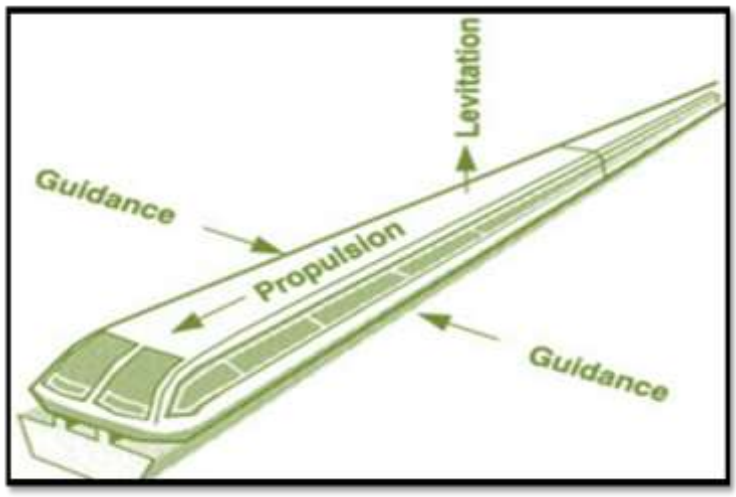


Figure 2-10: Basic principles of magnetic levitation. (Source: Shaik, 2018)

In addition, the guidance system is responsible for balancing the lateral displacement of the vehicle to keep it centred on the guideway (Rose, Peterson and Leung, 2008).

#### 2.3.1.1 Levitation

Levitation technology is the part of a Maglev system that keeps the vehicle gliding over an air cushion. The levitation of a train is dependent on its speed, as the coils are connected beneath the guideway, facing each other to constitute a loop. There are two methods to accomplish levitation: electromagnetic suspension (EMS); and electro-dynamic suspension (EDS).

##### 2.3.1.1.1 Electromagnetic suspension method

The EMS method uses the magnetic attraction between electromagnets and the guideway, as shown in Figure 2-11 (Lee, Kim and Lee, 2006). The magnets on the vehicles are wrapped around iron guideways and create lift by upward attracting forces. The resulting electromagnetic forces are usually independent of speed: there could be lifting forces at a zero speed at the end of the vehicle. In this case, the EMS requires a small gap of magnetic air of ≤25 mm (Cassat and Bourquin, 2011). Because of the small air gap in the EMS system, when speeds increase it is usually difficult to maintain control (Lee, Kim and Lee, 2006).

There are two types of levitation technologies in EMS: the levitation and guideway may be integrated, as in the Japanese HSST system and the Korean UTM system; or they may be separated, as in the German Transrapid system. The separated

type's electric power supply is rated higher than the integrated one, as it is difficult to control simultaneously both guidance and levitation because of the increasing interference between them during high-speed operation. For low-speed operation, the required number of electromagnets and controllers is less and comes at lower cost, while the difference in reluctance automatically generates the guiding force (Lee, Kim and Lee, 2006).

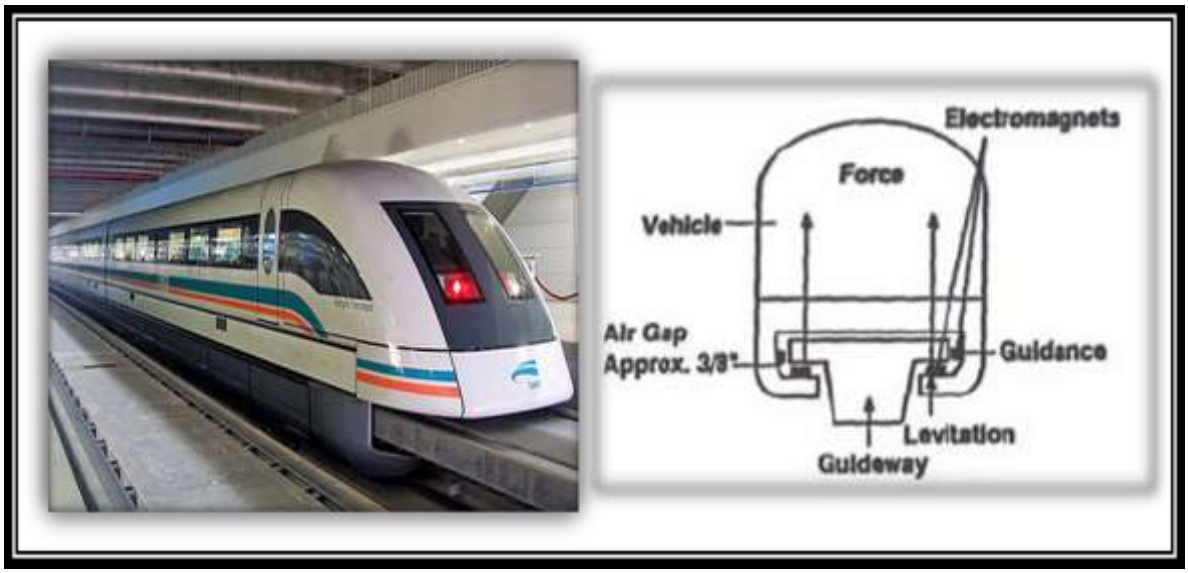


Figure 2-11: Electromagnetic suspension. (Source: Rose, Peterson and Leung, 2008)

Classical EMS technology includes the German Transrapid system, the Chinese CMS system, the Japanese HSST system and the Korean UTM system (Zhou *et al.*, 2010; Cassat and Bourquin, 2011).

#### 2.3.1.1.2 Electro-dynamic suspension method

The EDS method shown in Figure 2-12 was developed by Japanese engineers and uses magnets' same polarity to levitate trains by repulsive force, using the induced currents located in the conductive guideways to keep the two apart (Lee, Kim and Lee, 2006; Cassat and Bourquin, 2011). The repulsive forces are initially set up by temporal variation in a magnetic field in a conductor, and are exerted by both the rail and the train (Cassat and Bourquin, 2011; Chopade, 2017a). The repulsive force is located in the track, and is either created by the conducting strips in the track or induced in the magnetic field in wires (Chopade, 2017a). EDS technology is highly reliable across load variations so is stable magnetically, yet it needs sufficient speed to set up the induced current to achieve levitation (Lee, Kim and Lee, 2006).

In EDS technology, the magnetic air gap is large (100 mm) and there are no repulsive damping forces when the train is at a standstill. To permit this large air gap, the actual technology of Japan's JR-Maglev (MLX) is based on superconductivity, and at low speeds the system requires a bogie (≤100 km/h) (Cassat and Bourquin, 2011). A vehicle using the EDS system has a built-in current-carrying coil, and the flux produced by the current flowing through it induces a current in either conducting aluminium sheets or passive coils located in the guideway (Sharma *et al.*, 2014).

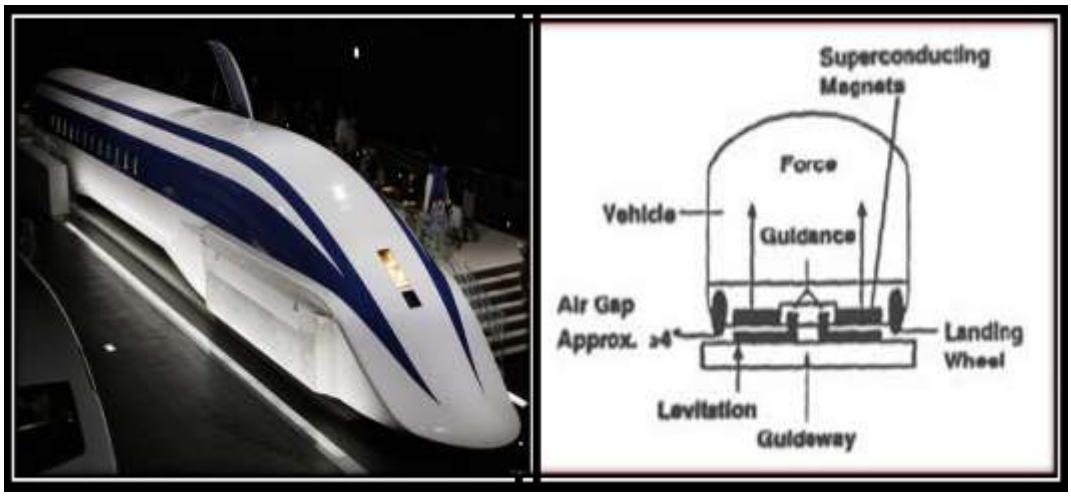


Figure 2-12: Electro-dynamic suspension. (Source: Rose, Peterson and Leung, 2008)

The main difference between EMS and EDS Maglev trains is that the former use standard electromagnets and, when a power supply is present, their coils only conduct electricity, whereas the latter use super-cooled coils as superconducting electromagnets to conduct electricity even when the power supply is turned off (Naufal, 2008). The linear motor is the most obvious propulsion system for a Maglev vehicle, using magnetic forces to produce thrust. While this can increase the speed of the train, however, it is not strong enough to move it along the track from stationary (Mustapha and Bababe, 2017). In order to control the air gap between the track and the train, the EDS system enables a suspension gap of up to 100 mm, larger than the EMS system (Zhou *et al.*, 2010). One of the most valued aspects of the attractive-force levitation used by the EMS system is its inherent instability: the electromagnets of each vehicle have to be actively controlled before they can levitate at a standstill, making the operation very safe (Cabral and Chavarette, 2015). For the superconducting Maglev, levitation and guidance coils are installed along both sides of the track, and they become electromagnets when an electric

current is induced, generating the force to push and pull the vehicles (Central Japan Railway Company, 2017). Some characteristics of EMS and EDS systems are compared in Table 2-8.

| **Characteristic** | **EMS** | **EDS** |
|---|---|---|
| Mode type | attraction mode | repulsive mode |
| Magnets | iron cored electromagnets | superconducting coils |
| Guideway | 10–15 mm | 100–150 mm |
| Guideway components | laminated strips | aluminium strips |
| Stability | inherently unstable | dynamically stable |
| Feedback control | necessary to maintain dynamic stability | Necessary |
| Compatible drive system | linear induction motor | linear synchronous motor |
| Example | Transrapid | MLX |

Table 2-8: Characteristics of EMS and EDS systems. (Source: Sharma *et al.*, 2014)

Most Maglev trains are of the EMS type, and guideways are mostly elevated, U-shaped and double track, with spans and track gauges of 24.8 m and 2.8 m, respectively, as shown in Table 2-9.

| **Maglev system** | **Shanghai, China** | **HSST, Japan** | **Transrapid, Germany** | **JR, Japan** | **Korea** |
|---|---|---|---|---|---|
| Suspension | EMS | EMS | EMS | EDS | EMS |
| Section | I-shaped | U-shaped | U-shaped | U-shaped | U-shaped |
| Guideway | elevated | Elevated | elevated (at grade) | elevated (at grade) | elevated |
| Track gauge | 2.8 m | 1.7 m | 2.8 m | 2.8 m | 2.8 |
| Span length (elevated) | 24.8 m | 30 m | 24.8 m | - | 25–30 m |
| Guideway structure | double track | double track | double track | double track | double track |

Table 2-9: Guideway structures and suspension systems. (Source: Yaghoubi, Barazi and Aoliaei, 2012)

#### 2.3.1.2 Propulsion

In the Maglev system, a contactless propulsion mechanism moves the vehicle body forward. Linear motors are used to produce both thrust, without any mechanical conversion, and the necessary braking forces. LIMs and synchronous motors are

the most popular, and are explained in detail in the following sections (Rose, Peterson and Leung, 2008).

#### 2.3.1.2.1 Linear induction motor

The LIM is used in propulsion systems to provide the properties of force and power consumption to travel through deep underground tunnels. It has many advantages over other systems of conventional propulsion, such as giving excellent acceleration and deceleration and the ability to climb steep gradients. The control equipment is installed beneath the deep underground GTX (Great Train Express) bogie, while the reaction plate is positioned on the rail (Park, Lee and Lee, 2012).

#### 2.3.1.2.2 Linear synchronous motor

The linear synchronous motor (LSM) used in propulsion systems contains the magnetic source within itself, while its motion is in synchrony with a travelling magnetic field produced by either switched currents or AC. The levitation-propulsion modules are located on the sides of each vehicle. This system requires data from on-board magnets to give the vehicle's exact position to guarantee that it is matched to the travelling magnetic wave in the guideway, produced by the stator winding (Mustapha and Bababe, 2017). In the superconducting Maglev system, the north and south poles of the magnetic field produced by passing current through the propulsion coils, located on the ground, propel the vehicle forward by the attraction of opposites. Moreover, a repulsive force can act between the same poles between the superconducting magnets built into the vehicles and the ground coils (Central Japan Railway Company, 2017). The active part of the motor for low-speed Maglevs is located within the vehicle, while for the high-speed Maglevs such as Transrapid and JR-Maglev it is located in the infrastructure (Cassat and Bourquin, 2011).

### 2.3.1.3 Guidance

The lateral guidance system enables the train to stay on the track and uses a system of electromagnets located in the undercarriage to stabilize its left and right movement (Train, 2011). Concrete or steel beams supported by a concrete substructure are used to construct a Maglev guideway in three ways: elevated, to avoid interference from existing infrastructure of other modes of transport and ground-surface activities; in tunnels, to direct it under densely populated areas; and

at-grade, if the land is available, where the system's safety can be maintained (American Magline Group, 2002).

In the EDS system, the principle of null-flux coils provides the guidance, achieved by cross-coupling the conducting coil mounted on the guideway, which is also used as the LIM framework for propulsion (Sharma *et al.*, 2014). By contrast, in the EMS mode guidance is provided by the magnetic guidance forces generated by the interaction between separate sets of electromagnets carried by vehicles and ferromagnetic rails on the sides of the guideway structure (Sharma *et al.*, 2014). The vehicles are kept in the centre of the guideway at all times by exerting a repulsive and an attractive force on both the near and far sides, especially when the vehicle moves off centre in either direction (Central Japan Railway Company, 2017).

#### 2.3.1.3.1 Repulsive force

Coils connected to each other on either side of the track exert a force, as shown in Figure 2-13, in such a way that the net electro-motive force (EMF) in the coils is induced to become zero. The net magnitude of induced EMF increases as the train displaces to either side to produce a repulsive force that centralizes each vehicle on the guideway (Rose, Peterson and Leung, 2008).

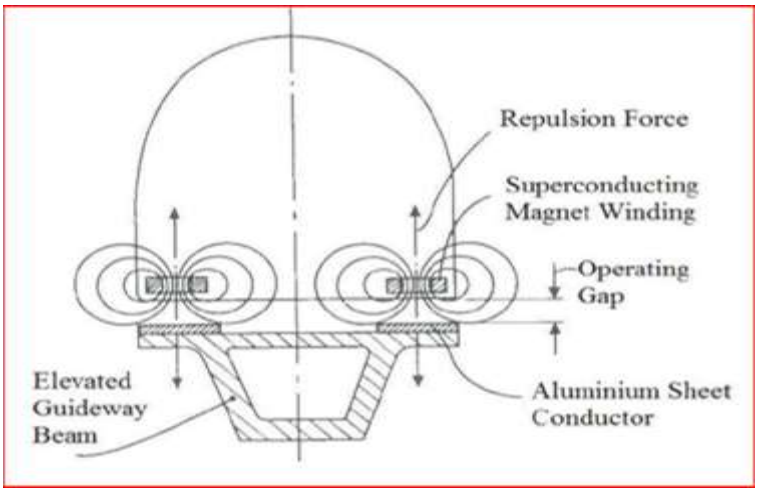


Figure 2-13: Magnetic repulsion force. (Source: Sharma *et al.*, 2014)

The Japanese MLU and MLX use the magnetic-repulsive guidance technique. MLU technology integrates the guidance with the propulsion system, while MLX technology integrates it with the levitation system. In the Transrapid system, the magnetic-repulsive force is between the coils connected to the sides of the train and

the on-board electromagnets. At higher speeds, the propulsion and levitation systems are separated from each other to avoid any interference (Rose, Peterson and Leung, 2008).

#### 2.3.1.3.2 Attractive force

The magnetic-attractive force generated between the reaction rails controls the lateral displacement and the on-board electromagnets, as shown in Figure 2-14. In the operating gap, a sensor detects the air gap between the reaction rail and the electromagnets (Rose, Peterson and Leung, 2008).

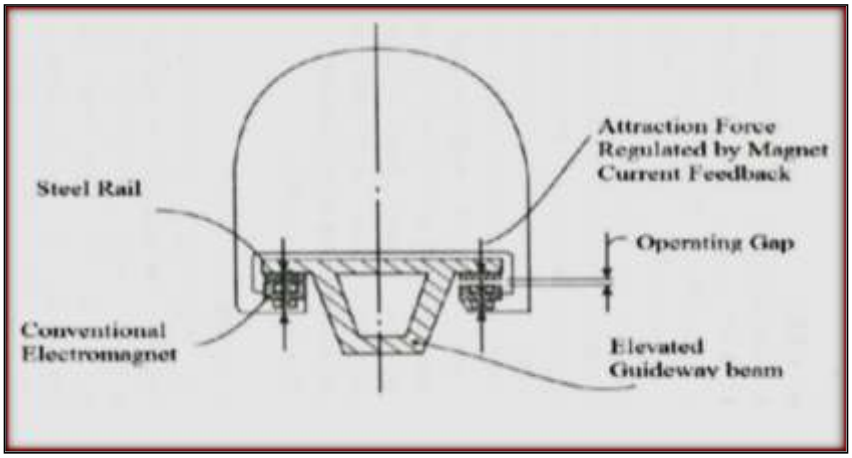


Figure 2-14: Magnetic-attractive force. (Source: Sharma *et al.*, 2014)

The air gap decreases the path of induction of the electromagnetic flux and increases the reluctance as soon as the vehicle becomes laterally displaced. The Japanese HSST system uses magnetic-attractive force guidance that is integrated with its levitation and guidance systems (Rose, Peterson and Leung, 2008).

### 2.3.2 Magnetic levitation in various countries

Maglev systems on the world market rely on a mechanical air gap between the track and the train This of a type dependent on the system's speed (Cassat and Bourquin, 2011). Superspeed Maglev systems are limited to two types: the German and Chinese Transrapid system; or the Japanese MLX system. However, a Maglev system is closer to an aeroplane than to road transport or conventional rail; moreover, it will become possible to design systems using lightweight guideways. For example, in 1999 a manned Japanese Maglev train broke the speed record by travelling at about 554 km/h around the 44 km-long test track, approaching airline speeds (Johnson *et al.*, 1989). No Maglev train currently has a double-decker

arrangement for passengers, and in future this might come to represent a limitation in terms of station length and capacity (Cassat and Bourquin, 2011).

#### 2.3.2.1 Chinese Shanghai Maglev line

In 1999, Chinese experts felt that it would be a significant achievement to develop and construct a high-speed Maglev system for Shanghai, in a world first at that time (Dona and Singh, 2017). The Shanghai Maglev Transportation Development Company (SMTDC) was founded in August 2000 to accomplish the project, using the German Transrapid for its guideway. Construction started in March 2001, and a demonstration of the first-ever operational Maglev system was held in December 2002. Commercial operation began in 2004 and showed how high speeds could be reached with Maglev trains (Dona and Singh, 2017).

The length of the Shanghai Maglev line is 30 km, with trains every 10 mins from Pudong International Airport to Lujiazui Financial District from 6:45 am to 9:40 pm (Dona and Singh, 2017). The trains are 153 m long, 4.2 m high and 3.7 m wide, with a two-class cabin that accommodates up to 574 passengers (Akamaihd, 2002). The service operates every 15 to 20 mins, and a one-way ticket costs €6.20 and a return €9.80 (Smith, 2017). There are three sets of five-section TR-08 trains, each with an average capacity of 100 passengers. The double-track route starts at the station in Longyang Road and ends at Pudong International Airport (Dona and Singh, 2017).


Figure 2-15: Shanghai Maglev train. (Source: Edwin, 2015)

The system has four main parts: the vehicle; the guideway; the operational control; and the power supply. The vehicles are electromagnetic for both elevation and propulsion, as shown in Figure 2-15, and include on-board batteries, a levitation control system and an emergency braking system (Dona and Singh, 2017). Along the route, the guideway directs the train and spreads the load from the train onto the ground. Generally with Maglevs, an operation control system is essential when an LIM is used; while the LSM is a highly efficient motor, it requires an active guideway, significantly increasing costs (Anisimow *et al.*, 2004). The power supply for the whole Shanghai Maglev system encompasses the substations, switch stations, other power supply equipment and trackside feeder cables (Dona and Singh, 2017).

#### 2.3.2.2 Chinese Changsha Maglev line

On May 2016, China launched the Changsha Maglev service between Changsha South railway station and the local airport, some 18.55 km, with a maximum speed of 100 km/h. Travel time is about 19.5 mins, and the line may help to reduce road traffic along the route (Dona and Singh, 2017). The fleet uses the EMS and LIM propulsion system. Each train is 48 m long, with an average capacity of 363 passengers (Barrow, 2016), and has a middle car and two head cars that can run in either direction, as shown in Figure 2-16, consisting of 10 electromagnetic modules and 20 suspension points (Jingfang, Zhiqiang and Xin, 2017). This line uses Chinese Maglev technology and has an intermediate station at Langlizhen.


Figure 2-16: Changsha Maglev line. (Source: Railway Pro, 2017)

In April 2020, the Zhejiang provincial government announced its plans to construct a Maglev train running 400 km at a speed of 430 km/h to connect southwest Shanghai to Ningbo in the south via Hangzhou, the Zhejiang capital. It intends to put the new line into operation around 2035 to revitalize the local economy through investment in transport infrastructure (Tabeta, 2020).

Regarding high-speed Maglev development, in 2020 at Shanghai's Tongi University a vehicle running on a Maglev line, as shown in Figure 2-17 (Tracy, 2020), successfully conducted its maiden run.


Figure 2-17: Shanghai–Hangzhou Maglev line. (Source: Tracy, 2020)

This high-speed service intended to connect Shanghai to Hangzhou, a distance of 175 km, and is to open to the public in 2025: citizens will be able to reach central Shanghai in just 20 mins (Cao Qingqing, 2020).

#### 2.3.2.3 South Korean Incheon Airport Maglev

The Korea Institute of Machinery and Materials (KIMM) gave funding in 1989 for a research and development project for a low-to-medium speed Maglev system using the EMS system and LIM propulsion. KIMM and Hyundai Rotem developed this system, enhancing their UTM-02 model to attain a nominal air gap of 8 mm. Incheon Airport Maglev (IAM) line has been working on this since 2007 as a test project, as this type of system allows the Maglev to work without noise or vibration or any need for wheels (Dona and Singh, 2017). The length of the IAM line is 6.1 km and it has six stations, with a design speed of up to 110 km/h and a maximum of 80 km/h. The

line has four Maglev trains, each consisting of two carriages, as shown in Figure 2-18, to carry up to 230 passengers at 15-min intervals between 9:00 am and 6:00 pm. South Korea started passenger operation in early 2016, making the country only the second in the world to launch urban Maglev technology (Dona and Singh, 2017).

Figure 2-18: Incheon International Airport Maglev. (Source: Rail Travel Station, 2019)

Now, South Korea has the ability to sell Maglev technology, and countries worldwide have expressed interest, such as Russia, Malaysia, the United States and Indonesia (Dona and Singh, 2017).

#### 2.3.2.4 Japanese MLX-JR-Maglev

The JR-Maglev is a system developed by the Japan Railway Technical Research Institute, and the JR-Maglev MLX01 is one of the country's latest designs. In Yamanashi prefecture, Japan has built a demonstration line as part of the planned Chuo Maglev Shinkansen line (CMS) (Maglev Board, 2018). The line will connect Tokyo and Osaka via Nagoya over a total length of 500 km and will be designed for a maximum speed of 505 km/h (Dona and Singh, 2017). The president of JR-Central, Masayuki Matsumoto, disclosed in 2007 that a commercial Maglev service between Tokyo and Nagoya will commence in 2025 (Maglev Board, 2018).

Figure 2-19: Japanese MLX Maglev train. (Source: Bonsor and Chandler, 2019)

In 2003, a three-car MLX01 Maglev train achieved a maximum speed of 581 km/h, faster than any wheeled train at that time and exceeding to the TGV record of 574.8 km/h set in 2007. The Japanese Maglev is technically able to reach higher speeds; as shown in Figure 2-19, it uses modern superconducting magnets to achieve the repulsive type of EDS, and it has a larger air gap (Maglev Board, 2018). To promote its construction, when the whole line is in operation the Maglev line is expected to run through nine prefectures, including the joint government groups of Tokyo and Osaka. One of the reasons why the Japanese government chose the EDS system is its wider air gap. In the event of an earthquake, the magnets of a Transrapid system in the EMS system, especially, could touch the stator due to its air gap of just 10 mm. The Japanese system has an air gap of about 100 mm and is self-stable, moreover it uses an LSM for its driving system (Maglev Board, 2018).

#### 2.3.2.5 Japanese Linimo Maglev line

The Japanese Linimo Maglev line was constructed for World Expo 2005, running from the Higashiyama subway line at Fujigaoka to the exhibition's satellite site at Yakusa. The Aichi Rapid Transit Company (ARTC) operates this line, and its vehicles levitate at 8 mm above the guideway, reaching a top speed of 100 km/h. The length of the line is 8.9 km and it has nine stations, transporting about 31,000 passengers daily throughout the World Expo. At the end of the event, the number

of passengers was reduced to 12,000 per day, and the Linimo line now serves the local community from 5:50 am to 12:05 am (Dona and Singh, 2017). This type of High-Speed Surface Transport (HHST), as shown in Figure 2-20, has frequent stations on an elevated guideway. The end-to-end trip takes just 15 mins, with 6 and 10 mins between vehicles during the peak and off-peak periods, respectively (Latino and Yokobri, 2009).


Figure 2-20: Linimo Maglev train. (Source: Gizmo Highway, 2011)

The Linimo Maglev is the first HSST commercial Maglev train in Japan and the second in the world to be propelled by LIM, using the attraction force of normal conductive magnetics for its levitation. The guidance and levitation systems provide the vehicles with primary suspension, while air springs and lateral mechanical linkages act as secondary suspension (Yasuda *et al.*, 2004).

#### 2.3.2.6 United Kingdom

The Birmingham International Maglev shuttle in Figure 2-21 was the first commercial Maglev train, opening in 1984 to connect the terminal at Birmingham International Airport to the nearby Birmingham International railway station. The line is just 600 m long (Bansal, 2014) and the train ran at a speed of 40 km/h, using LIM for its propulsion. It was levitated by electromagnets (BBC News, 1999).

Figure 2-21: Birmingham International Maglev shuttle. (Source: BBC News, 1999)

This system operated at a height of 15 mm above its track, and after 11 years it was closed in 1995 due to design and maintenance problems, as a further layer of fibreglass had had to be added to improve its crash worthiness. This made the cost of replacement and maintenance too high. In this case, the Maglev had radar rather than a conventional speedometer, and it was of little use at low speeds, especially in winter, and the project had to be realigned. Moreover, the additional weight prevented the electromagnets from lifting the train above the track, leading to the construction of an entirely new vehicle (BBC News, 1999).

### 2.3.3 Advantages and disadvantages of Maglev

Mokhim (2015b) mentions the advantages of magnetic levitated transport systems. Speed is one, as the Maglev is a floating train that travels extremely fast, reaching speeds of up to 500 km/h. Moreover, it has great potential for further development as it overcomes the main obstacles to increasing HSR speeds, which is the mechanical contact between rail and wheels and in the power supply system (Luguang, 2002). Maglev can match gate-to-gate air travel times on routes under 1,000 km, as it can accelerate and decelerate at up to 1.5 m/s and reach 300 km/h in around 5 km (Holmer, 2003). Additionally, it can attain its maximum speed of 500 km/h in 23 km, at around 4 mins 16 seconds, as shown in Figure 2-22.

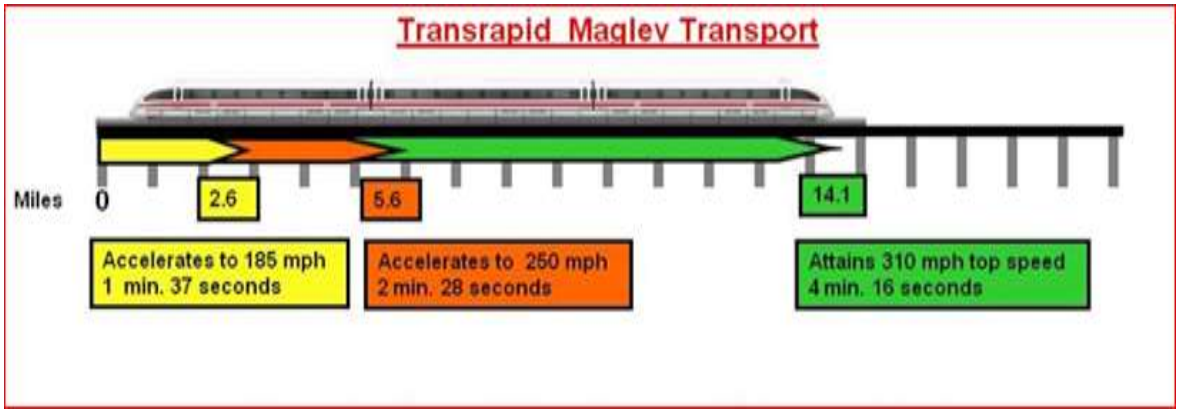


Figure 2-22: Maglev enables higher average speed. (Source: Holmer, 2011)

Maglev is less noisy than normal trains because there are no wheels rolling along the ground; the only major source of noise is from displaced air. Moreover, Maglev and its track require little maintenance, seen as the primary advantage, since the train never touches the track and so wear and tear on parts is minimal. In theory, this means that the trains and track need no maintenance at all and the cost of maintaining the rail is very low, since checks and frequent repairs are not required (Abeye *et al.*, 2012; Chopade and Sharma, 2013).

As Maglev trains float, while there is air resistance there is no friction. The trains are equipped with state-of-the-art safety systems to keep the operation under control, especially when cruising at high speeds, and these determine the technical feasibility of deploying Maglev (Sagar, 2016). For example, a Maglev can reach 300 km/h in only 5 km after a station, going uphill, and steep gradients are possible (Chopade and Sharma, 2013). Rain, ice and snow, just like natural hazards such as sandstorms, have little impact on Maglev systems because the trains do not depend on friction for movement; moreover, Maglev is suited to icy conditions because there are no overhead power lines that would be subject to freezing, as with conventional rail. Both the propulsion and guidance systems are located under the guideway to protect them from snow and rain. Due to the wind created by Maglev at high speed, snow tends not to accumulate on the guideway: even if it did, the train would run normally because it does not touch the rails (Luu and Nguyen, 2005). The principle of switching for a Maglev system is very simple, and there is no difficulty in changing to the other direction since there is a driving cab at each end of the train. The structure employs permanent magnets at a regular interval along a segment of track,

separated into two equal and diverging rails. The switch blades for Maglev are very long, at least the length of one carriage (Fiske *et al*., 2010).

Maglev trains are energy efficient and experience no rolling resistance, leaving only electromagnetic drag and air resistance; thanks to the levitation and the absence of physical contact between the vehicle and track, they do not waste energy in overcoming friction (Seminarsonly, 2009; Wilson, 2015). Maglev transport can use renewable sources of energy such as wind and solar power. It can carry enormous loads of people at lower cost than our current rail, car, bus and air travel. Moreover, as Maglev train and track operating costs are much lower and there is less wear and tear associated with the moving parts of a conventional train, there are long-term operational advantages (Chadha *et al.*, 2009). As there is no contact between the guideway and train, the lifespan of Maglev parts is much longer, so it is again cheaper in terms of repair and maintenance costs (Wilson, 2015).

As a result, the developers of Maglev claim that their system can reach higher speeds with lower energy consumption, attract more passengers, involve lower life-cycle costs and produce less vibration and noise than other transport modes, including HSR (Vuchic and Casello, 2002). In addition, the vehicles are more in line with environmental issues and cause less disturbance to nature by causing less pollution, vibration and noise and consuming less energy. The Maglev guideway has lower dead loading and, thanks to the elevated guideways, potentially occupies less land (Yaghoubi, Barazi and Aoliaei, 2012).

On the other hand, there are several disadvantages to Maglev trains. First, the guide routes are more costly than conventional steel railways, as the guideways do not match existing lines and a new set of tracks has to be built from scratch (Mokhim, 2015a). Also, to produce the strong magnetic fields to lift the train vehicles over a guideway Maglev requires rare-earth elements such as yttrium, scandium and 15 lanthanides. These may be expensive (Boslaugh, 2020). Moreover, there is an incompatibility with existing infrastructure in that Maglev trains cannot do what HSR does by travelling fast on high-speed lines and then completing the journey on classic rail lines. For this reason, unless two very large destinations are being connected it is difficult to construct Maglev lines that are commercially feasible,

whereas HSR can serve nearby cities in addition to the two end destinations by running on normal tracks that branch off the HSR line (Mokhim, 2015a).

Another disadvantage of Maglev is the weight of the large electromagnets in many EDS and EMS designs. Moreover, from a technical perspective, it has enormous switching challenges to direct a vehicle perfectly from one track to another. There are unique issues such as advanced guideway switch management, high-speed forces and frost wedging of guideways (Thorstrand, 2020). The movement of large parts of the guideway is considered to be a part of the switching system challenges, as this is often far more technically advanced than in conventional rail systems (Kemp and Smith, 2007). To achieve the desired curvature on the Nagoya Linimo EMS and Shanghai Transrapid Maglev lines, the switches bend a portion of rail as long as 150 m, as shown in Figure 2-23.

Figure 2-23: Switching system on the Linimo line in Nagoya, Japan. (Source: Thorstrand, 2020)

A similar system is used by the Chuo Shinkansen, bending the entire U-shaped guideway (Thorstrand, 2020).

In terms of energy consumption, larger train cars are difficult to levitate, requiring more energy and making the system less efficient (Chopade and Sharma, 2013). Energy is required to operate the air conditioning, lighting and heating, as well as to levitate, accelerate and stabilize the movement of the train (Ilonidis, 2010).

In 2006, a Transrapid high-speed Maglev train that floats on powerful magnetic field crashed into a maintenance vehicle on an elevated test track in northwest Germany, killing 23 and injuring 10 others. The accident was caused not by a technical failure

of the Maglev train but by human error (Alfano, 2006). In terms of the guideways, even though over time the costs are less than rail, it is difficult to justify spending so much upfront (Wilson, 2015).

## 2.4 Development of Hyperloop Technology

### 2.4.1 Feasibility of Hyperloop

In 1909, rocket pioneer Robert H. Goddard proposed a transport concept involving high-speed passenger-carrying pods travelling in an evacuated tube, or vacuum. Later, the main idea behind the Maglev train was introduced by Bachelet. The Rand Corporation developed these ideas in 1972 into its Very High-Speed Transport System (Opgenoord and Caplan, 2017). Next, in a White Paper, the Hyperloop transport concept was developed as an alternative to the California High-Speed Rail (CAHSR) project. It proposed to combine the benefits of lower overall costs and shorter travel times with superior performance (Chin et al., 2015).

The design for the Hyperloop uses a combination of magnetic acceleration and low air pressure that will transfer passengers from the Los Angeles region to San Francisco, as shown in Figure 2-24, following the Interstate 5 corridor, in about 30 mins (Nalam, Medepalli and Motukuri, 2018).

Figure 2-24: Artist's impression of Hyperloop from Los Angeles to San Francisco. (Source: Davies, 2015)

In terms of ground transportation systems, Hyperloop represents a vision of travelling faster than an aeroplane at a fraction of the cost, becoming the next achievement in transport (Heath, 2018). Many companies are currently involved in

its development, which could see passengers travelling in capsules floating in low-pressure tubes (Ranger, 2018). The Hyperloop champion, Elon Musk, founded his own tunnelling business, the Boring Company, on the basis of a tube running through a tunnel; another option is for the tube to run above ground. The Boring Company has conditional approval from Maryland's Department of Transportation in the United States to begin construction of a Hyperloop tunnel from Washington to Baltimore, and there is a similar plan for a tunnel beneath Culver City, California (Heath, 2018).

The main concept of Hyperloop is to enclose a passenger pod in a partial vacuum in a tube, suspending it on an air bearing. This is different from existing HSR as it eliminates the rails, similar to other vacuum-tube systems such as VacTrain (Chin *et al.,* 2015). The aim of Hyperloop is to improve current systems, including rail, air, water and road transport, and to travel at a top speed of 1,200 km/h and an average speed of 600 to 966 km/h yet to be as accessible and convenient as a train (Musk, 2013).

Decker *et al.* (2017) explain the concept of the Hyperloop as a cheaper, faster alternative to conventional rail, cars and aeroplanes, which are either expensive or slow, or both. In 2012, the first public mention of the Hyperloop concept was of a reduced-pressure tube on a pressurized base, driven by LIMs and air compressors on an air bearing (Nalam, Medepalli and Motukuri, 2018). It involves capsules travelling through a tube on a cushion of air, featuring aerodynamic lift and pressurized air. The capsules (pods) are accelerated by a magnetic linear accelerator attached to the tube at various stations, with rotors in every capsule. Passengers can enter or exit at stations located at branches along the tube's length or at either end (Musk, 2013).

### 2.4.2 Main components of Hyperloop system

Hyperloop is based on Maglev principles, consisting of a capsule in a tube for high-speed travel. The three main components are the propulsion, levitation and structure, as shown in Figure 2-25.

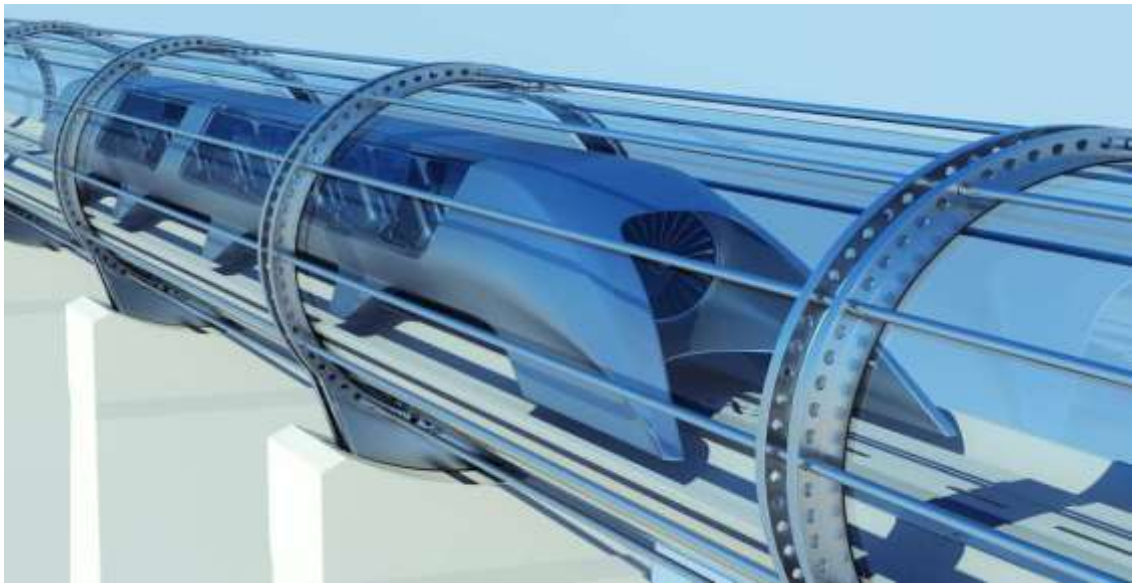

Figure 2-25: Hyperloop transport technology. (Source: Looveren, 2017)

#### 2.4.2.1 Propulsion system

The propulsion is provided by a LIM that benefits from carrying a rotor to make it efficient and for braking at the other end of the tube, to recover a large amount of the energy (MIT Hyperloop Team, 2017). The system is not particularly costly, and building the tube on pillars above the ground has the triple benefit of saving money, protecting it from earthquakes, snow and rainfall, and allowing solar panels to be placed on top. In this case, the energy from the solar panels more than meets the operational requirements of the Hyperloop and can be stored in battery packs overnight and in rainy or cloudy conditions (Kale *et al.*, 2019).

The Hyperloop capsule has a compressor mounted at the front to redirect all the air to behind the capsule. It is usually to be propelled by two electromagnetic motors (Nalam, Medepalli and Motukuri, 2018). Hyperloop uses a LIM to accelerate and decelerate the capsule, with several important benefits over a permanent magnet motor: lower material costs; a lighter, smaller capsule; and stabilizing the lateral forces exerted by the stator on the rotor to 13 N/m, as shown in Figure 2-26 (Musk, 2013). The stator is to be placed along the length of the tube to accelerate the capsule, while the rotor is located on the capsule to transfer the momentum through the linear accelerators, with a gap between them of 20 mm on either side. The stator is to be mounted at the bottom of the tube over the entire 4 km, as it takes between 300 and 760 m to accelerate and decelerate and is around 0.5 m wide, 0.1 m tall and 800 kg in weight (Awasthi, 2016). The tube is to incorporate the stator, which

powers the vehicle, while the rotor is placed on the vehicle to achieve both its power requirements and weight savings (Pandey and Pallissery, 2017).

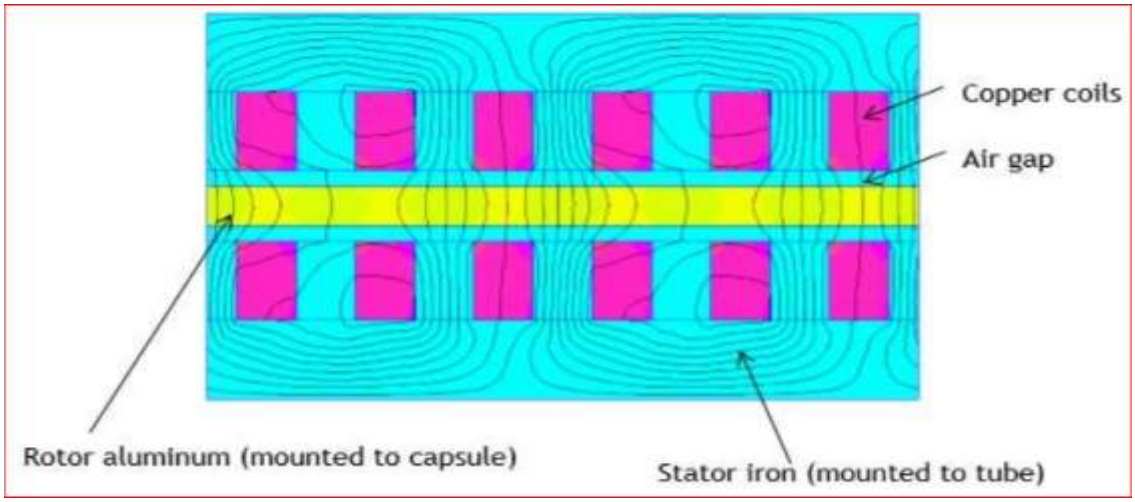


Figure 2-26: Hyperloop propulsion system. (Source: Mathur, 2017)

The rotor of the LIM in the capsule contains an aluminium blade in a skin of 0.01 m to decrease weight and cost; this is to be 15 m long, 0.5 m tall and 0.00055 m thick (Awasthi, 2016). An external LIM is to be used to propel the capsule to near sound velocity and plays an important role in producing motion in a straight line rather than rotationally (Kale *et al.*, 2019). The propulsion system includes a compressor to be located at the front of the capsule, as a LIM is used to accelerate and decelerate the capsule (Jithendra, 2015).

#### 2.4.2.2 Levitation system

The Hyperloop levitation system is designed to reduce friction during high-speed travel and to use a passive Maglev system to suspend the capsule above the track, which requires zero power input for levitation to occur at a given speed (Decker *et al.*, 2017). The braking system uses an EDS Maglev system to slow the capsule down at upwards of 2.4 G and an emergency braking system has been designed. The EDS was chosen for its substantial gap height, scalable with increasing the length over distance (L/D) with speed and compatible with the track (MIT Hyperloop Team, 2017). The capsule can be levitated using a high-pressure air cushion, while there is an axial-flow air compressor at its nose to decrease aerodynamic drag. The air compressor is at the bottom of the capsule, with nozzles for levitation (Hodaib and Fattah, 2016). The Hyperloop capsule uses an innovative magnetic system for

its levitation, consisting of both permanent magnets and electromagnets to generate controlled lift that helps pod levitation, as in Figure 2-27 (ESTECO Academy, 2018).

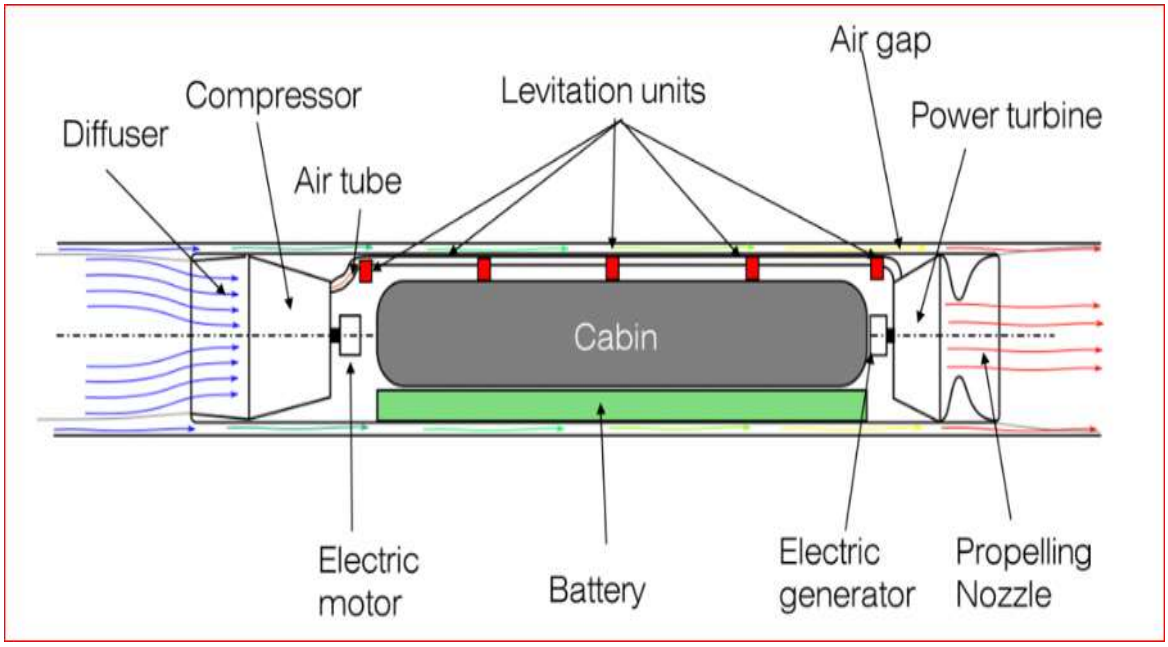


Figure 2-27: Hyperloop levitation system. (Source: ESTECO Academy, 2018)

At the bottom of the capsule, an aluminium (passive) track and permanent magnets are placed in a Halbach array,[3] as the motion of permanent magnets induces a magnetic field when the capsule moves forward. These magnets levitate the capsule and create eddies, which can be minimized by silicon steel lamination (Jithendra, 2015). Passive magnets are strategically placed on top of the capsule to allow individual fine control of the magnets' attraction and repulsion (Nalam, Medepalli and Motukuri, 2018).

### 2.4.3 Main parts of Hyperloop

Hyperloop consists of a low-pressure tube and capsules that can be transported at either low or high speed during a journey. The compressor fan shown on the front

[3] Halbach arrays are sets of magnets to generate the lift and thrust for the pods.

of the capsule in Figure 2-28 is designed to avoid the effect of the Kantrowitz limit,[4] sucking the air from the front of the tube and exhaling it to air bearings, making it possible to transfer huge volumes of air away from the nose (Jain, 2016; Pandey and Pallissery, 2017). The Kantrowitz limit can be avoided by increasing the ratio between cross-sectional areas of both capsule and tube and allowing more air to pass around the capsule at a lower velocity (Opgenoord and Caplan, 2017).

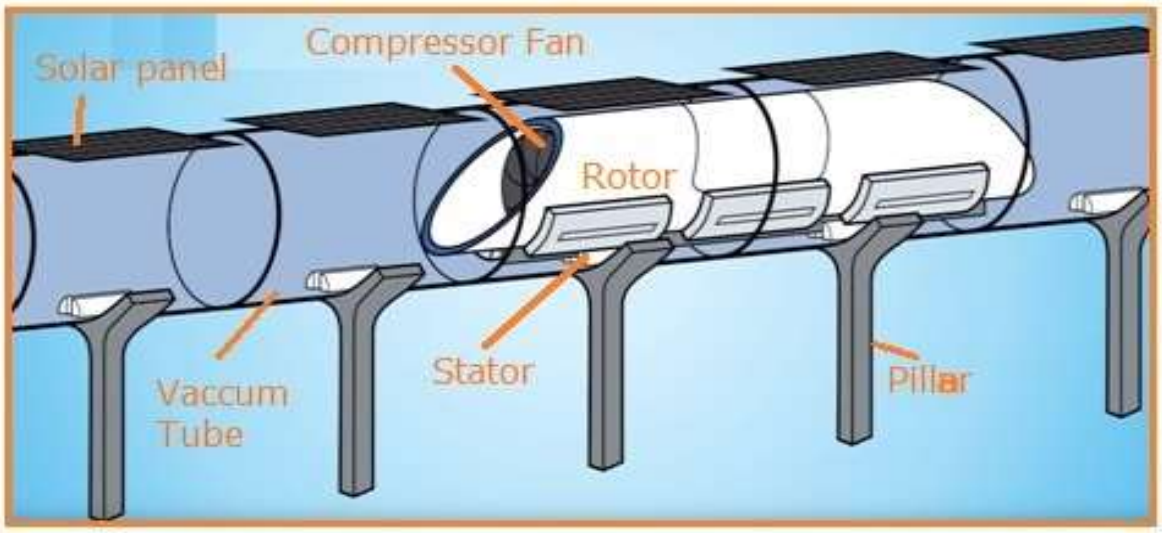


Figure 2-28: Main parts of Hyperloop system. (Source: RF Wireless World, 2015)

The compressor is powered by an 865 kW on-board electric motor, of an estimated mass of 275 kg, to include power electronics (Mathur, 2017). The air bearing is another part of the Hyperloop system to provide suspension to the capsule and make travel smoother (Pandey and Pallissery, 2017).

#### 2.4.3.1 Capsule

The capsule is designed to transport passengers at a very high speed. It has six permanent magnets embedded in its bottom to interact with the levitation solenoids. In addition, there are two permanent magnets on each side of the capsule to interact

[4] The Kantrowitz limit is a fundamental concept arising in the Hyperloop when air is forced through the space between the capsule and the inner wall of the tube.

with the propulsion solenoids (Abdelrahman, Sayeed and Youssef, 2018). Passengers are to travel in pressurized capsules, floating on a frictionless magnetic cushion, which are powered by a LIM, embedded rechargeable batteries and electromagnetic propulsion. Each passenger capsule is planned to have a total gross weight of 15,000 kg and a length of 30 m to carry an average of 28 to 40 passengers (Janić, 2018). The maximum width and height are 1.35 m and 1.10 m, (Musk, 2013), so the required aerodynamic power is to be around 285 kW at a speed of 1,120 km/h with a drag force of 910 N (Janić, 2018). For capsule safety, the HTT has developed a skin material called Vibranium, eight times stronger than aluminium and 20 times stronger than steel alternatives for integrity and stability at a wide range of temperatures. It can transmit critical information more instantly and wirelessly. Moreover, it is much lighter than steel and aluminium, helping to reduce the energy required to propel the capsule (Hawkins, 2016).

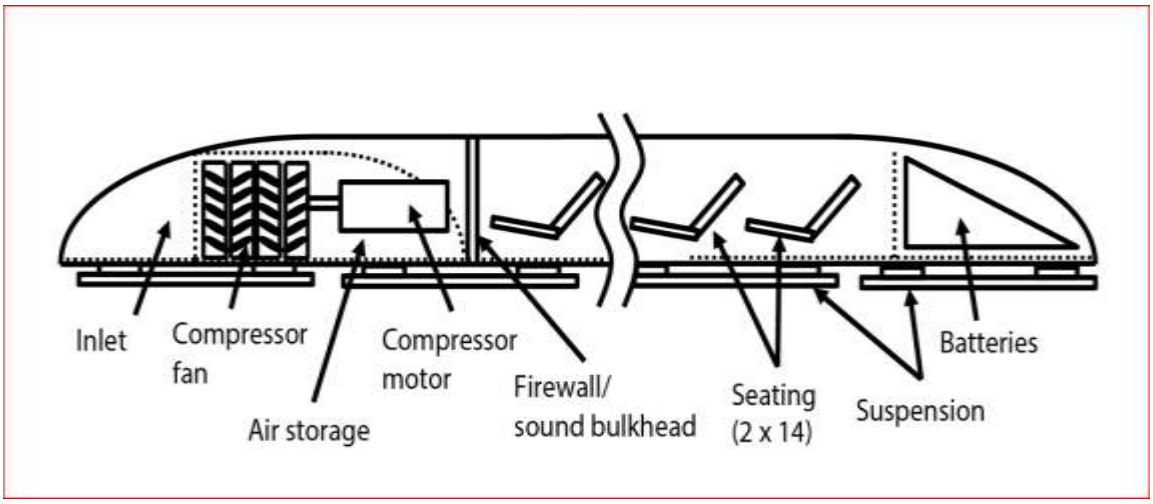


Figure 2-29: Hyperloop passenger capsule. (Source: Anthony, 2013)

The capsules are operated by a supporting thrust air bearing, using aerodynamic lift and a compressed air reservoir (Chopade, 2017b). The overall interior weight is estimated at 2,500 kg, including the restraint system, seats, interior and door panels, luggage sections and entertainment displays, as in Figure 2-29. The on-board compressor is an important feature that allows the capsule to traverse the narrow tube smoothly without checking the flow between it and the tube walls. This is to be powered by a 325 kW on-board electric motor with an estimated mass of 169 kg, and 1,500 kg of batteries will provide 45 mins of on-board compressor power. These are charged at stations and changed at each stop (Musk, 2013).

#### 2.4.3.2 Tube

The Hyperloop tube is of steel or a material made from a mixture of fibre and glass that has a little elasticity, specifically sized for optimal airflow around the capsule to improve the performance and energy consumption at the anticipated speeds (Musk, 2013; Nalam, Medepalli and Motukuri, 2018). It can be built above ground on pillars or underground to eliminate the dangers of grade crossing (Jain, 2016). Earthquake risk can be dramatically mitigated by building the Hyperloop system on multiple pillars and may obviate the need for expansion joints. The geometry of the Hyperloop tube is dependent on the capsule size, with an inner diameter of 2.23 m and a cross-sectional area of 3.91 $m^2$. Figure 2-30 shows how the closed-loop tubes are welded side by side to allow capsules to travel in either direction on elevated pillars placed every 30 m for support and covered in solar panels to provide the energy required by the system (Musk, 2013; Kumar and Khan, 2017).

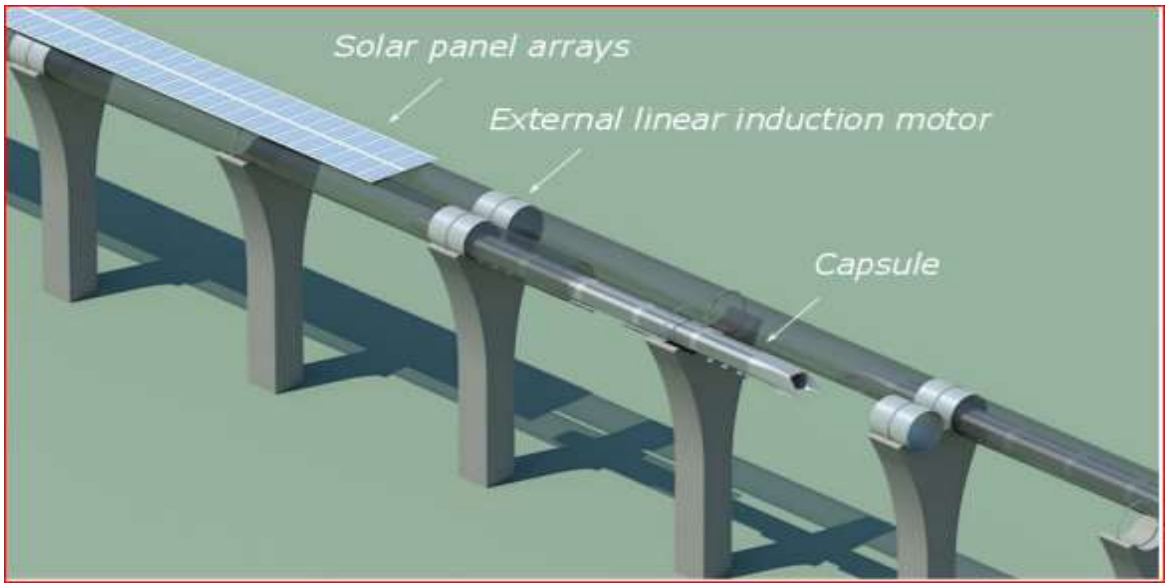


Figure 2-30: Hyperloop passenger tube. (Source: Coelho, 2016)

The thickness of the Hyperloop tube's wall is between 0.02 and 0.023 m to give it sufficient strength, bearing in mind the pressure differential, the loading of capsule weight and the bending and buckling between pillars (Musk, 2013). Vacuum pumps are installed to evacuate and maintain the required level of vacuum inside the tube and in the stations' chambers, and LIMs are located along the tube to accelerate and decelerate the capsule to the speed appropriate to each section of the route (Van Goeverden *et al.*, 2018).

#### 2.4.3.3 Pillars

In Hyperloop, the tube is to be elevated on pillars oriented vertically, as shown in Figure 2-31, to keep it constrained, and the spacing is crucial to retain the tube to meet its structure's design objective. The average spacing between pillars is 30.5 m and they are to be 6.1 m tall, and perhaps higher in hilly areas to avoid obstacles. Reducing this spacing may increase resistance related to seismic load and the capsule's lateral acceleration, as well as limiting the deflection of the tube that keeps the capsule steady and makes the journey more enjoyable (Musk, 2013).

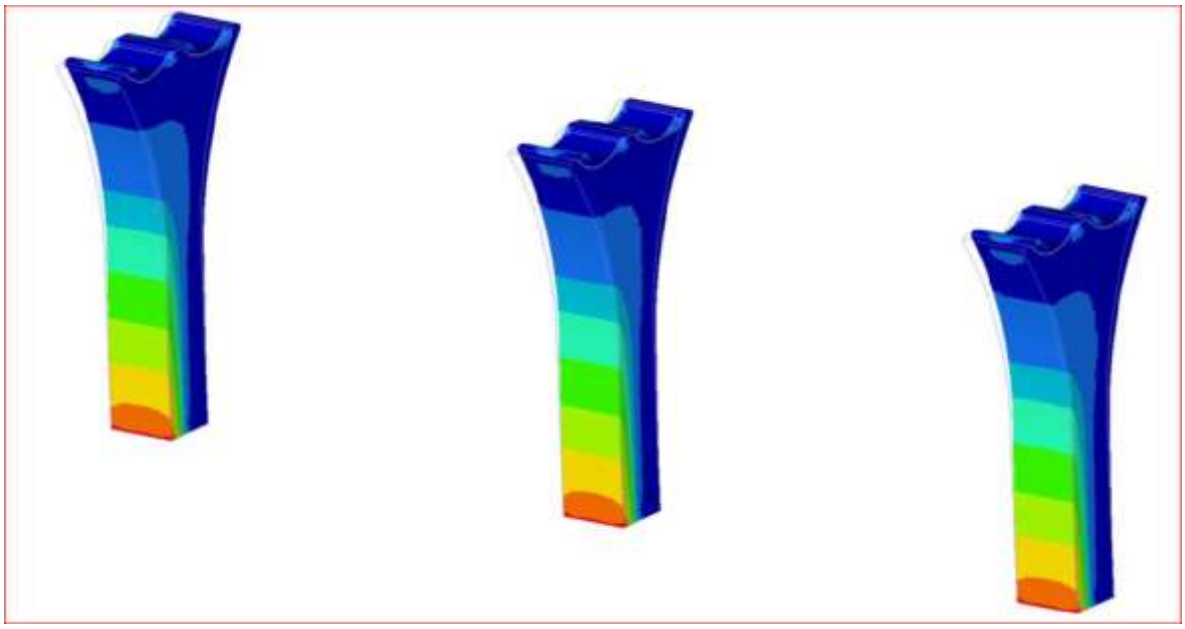

Figure 2-31: Hyperloop pillars. (Source: Musk, 2013)

#### 2.4.3.4 Station

The Hyperloop station is commonly integrated into the tube, and it is to consist of three modules. First is the vacuum tube's arrival chamber. This accepts the arriving Hyperloop capsule and sends it onto the second module at normal atmospheric pressure, where passengers disembark and embark. Next, the capsule proceeds to the departure chamber, again at normal atmospheric pressure initially. The capsule remains here until the air is evacuated from the chamber, then it proceeds along the tube. The three chambers are separated by closed doors to enable the required air pressure to be established and maintained appropriately (Van Goeverden *et al.*, 2018).

The design of the Hyperloop station is based on a looped track, using turntables and parallel platforms to enable an efficient flow of capsules from which passengers can disembark and embark (Sergeroux, 2016). Hyperloop stations contain a two storey-sufficient building, as all facilities are concentrated inside a single-looped elevated track that encircles the outer wall. Thus, each station can allow access to three capsules to match the requirement for 840 passengers per hour in peak hours, assuming that a capsule with 28 people departs every 2 mins (Sergeroux, 2016).

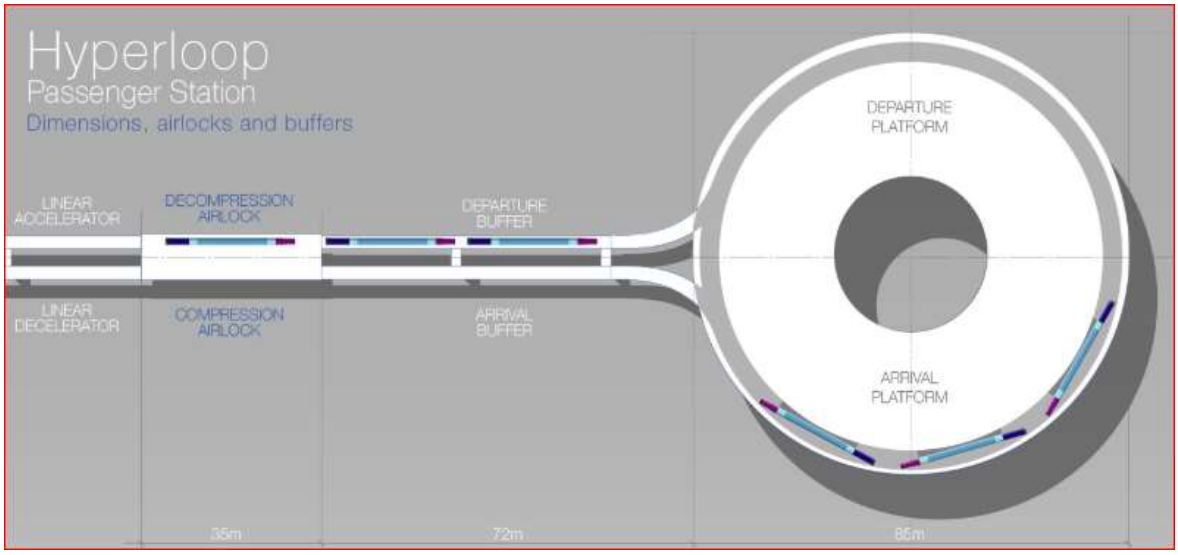


Figure 2-32: Hyperloop passenger station. (Source: Sergeroux, 2016)

Six steps are presented in Figure 2-32, from linear deceleration to linear acceleration. First, the capsule enters the compression airlock, where the pressure in the tube is equalized to atmospheric pressure. This step takes less than a minute. Second, the capsule parks in the arrival buffer space and remains for a maximum of 5 mins until all three capsules have entered the buffer. Third, all three capsules arrive at the arrival terminal; passengers have just 3 mins to disembark. Fourth, the three capsules prepare to depart; again, passengers have just 3 mins to embark. Fifth, the departing capsules taxi from the buffer, as each needs to wait its turn to enter the decompression airlock. Finally, the capsules enter the decompression airlock, where the pressure is equalized to the track's low pressure. This takes one minute (Sergeroux, 2016).

### 2.4.4 Proposed Hyperloop routes worldwide

Since the Hyperloop concept was first introduced to the world, three main companies have been working on its design: Virgin Hyperloop One; Hyperloop Transportation Technologies (HTT); and TransPod (Nalam, Medepalli and Motukuri, 2018). In 2016, the American transportation technology company, Hyperloop One, started comprehensive proposals to build Hyperloop networks, connecting countries and cities worldwide. It announced the 10 winning routes to connect about 53 urban centres for a total population of 150 million people in five countries, as in Table 2-10, with a total distance of 6,628 km (Simon and Choi, 2017).

| Country | Route | Team | Length (km) | Urban centres | Population |
|---|---|---|---|---|---|
| United Kingdom | Edinburgh–London | HypED | 666 | 4 | 19,151,514 |
| | Liverpool–Glasgow | Northern Arc | 545 | 6 | 9,715,488 |
| United States | Chicago–Columbus–Pittsburgh | Midwest Connect | 785 | 3 | 13,800,000 |
| | Cheyenne-Denver-Pueblo | Rocky Mountain Hyperloop | 580 | 10 | 4,831,000 |
| | Dallas–Laredo–Houston | Texas Triangle | 1030 | 5 | 18,771,000 |
| | Miami–Orlando | Miami/Orlando Hyperloop | 414 | 2 | 8,500,000 |
| India | Bengaluru–Chennai | AECOM India | 334 | 6 | 17,710,000 |
| | Mumbai–Chennai | Hyperloop India | 1102 | 10 | 43,190,000 |
| Mexico | Mexico City–Guadalajara | Mexloop | 532 | 4 | 33,530,000 |
| Canada | Toronto–Ottawa–Montreal | HyperCan | 640 | 3 | 13,326,000 |

Table 2-10: 10 Winners of Hyperloop One Global Challenge. (Source: Simon and Choi, 2017)

In 2019, Virgin Hyperloop One announced a study to build the world's longest Hyperloop test site, 35 km long, in KAEC in KSA, as shown in Figure 2-33. This proposed line is not included in Table 2-10 as it was announced only in 2019. Its main idea is to reduce travel time not only across the KSA but throughout the Gulf Corporation Council, which includes Kuwait, the United Arab Emirates (UAE), Qatar, Bahrain and Oman. For example, travel time would be reduced from 8.5 hours to 48 mins between Riyadh and Abu Dhabi, and from 10 hours to 76 mins between Riyadh and Jeddah (Hart, 2019).


Figure 2-33: Saudi-Virgin Hyperloop One's Vision 2030 passenger pod. (Source: Lavars, 2018)

Next, in 2013, HTT was founded by JumpStarter Inc. to design, manufacture and build the fastest, safest, most environmentally friendly and highly profitable passenger transport system (Cooke, 2016). HTT signed agreements in the United States, India, France, UAE, Brazil, the Czech Republic, Korea, Slovakia, Ukraine, Indonesia and China (Businesswire, 2020). For example, an agreement was signed in 2016 with the government of Slovakia to explore building a local Hyperloop system with a vision of creating international routes to connect Bratislava with Budapest in Hungary and Vienna in Austria. This agreement will boost collaboration and innovation between Slovakia and all European countries, and will lead to increased demand for Hyperloop worldwide (PRNewswire, 2016).

In the UAE, the only modes of transport currently connecting the two largest cities of Abu Dhabi and Dubai are car, taxi and bus. This lack of competition makes the country an attractive market for the Hyperloop system (Taylor, Hyde and Barr, 2016). HTT will start constructing the world’s first commercial Hyperloop over a distance of 10 km, and the first phase is expected to be completed in time for World Expo 2020 in the UAE (Walsh, 2018). As Hyperloop technology is expanding worldwide, China, which leads the world in terms of HSR lines, is looking to Hyperloop for a more efficient high-speed solution to connect the cities of Tongren and Guiyang over a length of 400 km (Wong, 2018) (Figure 2-34).

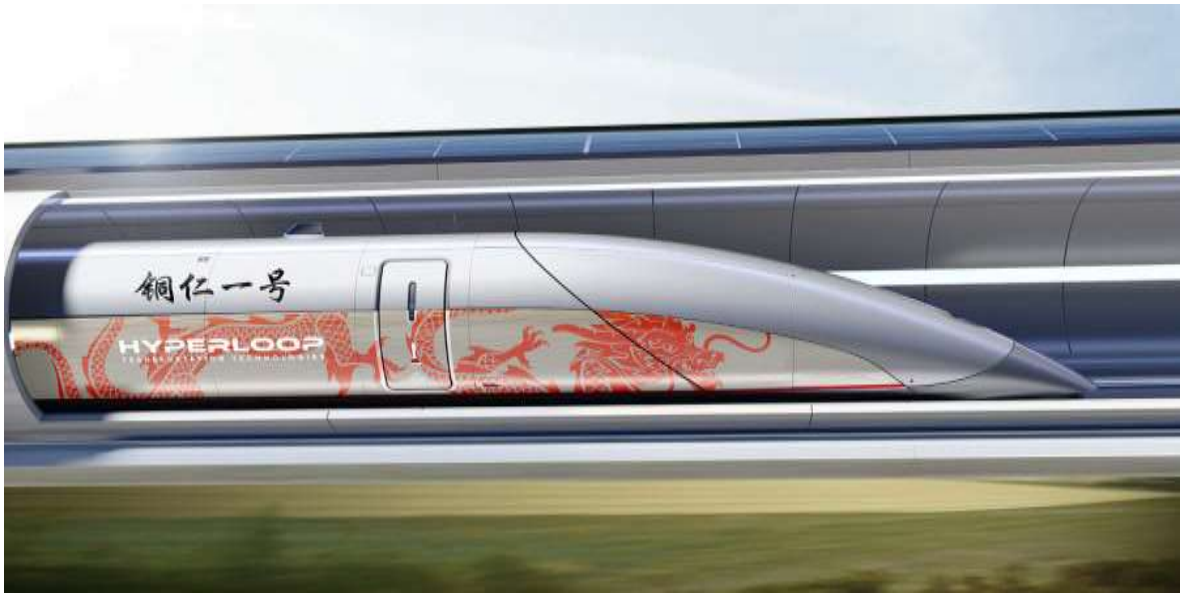


Figure 2-34: First Hyperloop planned for China. (Source: Wong, 2018)

Third, TransPod is a Canadian company that has a vision to connect people, cities and business by sustainable high-speed transport. In its Hyperloop system, TransPod capsules are driven by LIM and air compressors. They are designed to travel at a maximum speed of 1,200 km/h and for the system to be compatible with renewable energies, including solar generation, to minimize carbon emissions. It will help to enhance reliability, allowing a stronger business case for the Hyperloop system and improving its operational performance. TransPod is exploring several routes worldwide, focusing on countries with strong demand for new transport systems and a high-density population (Brown, 2017).


Figure 2-35: Canadian corridor between Toronto and Montreal. (Source: Janzen, 2016)

Most of the routes proposed by TransPod system are in Canada, including the Toronto–Montreal corridor via the cities of Kingston and Ottawa, and Toronto–Windsor and Calgary–Edmonton, as shown in Figure 2-35 (Brown, 2017; Nalam, Medepalli and Motukuri, 2018).

### 2.4.5 Advantages and disadvantages of Hyperloop

Nalam, Medepalli and Motukuri (2018) identify some advantages of Hyperloop technology, such as speed, efficiency, cost, safety, low power consumption, convenience and immunity to weather and earthquakes. First, it is far faster than existing modes of transport such as conventional rail, HSR, Maglev, air and car travel. The proposed maximum speed of Hyperloop is 1,159 to 1,223 km/h, with an average of 966 km/h, which could result in a 45-min saving on trips longer than 645 km. For example, a Hyperloop capsule could make the trip from San Francisco to Los Angeles in roughly 43 mins, as in Table 2-11, with no intermediate stops. This is a distance of about 640 km at an average speed of 1,080 km/h. This compares to 1 hour 30 mins (air); 6 hours 40 mins (car); 3 hours 50 mins (rail); and 2 hours 58 mins (HSR) (Virgin Hyperloop One, 2018). As a result, introducing Hyperloop transport technology removes the obstacles of distance and time, making it possible for people to live in a completely different city or part of the country from where they work ( B1M Limited, 2018).

| Transport mode | Travel speed (km/h) | Travel time |
|---|---|---|
| Virgin Hyperloop One | 1,080 | 43 mins |
| HSR | 300 | 2 hr 58 mins |
| Air | 841 | 1 hr 30 mins |
| Classic train | 220 | 3 hr 50 mins |
| Car | 112 | 6 hr 40 mins |

Table 2-11: Travel time of transport modes, including Hyperloop, San Francisco to Los Angeles. (Source: Virgin Hyperloop One, 2018)

Second, the Hyperloop is a safe transport technology, since it is not built at grade and can be operated only on pillars or underground, reducing the risk of collisions with other modes of transport (Upbin, 2016). Third, the low-pressure environment minimizes energy consumption, even at high speeds, and a high percentage of Hyperloop's overall energy consumption goes towards overcoming drag. The

energy cost of the system is less than any other current mode of transport; the fully electric Tesla Model S is the only one to come close in terms, as shown in Figure 2-36 (Musk, 2013).

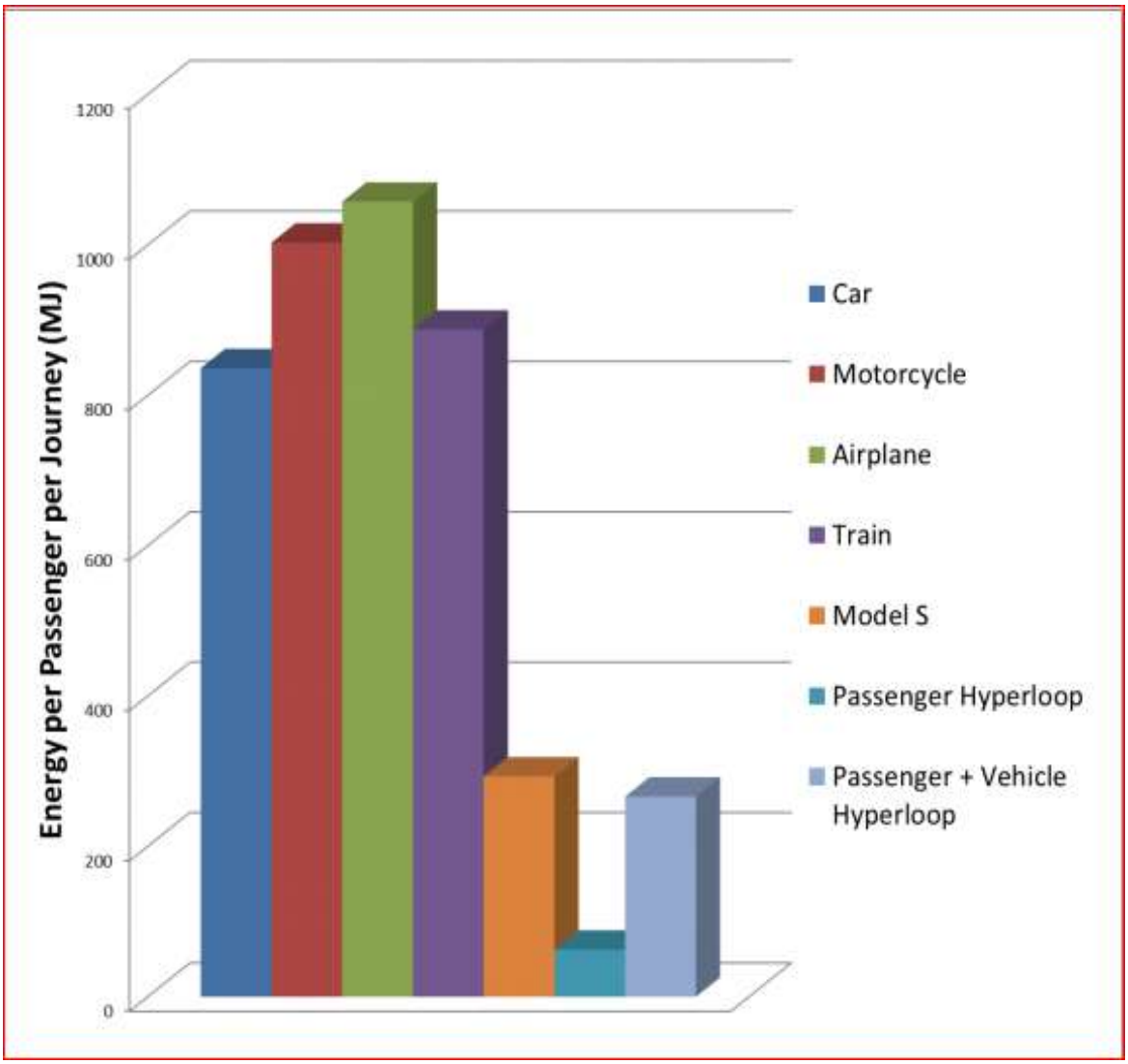


Figure 2-36: Energy cost per passenger for modes of transport, San Francisco to Los Angeles. (Source: Musk, 2013)

Fourth, the internal Hyperloop's capsule would be immune to adverse weather conditions such as fog and snow, and would also be earthquake resistant. The pillars used to raise the tube above the ground have a small footprint that limits any damage in the event of an earthquake (Kale *et al.*, 2019).

On the other hand, there are disadvantages to the Hyperloop system, including optimal land usage, limited capsule space, excess heat on Hyperloop's tracks, and the risk that low pressure and high speeds may cause passenger discomfort.

First, if it is to operate at maximum efficiency Hyperloop can travel only in straight lines, so it needs to cross both public and private land. Second, passengers will not be able to move freely during their journey but must lie down for at least 30 mins, depending on the route length, with restricted legroom (see Figure 2-37). Moreover, a crack in the Hyperloop capsule for any reason would lead to them being exposed to a vacuum, causing them to die (Follett, 2016).

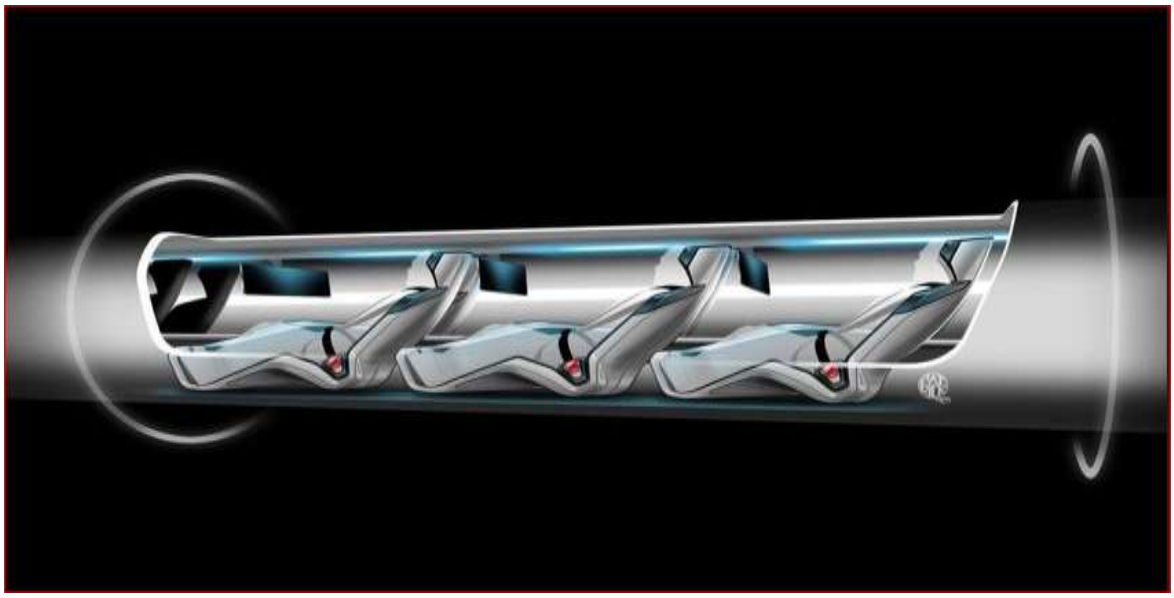

Figure 2-37: Cutaway of the passenger capsule. (Source: Ramachandran, 2013)

Third, investment in the Hyperloop transport system needs to be high, as the entire infrastructure is yet to be constructed (Markvica *et al.*, 2018). Fourth, passengers may experience dizziness due to the high speeds of 1,200 km/h, vibration and crowding. Finally, the Hyperloop's tube is to be built from steel, and its shape may change and due to high temperatures, especially along routes passing through deserts (Follett, 2016).

## 2.5 Summary

Based on the literature, the service characteristics of the HSGT technologies in this study are considered as inputs of the TSCM to be developed and to give an overall perspective of capacities, speeds, length of vehicles, and so on. As there are several HSR and Maglev lines in operation worldwide, it is helpful and informative to look at different countries' schemes and manufacturers to become familiar with the range of HSGT technologies.

As well as an overview of the total construction costs of various lines worldwide, HHSR in Saudi Arabia was studied in depth and useful data were obtained, such as the average speed of 300 km/h, capacity of 417 seats and fare structure.

In the following chapter, several total social cost models for case studies worldwide will be reviewed, with a focus on the three HSGT systems and their main service characteristics.

## 2.6 Rail and Equity

Spatial equity is a measure of the ease with which someone can travel from their origin to their destination via a given mode of transport. It refers to the geographical location of an individual, group or region affected by a transport infrastructure project. The implications of spatial equity derive from alterations to distribution of access for urban groups (Pagliara *et al.*, 2016). Equity effects began to be considered as a part of transport infrastructure development because equity issues were identified in the main access benefits, concentrated on urban areas with an HSR system. For locations that either have or do not have an HSR service along a given line, there are significant negative impacts on spatial equity arising from the increase in speed from 220 km/h to 300 km/h (Pagliara *et al.*, 2016).

In the transport decision-making process, public engagement can be defined as the process of involving, identifying and incorporating stakeholders' needs, values and concerns, whilst the engagement tools are designed to achieve an accepted solution from engaging stakeholders to a transport problem. Greater input from stakeholders, as well as their support for decisions, must be taken into account as they become engaged at the early stages of the transportation planning process (Pagliara, Hayashi and Ram, 2018).

As equity is considered an essential in sustainable development, HSR's introduction and expansion have raised concerns that also apply to Maglev and Hyperloop. For example, the fares of these modes are generally much higher than those on classic rail services. In China there has been debate on whether HSR services potentially cause social exclusion, mainly among social groups that put a lower value on time or have a low income. Many issues present an increasing challenge to socially

intermediate cities or vulnerable groups. These include population growth, urbanization and a lack of coordination between the various types of transportation infrastructure (Ren *et al.*, 2020).

## 2.7 Conclusion

This chapter has reviewed the development of three HSGTs in terms of existing and proposed lines worldwide. HSR's total network is 62,779 km across more than 21 countries, with 51,581 km in operation and 11,198 km under construction, while Maglev has a total network length of 359 km, with 73.4 km in operation and 285.6 km under construction. Hyperloop has a more than 6,628 km lines proposed, worldwide.

There are four acknowledged exploitation models for HSR systems: exclusive; mixed high-speed; mixed conventional; and fully mixed, as adopted in Japan, France, Spain and Germany, respectively.

In terms of the benefits of the HSGT technologies, HSR involves saving time, an increase in comfort and a reduction in accidents, avoidance of congestion at airports and a reduction in environmental impact. Maglev has the advantages of speed, less noise, energy efficiency and low maintenance costs thanks to parts' longer lifespan due to no contact between the train and guideway. Hyperloop technology is considered to be a fast transport mode that can be cheap, efficient and convenient, has low power consumption and is immune to earthquakes.

On the other hand, there are disadvantages to HSR, such as taking up land and causing damage to the environment due to the need to avoid curving tracks, and to avoid charging high fares that might restrict demand. The disadvantages of Maglev are closely related to its infrastructure, including the difficulties of switching from one track to another, and the requirement for more energy to levitate larger Maglev trains. Hyperloop has some disadvantages compared to HSR and Maglev, and they relate to technical issues such as the tight space in capsules, maintaining low pressure in the tube and travel sickness due to the extremely high speeds.

# Chapter 3. Methodological Review

## 3.1 Introduction

This chapter starts by reviewing the methodology of total social cost models in section 3.2 and presenting the results of various case studies. It includes models for both urban and inter-urban transport systems to determine only operator cost or, in some cases, both operator and user costs.

The chapter also reviews previous models designed to forecast demand for new transport systems in studies from countries such as Italy and Vietnam. These models are reviewed in section 3.3 and are based on projections of future population. An explanation of exogenous and endogenous demand is given, and evidence is presented for HSR demand worldwide. Section 3.4 reviews elasticity of demand models, which usually relate demand to GDP, fares, generalized journey time, level of service, and so on. In section 3.5, SP methods are reviewed, including definitions, the types of surveys and their application to transport mode choice in order to determine their utility and probability functions. Section 3.6 identifies that there is a gap in knowledge with respect to the total social cost on inter-city ground transport and proposes a methodology to fill this gap. This involves an integrated modelling framework that brings together the methods reviewed in the chapter in order to deal with issues such as the endogeneity of demand and the need to identify induced demand. Section 3.7 concludes the chapter with a summary of the key findings.

## 3.2 Review of Total Social Cost Models

Meyer, Kain and Wohl (1965) developed a cost function for the operation of an urban transport system, taking an engineering approach. The function determines the cost of a specific urban mode of public transport on the basis of total travel distance, the number of vehicles and the infrastructure construction and maintenance costs, as follows:

$$TC = \alpha nU + \beta M + \gamma L + S \qquad \text{Equation 3-1}$$

where TC represents the total cost of operating a public transport service, $\alpha$, $\beta$ and $\gamma$ represent the cost per vehicle unit employed, direct cost on the basis of miles of

travel performed and the cost on the basis of miles of roadway required, respectively. U, M, L and S denote the size of the vehicle fleet required, the number of vehicle miles travelled in this period, the lane-miles of roadway needed and the costs of structure, road, right-of-way, roadbed, and so on, respectively, while n represents the number of vehicular units operating as a train or coordinated group (Meyer, Kain and Wohl, 1965).

Another cost function for public transport technologies was developed by Brand and Preston (2003) to calculate the operator costs of public transport systems without a network on a stand-alone corridor in the TEST (Tool for Evaluating Strategically Integrated Public Transport) project. In this case, the total annual operator cost (TOC) is determined as follows:

$$TOC = OC^T + OC^D + OC^V + OC^R + CC^{ann} \qquad \text{Equation 3-2}$$

where $OC^T$, $OC^D$, $OC^V$, $OC^R$ represent the time, distance, vehicle and route-maintenance related to costs arising in operation, while $CC^{ann}$ denotes the annual capital investment costs of the infrastructure and vehicles that are needed. Using this model, the total operator costs can be calculated for annual levels of passenger demand (Brand and Preston, 2003).

An alternative cost model was developed by Campos, de Rus and Barron (2007a) to estimate only the operator costs of an HSR line that are associated with the infrastructure and rolling stock, as follows:

$$TC = \sum_{t=1}^{T} \frac{IC_t^C + IC_t^M + RSC_t^A}{(1+i)^t} + \frac{RSC_t^O + RSC_t^M}{(1+i)^t} \qquad \text{Equation 3-3}$$

where T represents the total duration of the project, and $IC^C$ and $IC^M$ the infrastructure construction and maintenance costs, respectively. $RSC^A$, $RSC^O$ and $RSC^M$ represent the rolling stock's acquisition, operation and maintenance costs.

For the infrastructure costs, all components related to the investment of HSR project are included, such as construction and maintenance of the tracks, the stations and terminals along and at the end of the line, the sidings, signalling systems and power supply. For the infrastructure maintenance costs, materials, spare parts, materials,

and so on, are included. The rolling stock costs of the trains serving the line are split into three categories: acquisition; operation; and maintenance (Campos, de Rus and Barron, 2007a).

Tang, Boyles and Jiang (2015) developed a total costs model for HSR that includes only the operator cost in order to mitigate increases in petrol prices, as follows:

$$TC(t) = C_c + C_{OMi} + (C_{OMa} * t) + (C_V * t) \quad \text{Equation 3-4}$$

The model has four parts: construction cost ($C_c$); initial operation and maintenance costs ($C_{OMi}$); annual operation and maintenance costs ($C_{OMa} * t$); and annual vehicle purchase cost ($C_V * t$) (Tang, Boyles and Jiang, 2015).

Li and Preston (2015) constructed a cost model to analyse the total social cost (TSC) of various public urban transport modes on the basis of their characteristics and daily level of passenger demand, as follows:

$$TSC = TOC + TUC + TEC \quad \text{Equation 3-5}$$

where TOC represents the total operator cost, to include all capital investment by operators of public transport services, and TUS is the total user cost, to include passenger walking time, waiting time and in-vehicle time. User time is converted to a cost by multiplying it by the value of time. Finally, TEC is the total external cost, based on external impacts such as accidents and air pollution. The model was used to compare the 'straddle bus' to the existing conventional bus on the main corridor along Minzu Avenue in Nanning, China, on the basis of operator cost, user cost, external cost, level of forecast passenger demand and level of service (Li and Preston, 2015).

Jansson, Holmgren and Ljungberg (2015) developed a total costs function for each mode of transport (bus, train or air) on Sweden's Stockholm–Sundsvall line by combining three individual costs: producer surplus; user surplus; and possible system-external cost:

$$TC = TC_{prod} + TC_{user} + TC_{ext} \quad \text{Equation 3-6}$$

In terms of the producer cost of a bus, it is assumed that all buses are fully occupied, while the daily traffic operation costs of a bus service operator are estimated by multiplying the number of buses in operation and the daily cost of a bus. The capital and running costs of a bus include garaging, repair and maintenance, and the drivers' wages (Jansson, Holmgren and Ljungberg, 2015). The daily cost of a bus is a function of its chief attributes, such as size and speed, while wages are assumed to be fixed. User costs include the cost of walking and waiting to catch the bus, the cost of the riding time and that of walking onwards to the final destination. Average walking time to/from bus stops relates to the distance between parallel bus routes running in the same direction, while waiting at the bus stop relates to the time between buses, known as the headway. The cost of riding time is calculated by multiplying the hourly cost of riding time and the length of the trip, then dividing by the overall speed (Jansson, Holmgren and Ljungberg, 2015).

A full-cost model was developed by Levinson *et al.* (1996) for inter-urban travel in the context of independent modes of transport along the Los Angeles–San Francisco corridor: air; road; and HSR. This combines infrastructure cost, carrier cost and social cost:

$$FC = ICC + IOC + CCC + COC - Ct + UCC + UOC - UT + UTC + SEC + SNC + SAC \qquad \text{Equation 3-7}$$

where ICC and IOC represent infrastructure construction cost and the cost of operating and maintaining the infrastructure, respectively, while CCC, COC and CT represent the carrier's capital cost to purchase a vehicle, to operate it and to maintain it and the transfers to infrastructure, respectively. The user costs include the expenses of the users, paid as user capital cost (UCC), fares to ride on carriers (UOC) and user transfers (UT), which are cost transfers to carriers, infrastructure and accident insurance. UTC and UCC represent users' travel time cost and congestion cost, which relate to the time spent travelling in uncongested and congested conditions, respectively, multiplied by the monetary value of time. Finally, SEC, SNC and SAC represent the net external cost to society from emissions (SEC), accidents (SEC) and noise, respectively, in using transport services (Levinson *et al.*, 1996).

## 3.3 Review of Forecasting Demand Model

Forecasts of travel demand are used to give dimensions to the construction aspects of transport infrastructure projects and are commonly future-year predictions, based on precise base-year observed flows (Flyvbjerg, 2005; Daly *et al.*, 2011). A forecasting demand model generally starts with a representation of existing modes of transport for leisure and business travel. After that, it covers population growth, GDP per capita and other components (MVA Consultancy, 2009). Travel demand forecasting is a key element in the field of transportation, as it allows predictions of the volume of traffic over a given transportation component in future and the targets of interest to transport engineers and planners (Flyvbjerg, 2005; Asad, 2015). It is an important part of the planning and evaluation of any transport infrastructure project, based on competition between alternative modes such as road, air and rail transport, whose particular attributes will attract different travellers (Flyvbjerg, 2005).

Forecasting public transport demand is important because it is closely associated with urban transport planning (Tsai, Mulley and Clifton, 2014). Taking the level of demand at the time of making the decision to build the project as fixed is a common basis of inaccuracy in calculations of demand during the first years of operation. The estimation of a project's financial viability is dependent on the accuracy of the forecast for travel demand, usually covering traffic volume and its distribution between modes of transport (Flyvbjerg, 2005).

Direct public transport demand models are widely employed in rail demand forecasts, as updates to models' specifications are required (Tsai, Mulley and Clifton, 2014). They are commonly an attractive proposition, especially in areas with extensive zones, and are of two types. First is the pure direct demand type that relates travel demand directly to transport mode, passenger and journey attributes by means of a single estimated equation. Second is the quasi-direct method that employs a form of separation between total travel demand and mode split (de Dios Ortuzar and Willumsen, 2011).

The relationship between rail support and fares and socio-demographics and travellers' income has been investigated by providing several demand elasticities for each determinant (Tsai, Mulley and Clifton, 2014). In terms of fares, travellers are considered as a crucial part of the production process and are associated with

time inputs such as access/egress time, waiting time, in-vehicle time and interchange time. Waiting and access/egress times decrease with greater service frequency and better network coverage, respectively, while interchange and in-vehicle travel time decrease if there are direct routes (Paulley *et al.*, 2006). An accurate forecast of total passenger demand and competition between transport modes is commonly the input in planning, designing, evaluating and regulating transport systems, moreover it supports transport firms' marketing and strategic planning (Tsekeris and Tsekeris, 2011).

The main strategy behind forecasting intercity travel demand is to develop a series of models to establish predictable relationships between demographic characteristics, physical systems, travel behaviour and activity distributions (Peers *et al.,* 1976). Meanwhile, the process of taking a fixed base year and making forecasts relative to that year is known as pivoting, as accurate base-year flows commonly do not come directly from strategic travel demand models. The role of pivoting is to exploit experimental matrices to improve the accuracy of forecasts (Daly *et al.*, 2011).

### 3.3.1 Review of models to forecast travel demand

In the transport planning process, models of transport demand forecasting involve four steps of trip generation, trip distribution, mode choice and traffic assignment. Econometric models in the trip generation stage are established to forecast passenger transport demand in terms of passenger vehicle-kilometres travelled, on the basis of population projections. These models use travel distance and the purpose of trips on both weekdays and weekends. At this stage, the linear regression model can be expressed as follows:

$$y = \alpha + \sum_{i=1}^{k} \beta_i x_i$$ Equation 3-8

where y is the dependent variable, $x_i$ is the independent variables related to both the passengers' and the transport system's attributes and $\beta_i$ is the corresponding coefficients to be estimated during model calibration (Tsekeris and Tsekeris, 2011).

To forecast demand for a new service, trip rate models can be developed simply by dividing the number of rail or bus trips by the sum of catchment area characteristics, such as population. These models can be extended to regression models based on explanatory variables to forecast annual trips at any station. The number of trips $y_{ij}$ can be predicted by the gravity model of trip distribution, as follows:

$$y_{ij} = \alpha_i \, P_i \beta_j A_j \, f(d_{ij}) \qquad \text{Equation 3-9}$$

where $P_i$ is the projected trips produced from zone *i*, $A_j$ is the projected trips attracted to zone j, $d_{ij}$ represents the cost function of travel between the zone pair i–j (origin–destination) of time separation and $\alpha_i$ and $\beta_j$ are the corresponding balancing factors for the origin and destination in the gravity model to be calibrated (Tsekeris and Tsekeris, 2011).

The standard gravity model can be used to explain variation in HSR demand, as follows:

$$T_{ij} = K \, A_i A_j R_{ij}^{\,-\varepsilon} \qquad \text{Equation 3-10}$$

where $T_{ij}$ represents the number of HSR trips between zones i and j and the $A_i$ and $A_j$ represent the attractiveness of zones i and j. K is a constant and $R_{ij}$ indicates the measure of repulsion between zones i and j. In addition, $\varepsilon$ represents the elasticity of demand with respect to the repulsion factor that is often found as a negative elasticity (Tsekeris and Tsekeris, 2011).

The gravity model can either refer to all travel or be mode-specific, and is integrated with a mode-split model before use in determining HSR share. As a part of the gravity model, measuring attraction is commonly based on population and income, using the city's GDP, while the repulsion measure is dependent on distance or journey time and the generalized cost of income levels and out-of-pocket expenses (Preston, 2013). For public transport, users' time inputs in terms of access/egress time, waiting time, in-vehicle time and interchange time are an important part of the production process, and can be greater than the users' monetary inputs in price or fare terms (Preston, 2015). A basic demand function is developed to determine the demand for public transport in terms of rail trips, as follows:

$$Q_1 = f(P_1, P_2, \dots\dots, P_n, I, T)$$ Equation 3-11

where $P_1$ represents the price of rail travel and $P_2$,… $P_n$ the price of rival products, such as car, bus, and so on, while I and T denote income and taste, respectively. The basic demand function can be rewritten using the double log model, as follows:

$$Q_1 = Lna + bLnP_1 + cLnP_2 + dLnP_3 + eLnI$$ Equation 3-12

where a represents the mode-specific constant that incorporates the variable of taste (T) and b, c, d and e are coefficients (Preston, 2015).

The price can be replaced by generalized cost, as follows:

$$GC = P + vJT$$ Equation 3-13

where v represents the value of time and JT denotes the journey time, which includes in-vehicle, waiting and walking time (Preston, 2015).

In the social sciences, gravity models are used to forecast and describe behaviours, and their application to analysis of transport systems concerns forecasting demand along a corridor. Two steps have been determined for HS1 in the United Kingdom: first, analysis of the HSR services between London and Kent at 24 stations throughout Kent, for both HSR and conventional trains; and second, to establish the number of trips from each station, devising a correlation matrix of dependent and independent variables of station usage and a set of variables. The variables included in the model are journey time and cost between stations, the number of trains between stations, the population within 4 mins of each station and the parking available at stations, as follows (Pagliara and Preston, 2013):

$$T_i = f(JT_{ij}, c, NT_{ij}, Pop_i, CP_i)$$ Equation 3-14

where $T_i$ represents the number of trips in station *i*, while $JT_{ij}$ , $F_{ij}$ and $NT_{ij}$ denote journey travel time, the fare and the number of trains between *i* and *j*, respectively. $Pop_i$ and $CP_i$ represent the population within 4 mins in uncongested driving conditions from station *i* and the number of car parking spaces available at station *I*, respectively (Pagliara and Preston, 2013).

To predict the change in the number of trips between two years and compare the results for this model, there are two possibilities: first, to forecast the change in the number of trips on a corridor where HSR and conventional train are available from the change in time and cost; and second, to predict the number of trips using the introduction of a new HSR service (Pagliara and Preston, 2013).

In DDMs, estimated demand is a multiplicative function of activity and socioeconomic variables including population, income, travel time and cost for each zone pair and level of service attributes for the transport modes serving them, as shown:

$$T_{ijk} = \emptyset(P_i P_j)^{\theta_{k1}} (I_i I_j)^{\theta_{k2}} \prod_m [(t_{ij}^m)^{\alpha_{km}^1} (c_{ij}^m)^{\alpha_{km}^2}$$ Equation 3-15

where P is population, I is income and t and c are travel time and cost, respectively, between i and j by transport mode k, while θ and α are parameters of the model and ∅ is a scale parameter that depends on the trips' purpose. In addition, both $\theta k_1$ and $\theta k_2$ are elasticities of demand with respect to population and income, respectively, while $\alpha_{km}^1$ and $\alpha_{km}^2$ are elasticities of demand for travel time and cost, respectively (de Dios Ortuzar and Willumsen, 2011).

For travel demand, regression analysis is commonly used to enable researchers to find the best linear forecast equation, as travel demand is a function of a set of independent variables, as follows:

$$Y = a + b_1 x_1 + b_2 x_2 + \cdots \ldots \ldots \ldots + b_n x_{n+e \ldots\ldots\ldots}$$ Equation 3-16

where Y represents a trip that is dependent on some variables, a represents the intercept of the regression plane, $b_{1,\,2,\,n}$ represents partial regression coefficients and $x_{1,\,2,\,n}$ represents independent explanatory variables (Ogunbodede and Ale, 2015). As a part of the semi-logarithmic linear formulation, Ristea (2016) forecasts UK travel demand for HS2 and HS3 using the log-linear model, as follows:

$$Ln(Y) = a + bx_1 + cx_2 + dx_3 + ex_4 + fx_5 + gDV_1$$ Equation 3-17

To establish the feasibility of HSR in Indonesia, Vikannanda (2018) calculated the 2030 level of demand using the log-log DDM, as follows:

$$Ln(Q) = a + blnP + clnI + dlnS + elnUMP$$ Equation 3-18

where Q represents the dependent variable of demand and P, I, S and UMP represent the independent variables of population, GDP, speed and unemployment, respectively (Vikannanda, 2018).

Garcia *et al.* (2016) predicted demand for the proposed Brazilian HSR project connecting Rio de Janeiro and Sao Paulo in order to calculate the total costs, using the following equation:

$$D(t) = f * Demand_{initial}$$ Equation 3-19

where D(t) represents the evaluation of future demands and *f* is a factor that can have values of 0.6 or 0.8, representing 60% or 80% of the given initial demand when t=1 (Garcia *et al.*, 2016).

### 3.3.2 Overview of forecasting demand case studies

In the field of transport, travel demand forecasting approaches are summarized and recommended for case studies worldwide. In this case, a separate model was used for each of the three case studies, similar to the case presented in this research and showing the impact of the introduction of new HSR technology on the current modes of transport, such as car, air, bus, and conventional rail, that serve a corridor.

In the United States, the multinomial choice model was used to forecast travel demand between HSR, air and road travel alternatives along the California corridor, as estimating costs commonly relate to demand. For this model, four factors were considered – mode, fare and service headway for both HSR and air travel – while the coefficients of each factor were the same across transport modes (Levinson *et al.*, 1997).

| **Market segment** | **Ridership** | **Distance (km)** | **Passenger-km** |
|---|---|---|---|
| South California–Northern California | 7,648,000 | 677 | 5,177,696,000 |
| Fresno–Northern California | 326,000 | 291 | 94,866,000 |
| Fresno–Southern California | 635,000 | 386 | 245,110,000 |
| Bakersfield–Northern California | 121,000 | 462 | 55,902,000 |
| Bakersfield–Southern California | 371,000 | 215 | 79,765,000 |
| **Total** | 9,101,000 | | 5,653,339,000 |

Table 3-1: Annual 2010 HSR ridership and distance. (Source: Levinson *et al.,* 1997)

The Caltrans state-wide model was devised in 1996 to estimate car trips to forecast 2010 demand, while air trips were based on the 1992 CalSpeed air passenger survey. Demand was forecast to rise to 5.6 billion passenger-kms, as shown in Table 3-1, yet this represented just one of many possible demand estimates for this study, and its general results were expected to be insensitive to minor variations in demand (Levinson *et al.*, 1997).


Figure 3-1: Map of California High-Speed Rail line (CAHSR). (Source: Taylor, 2014)

The future market share of HSR in metropolitan areas along California's HSR corridor was forecast as shown in Figure 3-1, based on a three-stage HSR demand-forecasting process (Charles River Associates Incorporated, 2000). In the first, travel demand for existing intercity transport modes, including air, private car and conventional rail, was estimated by using a DDM. Forecasting travel demand models incorporate the number of trips on existing modes of transport in future years, given the projected changes to various input variables such as population, level of service and income (Brand *et al.*, 1992; Charles River Associates Incorporated, 2000). For example, a model for air and private car demand was based on changes in socioeconomic variables, while conventional rail trips were

kept constant at the base-year level. As a result, the greatest contribution to HSR ridership was the 44.9% that was diverted from local air services, while private car trips contributed 41.9% of total ridership, as in Table 3-2 (Charles River Associates Incorporated, 2000).

| **Source** | **Ridership** | **Percentage of total (%)** |
|---|---|---|
| Local air | 14,373,650 | 44.9 |
| Connect air | 278,046 | 0.9 |
| Conventional rail | 1,915,011 | 6.0 |
| Private car | 13,404,305 | 41.9 |
| Subtotal | 29,971,012 | 93.7 |
| Induced | 2,031,091 | 6.3 |
| **Total** | 32,002,103 | 100.0 |

Table 3-2: Total intercity ridership in 2020 by source for funding scenario. (Source: Charles River Associates Incorporated, 2000)

In the second, the share of total trips made by each existing transport mode that can be expected to divert to the HSR mode is estimated using functional separation for each existing mode and market segment. Users of existing and future air, rail and car travel will divert to HSR in varying proportions when the same HSR option is offered, mainly dependent on the new rail service's actual speed, fares, station locations, frequencies and facilities (Brand *et al.*, 1992).

The third stage is to estimate induced travel demand by incorporating the utility function of mode-choice models. Induced demand can be defined as the number of trips that are not yet being made, whether on existing modes of transport or to alternative destinations. To forecast this demand associated with the introduction of a new HSR mode of transport, it is necessary to calculate the reduction in the equivalent price. The introduction of new transport mode commonly captures a large share of the market and may result in major improvements to the ease of travel (Brand *et al.*, 1992).

In 2000, total HSR ridership between the Los Angeles and San Francisco metropolitan regions was forecast to exceed 32 million by 2020, as shown in Table 3-3, with further trips being made between either San Francisco or Los Angeles to Central Valley. Trips between Los Angeles and San Francisco made the greatest

contribution of 35.2% to system ridership, followed by trips between the Los Angeles or San Francisco regions and Central Valley, at 16.4% (Charles River Associates Incorporated, 2000).

| Market segment | Ridership | Percentage of total (%) |
|---|---|---|
| Los Angeles–San Francisco | 11,269,050 | 35.2 |
| Los Angeles/San Francisco–Valley | 5,233,698 | 16.4 |
| Valley–Valley | 768,334 | 2.4 |
| Sacramento–Los Angeles | 3,384,964 | 10.6 |
| Sacramento–San Francisco | 1,690,169 | 5.3 |
| San Diego–Los Angeles | 5,304,220 | 16.6 |
| San Diego–San Francisco | 2,260,634 | 7.1 |
| Other | 2,091,034 | 6.5 |
| **Total** | **32,002,103** | **100.0** |

Table 3-3: Total intercity ridership in 2020 by source for funding scenario. (Source: Charles River Associates Incorporated, 2000)

In a 1976 study of the Sacramento–San Francisco Bay corridor via Stockton, a set of structural models were developed to estimate intercity travel. These are of two distinct types: probabilistic choice and direct demand (Peers *et al.,* 1976).

Probabilistic choice models are used to estimate the probability of choosing one of the available transport alternatives, or the likelihood of a traveller making a trip conditional on decisions such as trip frequency, transport mode, destination, choice of route, time of day and purpose (Peers *et al.,* 1976).

By contrast, aggregate direct travel demand models estimate future travel demand in the Sacramento–San Francisco Bay corridor on the basis of the availability of and need for data, model-use experience and subsequent costs in both money and time (Peers *et al.,* 1976). The data required were reformatted onto zones across the corridor. Some 90 zones were included in the Bay Area, while data on road networks were derived mainly from the California Department of Transportation for the base year. Surveys were conducted in conjunction with home-interviews to develop the attraction-zone socioeconomic data relating to employment groups (Peers *et al.,* 1976).

Ben-Akiva *et al.* (2010) presented a framework developed for an Italian case study involving 220 zones across all regions, as shown in Figure 3-2, to forecast the origin–destination passenger demand for HSR services. This framework uses three integrated demand models: national demand growth; mode-choice; and induced demand.


Figure 3-2: High-Speed Rail network of Italy. (Source: Ben-Akiva *et al.*, 2010)

In this study, the main Italian cities such as Rome, Naples, Turin and Milan were divided into 13, 8, 6 and 10 zones, respectively. In its demand growth model, a linear regression model evaluated the evolution of traffic over two years, mainly based on GDP and changes in oil price over two successive years (Ben-Akiva *et al.*, 2010). This was used to derive demand elasticity with respect to GDP growth for periods of both recession and an expanding economy, while assumptions were made about the threshold between these periods. Meanwhile, the mode-choice model was constructed from a set of nested logit models, using the nesting structure to capture higher degrees of substitutions between the transport alternatives of car, air, High-Speed Trenitalia and High-Speed Nuova Transport Viaggiatori (NTV) (Ben-Akiva *et al.*, 2010). In 2012, in the world's first case of competition between HSR operators

along the same corridor, the new HSR operator NTV entered the HSR market and competed with Trenitalia (Cascetta and Coppola, 2014).

Models based on gathering disaggregate data by means of a Revealed Preference (RP) and Stated Preference (SP) survey have used the maximum likelihood method for estimation. Finally, the induced demand model mainly concerns the relationship between the dependent variable of existing HSR demand and the existing travel costs and times of HSR, as well as including socioeconomic variables related to employment and population in zones connected by HSR services (Ben-Akiva *et al.*, 2010).

In Vietnam, intercity transport demand is increasing year by year due to economic development and a growing population. Traffic congestion is noted along many corridors and at railway stations, bus terminals and airports, especially at holiday times. To solve the current problem and also meet future demand, the Vietnamese government has decided to upgrade the infrastructure on the conventional rail route (Le *et al.*, 2018); moreover, construction of a new HSR line in the near future is being considered to connect the main cities of Ho Chi Minh city in the south and Hanoi in the north. This line will serve almost all city centres in the coastal area, home to 60% of Vietnam's population (Le *et al.*, 2018).

Le *et al.* (2018) used the integrated intercity forecasting travel demand model to represent trip generation and frequency, travel mode-choice behaviour and destination choice. This model uses a combined estimation of multiple data sources including SP, RP and aggregate trip data, as well as an explicit behavioural framework for intercity travel, to characterize and capture induced demand (Yao and Morikawa, 2005). The distance from Hanoi to Ho Chi Minh is about 1,700 km, taking around 30 hours by conventional rail or bus and almost 2 hours by aeroplane. In 2010, these two largest cities had populations of over 6.5 and 7.5 million, and year on year there is increasing demand for intercity transport. Quality of service on the other transport modes was found potentially to affect demand for HSR, especially if a low-cost airline were to become available (Le *et al.*, 2018).

HSR may alleviate heavy traffic along air and road corridors and improve interregional accessibility, and the construction of new HSR tracks is usually

dependent on the potential for some rail, air and car travellers to be diverted to the service (Borjesson, 2014). Endogenous passenger demand is related to user benefits such as waiting time, service frequency and in-vehicle time during the whole journey. The fact that passengers are willing to use a service on the basis of its quality shows this demand to be an endogenous variable: the operator of public transport will change its supply in the long term. On the other hand, exogenous demand can be considered as fixed demand that generates waiting time and in-vehicle time in order to establish the level of endogenous demand (Li, 2015). In a framework that includes demand and travel costs, exogenous and endogenous growth forecasting and logit modelling for mode-choice are mainly based on SP surveys (Atkins, 2012).

Forecasting HSR demand requires the integration of three modules: diverted demand; induced demand; and economy-based demand growth (Table 3-4). In this case, diverted demand is a variation of generalized travel cost on HSR services, which can induce a shift between alternative railway services and from other modes of transport such as air, car and bus. By contrast, induced demand is directly dependent on generalized travel cost (e.g. increases in trip frequency and change of trip destination). It is indirectly due to increased mobility in changing lifestyles (e.g. workers start to commute, so need to make more frequent trips) and land use (e.g. number of residents, activities and jobs) (Cascetta and Coppola, 2011).

| | | |
|---|---|---|
| **Endogenous factors** | Diverted demand | Shift from air, car or bus to HSR |
| | | Shift from conventional rail to HSR |
| | Direct induced demand | Increased trip frequency due to change in trip destination |
| **Exogenous factors** | Indirect induced demand | Increased mobility due to change in lifestyle and land use |
| | Demand growth | Increased mobility due to economic growth |

Table 3-4: Taxonomy of impacts on HSR demand. (Source: Cascetta and Coppola, 2011)

For exogenous changes related to society (e.g. GDP, population and employment growth) and endogenous changes related to the specific courses of action that are taken on the transport network (e.g. service frequency), forecasting demand commonly helps to understand the impact on demand for travel in the development and assessment of transport projects ('Guidance Note', 2019).

The exogenous changes related to rail demand are caused by the factors in Table 3-5, which are assumed to be beyond the control of the rail industry.

| **Exogenous factors** | **Endogenous factors** |
|---|---|
| Population | Rail fares |
| GDP | Rolling stock |
| Employment | Punctuality of rail services |
| Car ownership costs (e.g. fuel/maintenance) | Reliability of rail services |
| Cost of travel by other modes (e.g. bus, underground or air) | Station facilities |
| Journey time by other modes | Rail journey times |
| | Crowding |

Table 3-5: Examples of exogenous and endogenous factors. (Source: 'Guidance note', 2019)

On the other hand, endogenous aspects are assumed to be under the rail industry's control, such as the fares, punctuality and reliability of services, journey times, and so on ('Guidance Note', 2019). The traditional definition is that exogenous variables are determined from outside the model, while endogenous variables are determined by the economic model. The exogenous variables are independent of the error terms in the model since they are predetermined (Maddala and Lahiri, 1992). For example, both types of variable are classified in simultaneous demand and supply equation models, using a form from agricultural production as follows:

$$q = a_1 + b_1 p + c_1 y + u_1 \rightarrow \text{demand function} \qquad \text{Equation 3-20}$$

$$q = a_2 + b_2 p + c_2 R + u_2 \rightarrow \text{supply function} \qquad \text{Equation 3-21}$$

where q represents the quantity and p, y and R the price, income and rainfall, respectively, while $u_1$ and $u_2$ represent the error terms. The supply of wheat depends on the price of the wheat and the rainfall at the time, as supply is influenced by rainfall. In this case, the p and q are endogenous variables while y and R are exogenous variables, because the farm cannot control them, although the regressions of p and q can be estimated on y and R by ordinary least squares since the exogenous variables are independent of the error terms (Maddala and Lahiri, 1992).

The demand growth model is a linear regression model that relates the volume of demand to general economic factors, such as GDP and the percentage variation in

oil prices over two years. In this case, the elasticity of demand with respect to GDP growth can be derived from the demand growth model for periods of both an increasing economy and economic recession (Cascetta and Coppola, 2011).

Rail demand forecast models can be either aggregate or disaggregate. In aggregate models, the forecast is mainly based on the aggregate demand elasticity values of railway and car travel times, variations in GDP, car ownership, fuel costs and population (Cascetta and Coppola, 2014). Elasticity of demand for HSR would show that, should their travel time improve, passengers are relatively willing to switch to HSR. It measures how sensitive they are to potential changes to travel times and prices. The demand elasticity for HSR systems that offer higher speeds shows that it is greatest for distances of between 300 km and 800 km (Zschoche, Bente and Schilling, 2013).

Disaggregate models can be multimodal or mono-modal. Multimodal models are based on a simulation of the competition between rail and other modes of transport, such as car and air for long-distance passenger models, or between rail services such as intercity and HSR. In this model, the explicit timetables of all competing transport modes are used together with a nested logit model of mode, operator, service and run time (Cascetta and Coppola, 2014).

In an urban context, a mono-modal strategy is mainly employed to simulate demand and forecast the impact of a new transport technology or an improvement in the overall performance and demand, for example of HSR (Cascetta and Coppola, 2014).

Additional demand due to improvements to the rail service level is known as rail-induced demand, as these may affect users' decisions in terms of trip generation, distribution, scheduling, frequency and mode choice. Diverted and induced demand are not separate; changing from another mode to rail after it has commenced operation is regarded as induced demand rather than diversion of traffic. In this case, induced demand is defined as the increase in travel resulting from improved travel conditions such as shorter travel time, greater reliability, fare reductions, and so on. For example, as trips become more frequent, more comfortable and/or cheaper, induced demand may depend directly on the generalized journey cost. On

the other hand, it can depend indirectly on the relocation of people's workplace or home, modifications to people's lifestyle in terms of starting to commute and changes in land use regarding activities, jobs and residence (Gorham, 2009). Diverted demand occurs when travellers switch their journey from another mode or alter their time of travel. For example, to avoid peak period congestion travellers might travel to work earlier than they would otherwise like (Gorham, 2009).

As an example, the rapid development of Chinese railways in recent years has exerted a major influence on the structure of intercity passenger transport. There was a commitment to solve the issue both through satisfying current demand and forecasting predicted demand over the next 20 to 30 years (He *et al.*, 2017). In this case, between 2000 and 2014 data were collected from 26 provinces and three municipalities in China. Elasticity models were devised, such as the HSR elasticity model, the distributed lag model, the elasticity-based model and the rail efficiency model. In the first, both HSR-kilometres and conventional rail-kilometres were included to show the individual influence of each type of rail, while the second was employed to consider the demographic and economic factors and the time lag effect (He *et al.*, 2017).

In general, HSR technology is presented as a solution to congested airports and roads and as an efficient response to incremental increases in demand in the coming years. Demand is considered to be a significant component to obtain a positive financial return, and the case for HSR investment is heavily dependent on existing demand in the corridor in question (de Rus and Nombela, 2007). Preston (2013), after making 39 observations, presented the growth in demand for five services over time. Three groups of Japanese HSR lines appeared to experience strong growth in demand of 94% between 1984 and 2011, as shown in Table 3-6.

| Line | Year | Level of demand (million passengers) |
|---|---|---|
| TGV Sud-Est | 1987 | 19.2 |
| TGV Atlantic | 1995 | 29 |
| TGV Nord | 1994 | 20 |
| TGV Connexion | 2000 | 16.6 |
| TGV Rhone-Alpes | 1995 | 18.5 |
| TGV Mediterranée | 2001 | 20.4 |
| Madrid–Seville | 1998 | 3.6 |
| Madrid–Barcelona | 2009 | 5.4 |
| Tokyo–Osaka | 1970 | 80 |
| Seoul–Busan | 2010 | 28 |
| HS1 International | 2011 | 9.7 |
| HS1 Domestic | 2011 | 8.4 |
| Tokaido & Sanyo | 1984 | 128.3 |
| Tokaido & Sanyo | 2011 | 207.4 |
| Tohuku | 1984 | 24.1 |
| Tohuku | 2011 | 76.1 |
| Joetsu | 1984 | 11.3 |
| Joetsu | 2011 | 34.8 |
| Hefei–Nanjing | 2012 | 21.3 |
| Beijing–Tianjin | 2012 | 21 |
| Qingdao–Jinan | 2012 | 28 |
| Shi–Tai | 2012 | 22.3 |
| Hefei–Wuhan | 2012 | 11 |
| Coastal HSL | 2012 | 15.1 |
| Wuhan–Guangzhou | 2012 | 19.7 |
| Zhenghou–Xian | 2012 | 5.8 |
| Chengdu–Dujiangyan | 2012 | 4.7 |
| Shanghai–Nanjing | 2012 | 29.2 |
| Shanghai–Hangzhou | 2012 | 28.3 |
| Nanchang–Jiujiang | 2012 | 30.2 |
| Changchun–Jilin | 2012 | 8.4 |
| Hainan East Circle | 2012 | 6.4 |
| Beijing–Shanghai | 2012 | 24.8 |
| Italy HS Network | 2012 | 12.1 |
| Chinese Taipei HSR | 2007–2013 | 36.6 |
| G-Line (Gyeongbu) | 2004 | 22.2 |
| G-Line (Gyeongbu) | 2011 | 39.1 |
| H-Line (Honam) | 2004 | 4.2 |
| H-Line (Honam) | 2011 | 7.3 |
| **No. of observations** | | **39** |
| **Mean value** | | **29.2** |

Table 3-6: Evidence of HSR demand worldwide with a mean value. (Source: Preston, 2013)

The mean usage value of the included corridors was determined to be 29.2 million passengers, mainly based on the number of observations (39), and is known as actual passenger demand.

## 3.4 Review of Elasticity of Demand Models

The elasticity concept is defined as the ratio of a proportionate change in demand to the proportionate change of any factor that causes that demand to alter (Wallis, 2003). It is a measure of the understanding of demand change in a system's condition, since elasticity in demand for induced traffic means the rate of change in rail passenger-kilometres with respect to rail-kilometres (He *et al.*, 2017). To determine the level of demand, it can summarize demand's responsiveness to changes in various factors (Balcombe *et al.*, 2004).

In one study, to give the percentage change in travel distance by rail, the elasticity of an average trip distance is estimated for a particular HSR line in response to the percentage change in the generalized cost of rail trips over all origin–destination pairs (Borjesson, 2014). For example, demand is said to be elastic if a 1% change in a parameter causes a change in demand greater than 1%, and inelastic if the change is less (Wallis, 2003).

An example is that the elasticity of demand for business trips is extremely low, because employers are likely to disregard fare increases, especially for local trips. The elasticity is greater for those travellers with an alternative, such as access to a car, than for those without. The latter tend to have higher elasticity values in the long run (Paulley *et al.*, 2006).

Fares represent a major source of income for operators of public transport systems and are the most intensively studied factor of demand, as demand will decrease if fares are increased and vice versa. Both increases and decreases in revenue may result from a fare increase, depending on the relationship between demand and fare (Balcombe *et al.*, 2004). The value of fare elasticity is the ratio of the proportional change in demand to the proportional change in fares. For example, a fare increase will lead to increases in revenue if the value of elasticity is between zero and -1, while it will lead to decreasing revenue if drops below -1. Fare elasticity is dependent

on the mode, the time period over which it is being examined and the specific circumstances during operation (Balcombe *et al.*, 2004).

Oum, Waters and Yong (1992) reviewed empirical estimates of the elasticity of passenger demand, including the elasticities of aggregate market demand, mode-specific demand and mode choice. First, elasticity of market demand refers to the demand for transport among non-transport sectors of the economy. Second, it is important to differentiate between mode-choice elasticity and normal demand elasticity (Oum, Waters and Yong, 1992). Elasticity of demand with respect to service characteristics depends on the purpose and length of the journey, focusing on the four existing transport alternatives of car, bus, conventional rail and air (Balcombe *et al.*, 2004). A wide range of elements such as access/egress time, service interval and in-vehicle time convey the relative importance of service quality and incorporates a suitable demand forecast, using related elasticities. Thus, the service interval can be measured by frequency, total vehicle-kilometres per hour, headway and wait times. With respect to the vehicle-kilometres operated, the elasticity of demand for bus travel is approximately 0.7 in the long term and 0.4 in the short term, while for rail travel it is about 0.75 (Balcombe *et al.*, 2004).

Elasticity of demand also varies with the characteristics of the traveller, the time scale being considered and other factors related to the trip (Wallis, 2003). The value is influenced by the importance of the attribute, the strength of the competition, passenger and trip characteristics and the type of service. It tends to be greater for attributes that account for a larger part of the journey's total generalized cost. In terms of passenger characteristics, some groups are highly sensitive to price changes, while others are more sensitive to time changes (Wallis, 2003).

### 3.4.1 Review of models of demand elasticity

Demand elasticities can be calculated by applying the model to both a base scenario and one where there is a 10% increase in the given attribute over all trip relations, as the elasticity (ε) is calculated as follows:

$$T\varepsilon = \frac{\ln\left(D_{m1}/D_{m2}\right)}{\ln\left(x_{m1}/x_{m2}\right)} \qquad \text{Equation 3-22}$$

where $x_{m1}$ and $x_{m2}$ represent the attributes referring to mode m, in the base and change scenario respectively, while $D_{m1}$ and $D_{m2}$ represent the total demand referring to mode m, similarly. The elasticities for the number of daily trips are smaller than those for daily travel distance, because cuts in generalized travel costs cover both shorter and fewer trips (Borjesson, 2014).

In practice, the measurement of elasticity of demand is based on the size of the change in the explanatory variable, calculated as follows:

$$e_{Xi} = (\frac{\Delta y}{y} / \frac{\Delta x_i}{x_i}) \quad \text{Equation 3-23}$$

where $\Delta y$ represents the change in demand y and $\Delta x_i$ is the change in the explanatory variable $x_i$ (Balcombe *et al.*, 2004).

Elasticity can also be derived in a logarithmic form from the differential, as follows:

$$Elasticity = \frac{\frac{dy}{y}}{\frac{dx}{x}} = \frac{d(lny)}{d(lnx)} \quad \text{Equation 3-24}$$

This helps to make clear whether the elasticity is the same in both directions as well as giving the benefits of reversibility. For example, the original demand will be projected if the fare is increased by a certain amount and then reduced to its original level (Balcombe *et al.*, 2004).

In terms of the effects of demand interactions, cross-elasticity is used if there are competing modes of transport and a change in an attribute of one may affect demand for another. In this case, the cross-elasticity for a price change may be expressed as follows:

$$\eta_{ij} = \frac{\partial Q_i}{\partial P_j} \frac{P_j}{Q_i} \quad \text{Equation 3-25}$$

where $\eta_{ij}$ represents the cross-elasticity of demand for service *i* with respect to the price of service j, while $Q_i$ and $P_j$ represent demand for service *i* and the price for service *j*, respectively (Balcombe *et al.*, 2004).

Cross-elasticity can be used to find the effects of changes to the price of one mode of transport on the use of another. For example, the cross-elasticity of public transport with respect to petrol is 0.3 if there is an increase of 3% in demand of public transport when petrol prices rise by 10%. In this case, the calculation of cross-elasticities related to direct elasticities is as follows:

$$e_{rt}=e_r\ D_r\frac{m_r}{m_t} \qquad \text{Equation 3-26}$$

where $e_{rt}$ represents the demand cross-elasticity for public transport (t) with respect to private (r) price, while $e_r$ represents the direct demand elasticity for private vehicle trips with respect to private vehicle (r) price. $D_r$ represents the proportion of private transport trips that switch to public transport, known as the diversion rate, while $m_r$ and $m_t$ represent the modal share for private transport (r) and for public transport (t), respectively (Wallis, 2003).

The price elasticity of demand is defined by Fibich, Gavious and Lowengart (2005) as the percentage change in the quantity demanded that results in a 1% change in price, as follows:

$$\varepsilon=\frac{\partial Q/Q}{\partial p/p}=\frac{\partial Q}{\partial p}*\frac{p}{Q} \qquad \text{Equation 3-27}$$

where $\varepsilon$ represents elasticity, p is price and Q is demand. Various factors can strongly affect the elasticity of price related to demand, such as the importance of the item in terms of expenditure, adjustment time and range of use (Fibich, Gavious and Lowengart, 2005). In general, elasticities based on cross-sectional data are higher than those based on time-series data and lower than those based on SP data (Kremers, Nijkamp and Rietveld, 2002).

In comparison with direct elasticity, cross-elasticity is harder to measure and more sensitive to the base market share of the two modes (e.g. rail and bus). It is not readily transferable to new situations and cities due to differences in their modal share (Wallis, 2003). Mode-choice elasticities are concerned only with switching mode and ignore any trip generation or changes to destinations. They are derived from empirical studies that usually examine the split in a fixed volume of demand

between modes of transport and from models of mode choice, including SP-based models (Wallis, 2003).

To estimate elasticities separately for each component of travel cost and time, the generalized cost approach applies the concept of generalized cost (GC) or generalized time (GT). GC is defined as a measure composed of the monetary cost of a trip and other elements of the journey time, such as access/egress time, waiting time, interchange and in-vehicle travel time (Wallis, 2003). The GC approach assumes an average cost equivalent by multiplying the time for each component by its unit value. After that, the cost components are added together to estimate the total GC for the trip, while the demand level can be determined as a function of GC rather than in terms of the individual cost components (Wallis, 2003). GC for public transport is generally expressed as follows:

$$\mathrm{g} = \mathrm{f} + \alpha_1 t_1 + \alpha_2 t_2 + \alpha_3 t_3 \qquad \text{Equation 3-28}$$

where the g and f represent the GC and the fare per trip, respectively, and $t_1$, $t_2$ and $t_3$ the walking time, waiting time and in-vehicle time components, respectively, while $\alpha_1$, $\alpha_2$ and $\alpha_3$ represent the corresponding unit value of time. In this case, an overall GC elasticity can be applied to estimate the responsiveness of demand for travel to these variables rather than the individual elasticities with respect to in-vehicle time, fares, and so on (Wallis, 2003). As a result, the GC approach is often preferable due to its consistent results over a range of cases, and it appears to be sensibly constant over a wide range of journeys with various elasticities and component costs. There is a relationship between each GC component and its corresponding elasticity in that the elasticities of any component are proportional to that same component's contribution to total generalized cost, as follows:

$$e_g/\mathrm{g} = e_f/\mathrm{f} = e_1/\alpha_1 t_1 = e_2/\alpha_2 t_2 = e_3/\alpha_3 t_3 \qquad \text{Equation 3-29}$$

In general, the elasticity of dependent variable Y with respect to an independent variable $X_i$ is given by the following function:

$$\mathrm{E}(\mathrm{Y}, X_i) = \frac{\partial Y}{\partial X_i}\frac{X_i}{Y} \qquad \text{Equation 3-30}$$

It can be defined as the percentage change in the dependent variable with respect to the percentage change in the related independent variable. For example, the elasticity of public transport demand to fare changes is often stated to be around -0.33. This means that demand is expected to decrease by about 0.3% when fares rise by 1%. The elasticities in the econometrics of a given demand function with respect to changes in an explanatory variable can be calculated as follows:

$$\mathrm{Y} = f(X_1, X_2, \dots\dots, X_n) \qquad \text{Equation 3-31}$$

where Y represents the dependent variable and f is a function of independent variables (de Dios Ortuzar and Willumsen, 2011).

### 3.4.2 Overview of elasticity of demand studies

Several case studies on demand elasticity are presented in this section. It is determined with respect to price, generalized journey time, frequency, and so on; moreover, the cross-elasticity for multiple transport modes is obtained for several corridors. Generalized journey time is considered to be the sum of in-vehicle time and waiting time, which leads to an elasticity of -0.14 for HS1 trains and -0.06 for conventional trains. These are low, because they are for London commuters in Kent, England. In this case, an increase of 10% in the journey time results in a decrease of 1.4% in the number of trips on HSR and 0.6% fewer trips on conventional rail (Pagliara and Preston, 2013). For example, the value of demand elasticity among males is higher than among females in certain countries, due to the increased likelihood of their having a car available. In addition, travellers with a high income usually have greater values because of their higher level of car ownership, so they have an alternative if fares increase. Fare elasticity by distance travelled decreases for rail, as the fare per unit of distance diminishes with increasing distance. Due to the effect of income on car ownership, rail income elasticity can be as much as 2: car ownership is higher in the rail market (Paulley *et al.*, 2006).

Roman, Espino and Martín (2010) present the direct elasticities of choosing HSR and cross-elasticities with respect to car attributes in their report on the Madrid–Zaragoza corridor in Spain, and refer to air travel attributes along the Madrid–Barcelona route, as in Table 3-7. In the former, in terms of travel time, cost, access/egress time and headway, the price and time elasticities of HSR were found

to be -0.55 and -0.59 respectively, compared to -0.72 and -0.38 for the latter. Moreover, the cross-elasticity of HSR for the Madrid–Zaragoza corridor for car use is 0.12 and 0.04 for travel price and time respectively, compared to 0.7 and 0.11 for air travel for the Madrid–Barcelona corridor (Roman, Espino and Martín, 2010). All the values obtained are below 1, which shows that demand for HSR is inelastic. For example, it means that a 1% increase in travel cost will reduce HSR travel demand by a smaller proportion. At -0.55, the direct elasticity of travel cost between Madrid and Zaragoza shows that, in broad terms, demand goes down by 5.5% if the cost of travel goes up by 10%.

| **Attribute** | **Direct elasticities** | | **Cross-elasticities for car attributes** | **Cross-elasticities for air travel attributes** |
|---|---|---|---|---|
| | **Madrid–Zaragoza** | **Madrid–Barcelona** | **Madrid–Zaragoza** | **Madrid–Barcelona** |
| Travel cost | -0.55 | -0.72 | 0.12 | 0.70 |
| Travel time | -0.59 | -0.38 | 0.04 | 0.11 |
| Access/ egress time | -0.36 | -0.44 | − | 0.51 |
| Headway | -0.05 | -0.07 | − | 0.01 |

Table 3-7: Elasticity values for HSR. (Source: Roman, Espino and Martín, 2010)

Also, the cross-elasticities of rail demand with respect to car attributes for a value of 0.12 show that if the cost of car travel increases by 10% along the Madrid–Zaragoza corridor, rail demand goes up by 1.2%.

When TGV was introduced, rail travel time was slashed by 30%. The implied elasticity of travel time with respect to number of trips was around -1.6, as elasticity dropped to -1.1 then was further reduced by 25%. For the Madrid–Barcelona and Madrid–Seville HSR lines, the elasticities for the number of trips were -1.3 and -1.2, respectively (Borjesson, 2014). In this case, demand for HSR was shown to fall to a lesser extent upon a 1% increase in travel costs (Roman, Espino and Martín, 2010). Moreover, using the binary logit technique to examine the mode share between HSR and air travel, the elasticity of travel demand was found to be lower for out-of-vehicle travel time and frequency than for trip cost. In response to changes in out-of-pocket costs and in-vehicle travel time, elasticity of travel demand was

established as an effective means to further the aims of policy guidance and promote the desired mode-split changes (Wang *et al.*, 2014).

After the introduction of HSR services between Florence and Bologna in Italy, there was an increase in demand of 91%, with an elasticity of -2.5. Demand also increased for the Milan–Naples corridor by 41%, corresponding to an elasticity of -1.3. The overall increase in the volume of HSR demand for passenger transport between these cities from 2009 to 2010 was estimated to be from 6.6 million to 10.9 million passengers and from 2.4 billion to 3.9 billion HSR passenger-km. Based on this increasing demand, the overall elasticity values averaged between -1.6 and -2.1 for passengers and between -1.5 and -2 for passenger-kilometres (Cascetta and Coppola, 2011).

He *et al.* (2017) defined the elasticity model as an essential method to investigate induced demand, and it has two advantages from an economic point of view. First, the log form can eliminate heteroscedasticity for every variable, in normal circumstances. Second, the slope coefficient is unaffected by the unit measure. The basic elasticity model is based on factors of rail passenger-kilometre, such as population and cost of travel time. This is because in China the elasticity of rail-kilometres is 0.301, with respect to rail passenger-kilometres, meaning that it will increase by 0.301% upon a 1% increase in rail-kilometres. In addition, both gross regional product and population were found to have a significant impact on rail passenger-kilometres (He *et al.*, 2017).

Passenger demand for rail is mainly dependent on the price elasticity of demand and travel time. However, the elasticity of demand for HSR indicates that passengers are relatively willing to switch to HSR if their travel time improves. In this study, the elasticity values measure passengers' sensitivity to potential changes of travel time and price. The demand elasticity of HSR systems with higher speeds has been observed to be greatest for journeys of 300 km to 800 km (Zschoche, Bente and Schilling, 2013).

Demand elasticity with respect to service characteristics varies with the purpose and the length of the journey. A study of four existing modes of transport – car, bus, conventional rail and air travel – suggests that a wide range of attributes such as

the access/egress time, the service interval and in-vehicle time usually convey the relative importance of aspects of quality of service and incorporate suitable demand-forecasting technique, using related elasticities. Therefore, the service interval can be measured as the inverse of service frequency. With respect to the vehicle-kilometres operated, the elasticity of demand for bus travel is approximately 0.7 in the long term and 0.4 in the short term, while it is about 0.75 for rail demand (Balcombe *et al.*, 2004).

A set of short-term direct elasticity values is recommended when assessing the effect of changes in public transport variables on the demand for public transport, as most short-term service level elasticity is derived from time-series data (Wallis, 2003). A New Zealand study assessed evidence on elasticities of demand for public and private passenger transport by applying the values in their forecast of impacts on demand for urban transport. Table 3-8 summarizes the range of short-run aggregate values of direct elasticity for both rail and bus modes in terms of fares, in-vehicle time and level of service (at frequencies of 20–30 mins) (Wallis, 2003).

| **Attribute** | **Rail** | | **Bus** | |
|---|---|---|---|---|
| | **Best estimate** | **Typical range** | **Best estimate** | **Typical range** |
| Fare | -0.30 | -0.20 to -0.50 | -0.40 | -0.20 to -0.60 |
| In-vehicle time | -0.50 | -0.30 to -0.70 | -0.30 | -0.10 to -0.50 |
| Service level | 0.35 | 0.20 to 0.50 | 0.35 | 0.20 to 0.50 |

Table 3-8: Summary of short-run aggregate values of public transport direct elasticity. (Source: Wallis, 2003)

However, the in-vehicle elasticity for rail (-0.50) is higher than that for bus travel (-0.30), and rail trips tend to be longer (Wallis, 2003). For example, a value of -0.30 shows that if fares go up by 10%, demand for rail goes down by 3% and for bus by 4%.

The generalized cost for urban bus travel is based on components of fare and service levels (access/egress time, waiting time and in-vehicle time) (Wallis, 2003). In this study, access/egress time, waiting time and in-vehicle time were converted into a cost by multiplying their values by the value of time (€0.082/min or €4.95/hour) and the value of 2, as the access/egress and waiting times are valued at double the in-vehicle time (Wallis, 2003).

## 3.5 Review of Stated Preference Methods

The SP method is defined as a non-market valuation that relies on answers to carefully worded questions in a survey, using monetary amounts, choices or other indications of preference (Brown, 2003). It is a form of quantitative market research that has been developed over the past twenty years to address the limitations of RP analyses (Wallis, 2003). The technique involves asking people hypothetical questions to estimate their value of cost and time, thus establishing the extent of their collective willingness to pay for a specific benefit. SP techniques are of great interest to transport researchers. The methodology is based on statements made by respondents about their preferences for various mode alternatives. These techniques have been used for the calibration of demand models in order to predict users' mode choices on the basis of variations in their preferences (Louviere, Hensher and Swait, 2000; Guzzo and Mazzulla, 2004).

In a study by Petrik, Silva and Moura, the aim of the SP survey in transport demand modelling is to determine and analyse participants' perceived difficulties on the basis of their social decision-making and to suggest possible solutions (Petrik, Silva and Moura, 2016). The options prevalent since 2002 are face-to-face, email, telephone interviews and online surveys, with several combinations (Pearce, Ozdemiroglu and Britain, 2002). The models continue to attract attention for forecasting demand (Beaton, Chen and Meghdir, 1997): the researcher builds an experimental design and asks respondents to choose their hypothetical choice from a set of alternatives (Grigolon, Kemperman and Timmermans, 2010).

In transport planning, there is growing use of SP surveys to understand the changing behaviour of commuters under conditions that are new or hypothetical (Rastogi, 2000). The most common types include choice data; that is, respondents give their reasons for choosing between alternative modes of transport in the actual market (Sanko, 2001). The surveys offer each of a group of respondents variations in journey attributes, such as in-vehicle time, service frequency and travel costs, and they are asked to choose (Wallis, 2003).

In transportation research, many aggregate approaches concerned with choice behaviour since the mid-1970s have been replaced by disaggregate choice models using alternative theoretical frameworks, as random utility theory has been

incorporated into the multinomial logit model. Choice models were developed for transport mode choice, involving a limited number of options, using both revealed and SP data (Grigolon, Kemperman and Timmermans, 2010). Because of its key role in public transport policy-making, the mode-choice of transport is considered to be one of the most important classic models. It is important to develop and use models that are sensitive to the specific attributes of travel that influence individuals' choice (de Dios Ortuzar and Willumsen, 2011).

### 3.5.1 Review of the Stated Preference Model

Modelling of mode choice is achieved by means of the discrete-choice model, based on respondents selecting the transport mode alternative that has the greatest utility to them (Sekhar, 2014). Its philosophy is to manage transport demand and to adjust existing systems to these demands. Mode choice is influenced by factors such as in-vehicle travel time, waiting time, travel cost, number of transfers and comfort. Various researchers consider the value of time to be an influencing parameter, meaning how much a passenger is willing to pay in order to avoid a slower trip (Sekhar, 2014). Each combination of attributes in both SP and stated choice experiments can be defined as an alternative that represents a transport mode, and it can include the name of that mode alongside a description or illustration of its attributes, besides just the travel times and costs (Hensher, 1994).

The utility of the technique of transport mode alternatives stems from its incorporation of various attributes such as travel time, travel cost, service frequency and access/egress time for air and rail (Ben-Akiva *et al.*, 2010). There are three main types used in the SP approach. First is choice, where respondents are asked to choose one of several alternatives, usually a pairwise comparison. Second is ranking, where respondents must rank the alternatives. The third is rating, where respondents rate the alternatives on a numeric scale (1–100) or a semantic scale (definitely prefer, probably prefer, indifferent, and so on) (Pearce, Ozdemiroglu and Britain, 2002).

In transport planning, the transport mode-choice model is one of the most important classic versions, while the travelling transport mode is the behavioural model regarded as the most appropriate (Khan, 2007). In this case, individual choice behaviour involves four elements. First are the characteristics of the decision-maker

that affect the outcome of their decision, such as their age, gender, income, social class, and so on. Second are the alternatives to create a choice situation from which the decision-maker must choose. Third are the attributes that influence the overall utility of the travel alternatives, such as cost, time, waiting time and number of transfers. Fourth are the attribute levels, which have a major influence on the statistical power of the stated choice experiment. The number of levels in the experimental design affects the likelihood of finding a nonlinear relationship between the attribute and the derived utility. The decision rule is the theoretical method by which the decision-maker has to choose between the available alternatives (Twaddle, 2011).

The utility of travelling mode is defined as its attraction for a specific trip by virtue of its attributes, such as access time, in-vehicle travel time, waiting time, interchange time and travelling and parking fees (Khan, 2007). This utility is mathematically represented as both linear and nonlinear functions of a mode with a number of attributes for the journey, weighted by the coefficients, as follows:

$$U_{mi} = \theta_1 X_{mi1} + \theta_2 X_{mi2} + \cdots + \theta_k X_{mik} \qquad \text{Equation 3-32}$$

The utility function for mode m for individual i ($U_{mi}$) is equal to k number of attributes multiplied by k number of weights attached to each attribute ($\theta_{1, 2, \ldots, k}$), which have to be determined from the survey data (Khan, 2007). In the field of transportation planning, there is increasing use of the mixed logit approach, which introduces respondents' variations in taste. In this case, its mathematical framework is based on the theory of utility maximization, which can also be used to determine the logsum or composite cost. Ma, Kockelman and Fagnant (2015) state that logsum differences are based on an assumption of random utility maximization, used to estimate the benefits and losses of users when their travel context is altered. In this study, travel demand is taken as a result of individual travellers' choice-context changes (e.g. travel cost and travel time). Additionally, differences in logsum values for these individuals are characterized by the change in a consumer's surplus (Ma, Kockelman and Fagnant, 2015). The probability ($P_{in}$) in the framework of an individual (i) selecting a mode n, of the total number of available modes of travel (M), is given as:

$$P_{in} = \frac{\exp(X_{in})}{\sum_{m \in M} \exp(X_{im})}$$ Equation 3-33

In general, the logit model is of two main types, namely multinomial (of which the binary may be considered a sub-set) and nested. The binary logit model limits to two the total number of available alternatives. Its main limitation is that it should be applied only if the alternatives in the choice set are independent of each other. The nested logit model is characterized by grouping together all the subsets of alternatives in nests, each represented by a combined alternative that competes with the choices in the nest above (Khan, 2007).

As a result of modal split models, in order to forecast the travel behaviour in the study area the size of the choice set in the selection of an appropriate mode-choice model needs to be established. For example, a binary model modal split model can be applied if the choice set consists of two transport modes or two levels (lower and higher) of alternative modes, which would be termed a nested or hierarchical logit model (Khan, 2007). The probability of choosing alternative $Pr_1$ in the binary logit model where only two options are available is as shown (Maeyer and Pauwels, 2003):

$$Pr_1 = \frac{1}{1 + e^{(v_2 - v_1)}}$$ Equation 3-34

The probability of choosing alternative i where there are more than two options available is shown below, which is based on its associated utilities (Maeyer and Pauwels, 2003).

$$Pr_i = e^{(v_i - v_k)} * Pr_k$$ Equation 3-35

In this model, alternative i will be preferred over option k ($Pr_i > Pr_k$) when the utility associated with option i is larger than the option associated with alternative k ($v_i - v_k > 0$). In this case, on a disaggregate level the decision-maker has the discrete option to choose or not choose a transport mode, while the logit model leads to expressions such as ($\frac{Pr_i}{Pr_k} = \frac{1}{0}$ or $\frac{0}{1}$) and the logarithm cannot be calculated for these values (Maeyer and Pauwels, 2003).

For the HSR pricing strategy for the Wuhan–Guangzhou corridor, the disaggregate choice model assumed utility maximization, while probability was given by an individual n choosing alternative I, as follows:

$$P_{in} = P(U_{in} > U_{jn}, i \neq j) \qquad \text{Equation 3-36}$$

In this case, $U_{in}$ is the utility of alternative i for individual n, while $U_{in}$ is the utility of alternative j for individual n (Yao *et al.*, 2013).

In terms of the maximum likelihood estimation, Gould, Pitblado and Sribney (2006) mention that any likelihood function can be written as a function of several parameters and both dependent and independent data variables, using the most general case, as follows:

$$Ln\ L = \ln L[(\theta_{1j}, \theta_{2j}, \ldots\ldots, \theta_{Ej}; y_{1j}, y_{2j}, \ldots\ldots, y_{Dj}): j = 1,2, \ldots, N] \qquad \text{Equation 3-37}$$

where j represents the observation index, N is the number of observations and D represents the number of dependent variables (D≥0). In addition, θ denotes the probability model parameters and E the number of equations (E≥0) (Gould, Pitblado and Sribney, 2006).

### 3.5.2 Overview of stated preference case studies

An SP survey was used in a study of a projected HSR link connecting Lisbon to Oporto in Portugal, a distance of 650 km, intended to compete with existing modes such as air, bus, conventional train and private car travel (Carballo-Cruz, 2007; Petrik, Silva and Moura, 2016). The survey presents statements about hypothetical situations involving modal choices for a user travelling along various corridors (Petrik, Silva and Moura, 2016). In the experiment, several attributes and assigned levels were used to generate hypothetical scenarios. Competition between transport modes usually concerns the level of noise, travel time and comfort; however, respondents now had to choose between a new service (HSR) and existing modes of transport on the basis of their attributes. A choice of transport mode was presented for nine scenarios that were assumed to have a strong influence on respondents' decision (Petrik, Silva and Moura, 2016).

The nesting structure was used for an Italian case study as part of the mode-choice model to capture the higher degrees of substitution among subsets of eight mode

alternatives based on four levels. The first included the offer quality and specifics of air, car and rail modes of transport, while the second used identical criteria for the choice between HSR or intercity services. In the third, the choice was between the operators of NTV and AVTR (Advanced Vehicle Transformation) for travellers who selected the HSR service, or between first and second class for those who selected the intercity service. In the fourth, the choice was between first and second class for travellers who selected the HSR service (Ben-Akiva *et al.*, 2010).

In the United States, demand modelling for California High-Speed Rail started with a series of surveys and the integration of several demand models. A multinomial logit model was used in a trip frequency model with the collected data in order to explain trip generation, as the model is segmented by the length and purpose of trips. However, from the choice set of zero, one, two, three, or more trips per day, most survey respondents selected zero. The multinomial composite impedance function captures the effect of travel impedance, as the destination choice mode is more important if there are many stations in a proposed intercity service (Zhang *et al.*, 2019).

In California HSR demand modelling, in order to run categorical outcome regressions in the SP survey the main mode-choice model is similar to that in the four-step model. The assumption is that all induced demand for this case study can be attributed to the new mode, especially when there is a much better level of service on the new service, so the proposed framework focuses on induced rather than diverted demand (Zhang *et al.*, 2019).

The data in the survey were obtained for analysis by econometric models to explain the induced travel demand using a set of influential factors. For example, the proposed modelling framework was applied to a case study in Texas via an online survey website, AYTM (Ask Your Target Market) to determine the induced demand on the San Antonio–Dallas corridor. Its chief benefit is its large membership pool to ensure good sampling of people at various geographical locations and of many socioeconomic backgrounds (Zhang *et al.*, 2019). The questionnaire started by asking respondents about their socioeconomic factors and experience of previous trips. A brief introduction presented the new mode, followed by questions to establish the induced demand, dependent on the mode’s hypothetical parameters.

Each respondent answered the induced trip questions eight times under different combinations of travel costs, travel times and departure frequencies (Zhang *et al.*, 2019).

As a result, since most innovative intercity transport technologies aim to reduce it, travel time was identified as an important influential variable. In addition, the estimated coefficients were used to understand the relationship between the speed of public transport systems and induced demand. Also, travel cost was considered as an important variable to determine travel demand. The value of time is another important finding of the survey, derived from estimated coefficients of time and cost based on the statistical analysis of SP survey results in the context of induced travel demand. For example, an assumed value of time of $20/hour means that travellers are willing to pay an additional $20 to travel by a mode of transport that saves them an hour of travel time (Zhang *et al.*, 2019).

SP techniques were also used for the Vancouver–Seattle–Portland corridor in order to understand people's travel preferences for and attitudes to the proposed Ultra-High-Speed Ground Transport (UHSGT) project. The attitudinal data were collected to evaluate people's inherent biases. In this case, using hypothetical situations the SP survey asked respondents to make choices between using their current transport modes (car, air, bus or rail) or a new HSR service (WSDOT, 2019). In this part of the SP survey, the decision by a user is based on shifting from their existing transport modes to a UHSGT that provides more reliable service, shorter travel time and less greenhouse gas emissions. The behavioural survey was used to forecast the model inputs for the UHSGT demand and revenue study. In this case, the mode-choice models were developed from statistical analysis of the SP data from an online survey that yielded about 2.5 thousand responses (WSDOT, 2019).

Yao *et al.* (2013) analysed the pricing strategy of an HSR system to improve occupancy in view of competition between modes of transport along the Wuhan–Guangzhou corridor, starting with theoretical analysis of the link between fare and market share then using disaggregate choice models with a nested structure. The analysis was based on SP data to establish the HSR's market share at a specific fare, set at a higher level on weekends and holidays and lower on weekdays (Yao *et al.*, 2013). The likelihood ratio indexes exceeded 0.2 for all models, which can be

considered to be satisfactory goodness of fit. It was found that passengers became more sensitive to variations in travel time upon an increase in their level of income. Meanwhile, the parameters of profession, trip purpose and age had a positive impact on the utility function, which means that passengers, especially civil servants and managers, preferred travelling by HSR for business. The results showed that high-income passengers are willing to pay more for a shorter trip – they put a high value on time – and tend to choose HSR (Yao *et al.*, 2013).

## 3.6 Overall Integrated Model

In this chapter, the total social cost model is an important part of the comparative assessment structure of this research. After obtaining the main service characteristics from the previous chapter's literature review of HSGT technologies, the models in worldwide case studies were examined. It was found that many cost models for urban (and inter urban) transport systems are based on an engineering approach, thus they include infrastructure construction and maintenance costs and the size of the required vehicle fleet. This review of cost models led to determining which parameters of operator costs should be included, such as for infrastructure and rolling stock. Studies have also been presented on the total social cost of urban public transport in China, Sweden, Japan and Vietnam, and these include operator cost, user cost and external cost.

Only two studies of total social cost models for intercity transport systems were found to focus on HSR projects, or to determine only the operator costs of various transport modes such HSR, air and road transport. From this chapter, the unit costs, values of external costs, values of time (and the weights of access/egress time and waiting time with respect to in-vehicle time) of the chosen HSGT technologies were obtained to develop the cost model for this research. The difference between the works reviewed and the main aim of this thesis is to undertake a comparative assessment of HSGT technologies based on operator cost, user cost and external cost. Previous studies have focused on urban transport modes, or examined only the operator cost or the environmental costs of various intercity transport modes.

After reviewing the cost functions for both urban and inter-urban transport modes, the following chapter's methodology review of demand models determines the

appropriate approach, such as linear regression methods and discrete-choice models, to build the demand models using both revealed and stated preference data.

Forecasts of annual levels of passenger demand were determined and used as input to the total social cost model for HSGT modes. In this case, econometric models were reviewed to forecast demand by projecting variables such as population, GDP and ticket price, using the linear regression model. Further independent variables were included, such as journey time, journey cost and the number of trains.

In terms of models, a linear-linear forecast equation was initially developed to assess which explanatory factors were statistically significant. In addition, the linear-log and log-log functions were tested to determine the demand for HSR as the same independent variables of population, income, speed and unemployment rate were defined for both models. As with previous global studies, this study tested all three models – linear-linear, log-linear and log-log – to select the best-fit model. The difference between this and previous global studies is the addition of service frequency, mean fare and monthly dummy variables. Although the unemployment rate was tested, due to insufficient variation in the data it was not statistically significant.

In elasticity demand models, demand is normally determined with respect to explanatory variables such as travel volumes, fares, petrol prices, travel costs and travel times. By contrast, this research uses demand with respect to generalized journey time, which includes in-vehicle travel time, service frequency and number of interchanges.

For SP discrete-choice models, the techniques of utilities and probabilities were reviewed, as the utility function is based on attributes such as access time, waiting time, in-vehicle time, parking fees and interchange time. The logsum or composite cost was also reviewed, as it is a part of the SP method used to estimate the benefits and disutility of travellers when their context of travel changes. A strategy of integrating the three models (the regression model, the elasticity demand model and the stated preference model) identified diverted/abstracted demand,

induced/generated demand and economy-based demand growth, and this was used to forecast demand for Hyperloop.

The overall integrated model is based on a combination of total social cost models and several demand models, as the output of the demand models is an input into the project's TSCM. For example, the HSR demand model is determined in Chapter 5, after testing other two linear-linear and log-log functions then selecting the log-linear demand model as the best-fit function on the basis of the Box-Cox test. The elasticity demand model is also covered in Chapter 5, based on the outcome of HSR's DDM with respect to generalized journey time.

In Chapter 6, the distributions and observations of SP experiments are described, based on usage of the Riyadh–Dammam rail service. Then, demand is forecast for HSR, Maglev and Hyperloop through the interaction of the regression model, the EDM and the SPM, as presented in Chapter 7. For example, demand for HSR for 2018 is forecast by the DDM (log-linear function) method to forecast future HSR demand for 2030, 2040 and 2050 on the basis of the elasticity of demand in 2018 with respect to income, taken as 1.5. The direct demand model is used to forecast total HSR demand and the SPM to work out the extent to which demand is abstracted (and generated). This informs the Hyperloop forecasts. In this case, demand for Hyperloop in 2018 is forecast by combining its generated and abstracted demand, based on the probability of SP and demand for existing transport modes, while Hyperloop demand for 2030, 2040 and 2050 is forecast by its elasticity of demand in 2018 with respect to income, using the same value of 1.5 as for HSR. On the other hand, demand for Maglev is forecast by the EDM with respect to HSR and Maglev's generalized journey time.

After this review of HSGT technologies, total social cost models and demand models, the next chapter applies the TSCM to the Riyadh–Dammam case study. This is done by describing the case and comparing its existing modes of transport in terms of travel cost, travel time and service frequency.

## 3.7 Conclusion

This chapter started by reviewing cost models for both urban and inter-urban public transport systems, based on elements such as the number of vehicles needed, the

length of the corridor, travel time, and so on. Many total social cost models are focused on calculating the operator cost of modes of public transport based on their characteristics and the level of demand. Others encompass producer costs, user costs and possible external environmental costs.

The construction costs of HSR lines in several countries were reviewed in this chapter, ranging from €5.5 to € 36.7 million at 2017 prices. The construction cost of HSR projects in Spain and France is lower than that in Japan and Germany, due to their design as passenger trains, as in Japan HSR does not mix traffic. Construction cost is minimized in France by avoiding building tunnels and viaducts, by purchasing expensive land to keep to straight lines and by adapting steeper grades.

For Maglev projects, the construction costs, including trains, were about €284.1 million/km at 2017 prices on the Japanese Chuo Shinkansen line (285.6 km), and it goes through difficult terrain. By contrast, the construction costs of Hyperloop tube were estimated at €10.3 and €34.0 million/km on pillars and in tunnels, respectively.

The user cost of HSGT systems comprises access/egress time, waiting time and in-vehicle travel time. Access and egress cost are based on the time taken to get from the origin to the HSGT technology's station (A) and onwards from the HSGT technology's station (B) to the final destination. The access and egress times differ, depending on whether by walking or travelling on a bus, metro or car. Waiting cost is strongly related to the quality of the HSGT service in terms of capacity, frequency, and so on, as passengers may experience extra delay if the level of demand is remarkably high or the trains/capsules are behind schedule in the rush hour. As part of user travel time, in-vehicle time is considered as an important factor, usually helping travellers to decide on their fastest transport mode.

Lastly, for each HSGT system discussed the external environmental cost was reviewed, which relates to air and noise pollution, accidents and impact on climate change. Both HSR and Maglev systems are already in operation. HSR accidents have been recorded in Germany (1998), China (2011) and Spain (2013), and there were 23 fatalities in the Lathen/Emsland accident on Germany's Maglev Transrapid test track on 22 September 2006.

The level of demand is used as the independent variable to determine total social cost. As the prediction of demand is commonly a crucial factor in planning and evaluating any transport infrastructure project before making the final decision, this chapter reviewed demand models such as the DDM, EDM and SPM. To obtain an overview of the transport planning process, this study adopted the four steps of trip generation, trip distribution, mode choice and traffic assignment in the demand forecasting models.

The gravity demand model for the United Kingdom's HS1 line, presented by Pagliara and Preston (2013), was reviewed to determine the number of trips by means of the independent variables of journey travel time and cost, number of trains, population and number of parking spaces. Also reviewed was the DDM based on the log-linear and log-log formulations by Ristea (2016) to forecast demand for the United Kingdom's HS2 and HS3 and by Vikannanda (2018) for Indonesia's HSR.

EDM was reviewed, since it comprises part of the forecasting travel demand models devised in this current study, starting with the definition of elasticity in transportation. The elasticity of demand can be determined from the growth in demand, using the elasticity of the generalized journey time, the fare or the GDP component.

SPM's use in forecasting travel demand was reviewed, asking about participants' preferences for alternative modes of transport as is usual in transportation studies. The utility and probability of the alternatives in the various studies are generally based on dissimilar attributes, such as in-vehicle time, access/egress time, interchange time, travel cost and service frequency.

Figure 1.4 shows how the models fit together (sub-section 1.2.2). First, a demand-forecasting model of conventional rail demand in Saudi Arabia is developed, and this is used to forecast HSR demand. Second, an elasticity model is developed to forecast Maglev demand in relation to HSR. Third, SP mode-choice models are used to estimate the demand for Hyperloop and HSR, abstracted from other modes. Finally, a logsum model is used to estimate the extent of the Hyperloop demand that is generated, based on its estimates of the generated volumes of HSR.

# Chapter 4. Application of the Total Social Cost Model

## 4.1 Introduction

In this chapter, section 4.2 reviews the operator cost, user cost and external cost of HSR technology, largely using estimated costs for infrastructure construction in Europe. User cost is expressed in terms of HSR access/egress time, waiting time and in-vehicle travel time, as well as the external environmental cost. An overview of operator cost, user cost and external cost of Maglev is presented in section 4.3 for existing and proposed Maglev projects. Section 4.4 reviews the total social costs of Hyperloop technology, based on proposed projects worldwide. To illustrate the application of the TSCM methodology developed in this study, this chapter considers KSA's proposed Riyadh–Dammam HSR line. Some brief background describing KSA's location, population, GDP, international tourism, and so on, is presented in section 4.5. Section 4.6 details the transport modes currently serving the corridor, such as conventional train, bus (coach), car and air transport, in terms of distances, numbers of routes and travel time. It also compares the estimated travel time, service frequency and travel cost (fare) of existing transport systems to those of the proposed HSR line.

## 4.2 High-Speed Rail Technology

### 4.2.1 Operator cost of High-Speed Rail

Building an HSR infrastructure usually requires a specific design to eliminate technical issues that may limit the speed of commercial operation, such as level crossings and frequent sharp bends unsuitable for high-speed travel. It is difficult to compare the construction costs of HSR projects due to the technical solutions implemented in each case (de Rus, 2012a). In many HSR projects, both in service and under construction, land and planning costs and the cost of the main stations are commonly excluded from the infrastructure construction cost (ICC) as the average cost per kilometre of HSR line ranges widely, from €10 to €40 million at 2009 prices (de Rus, 2012a, 2012b). Preston (2013) found that the average construction cost and the lowest cost for HSR lines were achieved in France and Spain, as shown in Table 4-1, ranging from €5.5 to 22.0 million and €9.7 to 24.9 million, respectively, at 2017 prices. The lower cost in Spain and France than in

Japan and Germany is due to the design of high-speed lines in these countries, which are for passenger transport only (Preston, 2013).

| Country | Construction cost (€ million per km) at 2005 prices | Consumer price index in January 2005 | Consumer price index in January 2017 | Index | Construction cost (€ million per km) at 2017 prices |
|---|---|---|---|---|---|
| France | 4.7–18.8 | 91.3 | 107.0 | 1.17 | 5.5–22.0 |
| Germany | 15.0–28.8 | 91.4 | 108.1 | 1.18 | 17.7–34.1 |
| Japan | 20.0–30.9 | 100.5 | D | 1.03 | 20.6–31.9 |
| Spain | 7.8–20.0 | 86.7 | 107.9 | 1.24 | 9.7–24.9 |

Table 4-1: Construction costs of new high-speed lines per route-km. (Source: Preston, 2013)

The lower construction costs in France and Spain are also due to the construction procedures adopted, the less populated areas, which are away from major urban centres, and the more homogenous geography. For example, the cost of constructing an HSR line in France is minimized by using steeper grades rather than building viaducts and tunnels, and by acquiring more expensive land and thus achieve a straighter alignment, leading to a reduction in both operating and maintenance costs. In Germany and Japan, construction costs are expensive since their HSR lines are both built in densely populated areas and involve blasting tunnels through mountains (Campos, de Rus and Barron, 2006). Construction costs in Spain and France are lower because steeper gradients are more acceptable here, in part because of powerful rolling stock and high fuel consumption (which have their own costs) and lower speeds than would be the case with more moderate gradients. Note that in Germany high-speed lines are also used by freight, which limits the operating gradients. As a result, the mean construction cost of HSR is about €22 million/km, with a standard deviation of €10 million, closely based on various factors such as the wage rate, planning, land prices, type of structures and track, capacity and operating speeds, and so on (Preston, 2013).

The HSR's energy consumption is 5% lower in France than Germany because of being developed directly by the rail operator rather than included in the infrastructure, as in other countries, together with its cheaper, nuclear source (de Rus, 2012). The infrastructure costs of building, maintaining and operating 500 km of HSR in Europe are presented in Table 4-2, as the construction cost varies from

case to case and usually depends on major factors such as land values, the amount of tunnelling involved and the costs involved in entering large cities (Nash, 2010).

| **Category** | **Total cost (€ million)** | **Unit** | **Cost per unit (€ thousand)** |
|---|---|---|---|
| Infrastructure construction cost | 6,000–20,000 | 500 km | 12,000–40,000 per km |
| Infrastructure maintenance cost | 32.5 | 500 km | 65 per km |
| Rolling stock cost | 600 | 40 trains | 15,000 per train |
| Rolling stock maintenance cost | 36 | 40 trains | 900 per train |
| Energy cost | 35.7 | 40 trains | 892 per train |
| Labour cost | 19.8 | 550 employees | 36 per employee |

Table 4-2: Estimated costs of a 500 km HSR line in Europe, at 2004 prices. (Source: Nash, 2010)

The operation of an HSR project is planned to commence after finishing the infrastructure (t), and planning itself usually accounts for up to 10% (ρ) of the total ICC. The rest (90%) goes on the infrastructure construction and superstructure costs (Almujibah and Preston, 2018). Over a year in an HSR's life-cycle, the construction and maintenance costs of the infrastructure may be expressed per unit length of the HSR line, as the unit cost of regular maintenance of a given HSR line can be assumed. Working on assumptions of train capacity, initial demand, line length and train commercial speed, 5% of the social discounting rate is considered for both the project infrastructure and acquiring rolling stock (Campos, de Rus and Barron, 2007a).

Regarding the acquisition of rolling stock, the total number of trains needed for an HSR corridor relates to the number of passengers and the service frequency. However, the risk of failure has a value of 1.5, associated with providing services versus the cost of acquiring, operating and maintaining an over-sized fleet, and in the real world this value ranges from 1.25 to 1.6 (Campos, de Rus and Barron, 2007a). The average unit cost of acquiring a train in a given period ranges between €45,000 and €50,000 per seat, as it is dependent on the number of trains. In the case study, an average of €47,500 per seat is used (Janić, 2017).

In France, the energy consumption of the new South-East line is 16.5 kWh/km at a speed of 300 km/h (Levinson *et al.*, 1997). In the case study, the unit value of energy was assumed to be €0.024 kWh-hour, based on 2015 electricity prices for industrial use in Saudi Arabia (US Commercial Service, 2015). The cost of administration and

sales is dependent on the numbers of employees and automated ticketing machines needed for a given level of forecast traffic demand. To calculate the fares to be charged on an HSR, it is critical to decide which kind of pricing should be followed, since the average fare is an important element of the generalized cost of travel (de Rus, 2011). To compute the average price of tickets in Spain, government revenue data from 2014 is usually used, divided by the number of passengers, as fares during the span of the investment are kept constant on most lines to reflect the competition from air services (Albalate and Bel, 2017). The average unit maintenance cost of a train is assumed to be €0.0124/seat-kilometre, dependent on the specific features of the trains and their seating capacity. Annual usage of a train is assumed to be 500,000 km per seat (Janić, 2017).

### 4.2.2 User cost of High-Speed Rail

In transport studies, user travel time is implicated in many attributes such as access/egress, waiting and in-vehicle travel time. Access/egress time is from one's door (e.g. school, work and home) to the first transportation infrastructure used in the city (A) (Allard and Moura, 2013). Access time is how long it takes to walk to the origin railway station, to take the metro or bus or to drive by taxi or car (Table 4-3).

| **Access mode** | **Access time (mins)** | |
|---|---|---|
| | **Madrid, Atocha Station** | **Barcelona, Sants Station** |
| Car (private or taxi) | 15 | 10 |
| Local train | 15 | 12 |
| Metro | 30 | 12 |
| Bus | 45 | 20 |

Table 4-3: Average time to access HSR stations in Madrid and Barcelona, by mode. (Source: Pagliara, Vassallo and Román, 2012)

Egress time is defined as the time taken from the first transportation infrastructure used in the city (B) to the final destination. The main difference between access and egress times is found to be mostly travel to and from the HSR station; egress has been found to be 32% slower than access, which may be due to greater familiarity with one's transport options at the origin than those at the destination, after a long-distance trip. In some studies, the coefficient for walking time is almost double that of in-vehicle travel time. In another study, access/egress time is taken to be the time required to go by foot to/from the Lisbon Portela International Airport, the Oriente

Railway Station and the Sete Rios Bus Terminal in the morning rush hour, on the basis of a walking speed of 4 km/h (Allard and Moura, 2013). The speed limit for driving in urban areas is normally 45 km/h and between 80 and 120 km/h on roads between cities (DeNicola *et al.*, 2016).

Waiting time is found to be one of the most important factors of total user cost for all modes of public transport, as it starts upon arrival at the terminal and lasts until the passenger embarks. It is a critical aspect of passenger service, and a railway passenger usually experiences several types of waiting, for various reasons. For example, their waiting might be prolonged if trains are running behind schedule, and during the rush hour most meet with some delay (Vansteenwegen and Vanoudheusden, 2007). By contrast, in-vehicle time is generally based on door-to-door travel time and is one of the most relevant factors affecting travellers' choice of mode of transport. For example, door-to-door in-vehicle time is reduced if there are fewer stops along the line.

The value of time (VOT) is expressed almost as relative to driving time, when waiting for a train; passengers equate one minute of waiting to 2.5 mins spent driving. In this study, the VOT is assumed to be €8.2/h, as it depends on aspects such as trip purpose, socioeconomic and demographic characteristics and the total duration of the trip (Levinson *et al.*, 1997). For example, in 2008 the VOT for private trips was estimated by a Swedish national forecasting model at €6.5/h, €12/h and €10/h for bus, car and rail, respectively, based on stated-choice data (Borjesson, 2014).

### 4.2.3 External cost of High-Speed Rail

Maout and Kato (2016) define external costs as those generated by transport users but paid for by their surroundings, the environment and society as a whole. They include air pollution, noise, accidents and climate change. The external costs associated with society and transport users cannot be estimated independently of policy interventions, as they usually refer to the difference between internal cost and social cost (Maibach *et al.*, 2008).

All modes of motorized transport emit significant quantities of air pollutants to a varying extent, harming human health, reducing visibility, damaging material and stressing forests and crops (Igor and Howaida, 2014). There are two types of

damage from air pollutants on buildings and materials: soiling of buildings' surfaces by dust and particles; and degradation due to acid air pollutants and corrosive processes, including $NO_x$ and $SO_2$ (Maibach *et al.*, 2008). To generate the electricity for HSR trains, the primary fuel is coal, oil or gas.

Due to the strong likelihood of diversity in terms of the primary energy source used in each country, it is complex to make comparisons of HSR's air pollution emissions (Campos, de Rus and Barron, 2007b). In rail transport, the main key cost drivers are vehicle speed, load factors, fuel type, the geographical location of power plants, and so on (Maibach *et al.*, 2008). The marginal cost of HSR's air pollution is 0.368 €/1,000 passenger-km (Albalate and Bel, 2017). For a load factor of 50%, reported values of energy consumption are 567 kJ/passenger-km for Japanese Shinkansen, 440 kJ/passenger-kilometre for French TGV and 1,702 kJ/passenger-kilometre for TVE (Wayson and Bowlby, 1989).

Electromagnetic radiation and catenary arcing problems in HSR electrical operation have been considered as an environmental danger, inducing high voltages near the wayside due to the electrical components (Wayson and Bowlby, 1989). The potential hazards of having conventional and HSR tracks lying adjacent need to be considered, such as the aerodynamic interaction between trains, the procedure for evacuating passengers onto the tracks, the risk of fire on the adjacent track, and so on (Saat and Barkan, 2019).

The noise generated by HSR can be categorized as pantograph noise, wheel and rail noise and aerodynamic noise. It usually relates to the speed of the train that is passing: faster speeds generate most noise (Pourreza, 2011). For example, aerodynamic noise is direct airborne noise, as shown in Figure 4-1, which is generally generated by airflow around the body of the train, the pantograph and wheel areas, and this is prevalent at speeds of over 300 km/h (Temple-ERM, 2013).

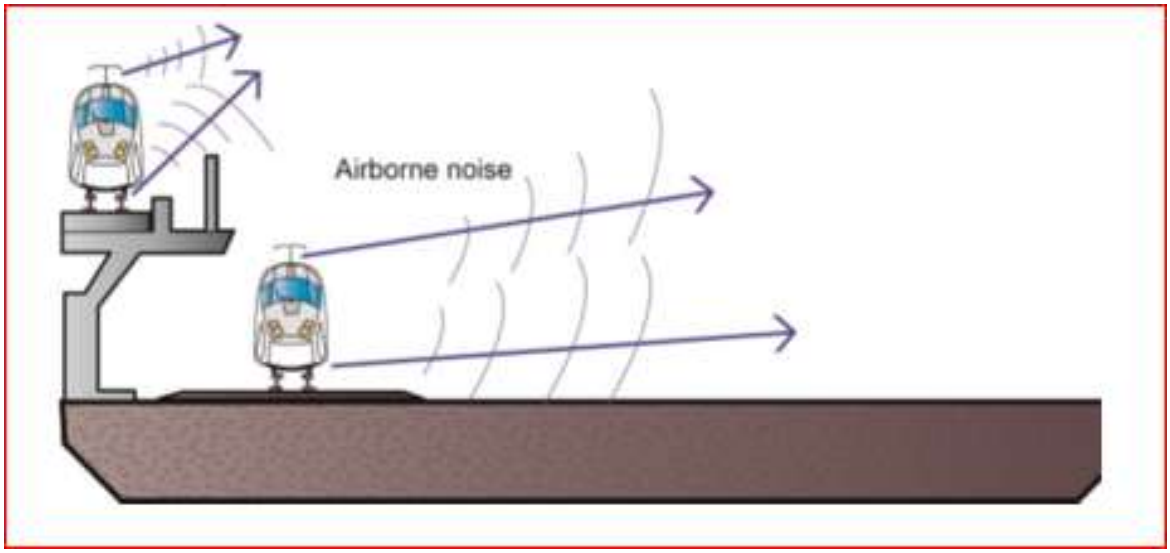


Figure 4-1: Direct environmental airborne noise from HSR. (Source: Temple-ERM, 2013)

In contrast to airborne noise, the ground-borne vibration generated by trains can have a major environmental impact on those living and working near a rail line. It involves noticeable movement of floors, shaking items from shelves, rattling windows, and so on (Hunt and Hussein, 2007).

In this study, noise costs fall into two categories: health and annoyance. First, at levels above 85 dB(A), transport noise can damage health, including hearing and cause nervous stress reactions such as changes in heartbeat frequency, hormones and blood pressure. Second, the annoyance can result in economic and social costs such as discomfort and limitations to the enjoyment of desired leisure activities (Maibach *et al.*, 2008). External HSR noise levels range from 80 to 90 dB(A) (Campos, de Rus and Barron, 2007b). The noise on board an HS train is an important aspect of the internal comfort, as high-speed operation usually generates rolling, aerodynamic, propulsion and equipment sounds (Maibach *et al.*, 2008).

The chief component of noise pollution by an electric train is the rolling of the steel wheels on the steel tracks, which is affected by the type of track, speed and conditions of both the rail's and the wheels' surfaces. The main cost drivers are foremost the type of brakes, then the presence of a noise barrier and the train's length (Maibach *et al.*, 2008).

This noise generally impacts on three land uses: land with residential buildings; quiet land with planned outdoor use; and land with daytime activities, such as schools,

businesses and libraries. Noise pollution for the population close to railway lines is usually avoided by erecting noise-mitigating barriers to keep the level down, decreasing it by around 20 dB(A) for a single barrier and 25 dB(A) for a double barrier (Janić, 2017). Noise is a major concern for HSR, and it needs to be reduced. For example, at 25 m from the tracks the French TGV is reported to generate 97 dB(A) at a speed of 272 km/h, and the German ICE 93 dB(A) at a speed of 300 km/h (Profillidis, 2014).

Levinson, Kanafani and Gillen (1999) evaluated the full cost of three intercity transport modes – air, road and HSR – in terms of economic investment along the California corridor linking Los Angeles to San Francisco. HSR produces less noise pollution for a given transport task than the other current transport modes, while its external noise cost has been estimated at €0.01803/1,000 passenger-km (Hume Regional Development, 2014). Estimates of HSR's expected noise cost are €0.0021/pkt and €0.0035/pkt at speeds of 200 km/h and 320 km/h, respectively, assuming five trains per hour (Levinson *et al.*, 1996).

Accident costs fall into many categories, such as medical and administrative, damage to materials and production losses. The strongest influences on the prevalence of rail accidents are the weather conditions, traffic volumes and degree of separation between transport systems, especially between types of trains (Maibach *et al.*, 2008). The HSR system is designed to reduce the possibility of accidents, and it has been proven by decades of safe operation to be the safest form of transport. Japanese Shinkansen is regarded as the world's safest HS service, as there have been no accidents due to collision or derailment since 1964. The only HSR accidents resulting in the injury and death of staff and passengers have been those in Spain, China and Germany in 2013, 2011 and 1998, respectively (Table 4-4).

| Country | No. of trains | Passengers on board | Year | Cause | Fatalities | Injuries |
|---|---|---|---|---|---|---|
| Germany | 1 | 287 | 1998 | Wheel breakup | 101 | 88 |
| China | 2 | 1630 | 2011 | Railway signal failure | 40 | 210 |
| Spain | 1 | 222 | 2013 | Extreme speed on bend | 79 | 139 |

Table 4-4: Main characteristics of fatal High-Speed Rail accidents. (Source: Janić, 2017)

Average external accident costs are usually calculated on the basis of up-to-date UIC accident statistics, and range from €0.08/train-km to €0.30/train-km in European countries at 2007 prices (Maibach *et al.*, 2008). The average accident cost on the proposed Melbourne–Canberra HSR line is estimated to rise to €1.23 per 1,000 passenger-km by 2036, compared to the total cost of passenger vehicle accidents in Australia, estimated at €14.09 billion (2009) to €22.95 billion (2011) (Edwards, 2012).

All transport modes, including HSR, emit pollutants and GHGs that can affect our climate, and this issue is one of the key topics of global research (Albalate and Bel, 2017). In this study, the energy-use impact is taken as dependent on average temperatures, due especially to warm-weather air conditioning (Maibach *et al.*, 2008). The embedded $CO_2$ emissions from constructing and maintaining an HSR line are often considerable because of the extensive use of concrete and steel, both of which are energy intensive to produce. As a result of traffic shifting from high-emitting modes of transport to a rail system upon the launch of a new HSR line, however, these emissions must be balanced by the consequent reduction in GHGs. In this case, current European power plants emit an average of between 410 and 443 g of $CO_2$ per kWh, as more than half of the power production is from the combustion of fossil fuels.

The proportion of open sections to tunnels on an HSR line is an important factor in the amount of embedded emissions. For example, for tunnel sections the emissions are assumed to range between 880 and 980 tonnes $CO_2$ eq. per rail-track km per year, and for open sections between 140 and 230 tonnes (Westin and Kågeson, 2012).

GHG emissions in Europe are planned to be cut to an average of 5.9 $gCO_2$/s-km, 1.5 $gCO_2$/s-km and 0.9 $gCO_2$/s-km by 2025, 2040 and 2055 (Janić, 2016). Meanwhile, the increase in temperature is an aspect of climate change that

represents a hazard to the rail network, as it causes increased track expansion. The ability of rail operators to maintain existing operating practices and avoid delays, especially during summer, is challenged by these temperature rises (Chinowsky *et al.*, 2017). The marginal cost to HSR from climate change is equal to €0.824/1,000 passenger-km, and this is the value used in this section (Albalate and Bel, 2017).

## 4.3 Magnetic Levitation Technology

### 4.3.1 Operator cost of Maglev

The total cost of the Shanghai Maglev project is €1.3 billion at 2017 prices as, due to its large population and vast area, for China the most appropriate system was the Transrapid (Dona and Singh, 2017). The total capital cost of this line includes the right-of-way clearance, on-site manufacture of the guideway, two stations, operation and control systems, cables, the power-feed system and switches.

The total cost of the Changsha Maglev project is about €1.07 billion, at 2017 prices, or €56.8 million/km, as shown in Table 4-5 (Dona and Singh, 2017).

| Maglev project | Country | Year of cost | Length (km) | Total project cost including trains (€billion) | 2017 consumer price index inflation | Project cost (€million/km) |
|---|---|---|---|---|---|---|
| Shanghai | China | 2004 | 30.0 | 1.07 | 1.6 | 56.8 |
| Changsha | | 2016 | 18.5 | 0.55 | 1.6 | 47.5 |
| Incheon Airport | South Korea | 2012 | 6.1 | 0.28 | 1.9 | 87.3 |
| Linimo | Japan | 2005 | 8.9 | 0.75 | 1.1 | 93.2 |
| Chuo Shinkansen | | 2016 | 285.6 | 73.77 | 1.1 | 284.1 |

Table 4-5: Total costs of Maglev projects. (Source: Dona and Singh, 2017)

By contrast, the estimated cost of the proposed Japanese Chuo Shinkansen Maglev line is around €73.8 billion, as the route includes 246.6 km of long tunnels through mountains, 4.1 km at grade, 11.3 km of bridges and 23.6 km of viaducts (Sato, 2014; Dona and Singh, 2017). The cost of the existing Linimo HSST Maglev (100 km/h) was approximately €88.5 million/km (McCourt, 2019). The South Korean IAM line's total cost was about €303 million, while its construction cost was €31.1 million/km at 2017 prices (Dona and Singh, 2017).

In general, the operation and maintenance (O&M) activities of a Maglev system include the maintenance of equipment, maintenance of the way, the cost of the trainset crew and other employees, energy cost and administration and insurance expenses (Ziemke, 2010).

The energy cost of Maglev trainsets depends heavily on the average operating speed, as higher speeds consume more energy per seat-kilometre. The Maglev Transrapid trainset, with six sections,[5] consumes around 20 kWh/km and 30kWh/km at speeds of 300 km/h and 400 km/h, respectively. The estimate for the operating and maintenance cost of Maglev systems is between €0.011 and €0.052 per seat-kilometre (Ziemke, 2010).

### 4.3.2 User cost of Maglev

Estimates of Maglev time information are based on distance from the road, calculated by dividing the distance of each origin–destination pair by the speed. For this study, in-vehicle travel time is computed from the number of stops, the distance and the number of transfers (Vyas and Rote, 1993). For example, the in-vehicle time for a non-stop Maglev express between two cities 600 miles apart is estimated at around two hours. In major metropolitan centres with more than one stop (i.e. airport, city centre), a wait of 2.5 mins is assumed at each stop. In terms of transfer, travelling to/from a smaller metropolitan statistical area might involve a transfer at a major hub, involving an average transfer delay of 30 mins (Vyas and Rote, 1993).

Regarding travel time, in areas where there is a constrained alignment the Maglev system performs better due its superior acceleration and braking rates, as well as its higher attainable speeds (Ziemke, 2010). The values for Maglev out-of-vehicle times, including access/egress time and waiting time, are calculated by multiplying the out-of-vehicle time of air travel by a factor of 0.75, assuming that metropolitan

[5] Six sections contain 500 passenger seats.

areas have more than a single Maglev station. As a result, the average distance to a Maglev station is less than the average distance to an airport (Vyas and Rote, 1993).

In terms of access to stations, the integration of a Maglev system in an urbanized area is generally simple due to its flexible alignment (Ziemke, 2010). For the Transrapid Maglev system, the minimum headway is dependent on the distance between propulsion blocks and power substations. As a one-drive control zone between two trains should remain free, there should be one propulsion block per track. For example, two propulsion blocks per substation control both trains, as the following train cannot enter the zone until the first has left. For the Maglev system, a minimum headway of 5 mins is technically feasible (Ziemke, 2010).

At a station, ‘dwell time’ is when the train comes to a standstill to allow passengers to embark and disembark and for essential technical procedures to be completed. For safety reasons, a Maglev train must be de-levitated and grounded before passengers can get in or out. As it is operated automatically, without a driver, the Transrapid Maglev has platform-edge doors to prevent passengers from entering the tracks. As a result, the overall dwell time of a Maglev train is around 30 seconds per stop, with six seconds to operate the platform-edge doors (Ziemke, 2010).

### 4.3.3 External cost of Maglev

In a Maglev system, the amount of land consumed depends on how the guideway is constructed. It has an appearance of a beam bridge, and pillars are necessary to create an elevated track. For example, the Transrapid Maglev route is usually raised on an elevated guideway for the most of the line, as in Shanghai (Ziemke, 2010), as shown in Figure 4-2.

An elevated guideway is suitable in areas where existing traffic routes must not be allowed to interfere with the Maglev line and in certain agricultural areas. In places with poor soils the guideway can be used without pillars, and this is frequently more economical (Transrapid International, 2002).

Figure 4-2: Transrapid Maglev train. (Source: Transrapid International, 2002)

For both elevated and at-grade guideways, a double-track guideway, centre-to-centre, measures 4.4 m for speeds of up to 300 km/h and 5.1 m for speeds up to 500 km/h, as shown in Figures 4-3 and 4-4. The standard beam span is 31 m, with a variable pillar height of 20 m so elevated guideways can adapt to the topography (Transrapid International, 2002).

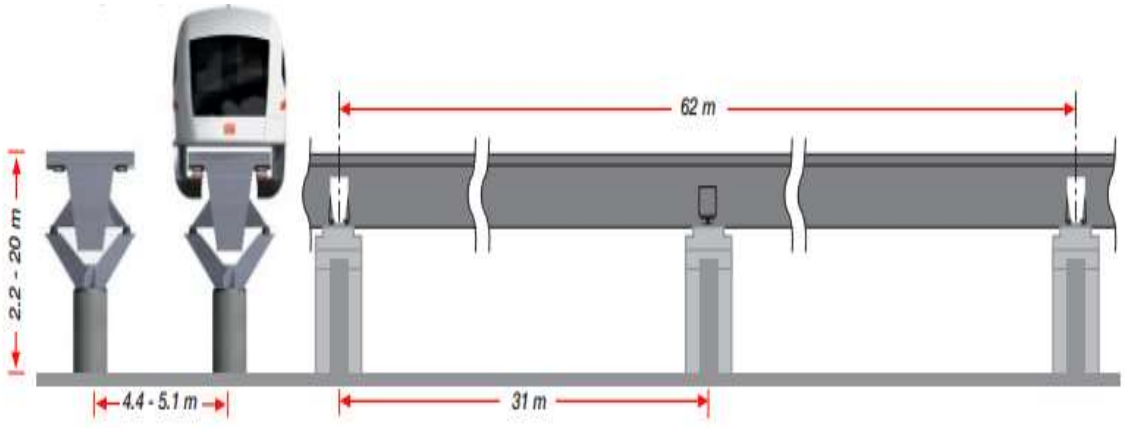


Figure 4-3: Elevated guideway. (Source: Transrapid International, 2002)

No land is required for an access road to the Transrapid Maglev for safety or for guideway maintenance (Ziemke, 2010). The at-grade guideway can be collocated in tunnels and cuttings, on primary civil structures such as stations and bridges, or along existing road and rail routes (Transrapid International, 2002).

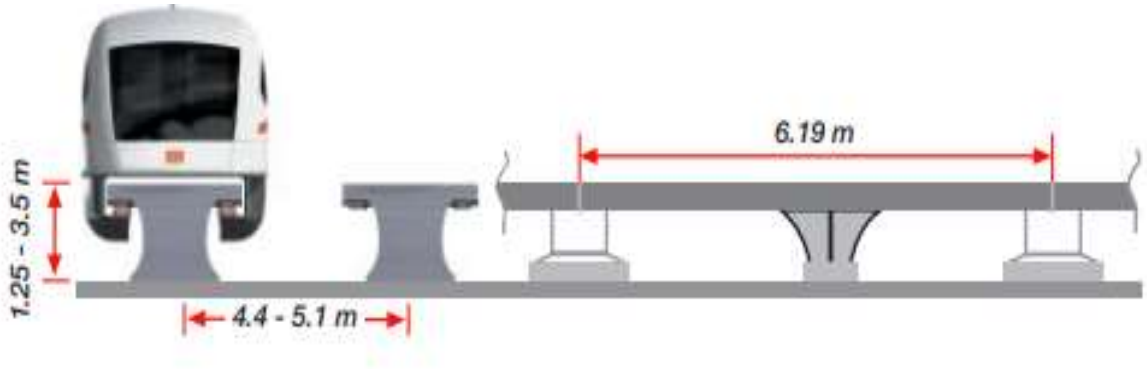


Figure 4-4: At-grade guideway. (Source: Transrapid International, 2002)

The areas of land needed for power substations and technical equipment are presented in Table 4-6. Some values are measures of ecological mitigation that might require further land.

| **Alignment** | **Land consumption ($m^2$ per m of double track)** |
|---|---|
| At-grade | 11.5 |
| At-grade plus mitigation measures (50%) | 17.0 |
| At a height of 5 m | 2.0 (elevated guideway) |
| At a height of 5 m plus mitigation measures (50%) | 3.0 (elevated guideway) |
| At a height of 12 m plus mitigation measures (50%) | 3.0 (elevated guideway) |

Table 4-6: Land consumption of the Maglev system. (Source: Ziemke, 2010)

The guideway infrastructure of Transrapid Maglev system can be seen to take very little space. For example, the land required for a standard elevated double-track guideway, including wayside equipment and substations, is around 2 $m^2$/m and about 12 $m^2$/m for an at-grade guideway (Transrapid International, 2002; Ziemke, 2010).

Energy consumption is considered to be the most important factor in environmental impact. It depends on the spacing of intermediate stations along the route, the route's geographical characteristics and the train's technology. For the Transrapid Maglev, the relative increase in energy consumption with speed is modest, due to its lower aerodynamic drag, as the energy consumption per kilometre is based on the average distance between stations (Ziemke, 2010). For example, the energy consumption of the Chuo Shinkansen and Transrapid Maglev systems along an open-air corridor at a maximum speed of 450 km/h is 78 Wh per seat-kilometre and

71 Wh per seat-kilometre, respectively (Eckert *et al.*, 2018). $CO_2$ emissions are highly dependent on the primary energy consumption and method and manner in which the raw materials generate the energy. For example, values of Transrapid's $CO_2$ emission range from 23 g to 33 g per seat-kilometre for speeds of 300 and 400 km/h, respectively (Transrapid International, 2002).

Maglev's noise emissions result from either aerodynamic, propulsion or guideway vibration. The first is dependent on aerodynamic drag, as its sources are the flow separation on the front and rear ends, the wake produced at the end and the flow interactions in the gap between the guideway and vehicle (Chen *et al.*, 2007; Ziemke, 2010). Additionally, noise emission at speeds over 250 km/h is due to the non-contact propulsion and levitation technology and amounts to 85 dB(A), as shown in Table 4-7 (Levinson *et al.*, 1996).

| **Speed (km/h)** | **Noise level (dB(A))** |
|---|---|
| 160 | 72 |
| 192 | 75 |
| 320 | 85 |

Table 4-7: Maglev noise levels at different speeds. (Source: Levinson *et al.*, 1996)

The Transrapid Maglev system produces magnetic fields along the guideway. The impact on passengers and the environment is low, at a value of 100 µT.

The Transrapid Maglev system is moderately unaffected by the weather since its propulsion components are situated beneath the guideway, protected from ice or snow, while there is a special vehicle to clear it away if it collects on the guideway itself. On the other hand, cross-winds and gusts have some effect on the Transrapid due to its guidance system and active control (Transrapid International, 2002).

On 22 September 2006, a Transrapid train on a test run in Emsland, Germany, crashed into a repair car that had been unintentionally left on the track. This was the first fatal accident involving a Maglev train (Cassat and Bourquin, 2011). It was running at 193 km/h at the time and had 29 people aboard, killing 23 and injuring 11.

On 11 August 2006, the Transrapid Shanghai Maglev line caught fire. This was caused by an electrical problem, and there were no injuries (Bonsor and Chandler,

2019). A damaged on-board storage battery was the possible cause. Smoke started rising from the second carriage after leaving Pudong International Airport station, as shown in Figure 4-5 (Xinhua, 2006).

Figure 4-5: Fire in Shanghai's Maglev. (Source: Xinhua, 2006)

## 4.4 Hyperloop Technology

### 4.4.1 Operator cost of Hyperloop

Van Goeverden *et al.* (2018) present an analysis and model of Hyperloop performance comprising five main categories of the operator costs of Hyperloop technology. First is the cost of constructing two parallel tubes and stations along them to operate capsules in both directions and the pillars to elevate the tubes. Second are the pumps needed to maintain vacuum conditions at specified parts within the tubes and stations. Third are the maintenance costs of the infrastructure. Fourth comes the fleet of Hyperloop capsules for the corridor, which can be either single or coupled together, operated by a magnetic linear accelerator located at stations to accelerate the capsules with the support of rotors attached to each. Finally come the maintenance and capsule control systems required to operate along the tube (Van Goeverden *et al.*, 2018).

Hyperloop capsules are to be operated in a low-pressure tube on a 0.5 to 1.3 mm cushion of air, using pressurized air and aerodynamics to reach their maximum speed of 1,220 km/h with a maximum inertial acceleration of 0.5 G The operational

performance involves a standard capacity of 28 seats per capsule and specific quality of service (Van Goeverden *et al.*, 2018).

The operator costs of Hyperloop include capital costs, operational costs and overhead costs. First, the capital costs comprise the infrastructure construction costs of tubes, pillars and stations, as well as the expense of purchasing the capsules. The capital cost of constructing a kilometre of tube is dependent on the local conditions, whether it is an empty area of flat, sandy soil, a highly urbanized area, over mountains or across moorland. The costs of building tubes raised on pillars or in tunnels are estimated at €10.3 million/km and €34.0 million/km, respectively, at 2015 prices, while the cost of a Hyperloop station is assumed to be €116 million, as in Table 4-8. The cost of a capsule is estimated at around €4.76 million and the average unit cost is thus €0.17 million per seat (Van Goeverden *et al.*, 2018).

| **Cost element** | | **Investment cost ($10^6$ €/km)** | **Annual cost ($10^6$ €/km)** | **Life span (years)** |
|---|---|---|---|---|
| Track infrastructure | Pillars, solid soil | 25 | 0.92 | 60 |
| | Pillars, weak soil | 35 | 1.28 | 60 |
| | Tunnel | 70 | 2.57 | 60 |
| Station | | 116 | 4.64 | 50 |
| Capsule | | 4.76 | 0.58 | 10 |

Table 4-8: Investment and annual capital costs for Hyperloop infrastructure and vehicles at 2015 prices. (Source: Van Goeverden *et al.*, 2018)

As an example, the estimated total construction cost of the Los Angeles–San Francisco Hyperloop route is €4.9 billion, to include guideway construction, stations and capsule fabrication. The cost of individual items for this route may be underestimated in the total construction cost of the Hyperloop system, as shown in Table 4-9. The cost is based on two tubes of a diameter of just 3 m, as the cost increases with the diameter. Some 25,000 concrete pillars might be needed along the route, and the cost will increase further if more are added. Total costs of €41 million/km and €102 million are estimated for tunnel construction and station construction, respectively (Taylor, Hyde and Barr, 2016).

| Element | Description | Cost (€million) |
|---|---|---|
| Tube construction | 1141 km of tube | 533 |
| Pillar construction | 25,000 | 2,090 |
| Tunnel construction | 24.5 km of tunnel | 492 |
| Propulsion | linear induction motors | 115 |
| Solar panels and batteries | panels cover both direction | 172 |
| Station and vacuum pumps | 2 stations | 213 |
| Permits and land | largely in I–5 ROW | 820 |
| **Total** | | **4,434** |

Table 4-9: Estimated cost of Hyperloop tube at 2015 prices. (Source: Taylor, Hyde and Barr, 2016)

Second, the operational cost includes the vehicle and station costs, the infrastructure and capsule maintenance costs, and the traffic management costs. In this type of cost, the cost of staffing the Hyperloop capsules and stations is dependent on the organization's stipulated numbers of employees per capsule and for control and ticket sales. For a single capsule and station, the numbers of full-time workers are assumed to be 2.14 and 5.15, respectively, with an average annual wage of €35,500. The annual operating cost for a single capsule and station is estimated at €75,000 and €180,000, respectively (Van Goeverden *et al.*, 2018). Traffic management cost is dependent on the challenges of the network, and is equal to the wage of one worker for each 1,000 km of tube, thus is €90/km (Van Goeverden *et al.*, 2018).

Hyperloop capsule cost is expressed per seat and seat-kilometre, as the capacity of a capsule is assumed to be a standard 28 seats, as shown in Table 4-10, with an average operating speed of 600 km/h and an average operation time of 15 hours per day (Van Goeverden *et al.*, 2018).

| Cost element | | Unit | Investment cost (€) | Maintenance cost (€) | Operating & overhead cost (€) | Total cost (€) |
|---|---|---|---|---|---|---|
| Track infra-structure | pillars, solid soil | Km | 917,000 | 91,700 | 100 | 1,008,800 |
| | pillars, weak soil | Km | 1,280,000 | 128,000 | 100 | 1,408,100 |
| | Tunnel | Km | 2,570,000 | 257,000 | 100 | 2,827,100 |
| Station | | Station | 4,640,000 | 464,000 | 200,000 | 5,304,000 |
| Capsule | | Vehicle | 580,000 | 58,000 | 82,500 | 720,500 |
| | | Seat | 21,000 | 2,100 | 3,000 | 26,100 |
| | | seat-km | 0.006 | 0.0006 | 0.0009 | 0.008 |

Table 4-10: Estimated annual costs of Hyperloop system at 2015 prices. (Source: Van Goeverden *et al.*, 2018)

Finally, the overhead cost is based on the capital and maintenance costs of real estate and staff costs. The real estate costs are marginal compared to Hyperloop's infrastructure capital and maintenance costs (Van Goeverden *et al.*, 2018).

For the proposed Hyperloop between Los Angeles and San Francisco, the total cost of the passenger transportation system is €44.3 million for 40 capsules, as shown in Table 4-11.

| Component | Cost (€million) |
|---|---|
| Capsule structure & doors | 8 |
| Interior and seats | 8.4 |
| Compressor and plumbing | 9 |
| Batteries and electronics | 4.9 |
| Propulsion | 4.1 |
| Suspension and air bearings | 6.6 |
| Component assembly | 3.3 |
| **Total** | **44.3** |

Table 4-11: Estimated annual costs of Hyperloop capsule at 2015 prices. (Source: Musk, 2013)

The cost of acquiring land could be reduced by building the Hyperloop on pillars and by using existing road and rail routes. The tubes of Hyperloop need to be straight if they are to achieve its potential operating speeds and, for passengers' comfort, keep

the lateral forces below 0.1 G (Walker, 2018). Furthermore, it is hard to implement straight lines in countries such as the United Kingdom that have dense urban space, hilly topography, numerous protected landscapes and expensive land values. On the other hand, building Hyperloop lines underground makes emergency evacuation and maintenance more difficult and increases the capital costs (Walker, 2018).

### 4.4.2 User cost of Hyperloop

In terms of the service quality, user travel time in the Hyperloop system consists of access/egress time, waiting time and in-vehicle travel time. First, access/egress time depends on the interconnectivity of the modes of transport from the user's door to the Hyperloop station and vice versa, and is generally based on traffic conditions and the speed of the transport systems (Van Goeverden *et al.*, 2018). Access/egress time is also dependent on the location of Hyperloop terminals (stations), as although having city-centre sites can reduce the time for passengers to go to/from the stations, the associated costs of land acquisition will be higher due to building in areas of high population density (Taylor, Hyde and Barr, 2016).

Second, waiting time is dependent on service frequency and is affected by delays to the schedule. Waiting time at a Hyperloop station will be shorter than the schedule delay if the frequency is more than six capsules per hour. Poor punctuality leads to increased waiting time, as it is generally associated with similar services regarding destination, route and intermediate stops (Van Goeverden *et al.*, 2018). Regarding frequency, it has been assumed that a Hyperloop will depart every 2 mins, or every 30 seconds during peak periods, and that this will reduce waiting time (Taylor, Hyde and Barr, 2016).

For the proposed Los Angeles–San Francisco Hyperloop line, a minimum of 28 seats per capsule and an average departure of 2 mins between capsules has been assumed, catering for 840 passengers per hour. As the proposed line requires up to 40 capsules in the rush hour, capacity can be increased by reducing the time between departures (Jain, 2016). A single tube on the proposed Los Angeles–San Francisco line would be able to transport about 7.4 million passengers per year with capsules departing every 30 seconds, each carrying 28 passengers (Nath, 2018).

Table 4-12 shows the daily passenger capacities for various Hyperloop capsule sizes for the proposed London–Edinburgh corridor.

| Transport type | Hyperloop small capsule | Hyperloop big capsule |
|---|---|---|
| Capacity (seats) | 28 | 40 |
| Departure times | 5:30am–10pm | 5:30am–10pm |
| Services per day | 568 | 398 |
| Services per hour | 32 | 22 |
| Departure frequency | every 113 seconds | every 163 seconds |
| Capacity per day | 15,904 | 16,520 |

Table 4-12: Capacity of different Hyperloop sizes. (Source: Walker, 2018)

Finally, the in-vehicle travel time of a Hyperloop system depends on the length of the corridor, the average speed and the dwell time at any intermediate stations. In this case, in-vehicle time and interchange time are generally correlated to door-to-door distance as, in the long-distance travel market, there are at least two interchanges between the access mode and the Hyperloop station, and between the Hyperloop station and the egress mode (Van Goeverden *et al.*, 2018). To predict mass-market demand for Hyperloop, it is vital to understand the main factors of travel time, such as in-vehicle travel time, security screening, reliability of journey time, boarding and VOT, among various wider factors such as convenience, crowdedness, cost and comfort (Walker, 2018).

### 4.4.3 External cost of Hyperloop

The external environmental indicators of a Hyperloop system include its noise, energy consumption, safety, land use and GHG emissions. People living or working close to a transport network can suffer annoyance and experience harm from the noise that is generated. In this study, the impact of noise is based on the level at the source, the duration of the exposure and the numbers of people affected.

It is hard for a Hyperloop system to produce external noise, because the capsule is not in contact with the tube and there is no vibration to be transferred. The only noise is from the vacuum pumps, but this will not be detected outside the tube, making the Hyperloop ultimately less environmentally damaging than current alternative modes of transport (Van Goeverden *et al.*, 2018; Walker, 2018). In this case, the energy consumed by the vacuum pumps is also considered. To maintain the required

vacuum in the Hyperloop tube, it is assumed that the pumps operate almost all the time (Janić, 2020). The Hyperloop system is estimated to be more energy efficient than other modes of transport, as it is to be propelled entirely by the electrical energy obtained from the solar panels placed on top of the tubes; indeed, the system will generate more than is needed (Van Goeverden *et al.*, 2018). Due to the rapid acceleration that enables the capsules to glide as a passive Maglev in a near vacuum, the Hyperloop system consumes little energy: an estimated 50 MJ per passenger (Walker, 2018). The system is expected to have no external safety concerns as it is designed on the fail-safe principle, using an emergency braking system. If any system on board fails, the capsule comes to a standstill (MIT Hyperloop Team, 2017; Van Goeverden *et al.*, 2018). In general, the Hyperloop system will not create GHG emissions from energy consumption. However, there are indirect emissions from the construction of its infrastructure, and these should be taken into account to estimate the system's life-cycle emissions of GHGs (Van Goeverden *et al.*, 2018). In the United Kingdom, for the proposed London–Edinburgh line the operational carbon emissions for Hyperloop are predicted to be in the region of 4 to 7 kg per passenger (Walker, 2018).

The cost of the land occupied by the Hyperloop system relates to the extent of the infrastructure needed and the land's value. In the case study, the Hyperloop system is planned to be elevated on pillars, so the effective occupation of ground is limited. The net area needed for a single kilometre of Hyperloop tube is about 0.5 hectare,[6] since the pillars are spaced on average at 30 m and there is limited opportunity to use the space on the ground between them (Van Goeverden *et al.*, 2018).

[6] One hectare is equal to 10,000 $m^2$, and is usually used to measure land.

## 4.5 Background to the Case Study

KSA as shown in Figure 4-6, is in the Middle East region, with an estimated size of 2.21 million square km. It shares borders with Kuwait, Jordan and Iraq to the north, Oman and Yemen to the south, UAE, Qatar, Bahrain and the Persian Gulf to the east and the Red Sea to the west (Ministry of Municipal and Rural Affairs, 2016).


Figure 4-6: Map of Saudi Arabia. (Source: Einstein, 2007)

In KSA, demographic surveys are an important source of the data essential to development planning in the social and economic fields at both national and domestic levels. The population increased by 8.17% from 2015 to 2019, from 31.6 million to 34.1 million people, as shown in Table 4-13, with an average annual increase of 2.52% (GMI, 2020).

| Year | Population (million) | Growth rate (%) |
|---|---|---|
| 2015 | 31.56 | N/A |
| 2016 | 32.28 | 2.28 |
| 2017 | 32.55 | 3.14 |
| 2018 | 33.55 | 6.31 |
| 2019 | 34.14 | 8.17 |

Table 4-13: Population of Saudi Arabia (2015–2019). (Source: GMI, 2020)

The discovery of oil changed the Kingdom from a pre-industrial to a modern industrial country and made it one of the richest developing nations; its wealth is from oil revenues (Al-Ahmadi, 2006). Saudi Arabia has experienced a massive boom since the discovery of Ghawar field, the largest oil field ever discovered (GMI, 2020).

According to the World Bank, KSA's GDP increased by 14% from 688.6 in 2017 to 786.5 billion US$ in 2018, as shown in Table 4-14.

| Year | GDP (billion US$) |
|---|---|
| 2013 | 746.65 |
| 2014 | 756.35 |
| 2015 | 654.27 |
| 2016 | 644.94 |
| 2017 | 688.59 |
| 2018 | 786.52 |
| 2019 | 792.97 |

Table 4-14: GDP of Saudi Arabia (2013–2018). (Source: World Bank, 2020b)

As it is one of the world's largest exporters and the sector contributes about 45% of the total country's GDP (Esmail, 2018), the Kingdom is dramatically dependent on the price of oil. After experiencing a global decline in oil prices that had an impact on the economy, the Saudi government decided to reduce the country's dependence on oil through developing a strategic development plan: Vision 2030. This will help the nation to diversify its economic base and focus on further development aspects to create jobs and raise income. Tourism is considered to be one of the most significant aspects of this transformation, and it is to contribute about 6.1% of total GDP. Existing tourism activities in Saudi Arabia are dominated by religious tourism, commonly known as pilgrimage tourism, which is undertaken by

Muslims worldwide (Abuhjeeleh, 2019). According to World Bank Data, the number of annual international tourists grew from 10 to 15 million from 2010 to 2018, respectively, as shown in Table 4-15.

| Year | Nos. of tourists (thousand) |
|---|---|
| 2010 | 10,850 |
| 2011 | 14,179 |
| 2012 | 16,332 |
| 2013 | 15,772 |
| 2014 | 18,260 |
| 2015 | 17,994 |
| 2016 | 18,044 |
| 2017 | 16,109 |
| 2018 | 15,334 |

Table 4-15: Nos. of international tourists visiting Saudi Arabia per year. (Source: World Bank, 2020a)

As a part of Vision 2030's tourism plans, the government aims to improve other attractions, such as the Kingdom's unique geographical appeal, culture and heritage. In accordance with Vision 2030, the transport and logistics sector has been assigned several key milestones (Abuhjeeleh, 2019). As a result, this study is considered very much part of Saudi Arabia's transport system development through introducing alternative of HSGT technologies.

## 4.6 Existing Transport Modes Along Riyadh–Dammam Corridor

The case study of the proposed Riyadh–Dammam line compares the total travel time and total travel costs (fares) of existing transport modes. The in-vehicle time for air transport is about an hour, while car, bus and conventional train travel take around 4 hours, 6.25 hours and 4.25 hours respectively, as shown in Figure 4-7. The bus takes the longest due to the speed limit on the Riyadh–Dammam road, followed by conventional rail due to the rolling stock used on this line (Toumi, 2018). CAF push-pull trainsets also serve the Riyadh–Dammam conventional line, and these operate at a higher speed of 180 km/h (Toumi, 2018).


Figure 4-7 Riyadh–Dammam corridor, using different transport modes. (Source: Google Maps)

### 4.6.1 Conventional train

The Saudi Railway Organization (SRO) has managed the Riyadh–Dammam conventional rail service since it opened for public service in 1981. It traverses the desert dunes via Hofuf and Bqaiq, covering 449 km in 4.5 hours. The track gauge is 1,600 mm and the line is equipped with the European Train Control System Level 1, the first implementation of this technology in the Arab world. In September 2018, the SRO increased the frequency between Riyadh and Dammam to 82 trips per week, between Dammam and Hofuf to 88 trips, and between Riyadh and Hofuf to 68. This total of 238 trips per week can be compared to the previous 35 (Alsugair, 2016).

Saudi Arabia has an ambition for a more extensive railway network, and projects are commencing in the eastern and western regions of the country. Forthcoming projects include the HHSR line (partly operational) connecting Mecca and Medina via Jeddah and Rabigh; the North–South rail (partly operational) linking Riyadh with Qurayyat via Majmah, Qassim, Hail and Al Jouf; and the Landbridge rail (planned) between Riyadh and Jeddah and Dammam and Jubail (Aldagheiri, 2010).

### 4.6.2 Bus

In Saudi Arabia, the bus service is regarded as a transport option along the Riyadh–Dammam corridor, and is provided by the Saudi Arabian Public Transport Company

(SAPTCO). SAPTCO was established in 1980 under government sponsorship and is managed by the Ministry of Transportation. According to the SAPTCO website, the trip takes about 6 hours, with fares ranging from €10.2 to €16 and 18 trips a day in each direction from 2 am to 12 midnight. Bus transport commonly makes multiple stops to serve places along the route.

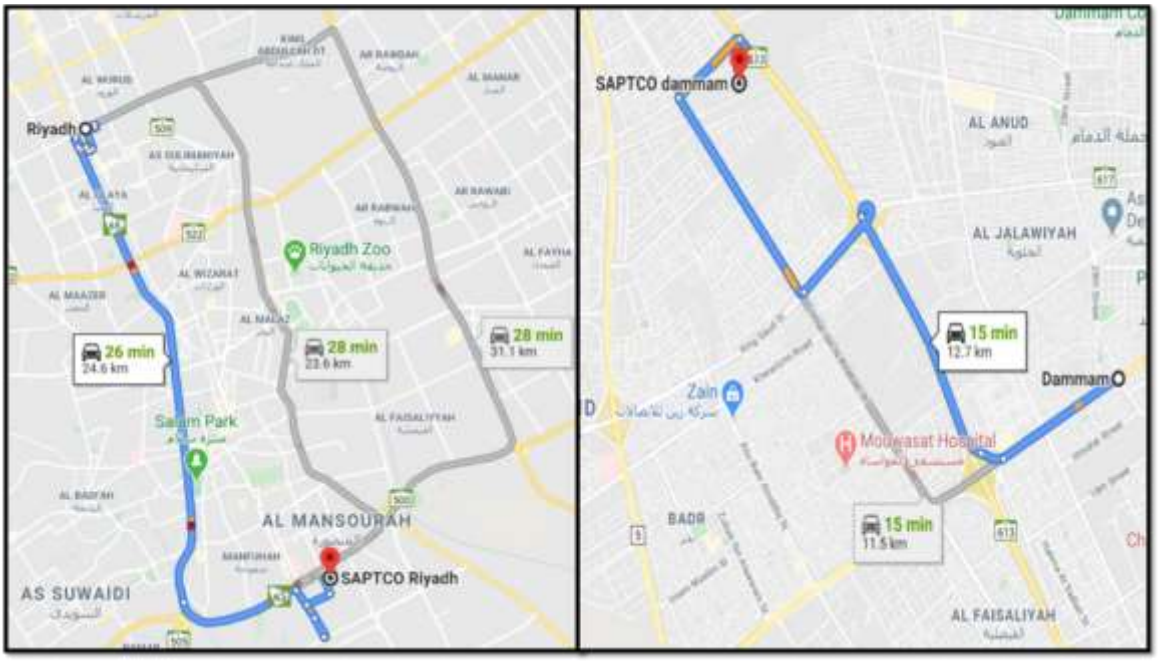


Figure 4-8: Driving to/from Riyadh SAPTCO station and to/from Dammam SAPTCO station. (Source: Google Maps)

As shown in Figure 4-8, Riyadh bus station is to the south of city and 24.4 km away, while Dammam's bus station is to the west of the city and 12.7 km away.

### 4.6.3 Car

A car is a personal mode of transport with a maximum capacity of five people. In Saudi Arabia, it is the most popular option and the dominant mode of intercity transport, and this has led to pollution, congestion and accidents. Riyadh has the highest rate of vehicle movement in the country, with vehicles entering daily from various cities across Saudi Arabia. More than 61,000 per day enter from Dammam (Ministry of Transport, 2017). Travel by car between the two cities is either direct on the Riyadh–Dammam main road, over a distance of 409 km, or via Hofuf city, over a distance of 474 km, as shown in Figure 4-9.

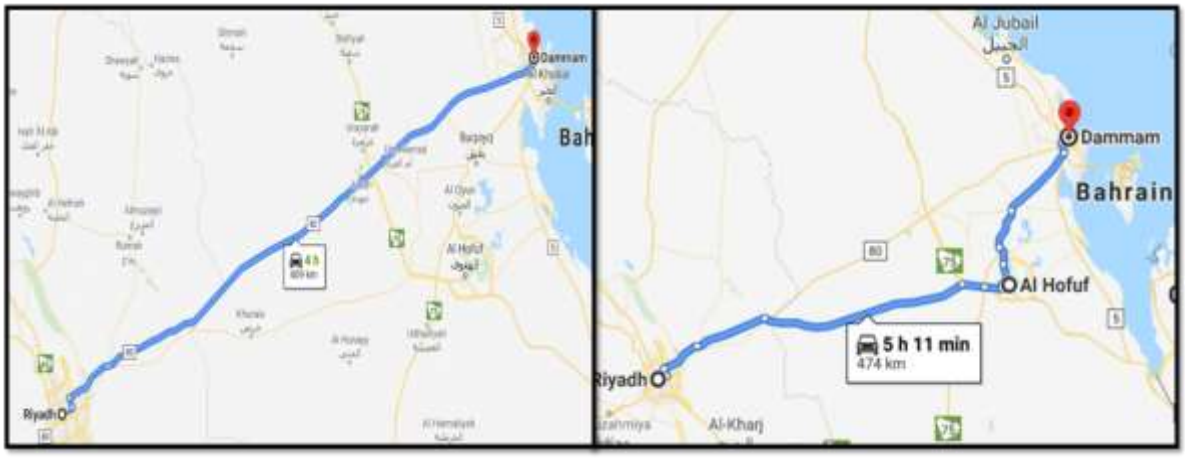


Figure 4-9: Driving on main road between Riyadh and Dammam and via Hofuf. (Source: Google Maps)

In 2018, KSA traffic police made the decision to increase the speed limit for cars on major roads from 120 km/h to 140 km/h (e.g. Riyadh–Dammam highway) in both directions (Toumi, 2018).

### 4.6.4 Air transport

The Saudi Civil Aviation Authority is developing its airport infrastructure by building 27 airports to serve all regions. The development includes three main international airports, namely King Abdulaziz International Airport in Jeddah, King Khaled International Airport in Riyadh and King Fahad International Airport in Dammam (General Authority of Civil Aviation, 2016). There are 21 flights from Riyadh to Dammam daily, on Saudi Airlines (Saudia), Flynas and Himalaya Airlines. The average flight time is one hour and 50 mins, including access/egress times (General Authority of Civil Aviation, 2016). In this study, one of the main reasons for including access/egress time in average travel time between the two cities by air is the rather remote location of their airports. On the other hand, by assuming that the travellers arrive at airports just in time for their flights, any waiting time is excluded.


Figure 4-10: Driving to/from Riyadh King Khalid Airport and Dammam King Fahd Airport. (Source: Google Maps)

King Khalid International Airport is to the north of Riyadh, as shown in Figure 4-10, at a distance of 36.7 km, while King Fahd International Airport is to the west of Dammam at a distance of 37.7 km.

## 4.7 Conclusion

Since it was discovered in 1938, oil has made KSA one of the richest countries in the Middle East, but the economy has become heavily dependent on its revenues. The Saudi government wishes to reduce this dependency and has launched a strategic development plan, Vision 2030, to diversify the economy into sectors such as tourism and to improve the Saudi business environment.

Part of this diversification includes the development of new HSGT systems such as HSR, Maglev and Hyperloop. This chapter has shown that there is sufficient documentary evidence to permit the computation of total social costs for these three modes.

The chapter has also shown that the Riyadh–Dammam corridor is a good case on which to apply the methodology developed in this study, as its length of 412 km is served by four transport modes: conventional rail, car, air and bus. Total travel time and cost are considered to be the chief factors behind travellers' choice of mode of transport between KSA's two main cities related to economic activity. Travel by air or conventional rail involves the longest access/egress time, due to the rather

remote location of the stations and airports. This also makes the total travel cost more expensive than just using the car.

# Chapter 5. Developing the Direct Demand Model

## 5.1 Introduction

This chapter develops a DDM for input into the TSCM. The DDM based on various parameters in order to estimate demand for HSR systems considered by this study. Section 5.2 shows the process of forecasting travel demand for HSR corridors worldwide, using the direct-demand regression model. A comparison is undertaken of linear-linear and log-linear functional relationships between the dependent and independent variables to select the best-fit model using the Box-Cox test. The DDM is based on the dependent variable of demand and independent variables of population, mean GDP per capita, mean speed, mean service frequency, mean fare and dummy variable per month.

SPSS software was used to determine the output regression analysis for both linear-linear and log-linear, which involved the model coefficients and Pearson's correlation between the independent variables themselves. It ascertained the model elasticity, the Shapiro-Wilk test of normality for residuals and causes of error such as autocorrelation, multicollinearity and heteroscedasticity.

Section 5.3 presents the EDM to forecast travel demand for a generic proposed Maglev system, based on generalized journey times for HSR and Maglev. The chapter ends with a summary in section 5.4 of the chosen log-linear DDM and the main parameters included in the EDM.

## 5.2 Direct Demand Model

To estimate the level of demand for potential HSR corridors worldwide, a direct-demand regression model was developed for application to the proposed Riyadh–Dammam HSR line. It features two functional relationships between the dependent and independent variables: linear-linear ($Q = a + bp$) and log-linear ($\log Q = a + bp$). The log-log was estimated, yet the parameter values were not plotted. It was decided to not use them, as some estimated parameter values were implausible.

In this section, multiple linear regression analysis is undertaken using aggregate, pooled cross-sectional and time-series data:

$$Y = \beta_0 + \beta_1 X_1 + \beta_2 X_2 + \ldots\ldots\ldots\ldots\ldots\ldots\ldots\ldots + \beta_n X_n$$ Equation 5-1

where

$Y$ = dependent variable or level of demand for the regression model

$X_1, X_2, \ldots\ldots\ldots\ldots, X_n$ = independent or explanatory variables that are used to predict the dependent variable (Y)

$\beta_0$ = intercept or the constant of the regression model

$\beta_1, \beta_2, \ldots\ldots\ldots, \beta_n$ = unstandardized regression coefficients for all predictors

For the cities along the proposed corridor, demand-level forecasts were based on independent socioeconomic variables such as the population, mean GDP per capita, number of trains per day, mean speed, mean fare and a dummy variable per month. The dummy variable was added to handle variations in these data sets. Observed historical demand was used as the dependent variable, based on combined data from the existing North–South and Riyadh–Dammam corridors for eight stations (Riyadh, Hofuf, Bqaiq, Dammam, Majmaah, Qassim, Hail and Al Jouf) between 2011 and 2018. IBM SPSS software was used to determine the coefficients' variables for the travel demand forecasting model, as it can help to show the correlation of each independent variable to the level of demand.

### 5.2.1 Historical data of demand

Historical demand data are essential to develop a demand-forecasting model. The aim was to forecast travel demand for the proposed case-study HSR line over the coming decade. However, because the line has not yet been built, the model must rely on secondary demand data. These secondary data were collected from the North–South (conventional) railway corridor that was opened in 2017 by the Saudi Railway Company (SAR) to connect Riyadh with Qurayyat via the cities of Majmaah, Qassim, Hail and Al Jouf, a length of 1,250 km. Moreover, data were gathered from the existing conventional Riyadh–Dammam rail line via Hofuf and Bqaiq, as shown in Figure 5-1. In this case, data were collected for the non-stop origin–destination pair of Riyadh–Dammam and parts of that route, with stops at the intermediate stations of Hofuf and Bqaiq.


Figure 5-1: Combined existing Riyadh–Dammam and North–South conventional lines[7]

The collected data include monthly figures from the North–South corridor between 2017 and 2018 and from the eight stations on the Riyadh–Dammam corridor between 2011 and 2018. For the Riyadh–Dammam conventional rail corridor the data covered eight years, yielding a total of 96 monthly observations. The North–South conventional rail line was opened to the public only in February 2017, hence there are just 22 full-month observations. The monthly passenger count on the Riyadh–Dammam conventional rail line is presented in Table 5-1, where it can be seen to have increased by 40% from 1.4 million in 2011 to 1.8 million in 2018.

[7] Note: The Haramain High-Speed Rail (HHSR) line shown in the figure was fully opened to the public only in October 2019, so it is not included in the historical demand data, while Qurayyat station is not yet operational.

| Month/ year | 2011 | 2012 | 2013 | 2014 | 2015 | 2016 | 2017 | 2018 |
|---|---|---|---|---|---|---|---|---|
| Jan | 90,155 | 114,911 | 108,456 | 62,386 | 115,191 | 117,416 | 123,732 | 159,302 |
| Feb | 100,177 | 100,853 | 89,743 | 124,761 | 100,558 | 101,522 | 89,600 | 148,212 |
| Mar | 108,113 | 122,398 | 115,726 | 87,341 | 124,906 | 122,290 | 132,073 | 156,792 |
| Apr | 98,190 | 107,421 | 101,577 | 133,001 | 107,005 | 111,389 | 143,072 | 166,398 |
| May | 110,159 | 105,402 | 96,080 | 99,818 | 105,023 | 118,236 | 122,359 | 139,338 |
| June | 104,606 | 113,637 | 99,245 | 112,281 | 98,942 | 85,814 | 90,274 | 139,848 |
| July | 110,802 | 79,036 | 73,909 | 106,057 | 101,026 | 113,599 | 124,671 | 155,641 |
| August | 116,917 | 100,300 | 95,098 | 78,864 | 118,950 | 120,057 | 128,565 | 163,746 |
| September | 105,315 | 86,106 | 102,307 | 118,428 | 118,296 | 107,916 | 122,533 | 139,724 |
| October | 121,011 | 98,132 | 88,957 | 93,580 | 108,227 | 110,672 | 132,580 | 143,630 |
| November | 129,351 | 86,396 | 113,481 | 150,110 | 109,984 | 124,923 | 136,938 | 153,264 |
| December | 100,335 | 95,975 | 95,128 | 81,102 | 108,575 | 117,433 | 138,254 | 147,814 |
| **Total** | **1,295,131** | **1,210,567** | **1,179,707** | **1,247,729** | **1,316,683** | **1,351,267** | **1,484,651** | **1,813,709** |

Table 5-1: Collated demand of the Riyadh–Dammam conventional rail line 2011–2018

For the last two years of data (2017 and 2018), demand increased strongly to 143,072 and 138,254 passengers in April and December, as in Figure 5-2. In 2018, demand on the Riyadh–Dammam corridor increased strongly in March, November and April to 156,792, 153,264 and 146,398 passengers, respectively. It is clear that the number of KSA rail passengers is affected by the three holidays that usually fall in these months: Eid Al-Fitr; Eid Al-Adha; and Saudi National Day.

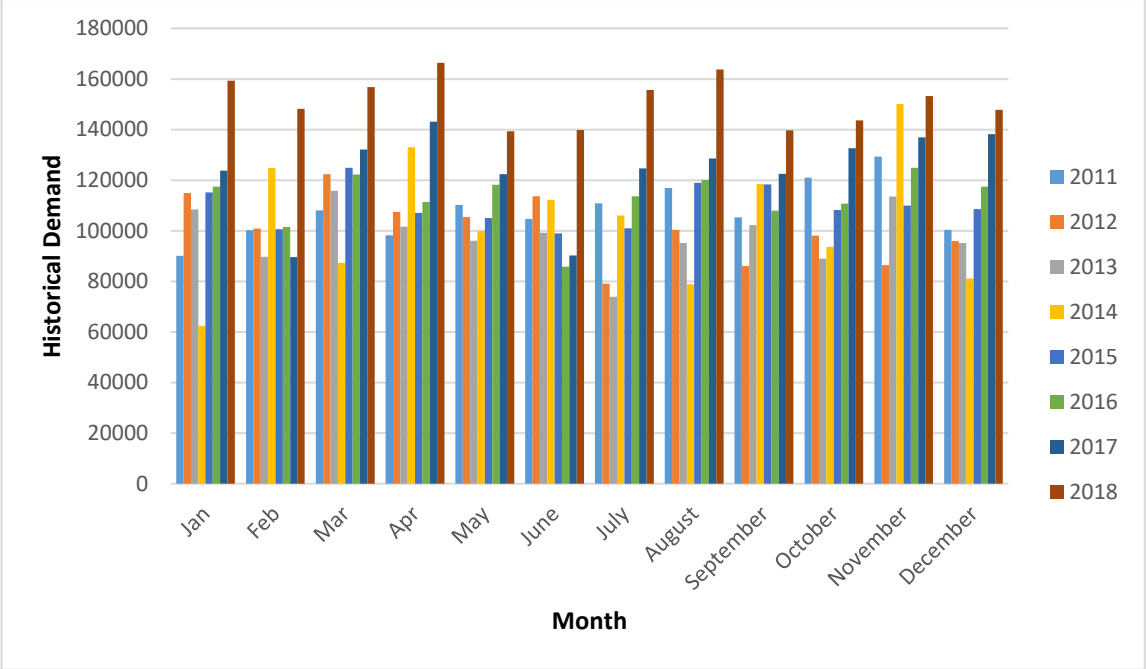


Figure 5-2: Passenger demand for existing Riyadh–Dammam conventional rail

On the North–South conventional rail line, passenger numbers increased by 134% from 159,189 in 2017 to 372,136 in 2018, as seen in Table 5-2.

| Month/year | 2017 | 2018 |
|---|---|---|
| January | 0 | 27,227 |
| February | 834 | 17,815 |
| March | 17,760 | 32,374 |
| April | 16,821 | 29,214 |
| May | 9,742 | 27,834 |
| June | 11,722 | 37,547 |
| July | 18,339 | 35,037 |
| August | 20,378 | 39,757 |
| September | 17,777 | 30,560 |
| October | 13,230 | 29,325 |
| November | 15,710 | 32,677 |
| December | 17,876 | 41,769 |
| Total | 159,189 | 372,136 |

Table 5-2: Collected demand of the North–South conventional rail line 2017–2018

As shown in Figure 5-3, demand increased strongly in both August and December 2018, to 39,757 and 41,769 passengers, respectively, and was also high in July and August, at 18,339 and 20,378 passengers.

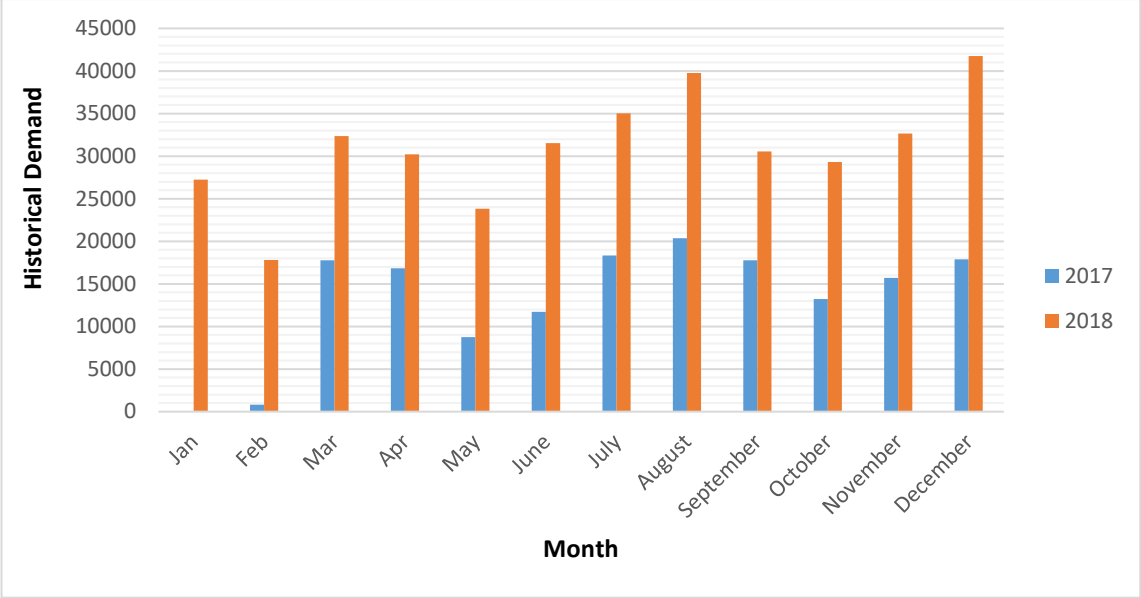


Figure 5-3: Passenger demand for existing North–South conventional rail

As a result, the combined data set comprises 12 and 20 directional origin–destination pairs[8] from the Riyadh–Dammam and North–South lines, respectively, making an overall total of 118 observations. Since the collected historical demand data are a combination of time-series and cross-sectional data, they are considered as pooled data.

### 5.2.2 Selecting the Covariates

Many factors (variables) are associated with models for forecasting travel HSR demand, such as population, mean GDP per capita, mean train service frequency and mean speed. In this case population, mean GDP per capita, mean service frequency, mean speed and mean fares are factors with a major impact on demand. Moreover, the data are available and can be collected easily. For example, in this case study the key to predicting HSR demand is the variable of mean speed, as by increasing its speed the rail service can be considered to be an HSR. In this case,

[8] Note: Riyadh–Dammam line has four stops = (4x4)-4=12 and North–South line has 5 stops = (5x5)-5=20. The overall monthly total of 118 was observed from (8 years x 12 months) = 96 for R–D line and (2 years x 11 months) = 22 for N–S line.

the variable specifications were also chosen to minimize correlation. For instance, the unemployment rate was tested; however, it was not reported because, due to insufficient data, it turned out to be insignificant.

#### 5.2.2.1 Population

Population is the main data parameter needed to establish and build a demand travel model, especially for cities with a population greater than 50,000. In this case, the average age has generally been increasing for many years and is expected to continue rising for the foreseeable future. An ageing population has significant effects on travel behaviour, such as the car-mode share, the percentage of work-related travel and the time of day (Cambridge Systematics *et al.*, 2012). For the proposed Riyadh–Dammam HSR corridor, population data were obtained from the Saudi General Authority for Statistics (SGAS). Table 5-3 presents the population statistics from 2011 to 2018 on the Riyadh–Dammam conventional rail corridor.

KSA's most populous city is Riyadh, whose population increased from about 5.4 million in 2011 to 6.8 million in 2018, making up 20% of KSA's total. In the same period, the population of Dammam, Bqaiq and Hofuf cities comprised 3%, 0.2% and 4% of the country's total, respectively.

| Year | Population of Riyadh | Population of Bqaiq | Population of Hofuf | Population of Dammam | Total |
|---|---|---|---|---|---|
| 2011 | 5,388,490 | 57,012 | 1,151,797 | 898,082 | 7,495,381 |
| 2012 | 5,571,362 | 58,947 | 1,190,887 | 928,560 | 7,749,756 |
| 2013 | 5,874,371 | 65,936 | 1,341,074 | 989,895 | 8,271,276 |
| 2014 | 6,070,810 | 67,983 | 1,392,422 | 999,135 | 8,530,350 |
| 2015 | 6,193,696 | 69,098 | 1,410,148 | 1,025,449 | 8,698,391 |
| 2016 | 6,294,999 | 71,777 | 1,420,683 | 1,060,097 | 8,847,556 |
| 2017 | 6,541,197 | 73,065 | 1,430,351 | 1,100,983 | 9,145,596 |
| 2018 | 6,796,505 | 75,907 | 1,448,756 | 1,132,660 | 9,453,827 |

Table 5-3: Population of cities along the Riyadh–Dammam included corridor (2011–2018)

Figure 5-4 shows that Riyadh has the highest population of the cities along the existing Riyadh–Dammam line, rising from 7.5 million in 2011 to 9.5 million in 2018.

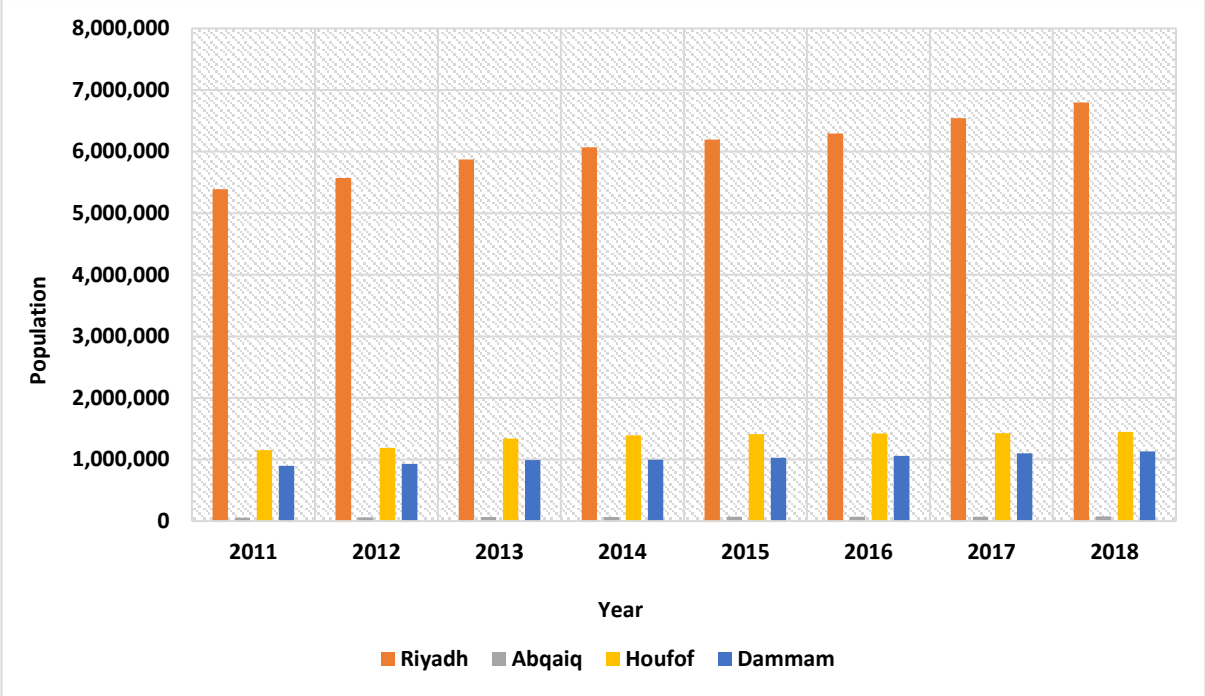


Figure 5-4: Population of cities along the existing Riyadh–Dammam rail route

Along the North–South railway corridor, the population of the cities of Al Majmaah, Al Qassim, Hail and Al Jouf are given in Table 5-4 and account for 0.5%, 2.2%, 1.6% and 1% of the total population of the country, respectively.

| Year | Population of Riyadh | Population of Al Majmaah | Population of Al Qassim | Population of Hail | Population of Al Jouf | Total |
|---|---|---|---|---|---|---|
| 2017 | 6,541,197 | 179,758 | 758,653 | 533,756 | 317,965 | 8,331,330 |
| 2018 | 6,796,505 | 184,505 | 779,991 | 538,640 | 328,156 | 8,627,796 |

Table 5-4: Population of the cities along the North–South included corridor (2017-2018)

The North–South line started operation in 2017 to serve a total population of 8.3 million, as shown in Figure 5-5.

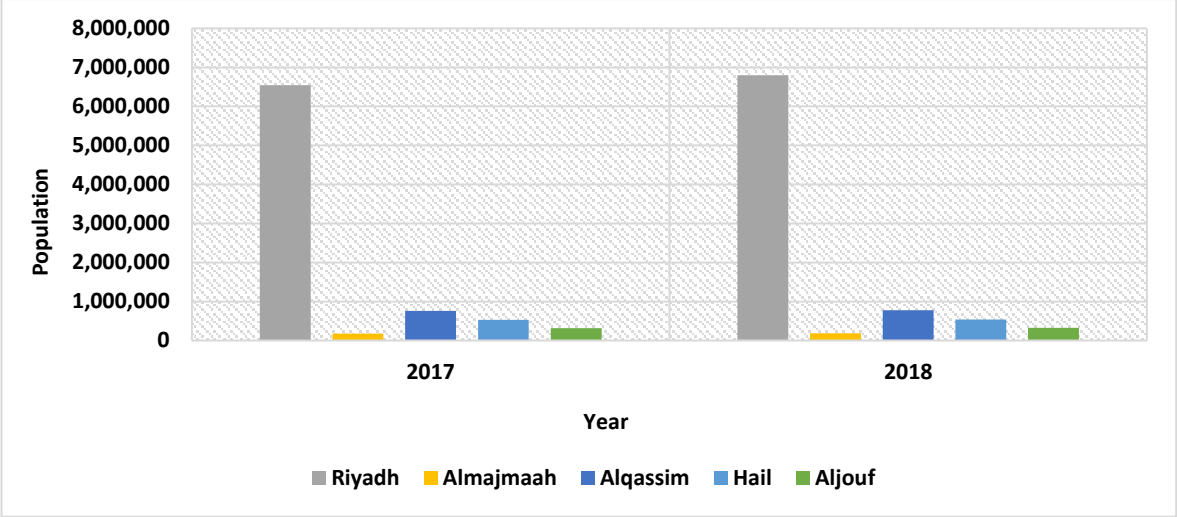


Figure 5-5: Population of cities along the existing North–South rail route (2017–2018)

### 5.2.2.2 Mean GDP per capita

GDP per capita is an important indicator of economic performance, identifying the average level of income in an urban unit. Actual GDP is obtained by dividing the nominal GDP per capita by GDP inflation to give the GDP per capita. For example, inflation is based on increases or decreases in an economy's prices relative to a base year. In general, GDP per capita can be measured by dividing the country's GDP by its total population. The collected data of mean GDP per capita for the case study's cities along the proposed HSR corridor are given in Tables 5-5 and 5-6, measured by the city's economic output that accounts for their population.

| Year | Riyadh GDP per capita (US$) | Dammam GDP per capita (US$) | Bqaiq GDP per capita (US$) | Hofuf GDP per capita (US$) | Mean GDP per capita (US$) |
|---|---|---|---|---|---|
| 2011 | 35,730.00 | 41,264.57 | 32,683.97 | 25,773.54 | 33,863.02 |
| 2012 | 38,231.25 | 44,153.28 | 34,971.99 | 27,577.80 | 36,233.58 |
| 2013 | 37,867.86 | 43,733.59 | 34,639.57 | 27,315.67 | 35,889.17 |
| 2014 | 37,486.81 | 43,293.52 | 34,291.01 | 27,040.81 | 35,528.04 |
| 2015 | 31,731.72 | 36,646.96 | 29,026.54 | 22,889.42 | 30,073.66 |
| 2016 | 30,571.58 | 35,307.12 | 27,965.31 | 22,052.56 | 28,974.14 |
| 2017 | 31,816.90 | 36,745.34 | 29,104.46 | 22,950.86 | 30,154.39 |
| 2018 | 34,913.69 | 40,321.82 | 31,937.25 | 25,184.71 | 33,089.37 |

Table 5-5: GDP per capita of cities along Riyadh–Dammam included corridor (2011–2018)

For example, in 2018 Dammam had a higher GDP per capita of US$40.3 thousand than Riyadh, Bqaiq and Hofuf, at US$34.9, US$31.9 and US$25.2 thousand,

respectively, as shown in Figure 5-6. Dammam is KSA's fastest-growing city and is the major administrative centre for the oil industry.

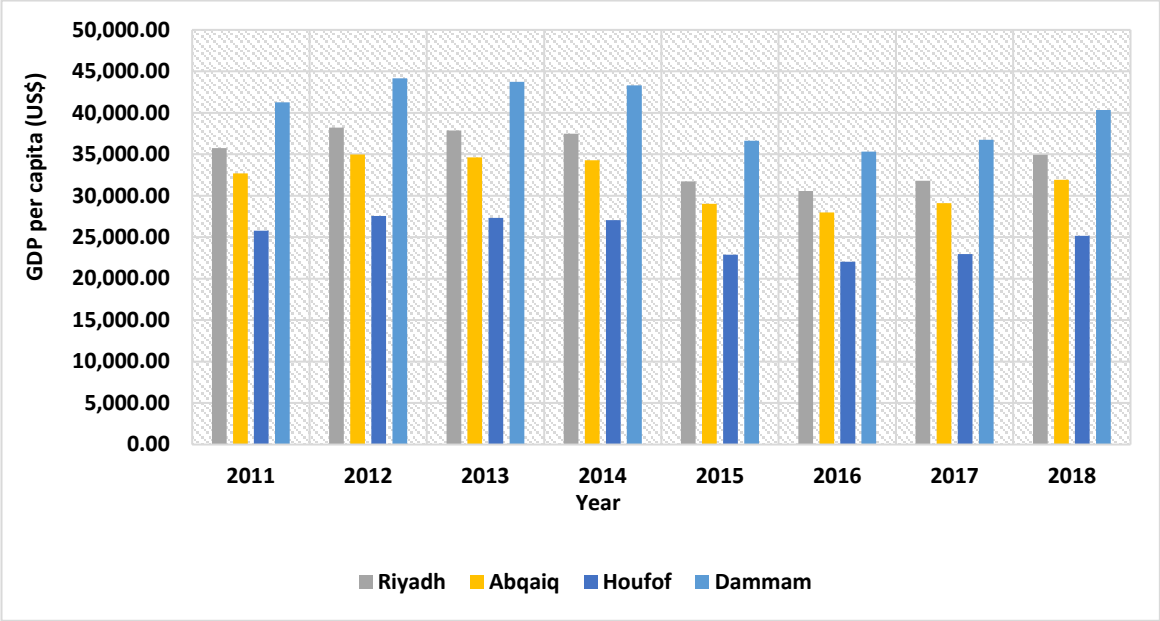


Figure 5-6: GDP per capita in cities along the existing Riyadh–Dammam rail route

In this analysis, GDP per capita represents the average real growth in income of people in cities along this corridor, determined by using the factor of inflation. As rail transport is a normal good, the number of passengers generally increases when income levels rise.

| Year | Riyadh GDP per capita (US$) | Al Majmaah GDP per capita (US$) | Al Qassim GDP per capita (US$) | Hail GDP per capita (US$) | Al Jouf GDP per capita (US$) | Mean GDP per capita (US$ ) |
|---|---|---|---|---|---|---|
| 2017 | 31,816.90 | 21,570.52 | 33,447.30 | 29,213.95 | 36,329.29 | 30,475.59 |
| 2018 | 34,913.69 | 22,190.36 | 39,314.20 | 30,185.35 | 40,605.58 | 33,441.83 |

Table 5-6: GDP per capita of cities along the North–South rail corridor (2017–2018)

On the North–South rail line in 2018, at US$40.6 thousand, Al Jouf had a higher GDP per capita than Riyadh, Al Majmaah, Al Qassim and Hail, at US$34.9, US$22.2, US$39.3 and US$30.2 thousand, respectively, as shown in Figure 5-7.

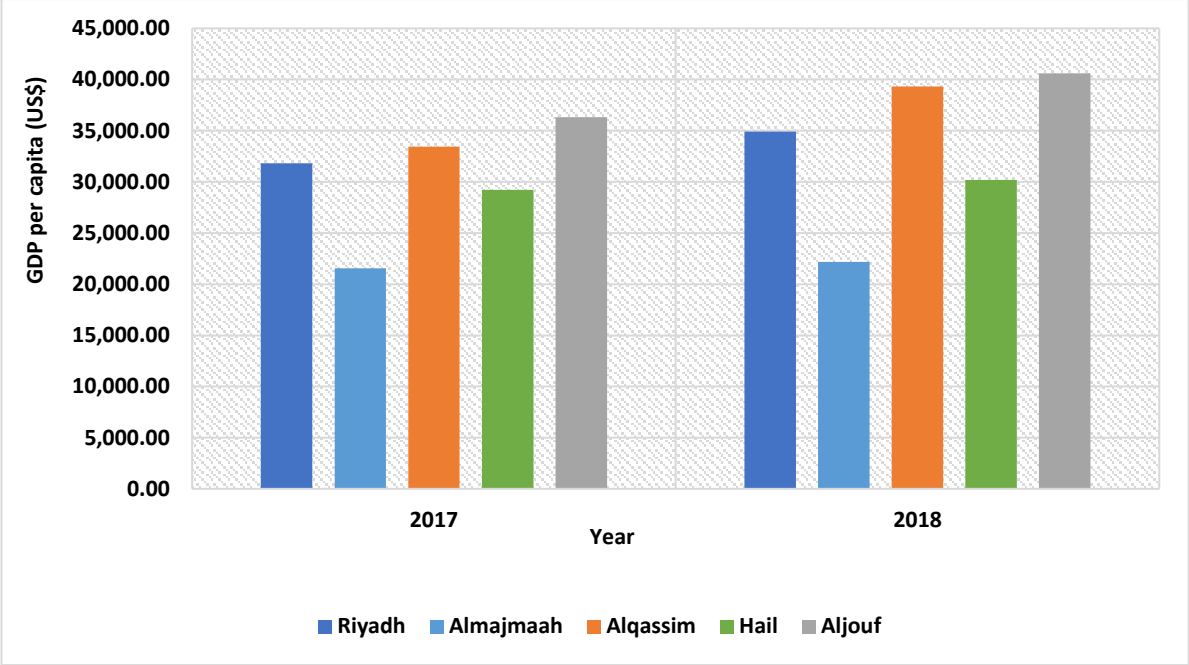


Figure 5-7: GDP per capita of cities along the existing North–South rail route

Al Jouf's high GDP per capita could be due to its location in the north of the country, bordering Jordan to the west and containing historical sites such as the Qadeer Palace, Kaf village, Az-Zabel and the Umar ibn Al-Khattaab mosque.

#### 5.2.2.3 Mean service frequency

In decision-making related to trip frequency, level of service is believed to be the main determinant. However, expected trip-frequency models are commonly employed to forecast the impact on the volume of demand in long-term and short-term scenarios (Cascetta and Coppola, 2014). The mean service frequency for the Riyadh–Dammam and North–South rail corridors was based on information provided by the SRO and SAR for their train timetables, as shown in Tables 5-7 and 5-8. The services on the Riyadh–Dammam line are:

- Dammam to Riyadh (direct)
- Riyadh to Dammam (direct)
- Dammam to Riyadh via Bqaiq and Hofuf railway stations
- Riyadh to Dammam via Hofuf and Bqaiq railway stations.

| City | Riyadh | Hofuf | Bqaiq | Dammam |
|---|---|---|---|---|
| Riyadh | 0 | 6 | 6 | 7 |
| Hofuf | 6 | 0 | 8 | 8 |
| Bqaiq | 6 | 8 | 0 | 8 |
| Dammam | 7 | 8 | 8 | 0 |
| **Mean train service frequency** | 7 | | | |

Table 5-7: Number of trains serving the Riyadh–Dammam Railway included corridor (2011–2018)

The North–South railway route operates four passenger trains daily along the line, each with 444 seats: 322 in economy class, 120 in business class and two wheelchair spaces. The two-night passenger trains per week can reach speeds of only 160 km/h, each with 337 seats: 238 in economy class, 42 in business class, one wheelchair space and 96 beds across 24 cabins.

| City | Riyadh | Al Majmaah | Al Qassim | Hail | Al Jouf |
|---|---|---|---|---|---|
| Riyadh | 0 | 3 | 4 | 2 | 1 |
| A Majmaah | 3 | 0 | 2 | 1 | 0 |
| Al Qassim | 4 | 3 | 0 | 2 | 1 |
| Hail | 2 | 1 | 2 | 0 | 1 |
| Al Jouf | 1 | 0 | 1 | 1 | 0 |
| **Mean train service frequency** | 2 | | | | |

Table 5-8: Number of trains per week serving the North–South railway included corridor (2017–2018)

#### 5.2.2.4 Mean speed

The mean speed for both corridors in this case study is dependent on the type of rolling stock, the distances and travel times between cities, information that was gleaned from the SRO and SAR main websites. In 2016, the SRO started operating passenger services on the Riyadh–Dammam line using new CAF push-pull trainsets that can reach 180 km/h, far faster than the other trains, which operate at between 120 km/h and 140 km/h. By contrast, the North–South corridor is served by diesel push-pull passenger trains, also made by CAF, and these run at speeds of up to 210 km/h. They are specially designed to operate in the harsh desert temperatures of up to 55$^{o}$C (Railway Technology, 2019).

### 5.2.2.5 Mean fares

Ticket prices on each line were noted from the information on the SRO and SAR websites. The mean fare for the Riyadh–Dammam line ranges from Riyals80 to 150 per trip for a distance of 449 km, dependent on the time of purchase. In this study, it is assumed that there are both economy and business fares on the Riyadh–Dammam conventional rail line.

| City | Riyadh | Hofuf | Bqaiq | Dammam |
|---|---|---|---|---|
| Riyadh | 0 | 57.57 | 68.25 | 79.65 |
| Hofuf | 29.4 | 0 | 7.35 | 13.65 |
| Bqaiq | 34.65 | 7.35 | 0 | 7.35 |
| Dammam | 79.65 | 13.65 | 7.35 | 0 |

Table 5-9: Ticket price for economy class on Riyadh–Dammam corridor (Riyals)

The average economy and business class fares between Riyadh and Dammam are Riyals80 and 150, as shown in Tables 5-9 and 5-10.

| City | Riyadh | Hofuf | Bqaiq | Dammam |
|---|---|---|---|---|
| Riyadh | 0 | 105 | 120.75 | 149.5 |
| Hofuf | 105 | 0 | 26.25 | 42 |
| Bqaiq | 120.75 | 26.25 | 0 | 26.25 |
| Dammam | 149.5 | 42 | 26.25 | 0 |

Table 5-10: Ticket prices for business class on Riyadh–Dammam corridor (Riyals)

The North–South rail line has an average economy-class fare of Riyals200 per trip for a journey of 1,250 km, as shown in Table 5-11.

| City | Riyadh | Al Majmaah | Al Qassim | Hail | Al Jouf |
|---|---|---|---|---|---|
| Riyadh | 0 | 55 | 80 | 125 | 200 |
| Al Majmaah | 55 | 0 | 55 | 105 | 0 |
| Al Qassim | 80 | 55 | 0 | 55 | 120 |
| Hail | 125 | 105 | 55 | 0 | 75 |
| Al Jouf | 200 | 0 | 75 | 200 | 0 |

Table 5-11: Ticket prices for economy class on North–South corridor (Riyals)

The average business-class for the whole journey is Riyals315, as in Table 5-12.

| City | Riyadh | Al Majmaah | Al Qassim | Hail | Al Jouf |
|---|---|---|---|---|---|
| Riyadh | 0 | 120 | 185 | 295 | 315 |
| Al Majmaah | 120 | 0 | 110 | 210 | 0 |
| Al Qassim | 185 | 110 | 0 | 160 | 265 |
| Hail | 295 | 210 | 160 | 0 | 200 |
| Al Jouf | 315 | 0 | 265 | 200 | 0 |

Table 5-12: Ticket prices for business class on North–South corridor (Riyals)

### 5.2.3 Years since opening

It takes years to develop predicted HSR demand, as transportation infrastructure planners are reluctant to base any decision to build an HSR line on the situation prevailing at the time. They sometimes use the traffic in the opening year as the basis for forecasting demand (Flyvbjerg, 2005). The average time from the start of a project to operation is about 16 years, as in Table 5-13.

| High-Speed Rail line | Planning started | Work started | In operation | Years of planning | Years of work |
|---|---|---|---|---|---|
| Berlin–Munich | 1991 | 1996 | 2017 | 26 | 21 |
| LGV Est European | 1992 | 2002 | 2016 | 24 | 14 |
| Madrid–Lyons | 1998 | 2001 | 2015 | 17 | 14 |
| Milan–Venice | 1995 | 2003 | 2028 | 33 | 25 |
| Madrid–Barcelona–French border | 1988 | 1997 | 2013 | 25 | 16 |
| Munich–Verona | 1986 | 2003 | 2040 | 54 | 37 |

Table 5-13: Estimated time from planning to operation of selected HSR lines. (Source: European Court of Auditors, 2018)

The number of years from opening the proposed HSR line is duly considered. The Riyadh–Dammam conventional rail service opened in 1981, and this information contributes to the forecasting demand model, as shown in Table 5-14.

| Year | Years since opening |
|---|---|
| 2017 | 36 |
| 2018 | 37 |
| 2030 | 49 |
| 2040 | 59 |
| 2050 | 69 |

Table 5-14: Years since opening the Riyadh–Dammam HSR line

#### 5.2.3.1.1 Monthly dummy variable

Garavaglia and Sharma (1998) define dummy variables as independent variables that take the value of either 0 or 1, and they serve as inputs in methods such as traditional regression or modelling paradigms. In this model, a dummy variable has been used to indicate the presence of HSR in a given corridor to differentiate between HSR demand and base-level rail demand, as well as other variables such as the GDP per capita of the departure and arrival destinations, average population density in cities along the route and travel time (Dorciak, 2015).

In this study, the dummy variable per month is shown in Table 5-15, using December as the base month.

| Month | Jan. | Feb. | March | April | May | June | July | August | Sep. | Oct. | Nov. |
|---|---|---|---|---|---|---|---|---|---|---|---|
| **Jan.** | 1 | 0 | 0 | 0 | 0 | 0 | 0 | 0 | 0 | 0 | 0 |
| **Feb.** | 0 | 1 | 0 | 0 | 0 | 0 | 0 | 0 | 0 | 0 | 0 |
| **March** | 0 | 0 | 1 | 0 | 0 | 0 | 0 | 0 | 0 | 0 | 0 |
| **April** | 0 | 0 | 0 | 1 | 0 | 0 | 0 | 0 | 0 | 0 | 0 |
| **May** | 0 | 0 | 0 | 0 | 1 | 0 | 0 | 0 | 0 | 0 | 0 |
| **June** | 0 | 0 | 0 | 0 | 0 | 1 | 0 | 0 | 0 | 0 | 0 |
| **July** | 0 | 0 | 0 | 0 | 0 | 0 | 1 | 0 | 0 | 0 | 0 |
| **August** | 0 | 0 | 0 | 0 | 0 | 0 | 0 | 1 | 0 | 0 | 0 |
| **Sep.** | 0 | 0 | 0 | 0 | 0 | 0 | 0 | 0 | 1 | 0 | 0 |
| **Oct.** | 0 | 0 | 0 | 0 | 0 | 0 | 0 | 0 | 0 | 1 | 0 |
| **Nov.** | 0 | 0 | 0 | 0 | 0 | 0 | 0 | 0 | 0 | 0 | 1 |

Table 5-15: Monthly dummy variables for the proposed Riyadh–Dammam HSR line

### 5.2.4 Direct demand regression model

The application of the DDM to forecast travel demand was examined in the case study cities of Riyadh and Dammam, using secondary data from sources such as SGAS, Public Transport Authority (PTA), SRO and SAR. It is usual to assume that demand functions are either multiple linear regression (linear-linear) or semi-log (log-linear), as these are easily handled and quite flexible (Tweeten, 2019).

#### 5.2.4.1.1 Linear-linear model

The multiple linear regression (linear-linear) demand function form was used, in which the dependent variable and the independent variables are measured in levels. In this study, the linear additive model was developed as a function of several

independent variables to forecast travel demand for the proposed HSR along the Riyadh–Dammam corridor on theoretical principles, with no intermediate stops:

$$D = a + b * Pob + c * MGP + d * MSF + e * MS + f * MF + g * DV \quad \text{Equation 5-2}$$

where

D= annual total passenger demand (passenger-km per trip) between two cities

$\mathrm{Pob}$ = population of cities served by the rail line (number)

$\mathrm{MGP}$ = mean GDP per capita (€/year)

$\mathrm{MSF}$ = mean service frequency (number of trains per day-direction)

$\mathrm{MS}$ = mean speed (km/h)

$\mathrm{MF}$ = mean fare (Riyals)

$\mathrm{DV}$ = dummy variable (0 or 1)

$\mathrm{a}$ = intercept of the regression model

$\mathrm{b, c, d, e\ and\ f}$ = unstandardized regression coefficients for all predictors of population, GDP per capita, mean service frequency, mean speed and mean fare, respectively.

#### 5.2.4.2 Log-linear model

The semi-log model (log-linear model) is another popular functional form in which the dependent variable is measured in logs and the independent variables in levels, as follows:

Log-linear or a semi-log (Ln Y = a + bX) Equation 5-3

The formulation of the model became as shown in the following equation:

$$Ln(D) = a + b * Pop + c * MGP + dMSF + e * MS + f * MF + g * DV \quad \text{Equation 5-4}$$

where Ln(D) represents the natural logarithm function of demand.

### 5.2.5 Regression analysis output

The data analysis output of the linear regression model was based on several dependent variables of historical demand for the Riyadh–Dammam and North–South conventional rail lines. The independent variables included population, mean GDP per capita, mean train service frequency, mean speed, mean fare and 11 monthly dummy variables.

#### 5.2.5.1 Descriptive analysis

The analysis of data focused on the descriptive analysis of both the dependent variable (demand) and the independent variables such as population, mean GDP per capita, mean train service frequency, mean speed and mean fare.

| Descriptive statistics | N | Linear-linear | | Log-linear | |
|---|---|---|---|---|---|
| | | Mean | Std. deviation | Mean | Std. deviation |
| Historical demand | 118 | 96,897.754 | 39,616.594 | 11.326 | 0.668 |
| Population | 118 | 8,518,241.085 | 568,296.001 | 8,518,241.085 | 568,296.001 |
| Mean GDP per capita | 118 | 32,811.206 | 2,561.466 | 32,811.206 | 2,561.466 |
| Mean train service freq. | 118 | 6.068 | 1.956 | 6.068 | 1.956 |
| Mean speed | 118 | 157.119 | 35.808 | 157.119 | 35.808 |
| Mean fare | 118 | 161.695 | 40.516 | 161.695 | 40.516 |
| Dummy Variable_Jan | 118 | 0.076 | 0.267 | 0.076 | 0.267 |
| Dummy Variable_Feb | 118 | 0.076 | 0.267 | 0.076 | 0.267 |
| Dummy Variable_Mar | 118 | 0.085 | 0.280 | 0.085 | 0.280 |
| Dummy Variable_Apr | 118 | 0.085 | 0.280 | 0.085 | 0.280 |
| Dummy Variable_May | 118 | 0.085 | 0.280 | 0.085 | 0.280 |
| Dummy Variable_June | 118 | 0.085 | 0.280 | 0.085 | 0.280 |
| Dummy Variable_July | 118 | 0.085 | 0.280 | 0.085 | 0.280 |
| Dummy Variable_Aug | 118 | 0.085 | 0.280 | 0.085 | 0.280 |
| Dummy Variable_Sep | 118 | 0.085 | 0.280 | 0.085 | 0.280 |
| Dummy Variable_Oct | 118 | 0.085 | 0.280 | 0.085 | 0.280 |
| Dummy Variable_Nov | 118 | 0.085 | 0.280 | 0.085 | 0.280 |

Table 5-16: Descriptive statistics. Analysed by SPSS

It was found that the population and mean GDP per capita in both the linear-linear and log-linear models have high values, 8.5 million and 32.8 thousand respectively, as shown in Table 5-16, followed by values of 161.7, 157.1 and 6.1 for mean fare, mean speed and mean train service frequency.

#### 5.2.5.2 Model coefficients

The model coefficients are given by the least square regression, as presented in Table 5-17 for the linear-linear model, to measure the extent to which the dependent variable increases/decreases when one independent variable increases or decreases by a single unit and the other variables are kept constant:

- For each one million-population increase in the catchment area, there is an increase of 18,378 in the monthly demand. This is calculated by multiplying the coefficient of population by one million.
- For each one thousand GDP per capita increase, there is a 3,512 increase in the monthly demand. This is calculated by multiplying the coefficient of mean GDP per capita by one thousand.
- For a unit increase in the mean train service frequency, there is a 13,550 increase in the monthly demand.
- For a unit increase in the mean speed, there is a 461 increase in the monthly demand.
- For a unit increase in the mean fare, there is a 497 decrease in the monthly demand.

In terms of the monthly dummy variables, there were increases in March, April, August, September and November to values of 7,551, 6,982, 3,837, 2,870 and 7,857, respectively. On the other hand, there were decreases in January, February, May, June, July and October to values of 1,226, 6,286, 1,027, 5,034, 2,614 and 491, respectively. The most important finding from the analysis is that increases in population, GDP per capita, speed and rail service frequency result in increased demand, while an increase in fare results in decreased monthly demand. In this case, the month variables were maintained to reflect the nature of the data and provide a fixed-effects type panel model, as a run test of the model was undertaken to check, by excluding the dummies, whether the adjusted R-squared goes up or not. In this case, it was found that the adjusted R-squared decreased slightly, indicating that including the monthly dummies in the model was justified; moreover, the dummies served to indicate the presence of HSR along a proposed corridor. The dummy data variable was presented in a month.

| Model | Linear-linear | | | | | Log-linear | | | | |
|---|---|---|---|---|---|---|---|---|---|---|
| | Unstandardized coefficient | | Standardized coefficient | T | Sig. | Unstandardized coefficient | | Standardized coefficient | t | Sig. |
| | Coefficient | Std. error | Beta | | | Coefficient | Std. error | Beta | | |
| (Constant) | -250,185.360 | 39,296.308 | | -6.367 | 0.000 | 6.462 | 0.592 | | 10.925 | 0.000 |
| Population | 0.018 | 0.005 | 0.264 | 3.616 | 0.000 | 2.391E-07 | 0.000 | 0.203 | 3.125 | 0.002 |
| Mean GDP per capita | 3.512 | 0.735 | 0.227 | 4.782 | 0.000 | 5.089E-05 | 0.000 | 0.195 | 4.603 | 0.000 |
| Mean service frequency | 13,549.690 | 3,056.480 | 0.669 | 4.433 | 0.000 | 0.246 | 0.046 | 0.721 | 5.351 | 0.000 |
| Mean speed | 460.612 | 118.770 | 0.416 | 3.878 | 0.000 | 0.004 | 0.002 | 0.233 | 2.430 | 0.017 |
| Mean fare | -497.297 | 112.510 | -0.509 | -4.420 | 0.000 | -0.006 | 0.002 | -0.376 | -3.658 | 0.000 |
| Dummy_Jan | -1,226.916 | 6,022.689 | -0.008 | -0.204 | 0.839 | -0.037 | 0.091 | -0.015 | -0.407 | 0.685 |
| Dummy_Feb | -6,286.360 | 6,022.689 | -0.042 | -1.044 | 0.299 | -0.106 | 0.091 | -0.042 | -1.169 | 0.245 |
| Dummy_Mar | 7,551.200 | 5,854.195 | 0.053 | 1.290 | 0.200 | 0.052 | 0.088 | 0.022 | 0.591 | 0.556 |
| Dummy_Apr | 6,982.700 | 5,854.195 | 0.049 | 1.193 | 0.236 | 0.032 | 0.088 | 0.013 | 0.361 | 0.719 |
| Dummy_May | -1,027.000 | 5,854.195 | -0.007 | -0.175 | 0.861 | -0.082 | 0.088 | -0.034 | -0.926 | 0.357 |
| Dummy_June | -5,034.500 | 5,854.195 | -0.036 | -0.860 | 0.392 | -0.084 | 0.088 | -0.035 | -0.952 | 0.344 |
| Dummy_July | -2,614.400 | 5,854.195 | -0.018 | -0.447 | 0.656 | -0.039 | 0.088 | -0.016 | -0.438 | 0.662 |
| Dummy_Aug | 3,837.100 | 5,854.195 | 0.027 | 0.655 | 0.514 | 0.039 | 0.088 | 0.016 | 0.446 | 0.656 |
| Dummy_Sep | 2,870.100 | 5,854.195 | 0.020 | 0.490 | 0.625 | 0.014 | 0.088 | 0.006 | 0.163 | 0.871 |
| Dummy_Oct | -491.700 | 5,854.195 | -0.003 | -0.084 | 0.933 | -0.050 | 0.088 | -0.021 | -0.570 | 0.570 |
| Dummy_Nov | 7,857.300 | 5,854.195 | 0.055 | 1.342 | 0.183 | 0.044 | 0.088 | 0.019 | 0.505 | 0.615 |

Table 5-17: Regression analysis output. Analysed by SPSS

The output of both linear-linear and log-linear DDMs showed that the independent variables of population, mean GDP per capita, mean train service frequency, mean speed and mean fare are highly significant.

For the log-linear model, there was an increase of 0.21 in monthly demand upon each one million increase in population and an increase of 0.05 upon each one thousand US$ increase in GDP per capita. Additionally, there were increases of 0.25 and 0.004 upon a unit increase in mean train service frequency and mean speed, respectively, while there was a 0.006 decrease upon a unit increase in the mean fare. Regarding the monthly dummy variables, there were increases in March, April, August, September and November to 0.052, 0.032, 0.039, 0.014 and 0.044, respectively, and decreases in January, February, May, June, July and October to values of 0.037, 0.106, 0.082, 0.084, 0.039 and 0.050, respectively.

#### 5.2.5.3 Model correlation

Model correlation analysis was used to determine which variables are significant and thus should be included in the model. Furthermore, Pearson's correlation was used to determine whether any independent variables could help to forecast the change in the dependent variable (historical rail demand), as shown in Table 5-18.

| Dependent variable | Independent variable | Linear-linear | | Log-linear | |
|---|---|---|---|---|---|
| | | R | P-value | R | P-value |
| Historical demand | Population | 0.293 | 0.001 | 0.174 | 0.060 |
| | Mean GDP per capita | 0.014 | 0.881 | 0.110 | 0.237 |
| | Mean train service frequency | 0.878 | 0.000 | 0.933 | 0.000 |
| | Mean speed | -0.424 | 0.000 | -0.561 | 0.000 |
| | Mean fare | -0.798 | 0.000 | -0.859 | 0.000 |
| | Dummy Variable_Jan | 0.038 | 0.685 | 0.048 | 0.604 |
| | Dummy Variable_Feb | 0.001 | 0.992 | 0.018 | 0.843 |
| | Dummy Variable_Mar | 0.039 | 0.674 | 0.021 | 0.823 |
| | Dummy Variable_Apr | 0.035 | 0.708 | 0.012 | 0.902 |
| | Dummy Variable_May | -0.027 | 0.772 | -0.040 | 0.664 |
| | Dummy Variable_June | -0.058 | 0.533 | -0.041 | 0.656 |
| | Dummy Variable_July | -0.039 | 0.673 | -0.021 | 0.824 |
| | Dummy Variable_Aug | 0.011 | 0.910 | 0.015 | 0.872 |
| | Dummy Variable_Sep | 0.003 | 0.974 | 0.004 | 0.970 |
| | Dummy Variable_Oct | -0.023 | 0.806 | -0.026 | 0.780 |
| | Dummy Variable_Nov | 0.042 | 0.655 | 0.017 | 0.852 |

Table 5-18: Regression coefficients

Pearson's correlation was used to limit the initial variables and measure their potential association with demand. In this case, in the linear-linear model, mean train service frequency was found to have a strong correlation to the level of demand of 88%, followed by the population, the dummy variables for November, March, January, April, mean GDP per capita, and dummy variables for August, September and February at values of 29%, 4.2%, 3.9%, 3.8%, 3.5%, 1.4%, 1.1%, 0.3% and 0.1%, respectively. For instance, the correlation between demand and mean fare, mean speed and dummy variables for May, June, July and October can be expressed as a negative correlation: the lower the fare, the more people will use the service.

For the log-linear model, mean service frequency was found to have the strongest positive correlation to the level of demand at 94%, while the mean fare is negatively correlated to demand, at a value of 87%.

In terms of the independent variables themselves, the population is strongly correlated to the mean speed of 57%, as shown in Table 5-19, followed by a mean fare of 21%, while it has a negative correlation to mean GDP per capita and a mean train service frequency of -51% and -2.1%, respectively.

| | | **Population** | **Mean GDP per capita** | **Mean train service frequency** | **Mean speed** | **Mean fare** |
|---|---|---|---|---|---|---|
| Population | Pearson correlation | 1 | -.505** | 0.021 | .569** | .209* |
| | Sig. (2-tailed) | | 0.000 | 0.819 | 0.000 | 0.023 |
| | N | 118 | 118 | 118 | 118 | 118 |
| Mean GDP per capita | Pearson correlation | -.505** | 1 | 0.135 | -.611** | -0.169 |
| | Sig. (2-tailed) | 0.000 | | 0.146 | 0.000 | 0.067 |
| | N | 118 | 118 | 118 | 118 | 118 |
| Mean train service frequency | Pearson correlation | 0.021 | 0.135 | 1 | -.710** | -.929** |
| | Sig. (2-tailed) | 0.819 | 0.146 | | 0.000 | 0.000 |
| | N | 118 | 118 | 118 | 118 | 118 |
| Mean speed | Pearson correlation | .569** | -.611** | -.710** | 1 | .748** |
| | Sig. (2-tailed) | 0.000 | 0.000 | 0.000 | | 0.000 |
| | N | 118 | 118 | 118 | 118 | 118 |
| Mean fare | Pearson correlation | .209* | -0.169 | -.929** | .748** | 1 |
| | Sig. (2-tailed) | 0.023 | 0.067 | 0.000 | 0.000 | |
| | N | 118 | 118 | 118 | 118 | 118 |
| | ** Correlation is significant at the 0.01 level (2-tailed). | | | | | |
| | * Correlation is significant at the 0.05 level (2-tailed). | | | | | |

Table 5-19: Pearson's correlation between only the independent variables

With respect to population, the mean GDP per capita and mean speed were found to be significantly correlated at the 0.01 level, and the correlation of mean fare was found significant at the 0.05 level. On the other hand, due to the multicollinearity, the correlation between mean fare and frequency was found to be high, at -0.929.

#### 5.2.5.4 Model regression statistics

The main finding in this chapter is the use of the regression model to forecast HSR demand. The model produced the R of 0.95 for the linear-linear function and 0.96

for the log-linear function, as shown in Table 5-20, which represents the correlation between the independent values and the observed value of the dependent variable. Additionally, the R-squared value for each model is 0.91 and 0.93, respectively, which represents the square of the coefficients, indicating that 91% of variation is explained by the regression.

| Model summary | Linear-linear | Log-linear |
|---|---|---|
| R | 0.952 | 0.962 |
| R-squared | 0.906 | 0.925 |
| Adjusted R-squared | 0.891 | 0.913 |
| Std. error of the estimate | 13,090.378 | 0.197 |
| R-square change | 0.906 | 0.925 |
| F change | 60.663 | 77.682 |
| df1 | 16 | 16 |
| df2 | 101 | 101 |
| Sig. F change | 0.000 | 0.000 |

Table 5-20: Regression analysis output. Analysed by SPSS

The value of R-squared tends to increase if there are more independent variables included in the model; however, a higher value of adjusted R-squared commonly indicates that a more suitable demand model is produced. In these two models, there is an estimated standard error of 13,090.4 and 0.20, being a measure of the variation of an observation made around the computed regression line. Because of the different dependent variables, these are not comparable: the first is an absolute measure (within 13,000 passengers), while the second is a relative measure (exp (0.2) = 1.22 – within 22%).

#### 5.2.5.5 Model ANOVA

Table 5-21 shows the total variance of regression and residual that can be explained by the independent variables. Additionally, the sum of squares represents the sum of the three variances of regression, residual and total.

| | Sum of squares | Df | Mean square | F | Sig. |
|---|---|---|---|---|---|
| **Linear-linear** | | | | | |
| Regression | 166,321,360,500 | 16 | 10,395,085,030 | 60.663 | .000b |
| Residual | 17,310,000,000 | 101 | 171,358,006 | | |
| Total | 183,631,360,500 | 117 | | | |
| **Log-linear** | | | | | |
| Regression | 48.257 | 16 | 3.016 | 77.682 | .000b |
| Residual | 3.921 | 101 | 0.039 | | |
| **Total** | 52.178 | 117 | | | |

Table 5-21: Model ANOVA regression analysis output. Analysed by SPSS

In this case, df represents the degrees of freedom associated with the variance sources, which is 117 degrees of freedom. The mean square is determined by dividing the sum of squares of regression by the number of independent variables (16) and the residual by the total of degrees of freedom (101). In the 'Mean square' column, the mean square regression and the mean square residual are presented in the first and second rows, calculated by dividing the sum of squares by the degrees of freedom. The F parameter is the ratio of the regression and residual terms and is calculated by dividing the mean square of regression by the mean square of residual to give values of 61 and 78 for the linear-linear and log-linear models, respectively.

#### 5.2.5.6 Model elasticity

Demand will change with elasticity in a fashion corresponding to independent variables such as population, mean GDP per capita, mean service frequency, mean speed and mean fare, as shown in Table 5-22. Elasticity can be computed as the coefficient multiplied by the mean value of the independent variable divided by mean demand. For example, the elasticity of mean train service frequency is calculated by multiplying the value of 13,549 by 6.07 and dividing it by 96,897 to get a value of 0.85. The elasticity of service frequency can be determined for 2030, 2040 and 2050, using the estimated mean train service frequencies of 20, 25 and 30 to achieve values of 2.8, 3.5 and 4.2, respectively.

| Descriptive statistics | Linear-linear | | | Log-linear | | |
|---|---|---|---|---|---|---|
| | Mean | Coefficient | Elasticity | Mean | Coefficient | Elasticity |
| Historical demand | 96,897.8 | | | 11.326 | | |
| Population | 8,518,241.1 | 0.018 | 1.616 | 8,518,241.1 | 2.39E-07 | 2.037 |
| Mean GDP per capita | 32,811.21 | 3.512 | 1.189 | 32,811.21 | 5.09E-05 | 1.670 |
| Mean frequency | 6.068 | 13,549.690 | 0.848 | 6.068 | 0.246 | 1.494 |
| Mean speed | 157.119 | 460.612 | 0.747 | 157.119 | 0.004 | 0.683 |
| Mean fare | 161.695 | -497.297 | -0.830 | 161.695 | -0.006 | -1.002 |
| Dummy_Jan | 0.076 | -1,226.916 | -0.001 | 0.076 | -0.037 | -0.003 |
| Dummy_Feb | 0.076 | -6,286.360 | -0.005 | 0.076 | -0.106 | -0.008 |
| Dummy_Mar | 0.085 | 7,551.200 | 0.007 | 0.085 | 0.052 | 0.004 |
| Dummy_Apr | 0.085 | 6,982.700 | 0.006 | 0.085 | 0.032 | 0.003 |
| Dummy_May | 0.085 | -1,027.000 | -0.001 | 0.085 | -0.082 | -0.007 |
| Dummy_June | 0.085 | -5,034.500 | -0.004 | 0.085 | -0.084 | -0.007 |
| Dummy_July | 0.085 | -2,614.400 | -0.002 | 0.085 | -0.039 | -0.003 |
| Dummy_Aug | 0.085 | 3,837.100 | 0.003 | 0.085 | 0.039 | 0.003 |
| Dummy_Sep | 0.085 | 2,870.100 | 0.003 | 0.085 | 0.014 | 0.001 |
| Dummy_Oct | 0.085 | -491.700 | 0.000 | 0.085 | -0.050 | -0.004 |
| Dummy_Nov | 0.085 | 7,857.300 | 0.007 | 0.085 | 0.044 | 0.004 |

Table 5-22: Elasticity of independent variables with respect to demand

On the other hand, the elasticity of mean speed with respect to historical demand has values of 1.331, 1.426 and 1.521 for 2030, 240 and 2050, respectively, while the elasticity of GDP per capita with respect to the dependent variable of demand is 1.485, 1.676 and 1.889, respectively. The elasticity of the mean fare with respect to demand is -2.565, -3.593 and -4.619 for the assumed years of 2030, 2040 and 2050, while the elasticity of the population for these same years is 0.022, 0.025 and 0.027, respectively.

### 5.2.6 Residual analysis

Residual analysis was conducted to test whether the model contains any significant error and to ascertain whether any errors are normally distributed. The normality test is considered to be one of the assumptions behind regression analysis, as shown in Table 5-23. This is supported by the values from Shapiro-Wilk test.

| | | | Statistic | df | Sig. |
|---|---|---|---|---|---|
| Historical demand | Population | 7,495,381 | 0.977 | 12 | 0.970 |
| | | 7,749,756 | 0.978 | 12 | 0.972 |
| | | 8,271,276 | 0.961 | 12 | 0.799 |
| | | 8,331,330 | 0.913 | 12 | 0.300 |
| | | 8,530,350 | 0.973 | 12 | 0.936 |
| | | 8,627,796 | 0.958 | 12 | 0.751 |
| | | 8,698,391 | 0.949 | 12 | 0.619 |
| | | 8,847,556 | 0.875 | 12 | 0.075 |
| | | 9,145,596 | 0.812 | 12 | 0.063 |
| | | 9,453,827 | 0.981 | 12 | 0.986 |
| | Mean GDP per capita | 28,974.14 | 0.875 | 12 | 0.075 |
| | | 30,073.66 | 0.949 | 12 | 0.619 |
| | | 30,154.39 | 0.812 | 12 | 0.013 |
| | | 30,475.59 | 0.913 | 12 | 0.300 |
| | | 33,089.37 | 0.981 | 12 | 0.986 |
| | | 33,441.83 | 0.958 | 12 | 0.751 |
| | | 33,863.02 | 0.977 | 12 | 0.970 |
| | | 35,528.04 | 0.973 | 12 | 0.936 |
| | | 35,889.17 | 0.961 | 12 | 0.799 |
| | | 36,233.58 | 0.978 | 12 | 0.972 |
| | Mean train service frequency | 2 | 0.937 | 12 | 0.173 |
| | | 7 | 0.997 | 12 | 0.999 |
| | Mean speed | 120 | 0.989 | 12 | 0.936 |
| | | 140 | 0.949 | 12 | 0.619 |
| | | 180 | 0.971 | 12 | 0.445 |
| | | 210 | 0.937 | 12 | 0.173 |
| | Mean fare | 100 | 0.977 | 12 | 0.970 |
| | | 150 | 0.997 | 12 | 1.000 |
| | | 240 | 0.937 | 12 | 0.173 |

Table 5-23: Test of normality for residual, based on Shapiro-Wilk test. Analysed by SPSS

The Shapiro-Wilk test statistic was used to check the null hypothesis for this test of normality to see whether the data were normally distributed, as the null hypothesis is rejected if the p-value is below 0.05. In SPSS output, the p-value was labelled ‘Sig.’ to confirm that all the p-values are above 0.05, so the null hypothesis was retained. The Shapiro-Wilk test thus indicated that the data are distributed approximately normally.

### 5.2.7 Causes of error

The three errors most likely to arise from the analysis of the model are autocorrelation, multicollinearity and heteroscedasticity.

#### 5.2.7.1 Autocorrelation

Autocorrelation is known as serial correlation, in terms of the relationship between variable and its lagged version over various time intervals. It can be a significant problem in analysing historical data. The Durbin-Watson statistic was used to test for autocorrelation from the statistical regression analysis in the residuals, which will always range between 0 and 4. There was no autocorrelation for the test value of 2, positive autocorrelation for value between 0 and less than 2, or negative autocorrelation, for values greater than 2 to 4 (Kenton, 2019). In this case, the result of the Durbin-Watson test was equal to 2.016 (greater than 2) for the linear-linear model in Table 5-24, which means that the data show a negative autocorrelation.

| Autocorrelation | Linear-linear | Log-linear |
|---|---|---|
| Durbin-Watson | 2.016 | 1.197 |

Table 5-24: Autocorrelation using Durbin-Watson test. Analysed by SPSS

On the other hand, for the log-linear model, the data revealed a positive correlation, based on the value of 1.197.

#### 5.2.7.2 Multicollinearity

In a regression model, multicollinearity arises when the independent variables are correlated to each other. The variance inflation factor (VIF) was used to identify this correlation and its strength, and looked only at intercorrelations between the explanatory variables (Maddala and Lahiri, 1992; Frost, 2017). Values of VIF start at 1 and have no upper limit. A value of 1 indicates no correlation between an independent variable and any other. There could be a moderate correlation at values of VIF between 1 and 5, yet not pronounced enough to warrant corrective measures (Frost, 2017).

| Collinearity statistics | Linear-linear | | Log-linear | |
|---|---|---|---|---|
| | VIF | Tolerance (1/VIF) | VIF | Tolerance (1/VIF) |
| Population | 5.697 | 0.176 | 5.697 | 0.176 |
| Mean GDP per capita | 2.417 | 0.414 | 2.417 | 0.414 |
| Mean train service frequency | 24.394 | 0.041 | 24.394 | 0.041 |
| Mean speed | 12.35 | 0.081 | 12.35 | 0.081 |
| Mean fare | 14.188 | 0.070 | 14.188 | 0.07 |
| Dummy Variable_Jan | 1.76 | 0.568 | 1.76 | 0.568 |
| Dummy Variable_Feb | 1.76 | 0.568 | 1.76 | 0.568 |
| Dummy Variable_Mar | 1.831 | 0.546 | 1.831 | 0.546 |
| Dummy Variable_Apr | 1.831 | 0.546 | 1.831 | 0.546 |
| Dummy Variable_May | 1.831 | 0.546 | 1.831 | 0.546 |
| Dummy Variable_June | 1.831 | 0.546 | 1.831 | 0.546 |
| Dummy Variable_July | 1.831 | 0.546 | 1.831 | 0.546 |
| Dummy Variable_Aug | 1.831 | 0.546 | 1.831 | 0.546 |
| Dummy Variable_Sep | 1.831 | 0.546 | 1.831 | 0.546 |
| Dummy Variable_Oct | 1.831 | 0.546 | 1.831 | 0.546 |
| Dummy Variable_Nov | 1.831 | 0.546 | 1.831 | 0.546 |

Table 5-25: Collinearity statistics. Analysed by SPSS

The results for VIF shown in Table 5-25 indicate that there are critical levels of multicollinearity for population, mean train service frequency, mean speed and mean fare, as their VIF values are greater than 5. Multicollinearity affects the statistical significance of the independent variable parameter values. The model should still do a relatively good job of predicting the same target variable as, provided the past pattern of multicollinearity continues into the future, there is no major impact on its accuracy. In this case, it affects only the variance associated with the prediction, reducing the quality of the independent variables' interpretation. As a result, the best strategy with multicollinearity is to drop either one of the variables that are too strongly correlated or a variable that is less correlated to the dependent variable. In this case, provided the pattern of multicollinearity that was detected persists into the future, the forecasts are unbiased (Maddala and Lahiri, 1992). In addition, using the baseline month of December for this study, on the basis of the interpretation SPSS did not drop any variables.

#### 5.2.7.3 Heteroscedasticity

The heteroscedasticity (or heteroskedasticity) test is defined as the change in variance of predicted values of dependent variable, given different values for the independent variables (Knaub, 2017). It is considered to be part of the classic assumption test in the regression model.

Stata software was used to perform the heteroskedasticity test for regression or residuals. A regression needs to be run for the test using the Stata command '*estat hettest'* to check whether the residuals are heteroscedastic or not, using the Breusch-Pagan/Cook-Weisberg test as shown in Table 5-26.

| | **Linear-linear** | **Log-linear** |
|---|---|---|
| Ho | Constant variance | Constant variance |
| Variable | Fitted values of historical demand | Fitted values of Ln historical demand |
| Chi2(1) | 2.190 | 58.120 |
| Prob>chi2 | 0.139 | 0.000 |

Table 5-26: Breusch-Pagan/Cook-Weisberg (heteroscedasticity test). Analysed by Stata

The test is also designed to identify any linear form of heteroscedasticity and to test the null hypothesis to ascertain whether the error variances are all equal versus the alternative, as the error variances are a multiplicative function of either one or more variables (Richard, 2020). In this case, the alternative hypothesis states that the relationship between the error variances and the predicted values of demand is such that an increase in one causes an increase in another. For example, the greater the error variance, the greater the predicted demand. A large chi-square would show that the heteroscedasticity is present (Choudhury and Chetty, 2018).

In this model, the chi-square was found to be small for the linear-linear model, showing that heteroscedasticity was not a multiplicative function of predicted demand values.

### 5.2.8 Box-Cox test

To compare the goodness of fit of linear-linear (D) and log-linear (LnD) models in which the dependent variable is in levels or logs, it is not valid to compare the R-squared since the total sums of squares in D and LnD are different. In this case, the Box-Cox test was used to make the residual sum of squares comparable by

transforming the data to the appropriate functional form of the independent variable (Maddala and Lahiri, 1992).

To choose between the linear-linear and log-linear models, each $D_i$ had first to be divided by the geometric mean of the Ds, determined by Stata software. Then the model was run for each case to estimate the two regressions and choose the smaller value of residual sum of squares, as shown in Table 5-27.

| Variable | Mean geometric | Residual sum of squares |
|---|---|---|
| Historical demand | 82,964.18 | 2.514 |
| Ln (historical demand) | 11.30 | 0.031 |

Table 5-27: Residual sum of squares values. Analysed by Stata

By using the Box-Cox test of the residual sum of squares between the two models, the linear-linear model was strongly rejected in favour of the log-linear model due to the value of RSS for the linear-linear model being 2.514, compared to 0.031 for the log-linear.

In this case, the SPSS was used for standard statistical analysis, including multivariate analysis. For the discrete-choice analysis, a more advanced statistical package was required. Several packages were considered (e.g. Biogeme, LIMDEP etc.), and Stata was chosen for its availability, documentation and user interface.

## 5.3 Elasticity of Demand Model

Demand for travel on a Maglev system can be forecasted by using the EDM, based on the GT between the proposed HSR and Maglev lines in terms of their chief service quality variables: journey times (in-vehicle time), frequency and service interval penalty. In this case, the service intervals can be determined in several ways, such as total vehicle-hours, frequency, headway, wait time and schedule delay. The GT approach represents the sum of in-vehicle travel time, service frequency specified as service headway and interchange time. The number of interchanges can be zero, denoting the equivalent change in demand upon a change in the number of interchanges. The EDM, based on the generalized journey time for both Maglev and HSR, was developed to forecast the initial annual demand for the first year of operating the Maglev system on the proposed line.

The concept of generalized journey time (GJT) is used when considering how demand for Maglev travel is affected by aspects of service quality that relate to the timetable of service interval penalty. The GJT approach is also defined as a measure of the quality of transport mode service between two stations, and it combines the sum of the in-vehicle time, service interval penalty and the number of interchanges required. In this case study, it was assumed that there is no interchange required along the proposed corridor and the calculation is as follows:

$$\mathrm{GJT} = \mathrm{IVT} + \mathrm{SIP} + \mathrm{IP} \qquad \text{Equation 5-5}$$

$\mathrm{GJT}$ = generalized journey time (mins)

$\mathrm{IVT}$ = in-vehicle time between two stations (mins)

$\mathrm{SIP}$ = service interval penalty (mins)

$\mathrm{IP}$ = interchange penalties for any interchanges required (number).

In-vehicle time (IVT) is calculated using the HSGT's average operating speed and the total distance between the two main stations, while the service interval penalty (SIP) is converted into an equivalent time effect and based on service frequency:

$$\mathrm{GJT} = \frac{\mathrm{Distance}}{Speed} + \frac{60}{Service\ frequency} \qquad \text{Equation 5-6}$$

The average interchange penalty is expected to vary with journey distance as it is assumed to be greater in terms of the minutes penalty for longer-distance trips. In this case, the interchange penalty varied with journey distance for interchanges between scheduled services, assumed to be like UK values, as in Table 5-28.

| Distance (km) | Interchange penalty (mins) |
|---|---|
| 0 | 10 |
| 24 | 15 |
| 48 | 19 |
| 80 | 25 |
| 113 | 31 |
| 191 | 40 |
| 241 | 55 |
| 322 | 65 |
| 482 | 85 |
| over 523 | 90 |

Table 5-28: Interchange penalties. (Source: Rail Delivery Group, 2011)

In terms of equivalent journey time, the service intervals range from 5 mins to 3 hours, as shown in Table 5-29:

| Service interval (mins) | Equivalent time penalty (mins) |
|---|---|
| 5 | 5 |
| 10 | 10 |
| 15 | 14 |
| 20 | 18 |
| 30 | 24 |
| 40 | 27 |
| 60 | 33 |
| 90 | 43 |
| 120 | 52 |
| 180 | 70 |

Table 5-29: Service interval penalties (mins). (Source: Rail Delivery Group, 2011)

As a result of the revised service frequency, total GJT fell from 114 mins (HSR) to 85 mins (Maglev), due to the faster operating speed.

Moreover, service frequency changes, in-vehicle travel time and interchange can be evaluated to determine total GJT. As the most popular option worldwide, the Transrapid Maglev system was selected for the model, with an average operating speed of 400 km/h and no interchanges along the 412 km-long Riyadh–Dammam corridor. For the model, HSR service frequency per hour was based on initial daily demand to illustrate how the forecast changes.

The forecast change in demand, using the GJT elasticity of value of -0.9 that was established for non-London ticket holders over 20 miles (Rail Delivery Group, 2011), was calculated as follows:

$$Forecast\ change\ (F_c) = \frac{\mathrm{T_M}}{\mathrm{T_{HSR}}} = \left(\frac{\mathrm{GJT_M}}{\mathrm{GJT_{HSR}}}\right)^{E} \quad \text{Equation 5-7}$$

where:

$\mathrm{T_M}$ = number of trips by Maglev (trains)

$\mathrm{T_{HSR}}$ = number of trips by HSR (trains)

$\mathrm{GJT_M}$ = generalized journey time by Maglev system (mins)

$\mathrm{GJT_{HSR}}$ = generalized journey time by HSR system (mins)

$E$ = elasticity of generalized journey time.

## 5.4 Conclusion

The demand model for this study was constructed from a combination of two models, the DDM and the EDM. The aim was to forecast the level of demand for HSR and for Maglev. In terms of the DDM, a comparison of linear-linear and log-linear functional relationships between the dependent and independent variables was examined to choose the best-fit method on the basis of the outcomes of the Box-Cox test.

In this case study, the dependent variable is historical demand along the Riyadh–Dammam and North–South conventional lines, while the independent variables are population, mean service frequency, mean GDP per capita, mean fare, mean speed and monthly dummy variables.

In terms of demand for the Riyadh–Dammam and North–South lines, from 2017 to 2018 there was an increase of 11% and 134%, respectively. The mean service frequency was seven trains per day for the Riyadh–Dammam conventional line and two for the North–South line, and the mean speed increased from 120 km/h in 2011 to 180 km/h in 2018 for Riyadh–Dammam and was 210 km/hr for the North–South

line. The mean fare increased from Riyals100 in 2011 to Riyals150 in 2012 for the Riyadh–Dammam line and was Riyals240 for the North–South line.

It was shown by descriptive analysis that both population and GDP per capita have top values of 8.5 million and 32.8 thousand, respectively. As a result of the model coefficients, an increase in monthly demand was indicated upon a unit increase in population, GDP per capita, mean service frequency and mean speed, yet a decrease upon a unit increase in mean fare. Mean service frequency and population were shown by Pearson's correlation to be strongly correlated to demand in the linear-linear and log-linear models, respectively. These two models exhibited a good fit, with R-squared values of 91% and 93%, respectively. In the residual analysis, the data were normally distributed: the Shapiro-Wilk test showed the p-values to be greater than 0.05, hence the null hypothesis was retained. As a result of using the Box-Cox test on the linear-linear and log-linear models, the latter was chosen for its smaller residual sum of squares.

Using EDM, travel demand for Maglev can be forecast on the basis of GJT for both the HSR and the Maglev proposed systems. The interchange penalties were obtained using the average distances and the service interval, which was determined by using the equivalent time penalty.

# Chapter 6. Developing a Stated Preference Model

## 6.1 Introduction

This chapter aims to forecast the number of passengers on the proposed Hyperloop line in the case study by determining how many travellers are willing to change their preferred choice of travel mode, or their SP. The SPM offers the transport options of air, conventional rail, bus and car or the proposed transport HSR and Hyperloop technologies. Many factors, over and above travel time, travel cost and service frequency, determine modal choice. For example, the flexibility of car travel and the necessity for advance reservations may impact on the cost of HSR and air travel; likewise, there are factors related to environmental impact and safety. Given the limitation of the SP design, which means that only a small number of variables can be considered, it was not possible to examine these factors; however, in the SP experiments the impacts of these missing variables were detected by the alternative-specific constants. In section 6.2, the mode-choice model is portrayed as a flowchart. It starts by identifying the study, then presents the attributes and modes of choice. Next comes questionnaire design, conducting a pilot survey and collecting the data before analysing them using Stata software. Section 6.3 presents the design of the experimental choice model, based on specific alternatives and attributes, variables and levels of attribute. A fractional factorial design was used in the two experiments, as presented in section 6.4, and was divided into three to construct efficient choice sets.

After designing the fractional factorial, the questionnaire was designed as in section 6.5 before undertaking a pilot survey, selecting respondents, securing ethical approval and ascertaining the appropriate sample size. Section 6.6 presents the data collection process in terms of distribution and observation, while section 6.7 summarizes the outcomes of both surveys.

## 6.2 Model Process

From a transit planning and demand modelling point of view, to assess the socioeconomics of a projected public transit infrastructure it is necessary to understand a traveller’s preferences for model of travel and behaviour concerning decisions about intercity public transport. Travel time and cost, as well as service

frequency, are increasingly relevant to current intercity passenger transport in view of rising demand and fuel prices.

In the four steps of classical urban transportation modelling, mode choice comes third, and it is one of the most important models. When a traveller plans any trip, in this model a specific transport mode is chosen from a set of transportation options, and data collection is vital to specify and calibrate the model's alternatives. In this case, an SP survey was constructed to examine the important characteristics that affect the selection of the mode of intercity travel and thus satisfy the requirements of a model of intercity mode-choice behaviour for the Riyadh–Dammam corridor. An SP survey was constructed to develop a model with statistically significant parameter values (which the models have, apart from service frequency), with a plausible magnitude of parameter values (which they have, in terms of the inferred value of time) and with a good fit (which they do not possess, possibly because of a degree of randomness in participants' responses).

From the framework shown in Figure 6-1, the first task for the case study was to identify the problem, followed by the selection of attributes and modes of choice. The next step in the methodology was to design questionnaires in both Arabic and English and to distribute them to participants after conducting a pilot survey to test the main survey tool's items. After that, to consider all six forms of intercity transport in the model the required data were collected from participants on trains and at railway stations along the Riyadh–Dammam corridor (Riyadh, Hofuf, Bqaiq and Dammam). This was followed by data analysis using Stata software, then determination of the utility and probability of all the transport modes in question.

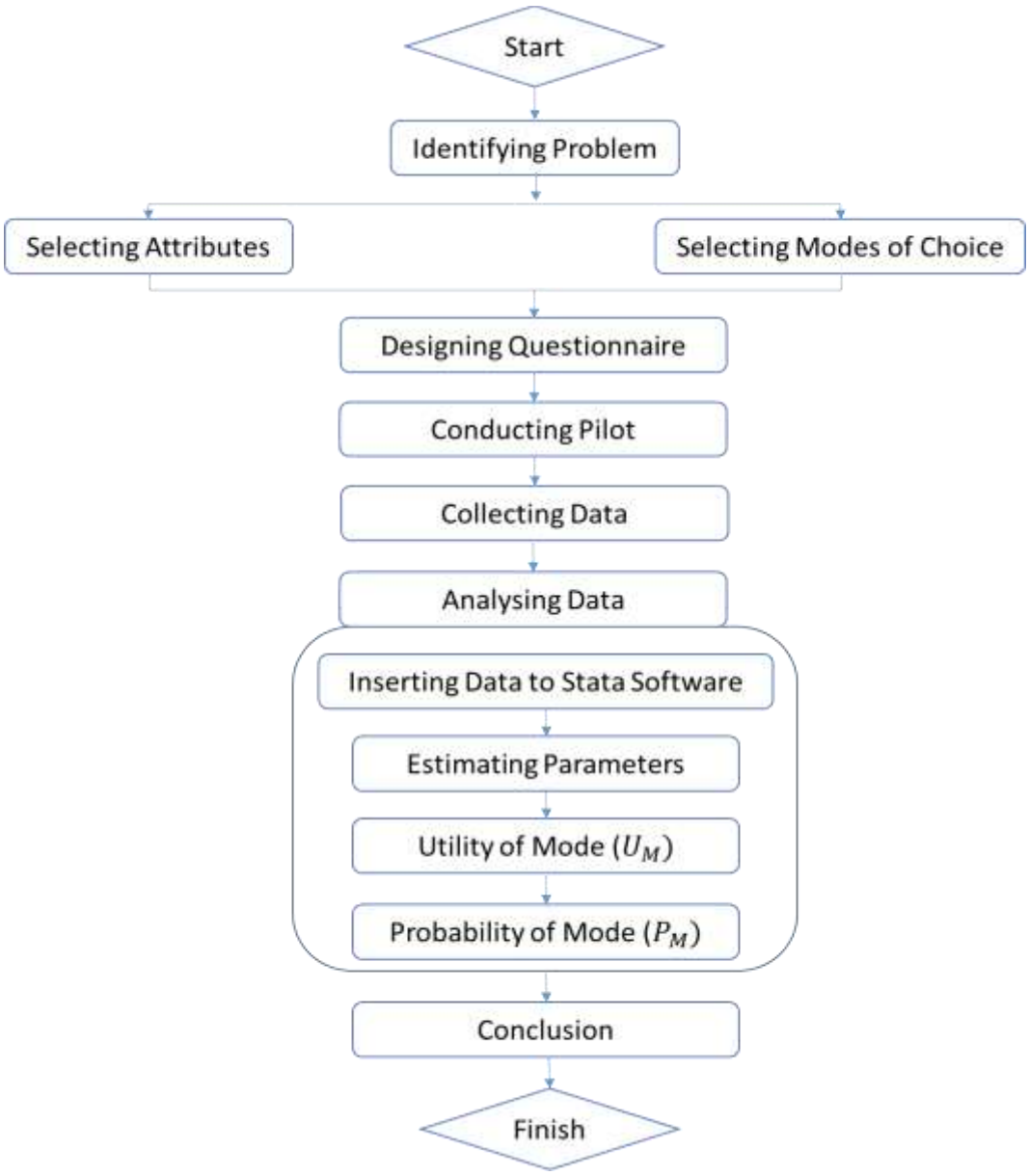


Figure 6-1: Flowchart of mode-choice model

The main target of this case study was travellers who usually use public modes of transport. This was so that changes in the attributes of their transport mode choices, whether with or without an available car, could be examined upon introducing the Hyperloop as a new option in terms of travel cost, travel time and service frequency.

Data collection was undertaken in the field, using the SP method. Two experiments were carried out to forecast the behaviour of travellers between Riyadh and Dammam. The main aim of the case study was to develop intercity mode-choice models through introducing HSR and Hyperloop to passengers from cities in the Riyadh–Dammam corridor as alternative transport technologies, collected data from them to obtain their opinions.

While a nested logit model could be used, the model of the transport systems serving Riyadh–Dammam travellers was based on the following experiments. The researcher asked each respondent to participate in two SP choice surveys. One concerned HSR and two public transport modes (classic rail and bus), nested into a composite mode of public transport. The other survey had air, HSR and Hyperloop travel options nested into a composite mode of public transport. Each mode alternative described three levels of the following attributes for the journey along Riyadh–Dammam corridor, both with and without an available car. The first attribute is total travel time with combined components for access/egress, waiting time and in-vehicle time. The second is service frequency, based on the expected travel demand. The third is total travel cost or fare, presented for either single or return trips for an individual or group of travellers, as separate costs were presented for first and standard class for rail (classic and HSR), Hyperloop and air transport.

The attributes in both surveys represent the level of service variables to help a researcher to define the global quality of the alternative in each choice situation. The questionnaires were distributed by the researcher on trains and at railway stations at varying times. Participants were asked to complete them manually then return them to the researcher during their journey or at the railway station. Participants were given information sheets and consent forms before starting the questionnaire, and the forms were collected after completion. Unless they needed help, people were left to complete the questionnaire on their own. As the majority of intercity travellers in Saudi Arabia are from many nations, both Arabic and English were spoken.

## 6.3 Design of Experimental Choice

The objective of experimental design is to create a stated choice experiment to minimize the choice sets. This avoids losing the ability to detect attributes' influence. In this case, a specific design of experimental choice was essential to establish the number of alternatives, attributes and attribute levels, as shown in Figure 6-2.


Figure 6-2: Framework of the design of choice experiment

The main reason for conducting two surveys is the impact of cars in Saudi Arabia, as they are the predominant mode of transport between the two cities. Besides the need to ascertain the impact of introducing a fast mode of transport mode such as HSR and Hyperloop, there was a requirement to test participants' attitudes both when there is a car available and when there is no car available. The rationale behind the selection of the attributes of travel time, travel cost and service frequency is that they are the most important variables in travel demand.

### 6.3.1 Alternatives and attributes

The set of attributes to be considered in the experimental choice design of the first experiment is presented in Table 6-1 for bus, HSR and classic rail: total travel time; total travel cost; and service frequency.

| Alternative / Attribute | Bus | HSR | Classic rail |
|---|---|---|---|
| Total travel time (mins) | √ | √ | √ |
| Service frequency (per day) | √ | √ | √ |
| Total travel cost or fare (SR) | √ | √ | √ |

Table 6-1: Combination of attributes and transport alternatives in first experiment

The second experiment has the same number of attributes as the first, but has four transport options of car, air, HSR and Hyperloop, as shown in Table 6-2. Air transport served as the base level, so that a similar design might be used for both experiments.

| Alternative / Attribute | Car | Air | HSR | Hyperloop |
|---|---|---|---|---|
| Total travel time (mins) | √ | √ | √ | √ |
| Service frequency (per day) | × | √ | √ | √ |
| Total travel cost or fare (SR) | √ | √ | √ | √ |

Table 6-2: Combination of attributes and transport alternatives in second experiment

### 6.3.2 Variables

The number of variables was based on a combination of the attributes and options of each mode of transport (alternatives). For the first experiment, nine variables

were considered, as shown in Table 6-3, which could be reduced to six if expressed as differences.

| No. | Mode comparison | Attribute |
|---|---|---|
| 1 | Bus | Total travel time |
| 2 | HSR | Total travel time |
| 3 | Classic rail | Total travel time |
| 4 | Bus | Service frequency |
| 5 | HSR | Service frequency |
| 6 | Classic rail | Service frequency |
| 7 | Bus | Total travel cost or fare |
| 8 | HSR | Total travel cost or fare |
| 9 | Classic rail | Total travel cost or fare |

Table 6-3: Nos. of variables for first experiment

For the second experiment, eight variables were considered as the design was based on differences, with air serving as the base level, as shown in Table 6-4.

| No. | Mode comparison | Attribute |
|---|---|---|
| 1 | HSR/Air | Total travel time |
| 2 | Hyperloop/Air | Total travel time |
| 3 | Car/Air | Total travel time |
| 4 | HSR/Air | Service frequency |
| 5 | Hyperloop/Air | Service frequency |
| 6 | HSR/Air | Total travel cost or fare |
| 7 | Hyperloop/Air | Total travel cost or fare |
| 8 | Car/Air | Total travel cost or fare |

Table 6-4: Nos. of variables for second experiment

### 6.3.3 Attribute levels

To reduce the number of choice sets presented, besides reducing the number of levels, blocking the design and the combination between the fractional factorial design and blocking strategy, one of the strategies was to use fractional factorial design (Hensher, Rose and Greene, 2005). A full factorial orthogonal design is one in which there are no correlations between the design variables. In a fractional factorial there are no main effect (first-order) correlations, but there may be second-order correlation between combination (interactions) of design variables.

In terms of each column in Table 6-5 and Table 6-7, the column for the total number of variables indicates the total for which the plan is available, while the column of three levels represents the number of variables at these three and identifies specifically the experimental conditions for which it can be used. In addition, the column for the number of tests required gives the total number of experimental trials needed to run one iteration of the experiment. The column for the master plan number indicates the plan in the master list from which the exact treatment combination is selected, as all possible combinations of levels can be taken for each of the variables. Finally, the column of using column numbers specifies the precise number to select from the master plan column, as the three-level factors are assigned to the columns containing 0s, 1s and 2s (Hensher, Rose and Greene, 2005).

In the first experiment, nine variables are shown in Table 6-3 at three levels (low, medium and high), which led to 27 tests being required, as the actual experiment was constructed using columns 1, 2, 5, 6, 7, 10, 11, 12 and 13, as mentioned in Table 6-9 of Master Plan 8, as in Table 6-5.

| Total no. of variables | Three levels | No. of tests required | Master plan no. | Using column nos |
|---|---|---|---|---|
| 9 | 9 | 27 | 8 | 1, 2, 5, 6, 7, 10, 11, 12, 13 |

Table 6-5: Index of experimental plan for first experiment

In this case study, travel time was set at the estimated access/egress time of 20 mins. Therefore, the model has the HSR operating at speeds from 200 to 350 km/h on a 412 km corridor to achieve attribute levels of 1.5 to 2.5 hours. For the attribute of travel cost, the levels were based on the fares of the existing HHSR serving the west of Saudi Arabia: SR170, SR226 and SR300. For the Riyadh–Dammam route, the frequency of the existing air service is about 21 flights daily, while conventional trains run eight times a day. In this case, to compete with these modes of transport the levels of frequency for HSR were set at one train every 15, 25 and 45 mins, respectively. This represents a range of 24 to 72 services day (assuming an 18-hour operating day). These higher levels of service are consistent with what is found in practice, not least because HSR can serve intermediate, medium-distance markets in a way that air travel cannot.

The completed design of the first experiment, with realistic levels for the attributes alternatives, is shown in Table 6-6.

| Mode | Bus | HSR | Classic rail |
|---|---|---|---|
| **Total travel time** | | | |
| Low variable | 6 hrs 00 mins | one hr 30 mins | 4 hrs 15 mins |
| Medium variable | 6 hrs 15 mins | 2 hrs 00 mins | 4 hrs 20 mins |
| High variable | 6 hrs 25 mins | 2 hrs 30 mins | 4 hrs 35 mins |
| **Service frequency** | | | |
| Low variable | Every 20 mins | Every 15 mins | Every 10 mins |
| Medium variable | Every 30 mins | Every 25 mins | Every 35 mins |
| High variable | Every 50 mins | Every 45 mins | Every hour |
| **Total travel cost / fare (SR)** | | | |
| Low variable | 68 | 170 | 79 |
| Medium variable | 94 | 226 | 110 |
| High variable | 104 | 300 | 137 |

Table 6-6: Attribute levels for nos. of alternatives in first experiment

For the second experiment, as in Table 6-4, eight variables were considered at the same number of three levels (low, medium and high), making a total of 27 tests required, as the actual experiment was constructed using columns 1, 2, 5, 6, 10, 11, 12 and 13, as in Table 6-10 of Master Plan 8, as indicated in Table 6-7.

| Total no. of variables | Three levels | No. of tests required | Master plan no. | Using column nos |
|---|---|---|---|---|
| 8 | 8 | 27 | 8 | 1, 2, 5, 6, 10, 11, 12, 13 |

Table 6-7: Index of experimental plan for the second experiment

For the proposed Hyperloop, the values of travel time and cost attributes were estimated from the CAHSR project's Hyperloop Alpha. The completed design of this experiment, with realistic levels of attribute alternatives, is shown in Table 6-8.

| Mode | Car | Air | HSR | Hyperloop |
|---|---|---|---|---|
| **Total travel time** | | | | |
| Low variable | 3 hrs 30 mins | One hr 50 mins | One hr 30 mins | 50 mins |
| Medium variable | 3 hrs 50 mins | One hr 50 mins | 2 hrs 00 mins | One hr 00 mins |
| High variable | 4 hrs 15 mins | One hr 50 mins | 2 hrs 30 mins | One hr 10 mins |
| **Service frequency** | | | | |
| Low variable | -- | Every hour | Every 15 mins | Every 20 secs |
| Medium variable | -- | Every hour | Every 30 mins | Every 30 secs |
| High variable | -- | Every hour | Every 45 mins | Every 40 secs |
| **Total travel cost/fare (SR)** | | | | |
| Low variable | 76 | 278 | 170 | 300 |
| Medium variable | 96 | 278 | 226 | 370 |
| High variable | 128 | 278 | 300 | 450 |

Table 6-8: Attribute levels for number of alternatives in the second experiment

## 6.4 Design of Fractional Factorial

Since for both experiments 27 tests were required for the design in the master plan, to be statistically efficient the fractional factorial was divided into three groups with the same number of choice sets, namely nine, as shown in Tables 6-9 and 6-10. In this case, the full fractional factorial design was employed, in which researchers can measure responses for all combinations of levels of the factors.

| Run | 1 | 2 | 5 | 6 | 7 | 10 | 11 | 12 | 13 | |
|---|---|---|---|---|---|---|---|---|---|---|
| **1** | 0 | 0 | 0 | 0 | 0 | 0 | 0 | 0 | 0 | **Participant 1** |
| **2** | 0 | 0 | 1 | 1 | 2 | 1 | 2 | 1 | 2 | |
| **3** | 0 | 0 | 2 | 2 | 1 | 2 | 1 | 2 | 1 | |
| **4** | 0 | 1 | 0 | 0 | 0 | 1 | 1 | 2 | 2 | |
| **5** | 0 | 1 | 1 | 1 | 2 | 2 | 0 | 0 | 1 | |
| **6** | 0 | 1 | 2 | 2 | 1 | 0 | 2 | 1 | 0 | |
| **7** | 0 | 2 | 0 | 0 | 0 | 2 | 2 | 1 | 1 | |
| **8** | 0 | 2 | 1 | 1 | 2 | 0 | 1 | 2 | 0 | |
| **9** | 0 | 2 | 2 | 2 | 1 | 1 | 0 | 0 | 2 | |
| **10** | 1 | 0 | 0 | 1 | 1 | 1 | 1 | 1 | 1 | **Participant 2** |
| **11** | 1 | 0 | 1 | 2 | 0 | 2 | 0 | 2 | 0 | |
| **12** | 1 | 0 | 2 | 0 | 2 | 0 | 2 | 0 | 2 | |
| **13** | 1 | 1 | 0 | 1 | 1 | 2 | 2 | 0 | 0 | |
| **14** | 1 | 1 | 1 | 2 | 0 | 0 | 1 | 1 | 2 | |
| **15** | 1 | 1 | 2 | 0 | 2 | 1 | 0 | 2 | 1 | |
| **16** | 1 | 2 | 0 | 1 | 1 | 0 | 0 | 2 | 2 | |
| **17** | 1 | 2 | 1 | 2 | 0 | 1 | 2 | 0 | 1 | |
| **18** | 1 | 2 | 2 | 0 | 2 | 2 | 1 | 1 | 0 | |
| **19** | 2 | 0 | 0 | 2 | 2 | 2 | 2 | 2 | 2 | **Participant 3** |
| **20** | 2 | 0 | 1 | 0 | 1 | 0 | 1 | 0 | 1 | |
| **21** | 2 | 0 | 2 | 1 | 0 | 1 | 0 | 1 | 0 | |
| **22** | 2 | 1 | 0 | 2 | 2 | 0 | 0 | 1 | 1 | |
| **23** | 2 | 1 | 1 | 0 | 1 | 1 | 2 | 2 | 0 | |
| **24** | 2 | 1 | 2 | 1 | 0 | 2 | 1 | 0 | 2 | |
| **25** | 2 | 2 | 0 | 2 | 2 | 1 | 1 | 0 | 0 | |
| **26** | 2 | 2 | 1 | 0 | 1 | 2 | 0 | 1 | 2 | |
| **27** | 2 | 2 | 2 | 1 | 0 | 0 | 2 | 2 | 1 | |

Table 6-9: Master plan for first experiment

In this case study, the design of the experiments' master plan was based on the strategy developed by Hensher, Rose and Greene (2005) for placing the values of the levels (0, 1 and 2).

| Run | 1 | 2 | 5 | 6 | 10 | 11 | 12 | 13 | |
|---|---|---|---|---|---|---|---|---|---|
| **1** | 0 | 0 | 0 | 0 | 0 | 0 | 0 | 0 | **Participant 1** |
| **2** | 0 | 0 | 1 | 1 | 1 | 2 | 1 | 2 | |
| **3** | 0 | 0 | 2 | 2 | 2 | 1 | 2 | 1 | |
| **4** | 0 | 1 | 0 | 0 | 1 | 1 | 2 | 2 | |
| **5** | 0 | 1 | 1 | 1 | 2 | 0 | 0 | 1 | |
| **6** | 0 | 1 | 2 | 2 | 0 | 2 | 1 | 0 | |
| **7** | 0 | 2 | 0 | 0 | 2 | 2 | 1 | 1 | |
| **8** | 0 | 2 | 1 | 1 | 0 | 1 | 2 | 0 | |
| **9** | 0 | 2 | 2 | 2 | 1 | 0 | 0 | 2 | |
| **10** | 1 | 0 | 0 | 1 | 1 | 1 | 1 | 1 | **Participant 2** |
| **11** | 1 | 0 | 1 | 2 | 2 | 0 | 2 | 0 | |
| **12** | 1 | 0 | 2 | 0 | 0 | 2 | 0 | 2 | |
| **13** | 1 | 1 | 0 | 1 | 2 | 2 | 0 | 0 | |
| **14** | 1 | 1 | 1 | 2 | 0 | 1 | 1 | 2 | |
| **15** | 1 | 1 | 2 | 0 | 1 | 0 | 2 | 1 | |
| **16** | 1 | 2 | 0 | 1 | 0 | 0 | 2 | 2 | |
| **17** | 1 | 2 | 1 | 2 | 1 | 2 | 0 | 1 | |
| **18** | 1 | 2 | 2 | 0 | 2 | 1 | 1 | 0 | |
| **19** | 2 | 0 | 0 | 2 | 2 | 2 | 2 | 2 | **Participant 3** |
| **20** | 2 | 0 | 1 | 0 | 0 | 1 | 0 | 1 | |
| **21** | 2 | 0 | 2 | 1 | 1 | 0 | 1 | 0 | |
| **22** | 2 | 1 | 0 | 2 | 0 | 0 | 1 | 1 | |
| **23** | 2 | 1 | 1 | 0 | 1 | 2 | 2 | 0 | |
| **24** | 2 | 1 | 2 | 1 | 2 | 1 | 0 | 2 | |
| **25** | 2 | 2 | 0 | 2 | 1 | 1 | 0 | 0 | |
| **26** | 2 | 2 | 1 | 0 | 2 | 0 | 1 | 2 | |
| **27** | 2 | 2 | 2 | 1 | 0 | 2 | 2 | 1 | |

Table 6-10: Master plan for second experiment

## 6.5 Design of Questionnaire

Designing the format of the SP survey involved selecting a layout and deciding on its length. Two main issues to be established in advance were the kind of data to be collected and how to collect them. The questionnaire has three parts. The journey section obtained participants' main purpose of travel, the number of travellers and type of ticket. Second, the respondent's socioeconomic characteristics were obtained by asking for their gender, age and occupation. Finally, by giving the various options of transport modes and imagining that the participant is making a journey in future along the Riyadh–Dammam corridor, their mode-choice preferences (SP) were ascertained.

### 6.5.1 Pilot survey

A pilot survey is the final stage before actual data collection, and aims to identify issues that might arise at the data collection stage, especially with the instrument

itself. To check for improvements to the instrument before collecting data, asking for feedback is worthwhile. In this case, the pilot survey was undertaken by asking about 10 participants, randomly selected, for feedback to ensure that there were no issues with its design and that all questions were clear. Six participants were male and four were female, and classic rail and HSR were chosen for Experiment 1 and Experiment 2, respectively. From the pilot survey conducted for this study with 10 respondents, the survey was estimated to take 15 mins.

### 6.5.2 Selecting respondents

Respondents were selected randomly, on the basis of availability (i.e. they volunteered), as the following had to be taken into account:

1. The researcher needed first to introduce himself to respondents.
2. The researcher needed to tell respondents about his occupation.
3. The researcher needed to explain the main aim of the study and the benefits from doing it (e.g. indirect benefits).
4. The researcher had to tell respondents about the estimated time to complete the survey, approximately 15 mins.
5. The researcher had to ask respondents if they had enough time for the survey and tell them that their time and help were greatly appreciated.
6. Respondents needed to read the participant information sheet and sign the consent form before starting the survey.

All respondents were made aware of the time required and signed the consent form.

### 6.5.3 Ethical approval

On 1 February 2018 ethical approval was granted by the University of Southampton Research Ethics Committee. Approval is one of the University's requirements for the collection of data using online surveys and questionnaires (see Appendix C: Ethics agreement number 40142).

### 6.5.4 Sample size

In advance of this study, a minimum sample size of 50 participants for each alternative was planned; however, during the data collection more travellers showed an interest in participating, as they were looking for improvements to the intercity

transport system. This raised the total to 456. It resulted from distributing 200 surveys each at Riyadh and Dammam railway stations, 140 on trains from Riyadh to Hofuf and from Dammam to Riyadh and 126 at Hofuf and Bqaiq railway stations. Both the peak and off-peak hours, weekdays and weekends were used.

## 6.6 Data Collection

The survey data were collected along the Riyadh–Dammam railway corridor, including the two intermediate stations of Bqaiq and Hofuf, as in Figure 6-3. The line opened in 1980 and is operated and maintained by the SRO, linking the Eastern Province's capital of Dammam with Riyadh, KSA's capital, over a total distance of 449 km taking 4.5 hours. The stations typically have ticket counters, waiting areas, information desks, shops and restaurants.

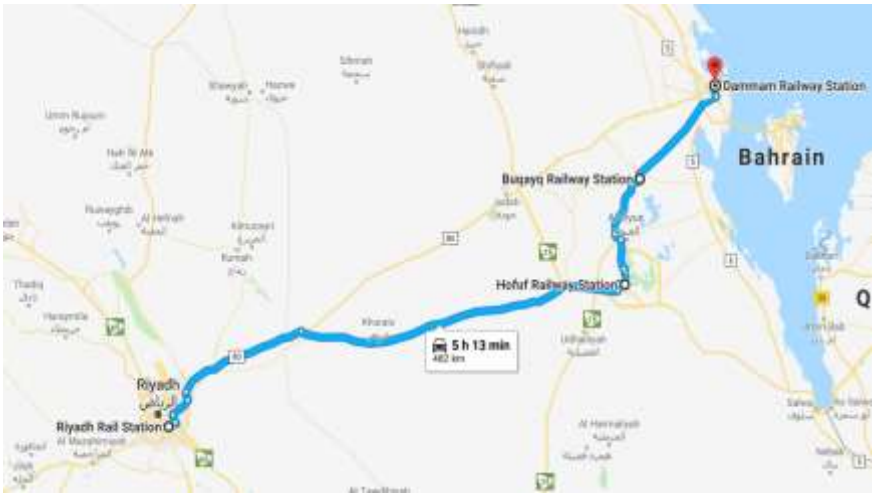


Figure 6-3: Conventional rail corridor of Riyadh–Dammam via Hofuf and Bqaiq. (Source: Google Maps)

### 6.6.1 Survey distribution

Questionnaires were distributed physically from 15 March to 15 May 2018. Permission was granted by the SRO and the PTA. Most respondents were surveyed at Riyadh and Dammam stations and on trains between cities along the line, yielding 135, 94 and 132 participants, respectively, as shown in Table 6-11. The rest of the respondents, 86 participants and nine participants, respectively, were surveyed at Hofuf and Bqaiq stations.

| Station/on train | No. of participants |
|---|---|
| Riyadh | 135 |
| Dammam | 94 |
| Hofuf | 86 |
| Bqaiq | 9 |
| On train | 132 |
| **Total** | 456 |

Table 6-11: Total number of participants in each station or on train

### 6.6.2 Survey observations

Table 6-12 presents respondents' main purpose, frequency, type of ticket, gender, age, occupation, and so on. Most were aged 25 to 34 years (35%), followed by 16 to 24 years (32%), 35 to 44 years (17%), 45 to 54 years (8%), 55 to 64 years (5%) and 65 to 74 years (1%). Females' participants dominated, at 54%, while 44% were male.

The journey's main purpose, for 35% of respondents, was to visit friends or relatives, followed by 20% commuting for education. Regarding trip frequency, 19% travelled once or twice per month, while the lowest percentage was 13% for those travelling three or more times per week. Only 13% were travelling for the first time; 87% frequently travelled by conventional train. Of all respondents, 67% were in standard (economy) class, while 32% were in first class and 1% were 'other'. Most, 68%, preferred to purchase their ticket in advance to avoid missing the train while queuing at the station if they were late due to traffic congestion, while 32% purchased their ticket on the same day.

| Category | Sub-category | Sample | Percentage (%) |
|---|---|---|---|
| Main purpose | Commuting to/from work | 69 | 15 |
| | Commuting for education | 90 | 20 |
| | Visiting friends or relatives | 158 | 35 |
| | On company business | 12 | 3 |
| | On personal business | 50 | 11 |
| | Shopping trip | 10 | 2 |
| | Travel to/from holiday | 30 | 7 |
| | Other | 37 | 8 |
| Group size | Alone | 227 | 50 |
| | With others | 229 | 50 |
| Frequency of trip | 3 or more a week | 61 | 13 |
| | Once or twice a week | 83 | 18 |
| | Once or twice a month | 85 | 19 |
| | Once every 2-3 months | 71 | 16 |
| | Once every 6 months | 79 | 17 |
| | Less often | 77 | 17 |
| First time | Yes | 61 | 13 |
| | No | 395 | 87 |
| Ticket type | First class | 147 | 32 |
| | Standard class | 307 | 67 |
| | Other | 2 | 1 |
| Advance purchase ticket | Yes | 309 | 68 |
| | No | 147 | 32 |
| Getting discount | Yes, Student | 93 | 20 |
| | Yes, Disabled | 14 | 3 |
| | Yes, Other | 3 | 1 |
| | No | 346 | 76 |
| Gender | Male | 200 | 44 |
| | Female | 256 | 56 |
| Age | 16-24 | 148 | 32 |
| | 25-34 | 159 | 35 |
| | 35-44 | 79 | 17 |
| | 45-54 | 37 | 8 |
| | 55-64 | 25 | 5 |
| | 65-74 | 4 | 1 |
| | ≥75 | 0 | 0 |
| | Not to say | 4 | 1 |
| Occupation | Full-time education | 131 | 29 |
| | Full-time employee | 177 | 39 |
| | Part-time employee | 12 | 3 |
| | Self-employed | 23 | 5 |
| | Unemployed | 23 | 5 |
| | Full retired | 27 | 6 |
| | Home-based | 47 | 10 |
| | Other | 6 | 1 |
| | Not to say | 10 | 2 |

Table 6-12: Survey observations sample and percentages

According to the data collected, 39% of respondents were full-time employees, followed by 29% and 10% in full-time education and home-based, respectively. In this case, the sample's representativeness was checked by comparing the survey statistics to national (or similar) statistics. However, the gender imbalance should be understood through representativeness and statistical power: for example, this study was conducted with 456 travellers on the Riyadh–Dammam conventional rail line, whose gender distribution was not balanced (e.g. 56% female and 44% male).

A total of 456 respondents participated in the discrete-choice survey experiment and were asked to choose their preferred mode of transport for this route. Therefore, a total of 4,104 observations were taken overall, as in Table 6-13:

| **Experiment 1** | | | **Total** | **Experiment 2** | | | | **Total** |
|---|---|---|---|---|---|---|---|---|
| **Bus** | **HSR** | **Classic rail** | | **Car** | **Air** | **HSR** | **Hyperloop** | |
| 242 | 2,215 | 1,647 | 4,104 | 592 | 772 | 1,760 | 980 | 4,104 |
| 6% | 54% | 40% | | 14% | 19% | 43% | 24% | |

Table 6-13: Observations and percentages in choosing transport mode

In the first experiment, while HSR and classic rail were chosen on 54% and 40% of the occasions that they were available, respectively, only 6% of participants opted for the bus service as it involves a long journey time. In the second experiment, HSR and Hyperloop were again selected often, at 43% and 24%, followed by air and car travel at 19% and 14%, respectively.

## 6.7 Conclusion

In this chapter, the SP model has been developed to forecast the level of demand for Hyperloop systems. The focus is on the Riyadh – Dammam case study but the method is generic and potentially transferable worldwide. By means of the case study, the model's framework is presented, starting with identifying the problem, selecting the alternatives and attributes, designing the questionnaire, conducting a pilot survey, collecting the data and then analysingit. An experimental choice survey was necessary to identify the transport alternatives, their attributes and levels. In the first experiment the options of bus, classic rail and HSR were presented as a scenario in which there is no car available, using the attributes of total travel time, travel cost and daily service frequency at low, medium and high levels. In the second

experiment, for the same attributes as in the first experiment, the alternatives of car, air travel, HSR and Hyperloop were offered: no service frequency was needed for the car option.

To design fractional factorial experiments, in both cases 27 tests were required from the master plan, divided into three groups for efficiency, with the same number of choice sets: nine. The questionnaire for the SPM was designed to take approximately 15 minutes, ascertained by means of a pilot survey, while respondents were selected on the basis of their availability. Ethical approval was achieved before starting data collection. Data from over 450 respondents were obtained, with the sample being broadly representative of the travelling population and exhibiting a sufficient degree of trading to permit model calibration, as detailed in the next chapter (section 7.4).

# Chapter 7. Application of Demand Models

## 7.1 Introduction

As travel demand forecasting is commonly concerned with predicting the response of travel demand, by mode of transport, to changes in one or more attributes such as travel costs, travel time and service frequency, this chapter focuses on the application of demand models.

Section 7.2 looks at forecasting travel demand for HSR, presenting the projected demand for 2030, 2040 and 2050 by means of a log-linear DDM. Section 7.3 predicts travel demand for Maglev transport technology using an EDM by means of comparing the GJT of Maglev with that of HSR. To forecast demand for the Hyperloop system, the SP method is employed in section 7.4, testing nested logit and multinomial logit models. The outcomes show that the multinomial logit model achieves statistically significant results for travel cost and travel time, using Stata software for analysis. As explained in the earlier sections on methodology, the reason behind using mixed methods (and software) is to construct contrasting models, that distinguish between revealed and stated preference data, and this involves the use of contrasting software.

## 7.2 Direct Demand (HSR)

The DDM was also used to determine the travel demand for HSR in the case study on the Riyadh–Dammam line proposed in 2018, based on the dependent variable of historical demand and independent variables of population, mean GDP per capita, mean service frequency, mean speed and mean fare. In this case, demand for HSR was obtained for 2030, 2040 and 2050, using the demand for HSR in 2018 as a base, as the service was assumed to commence operation at an initial frequency of 10 trains per day in each direction with a mean speed of 300 km/h and a mean fare of Riyals180. However, the initial number of trains needed depends on the demand that is forecast for the entire first decade. Further trains will continue be purchased for the years ahead on the basis of additional demand until final-year capacity is reached.

Choosing the best-fit regression model is a necessary part of demand analysis. In this case study, two forms of demand regression function were compared, namely the linear-linear and log-linear models. The comparison of the linear-linear model with the Box-Cox test, in which the dependent variable is measured in logs and the independent variables in levels, led to choosing the semi-log regression model (log-linear model). Thus, the demand function can be expressed as follows:

$$D = e^{(6.462+2.39x10^{-07}*Pop+5.09x10^{-05}*MGP+0.246*MSF+0.004*MS-0.006*MF+g*DV)}$$ Equation 7-1

To use the log-linear model, the values of independent variables such as population, GDP per capita, mean service frequency, mean speed and mean fare were estimated and used as the inputs for 2018.

| Year | Month | Population | Mean GDP per capita ($) | Mean train service frequency | Mean speed | Mean fare | Predicted passengers per month |
|---|---|---|---|---|---|---|---|
| 2018 | January | 9,453,827 | 33,089.37 | 10 | 300 | 180 | 420,554 |
| | February | | | | | | 392,514 |
| | March | | | | | | 459,699 |
| | April | | | | | | 450,597 |
| | May | | | | | | 402,048 |
| | June | | | | | | 401,245 |
| | July | | | | | | 419,714 |
| | August | | | | | | 453,762 |
| | September | | | | | | 442,559 |
| | October | | | | | | 415,122 |
| | November | | | | | | 456,036 |
| | December | | | | | | 436,406 |
| **2018** | | **Total demand per year** | | | | | **5,150,256** |

Table 7-1: Forecasting travel demand of proposed HSR line

In this case, the demand for HSR in 2018 achieved using the DDM was 5.2 million, as shown in Table 7-1. The prediction of population growth in the cities along the proposed lines adhered to the guidelines laid down by the Office of National Statistics (General Authority for Statistics, 2012; Office of National Statistics, 2018), while the prediction of GDP per capita used in the model was based on OECD data for GDP long-term forecasts (OECD, 2018).

The forecast demand for HSR for 2030, 2040 and 2050 is determined by using the elasticity for HSR with respect to income, which is assumed to be 1.5, using the total demand for HSR in 2018 as a base. In this case, it results from the multiplication of

the demand for HSR in 2018 (5,150,256) by the population change (1.06) and the GDP change to the power of 1.5, as shown in Table 7-2.

| Year | 2018 | 2030 | 2040 | 2050 |
|---|---|---|---|---|
| Population | 9,453,827 | 10,025,000 | 11,589,296 | 12,397,683 |
| GDP per capita | 33,089.37 | 40,963.30 | 46,249.70 | 52,124.69 |
| Population change | | 1.06 | 1.23 | 1.31 |
| GDP change | | 1.24 | 1.40 | 1.58 |
| **Total demand for HSR** | **5,150,256** | **7,522,552** | **10,432,991** | **13,353,471** |

Table 7-2: Forecast demand for HSR in 2030, 2040 and 2050

It was found that demand increases from 2018 levels (5,150,256) to 2030 (7,522,552), 2040 (10,432,991) and 2050 (13,353,471), by 46% and 103% and 159%, respectively. To verify this demand model, it was compared with the forecasts that were developed by Vikannanda (2018) for the Jakarta–Surabaya HSR. For the same initial year, 2030, a difference in demand was found for population growth over time. This calculated 152% and 165% higher growth in demand for the North line, at 18.9 million, and the South line, at 20 million, compared to that of the Riyadh–Dammam HSR line, at 7.5 million. In this case, lines are reported as having similar demand to the 7.5 million for Riyadh-–Dammam. For example, Changchun–Jilin carried 8.4 million in 2012 (PRC) and the H-Line (Honam) (South Korea) carried 7.3 million in 2011 (Korea) (Preston, 2013). The major difference in demand is due to the high density of population in Java, Indonesia, which had a population of over 141 million in 2018.

## 7.3 Demand Elasticity (Maglev)

The demand elasticity model is based on GJT, so forecasting travel demand for the proposed Riyadh–Dammam Maglev line involved the attributes of in-vehicle travel time, service frequency and any interchanges. In this case, it was determined that one HSR train per hour (19 trains/day in each direction) was to run. Due to the lower capacity of Maglev train (449 seats), a service of two trains per hour (41 trains per day-direction) was assumed for the Maglev line. This yields an equivalent time penalty of 24 mins and 33 mins for the Maglev and HSR lines, respectively, resulting from an assumed service interval of 30 mins and 60 mins, based on Table 7-3, so that there would be four trains and two trains, respectively, in both directions.

| Service interval | London intercity | Non-London inter-urban |
|---|---|---|
| 5 | 5 | 5 |
| 10 | 10 | 10 |
| 15 | 14 | 14 |
| 20 | 18 | 18 |
| 30 | 24 | 23 |
| 40 | 27 | 26 |
| 60 | 33 | 31 |

Table 7-3: Average service interval penalties (in mins). (Source: Rail Delivery Group, 2011)

For a service interval of 30 mins, people wait an average of 15 mins, which is then multiplied by 2 to make 30 mins. In this case, the value of 23 mins for non-London inter-urban travel is to allow for the fact that some well-organized people aim to turn up just before the train leaves rather than to arrive at random.

EDM was also used to determine the GJT of a Maglev system with an operating speed of 400 km/h, as there is no interchange on the 412 km proposed Riyadh–Dammam line, as in Table 7-4.

| Category | HSR | | Maglev | |
|---|---|---|---|---|
| | Service | GJT units | Service | GJT units |
| In-vehicle travel time | 83 mins | 83 mins | 62 mins | 62 mins |
| Service frequency | 1 per hour | 31 | 2 per hour | 23 |
| Interchange | 0 | 0 | 0 | 0 |
| **Total GJT** | | 114 mins | | 85 mins |

Table 7-4: Forecasting service frequency changes

In this case, the total GJT was determined. The forecast change in demand was calculated by dividing the GJT for a Maglev line by the GJT of a HSR line, based on the generalized elasticity of -0.9 by Rail Delivery Group (2011), as follows:

$$Forecast\ change\ (F_c) = (\frac{85}{114})^{-0.9} = 1.3024 \qquad \text{Equation 7-2}$$

This means that a Maglev line would operate at a capacity of 449 seats, compared to 604 seats on HSR, so the increases in service level and hence the demand uplift over time would be dissimilar (ArabianBusiness, 2018; Janić, 2018). In this case, the change in service boosted HSR demand by 30.24% to achieve a demand forecast for a Maglev system for 2018, 2030, 2040 and 2050, as in Table 7-5.

| Year | Demand for HSR | Increase (%) | Increase in demand | Demand for Maglev |
|---|---|---|---|---|
| 2018 | 5,150,256 | 30.24 | 1,557,437 | 6,707,693 |
| 2030 | 7,522,552 | 30.24 | 2,274,820 | 9,797,372 |
| 2040 | 10,432,991 | 30.24 | 3,154,937 | 13,587,928 |
| 2050 | 13,353,471 | 30.24 | 4,038,090 | 17,391,561 |

Table 7-5: Forecasting travel demand of proposed Maglev line

Therefore, demand for a Maglev system was found to increase by 46%, 103% and 159% from 6,707,693 in 2018 to 9,797,372 in 2030; to 13,587,928 in 2040; and to 17,391,561 in 2050. In this case, the exact same increase in demand was assumed for HSR and for Maglev for all years, as Maglev demand was based on demand for HSR and grew just by the percentage determined from the elasticity demand model. This is realistic provided the two modes have the same income and population elasticities, which seems probable.

## 7.4 Stated Preference (Hyperloop)

To forecast the case study's travel demand for Hyperloop, the SP method was used. The nested logit model (nlogit) was first tested to establish whether it was possible to use two- and three-level structures in the first and second experiments, respectively, and this was found not to be supported by the data. To choose a better model for this study, the nested logit and alternative-specific conditional logit (Aslogit) models were duly tested. In this case, initially estimates were made with Biogeme, but Stata was found to be more user-friendly.

### 7.4.1 Multinomial logit model

The multinomial logit model was also tested through Stata software, using alternative-specific conditional logit (Asclogit) to analyse the case study's SP data. Conditional logit is a special case where there are only attributes (choice specific variables) and no characteristics (individual specific variables). It was found to be a good fit for this study, as it is a specific case of the more general logit choice model and requires multiple observations of each case, each observation denoting an alternative that could be chosen (Stata Software, 2019). In the Stata script, the chosen alternative is represented by a value of 1, while zeros represent the alternatives that are not chosen. The three main explanatory variables are then listed, followed by the source of observations, the list of alternatives and, in this instance, a dummy variable indicating gender.

The Asclogit model is stated as follows:

Asclogit Chosen Cost Time, case (Observation) alternatives (Alternative) casevars (gender_male) nocons

The attribute of service frequency was eliminated from the SP study due to its statistically insignificant results. Its exclusion made little difference to the results of the other two attributes (i.e. cost and time) (see Appendixes F and G).

#### 7.4.1.1 Calibration results

In the first experiment, each participant chose from bus (A), HSR (B) and classic rail travel (C) on the basis of independent variables such as cost and time. The results, shown in Table 7-6, indicated that male participants prefer travelling by classic rail to either HSR or bus. Each participant completed a questionnaire with nine scenarios, multiplied by three transport modes, to give a potential total of 27 observations per individual, partitioned so each responded to nine scenarios.

The coefficients of predictors were interpreted in the same way as ordinary least squares (OLS) regression coefficients, as the expected value of the outcome variable changes by the regression coefficients upon a unit increase in the predictor variable.

The standard errors (std. err.) of the individual regression coefficients are used in the calculation of both the z test statistic and the confidence interval of the regression coefficients. In this case, the z test is the ratio of the coefficient to the standard error of the respective predictor while P>|z| represents the probability that the regression coefficient of the predictor is zero.

| | | | | | | |
|---|---|---|---|---|---|---|
| Alternative-specific logit | No. of obs = | | | | 12,312 | |
| Case variable: Observation | No. of cases = | | | | 4104 | |
| Alternative variable: Alternative | Alts per case: min = | | | | 3 | |
| | avg = | | | | 3 | |
| | max = | | | | 3 | |
| | Wald chi2(4) = | | | | 1163.09 | |
| Log-likelihood = -3636.2056 | Prob > chi2 = | | | | 0.0000 | |
| **Chosen** | **Coef.** | **Std. err.** | **Z** | **P>z** | **95% conf.** | **Interval** |
| Alternative Cost | -0.0029243 | 0.0004809 | -6.08 | 0.000 | -0.0038669 | -0.0019816 |
| Time | -0.4580496 | 0.0230736 | -19.85 | 0.000 | -0.503273 | -0.4128261 |
| A (Bus) (base alternative) | --- | --- | --- | --- | --- | --- |
| B (HSR) gender_male | 0.9337082 | 0.1273134 | 7.33 | 0.000 | 6841785 | 1.183238 |
| C (Classic Rail) gender_male | 1.40297 | 0.1202465 | 11.67 | 0.000 | 1.167292 | 1.638649 |

Table 7-6: Overall goodness of fit measure for first experiment

The z-values and p-values of the independent variables (e.g. cost and time) were found to be statistically significant. In this experiment, the number of observations in the dataset is 12,312, as there are non-missing values in the outcome and predictor variables. The Wald Chi-Square statistic was used to test the hypothesis that at least one of the predictor's regression coefficients is not equal to zero, while the number of 4 in parentheses indicates the degrees of freedom of the Chi-Square distribution and is defined by the number of predictors in the model.

Log-likelihood is used in the likelihood Ratio Chi-Square test of whether all regression coefficients of predictors in the model equal zero or not, and in this experiment it was -3,636.21.

For the second experiment, participants chose between car (A), air (B), HSR (C) and Hyperloop travel (D). Each participant completed a questionnaire with nine tables for each of the four transport modes, making a potential total of 36 observations each, partitioned so they responded to nine scenarios. In this case, the results shown in Table 7-7 indicated that most would prefer to travel by HSR than by car, air or Hyperloop. The total number of observations in the data set is 16,416 for 4,104 cases.

| | | | | | | |
|---|---|---|---|---|---|---|
| Alternative-specific logit | No. of obs = | | | | 16,416 | |
| Case variable: Observation | No. of cases = | | | | 4104 | |
| Alternative variable: Alternative | Alts per case: min = | | | | 4 | |
| | avg = | | | | 4.0 | |
| | max = | | | | 4 | |
| | Wald chi2(5) = | | | | 362.96 | |
| Log-likelihood = -5507.1743 | Prob > chi2 = | | | | 0.0000 | |
| Chosen | **Coef.** | **Std. Err.** | **z** | **P>z** | **95% Conf.** | **Interval** |
| Alternative Cost | -0.0018236 | 0.000349 | -5.23 | 0.000 | -0.0025075 | -0.0011398 |
| Time | -0.3542093 | 0.036687 | -9.65 | 0.000 | -0.4261149 | -0.2823037 |
| A (Car) (base alternative) | --- | --- | --- | --- | --- | --- |
| B (Air) gender_male | -0.1571196 | 0.089493 | -1.76 | 0.079 | -0.3325235 | 0.0182843 |
| C (HSR) gender_male | 0.520793 | 0.08041 | 6.48 | 0.000 | 0.3631929 | 0.6783931 |
| D (Hyperloop) gender_male | -0.1715499 | 0.097942 | -1.75 | 0.080 | -0.3635131 | 0.0204132 |

7-7: Output results of using Stata for second experiment

Significance is typically measured by the z-statistic or p-value in the regression readout. In this case, a z-statistic above 2 or below -2 was considered significant at the 95% level of confidence: all values of z-statistics in this model were found to be significant. For example, the figure of -5.23 in the z-statistic column was calculated by dividing the coefficient of cost (-0.00182) by the standard error (0.00349). As a result, the overall goodness of fit measure was used for both experiments with the service frequency excluded, as no difference was found in the outcomes, either with or without frequency.

#### 7.4.1.1.1 Maximum likelihood estimation

The most efficient approach to estimation of the multinomial logit model is maximum simulated likelihood. The model's structure is a flexible discrete-choice formulation that can provide broad patterns of competitiveness in intercity travel choice. The goodness of fit of a logit specification can be measured by using the log-likelihood index, as defined in the basic form shown below:

$$\text{Pseudo } R^2 = 1 - \frac{LL_e}{LL_b} \qquad \text{Equation 7-3}$$

where $LL_e$ represents the final log-likelihood of the estimated model and $LL_b$ that of the base model.

In this model, the maximum likelihood estimation uses multinomial logistic regression, which is an iterative procedure. The first iteration (0) is known as the log-likelihood of an no parameters at all null model, while the predictors are incorporated at the next one. In terms of goodness of fit this value seems low; however, the likelihood ratio (LR) test finds the goodness of fit for two competing statistical models from the ratio of their likelihoods. It needs to be compared to the appropriate critical statistic to find whether the model parameter values are significantly different from zero. In this case, it is based on the degrees of freedom that the final model uses relative to the base model. For this model, the LR test statistic was calculated by multiplying the difference between the start and end log-likelihood by -2, as follows:

$$LR=-2x(LL_b-LL_e) \qquad \text{Equation 7-4}$$

As a result, the pseudo-R-squared for a choice mode is equal to 0.045 and, for the first experiment, it was based entirely on the results presented in Table 7-8.

| | |
|---|---|
| Iteration 0: null Log-likelihood | -3805.9768 |
| Log-likelihood | -3636.2056 |
| Pseudo-R-squared | 0.0446 |
| Likelihood ratio (LR) chi-squared | 339.5424 |

7-8: Result of likelihood ratio and the pseudo R-square for first experiment

As a result, the likelihood ratio chi-squared test statistic is 339.54, showing that there is a chi-square distribution with the number of degrees of freedom being 4, and the log likelihood ratio test would seem to strongly support the model-which contrasts with the Pseudo R-Squared measure.

For the second experiment, the pseudo-R-squared is equal to 0.0041, as shown in Table 7-9 and the LR test statistics for adding time, cost, air transport, HSR and Hyperloop to the model is 45.2, as it is distributed chi-squared with degrees of freedom.

| | |
|---|---|
| Iteration 0: null Log-likelihood | -5528.4564 |
| Log-likelihood | -5505.8701 |
| Pseudo-R-squared | 0.0041 |
| Likelihood ratio (LR) chi-squared | 45.1726 |

7-9: Result of likelihood ratio and the pseudo R-squared for second experiment

In this case, the degrees of freedom equal the number of variables being added to the model, which in this model is 5 and the log likelihood ratio test would become to strongly support the model-which contrasts with the Pseudo R-Squared measure.

Both experiments found that the values of pseudo-R-squared are very small. Many textbooks suggest that a good fit is between 0.2 and 0.4, and the values for this study fall below this range. This could be partly due to the way that these are computed in Stata, based on the outcome of the SP experiments. In any event, the models reported were the best fit of those tested. Other specifications that could have been considered such as the cross-nested logit and mixed logit were not taken forward because of complications with providing total market forecasts. The low pseudo-R-squareds may reflect the highly hypothetical nature of the SP experiments, where participants were dealing with deeply unfamiliar choices, and that certain modes dominated the choices made.

#### 7.4.1.1.2 Variance in value of time

The value of time is based on the coefficients of travel time and travel cost, as presented in Tables 7-6 and 7-7, in terms of journey purpose, for both men and women, as it is calculated by dividing the coefficient of time by the coefficient of cost. In this case, the value of time was calculated at Riyals157 and Riyals194 per hour, respectively. Approximations of the mean and variance of a ratio related to value of time were based on the coefficient of cost and time parameters (Seltman, 2012). The standard error values were used from Tables 7-6 and 7-7, while the variance was calculated as follows:

$$\text{Variance (R) or (S)} = (\text{Standard Error})^2 \qquad \text{Equation 7-5}$$

The covariance of values of time and cost parameters was calculated as below:

$$\text{Covariance (R, S)} = \sqrt{Variance\ (R) * Variance\ (S)} \qquad \text{Equation 7-6}$$

The value of variance (R/S) was thus calculated as follows:

$$\text{Variance (R/S)} = \frac{(\mu R)^2}{(\mu S)^2}\left[\frac{Var(R)}{(\mu R)^2} - 2\frac{Cov(R,S)}{\mu R \mu S} + \frac{Var(S)}{(\mu S)^2}\right] \qquad \text{Equation 7-7}$$

where:

$\mu$R = time parameter value

$\mu S$ = cost parameter value

$Var(R)$ = variance of time parameter

$Var(S)$ = variance of cost parameter.

In this case, to check if the model has good precision the variance value of time was determined. For the first experiment, it was equal to 371.1, closely based on the time and cost parameters and the standard error, as shown in Table 7-10.

| | **Time parameter value (R)** | **Cost parameter value (S)** |
|---|---|---|
| Coefficient | -0.458 | -0.0029 |
| Standard error | 0.0231 | 0.0005 |
| Variance | 0.00053361 | 0.00000025 |
| Covariance (R,S) | 0.00001155 | 0.00001155 |
| Variance (R/S) | 371.1 | |

7-10: Variance of value of time for combined gender in first experiment

In this case, the standard deviation of the model is equal to 19.3. This is achieved by taking the square root of the variance (R/S) at the suggested 95% confidence interval, giving +/- 37.76, the product of multiplying 1.95 by 19.3. The value of time was set at Riyals157 +/- 37.76, which shows that the model has good precision and is consistent with the +/- 25% range for value of time advocated by WebTAG, based on UK studies (38/157 = 0.24) and the confidence levels of the estimated values of time in those studies.

In the second experiment, the variance of value of time is as in Table 7-11, which is based on the standard error for both cost and time parameters.

| | Time parameter value (R) | Cost parameter value (S) |
|---|---|---|
| Coefficient | -0.354 | -0.0018 |
| Standard error | 0.0367 | 0.00035 |
| Variance | 0.00134689 | 1.225E-07 |
| Covariance (R,S) | 0.000012845 | 0.000012845 |
| Variance (R/S) | 318.7 | |

Table 7-11: Variance of value of time for combined gender in second experiment

Additionally, the variance (R/S) of both the time and cost parameters is 318.7, using the same covariance values for both. As a result, the standard deviation is 7.9, achieved by taking the square root of 318.7 at the suggested 95% confidence interval, giving +/- 35.0, the product of 1.95 and 17.9. The value of time was set at +/- 35, given 35/194 = 0.18, which shows that the model has good precision.

#### 7.4.1.1.3 Mode-choice utility

The logit model is one of the most realistic for mode choice for travel between two major cities, based on a utility function that is defined for each mode before the combination of both experiments, using the multinomial model. This function represents the influence of the specific service characteristics of each mode, and consists of the attributes related to the decision-making process, expressed as:

$$\mathrm{U}_m = \mathrm{ASC} + \alpha Cost_m + \beta Time_m \qquad \text{Equation 7-8}$$

$\mathrm{U}_M$ = utility of travel by mode m

$\mathrm{ASC}$ = alternative-specific constant relating to mode

$\alpha \text{ and } \beta$ = weights associated with the attributes

$\mathrm{Time}_\mathrm{m}$ = time while travelling by mode m

$\mathrm{Cost}_\mathrm{m}$ = cost while travelling by mode m.

Each mode of transport's utility can be calculated, as participants can ascertain the value of each attribute such as total travel time and cost. These are combined then compared to the utility of each mode of transport, and the traveller opts for the mode with the greatest utility. In this case, the utility of each mode in the first experiment is presented as shown in Table 7-12, as each was analysed individually.

| Mode | Cost (Riyals) | Time (hr) | | Utility |
|---|---|---|---|---|
| Bus | 68 | 6 | U_Bus-L | -2.95 |
| | 94 | 6.25 | U_Bus-M | -3.14 |
| | 104 | 6.42 | U_Bus-H | -3.24 |
| | | | U_Bus-Mean Value | -3.11 |
| HSR | 170 | 1.5 | U_HSR-L | -0.25 |
| | 226 | 2 | U_HSR-M | -0.64 |
| | 300 | 2.5 | U_HSR-H | -1.09 |
| | | | U_HSR-Mean Value | -0.66 |
| Classic rail | 79 | 4.25 | U_ClassicRail-L | -0.77 |
| | 110 | 4.33 | U_ClassicRail-M | -0.90 |
| | 137 | 4.58 | U_ClassicRail-H | -1.10 |
| | | | U_ClassicRail-Mean Value | -0.92 |

Table 7-12: Utility of transport modes in first experiment (No Car Available)

In this first experiment, when no car is available, HSR scored the highest mean value of -0.66, compared to -3.11 and -0.92 for bus and classic rail, respectively. In the second experiment, with a car available, the utility of each alternative is seen in the results in Table 7-13.

| Mode | Cost (Riyals) | Time (hr) | | Utility |
|---|---|---|---|---|
| Hyperloop | 300 | 0.83 | U_Hyperloop-L | -1.01 |
| | 370 | 1 | U_Hyperloop-M | -1.20 |
| | 450 | 1.17 | U_Hyperloop-H | -1.41 |
| | | | U_Hyperloop-Mean Value | -1.21 |
| HSR | 170 | 1.5 | U_HSR-L | -0.32 |
| | 226 | 2 | U_HSR-M | -0.60 |
| | 300 | 2.5 | U_HSR-H | -0.91 |
| | | | U_HSR-Mean Value | -0.61 |
| Air | 278 | 1.83 | U_Air-L | -1.31 |
| | 278 | 1.83 | U_Air-M | -1.31 |
| | 278 | 1.83 | U_Air-H | -1.31 |
| | | | U_Air-Mean Value | -1.31 |
| Car | 76 | 3.5 | U_Car-L | -1.38 |
| | 96 | 3.83 | U_Car-M | -1.53 |
| | 128 | 4.25 | U_Car-H | -1.74 |
| | | | U_Car-Mean Value | -1.55 |

Table 7-13: Utility of transport modes in second experiment (Car Available)

HSR again scored the highest mean value of -0.61, compared to -1.21, -1.31 and -1.55 for Hyperloop, air and car travel, respectively.

#### 7.4.1.1.4 Stated preference probability

The SP method is generally used to identify behavioural responses in travel behaviour research, and the most common type is choice data; that is, supported by respondents' reasons for their choice of transport mode in the actual market (Sanko, 2001). In this case study, however, the discrete-choice method was used first to determine the probability of a transport mode being selected from the available alternatives in the experiments.

In the first experiment, without an available car, the probability of individual transport alternative was calculated as shown in Table 7-14, based on the utility presented in the previous section, using the mean value. For example, the probability of HSR was calculated as follows:

$$P_{HSR} = \frac{e^{U_{HSR}}}{e^{U_B} + e^{U_{HSR}} + e^{U_{CR}}}$$ Equation 7-9

$P_{HSR}$ = probability of HSR

$U_B$ = utility of travel by bus mode

$U_{HSR}$ = utility of travel by HSR mode

$U_{CR}$ = utility of travel by classic rail mode.

| **Probability** | **Middle value** | **Low value** | **High value** | **Mean value (average)** |
|---|---|---|---|---|
| Prob_Bus | 0.04 | 0.04 | 0.05 | 0.05 |
| Prob_HSR | 0.54 | 0.60 | 0.47 | 0.54 |
| Prob_ClasicRail | 0.42 | 0.36 | 0.47 | 0.41 |
| **Total probability** | 1 | 1 | 1 | 1 |

Table 7-14: Probability of transport modes included in first experiment (mean value)

As a result, total probability is equal to 1, resulting from 0.05, 0.54 and 0.41 for bus, HSR and classic rail travel, respectively.

In the second experiment, with a car available, the probability of Hyperloop travel was calculated as follows:

$$P_H = \frac{e^{U_H}}{e^{U_H} + e^{U_{HSR}} + e^{U_A} + e^{U_C}}$$ Equation 7-10

$P_H$ = probability of Hyperloop

$U_H$ = utility of travel by Hyperloop

$U_{HSR}$ = utility of travel by HSR

$U_A$ = utility of travel by air

$U_C$ = utility of travel by car.

The probability was calculated for each transport alternative individually, as in Table 7-15.

| Probability | Middle value | Low value | High value | Mean value (average) |
|---|---|---|---|---|
| Prob_Hyperloop | 0.23 | 0.22 | 0.23 | 0.23 |
| Prob_HSR | 0.41 | 0.37 | 0.45 | 0.41 |
| Prob_Air | 0.20 | 0.25 | 0.17 | 0.20 |
| Prob_Car | 0.16 | 0.16 | 0.16 | 0.16 |
| **Total probability** | 1 | 1 | 1 | 1 |

Table 7-15: Probability of transport modes included in second experiment (mean value)

The multinomial logit model for both experiments, when a car is available and when no car is available, is presented in Figure 7-1. In this case, air transport and Hyperloop have been added to the transport modes in the first experiment, when no car is available, whereas both bus and classic rail transport modes are added to the second experiment, when a car is available.

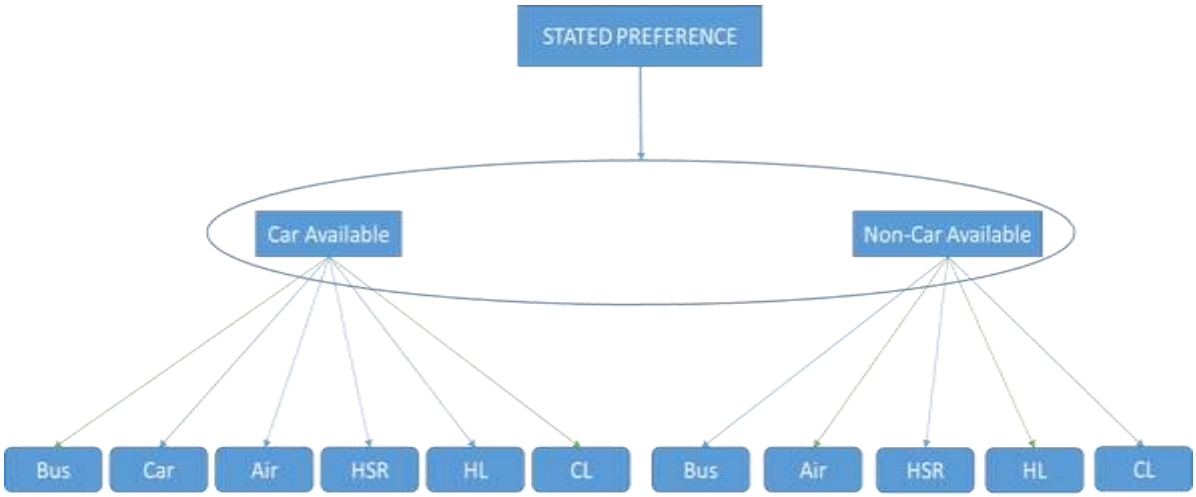


Figure 7-1: Multinomial logit structure between the two experiments

#### 7.4.1.1.5 Alternative-specific constant

To calculate the value of the alternative-specific constant for Hyperloop in the first experiment (bus, HSR and classic rail), that for the HSR-Hyperloop ratio in the second experiment (air, HSR, Hyperloop and car) was used to incorporate this mode of travel in both experiments, as follows:

$$\frac{\mathrm{ASC}_{\mathrm{HL/CA}}}{\mathrm{ASC}_{\mathrm{HSR/CA}}} = \frac{\mathrm{ASC}_{\mathrm{HL/NCA}}}{\mathrm{ASC}_{\mathrm{HSR/NCA}}} \qquad \text{Equation 7-11}$$

where

$\mathrm{ASC}_{\mathrm{HL/CA}}$ = alternative-specific constant of Hyperloop where Car is available

$\mathrm{ASC}_{\mathrm{HSR/CA}}$= alternative-specific constant of HSR where Car is available

$\mathrm{ASC}_{\mathrm{HL/NCA}}$ = alternative-specific constant of Hyperloop where Car is not available

$\mathrm{ASC}_{\mathrm{HSR/NCA}}$= alternative-specific constant of HSR where Car is not available.

In this case, the alternative-specific constant ratio was calculated as follows:

$$\mathrm{Ratio} = \frac{\mathrm{ASC}_{\mathrm{HL/CA}}}{\mathrm{ASC}_{\mathrm{HSR/CA}}} = \frac{-0.17}{0.52} = \mathbf{-0.33} \qquad \text{Equation 7-12}$$

The coefficients of -0.17 and 0.52 from Table 8-7 were used for the second experiment, where a car is available, and it was found that both Hyperloop and HSR were -0.33. The ratio of ASC in the second experiment, based on these coefficients, is used in the first experiment where no car is available, using the coefficient of HSR in Table 7-7.

For example, the alternative-specific constant value of Hyperloop for the first experiment was determined as follows:

$$\mathrm{ASC}_{\mathrm{HL/NCA}} = -0.33 * 0.93 = \mathbf{-0.31} \qquad \text{Equation 7-13}$$

As a result of the above calculation, the alternative-specific constant for combining transport modes was determined as shown in Table 7-16.

| **Mode** | **Alternative-specific constant** | |
|---|---|---|
| | **No car available** | **Car available** |
| Bus | 0 | -0.41=0.52-0.93 |
| HSR | 0.93 | 0.52 |
| Classic rail | 1.40 | 0.78=(1.40/0.93)*0.52 |
| Hyperloop | -0.31 =(-0.17/0.52)*0.93 | -0.17 |
| Air | -0.29 =(-0.16/0.52)*0.93 | -0.16 |
| Car | -- | 0 |

Table 7-16: Values of alternative-specific constant for possible split between the two experiments

To determine the utility of bus travel, the value of bus travel's alternative-specific constant in the second experiment was determined by subtracting the value of HSR when a car is available by the value of HSR when no car is available.

For the possible mode split between no car being available and available, the probability of bus was calculated by taking the exponential utility of the bus then dividing it by the sum of exponential utilities of all transport modes, as follows:

$$P_{Bus} = \frac{e^{U_{Bus}}}{e^{U_{Bus}} + e^{U_{HSR}} + e^{U_{CL}} + e^{U_{HL}} + e^{U_{Air}} + e^{U_{Car}}} \quad \text{Equation 7-14}$$

In this case, the probability of all the transport modes considered in the model gave the sum of 1, as in Table 7-17.

| **Mode** | **No car available** | | **Car available** | |
|---|---|---|---|---|
| | **Utility** | **Probability** | **Utility** | **Probability** |
| Bus | -3.06 | 0.03 | -2.74 | 0.03 |
| HSR | -0.66 | 0.37 | -0.61 | 0.29 |
| Classic rail | -0.82 | 0.32 | -0.89 | 0.22 |
| Hyperloop | -1.84 | 0.11 | -1.20 | 0.16 |
| Air | -1.54 | 0.16 | -1.07 | 0.18 |
| Car | -- | -- | -1.58 | 0.11 |
| **Total** | | 1.00 | | 1.00 |

Table 7-17: Utility and probability of transport modes included in the model

For example, bus travel has the least probability at 0.03, whether or not a car is available, because due to the protracted journey times it is a minority mode of transport in terms of participant choice.

### 7.4.2 Nested logit model

In empirical analysis, the nested logit (NL) model has become an important method for discrete outcomes (Heiss, 2002). The model's procedure was applied in both experiments, as there are two levels of nested structure in the scenario with no car available (first experiment). Bus and rail (HSR and classic rail) travel are nested at the upper level and HSR and classic rail travel are nested at the lower (Figure 7-2).

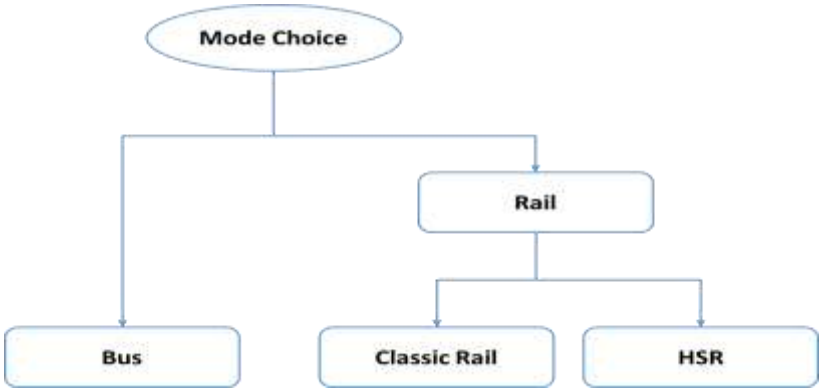


Figure 7-2: Two-level nested structure for first experiment

The results of the first experiment were determined in detail (see Appendix H) for where no car is available, and they are presented in Table 7-18. The outcome is that, based on the P>|z| values, all independent variables and alternative-specific constants apart from time were found to be insignificant.

| | | | | | | | |
|---|---|---|---|---|---|---|---|
| Non-normalized nested logit regression | | | | Number of obs = 12,312 | | | |
| Case variable: Observation | | | | Number of cases = 4104 | | | |
| Alternative variable: Mode | | | | Alts per case: min = 3 | | | |
| | | | | avg = 3.0 | | | |
| | | | | max = 3 | | | |
| | | | | Wald chi2(6) = 114.47 | | | |
| Log-likelihood = -3533.4927 | | | | Prob > chi2 = 0.0000 | | | |
| | **Chosen** | **Coef.** | **Std. err.** | **Z** | **P>\|z\|** | **[95% conf. interval]** | |
| Mode | bus_asc | 0.61850500 | 0.443812 | 1.39 | 0.163 | -0.2513512 | 1.488361 |
| | classic_asc | 0.60965450 | 0.438577 | 1.39 | 0.165 | -0.2499406 | 1.46925 |
| | hsr_asc | 0.51930970 | 0.418577 | 1.24 | 0.215 | -0.3010851 | 1.339704 |
| | Time | -0.18301480 | 0.033411 | -5.48 | 0.000 | -0.2484994 | -0.1175302 |
| | Cost | -0.00049590 | 0.000449 | -1.11 | 0.269 | -0.0013755 | 0.0003836 |
| **NonCarAvailable equations** | | | | | | | |
| | Bus gender_male | 0 (base) | | | | | |
| | Rail gender_male | 0.3970311 | 0.1393407 | 2.85 | 0.004 | 0.1239284 | 0.6701338 |
| **Inclusive-value parameters** | | | | | | | |
| type | /Bus_tau | 0.2631826 | 1.577155 | | | -2.827984 | 3.35435 |
| | /Rail_tau | 4.054995 | 1.781032 | | | 0.5642373 | 7.545754 |
| LR test for IIA (tau=1): chi2(3) = 194.36 Prob > chi2 = 0.0000 | | | | | | | |

Table 7-18: Outcome of nested logit analysis of first experiment

Because bus and rail do not vary within each case, the set of parameters of a single alternative, in this case ‘bus’, must be set to zero to identify the model. The inclusive-value or dissimilarity parameters measure the degree of correlation of random shocks within each of the two transport modes. In this case, the inclusive-value parameter for rail of greater than one implies that the model is inconsistent with random utility maximization.

The Independence of Irrelevant Alternatives (IIA) is the property of the conditional and multinomial logit models to force the odds of selecting one alternative over another in order to be independent, and additional alternatives in the choice sets will have the same proportionate effect on existing choices (Benson, Kumar and Tomkins, 2016). In this case, the scale parameter ‘tau’ was defined as the scale of the upper level divided by the scale of the lower level (Ozonder and Miller, 2019). The tau value of rail (4.1) was outside the acceptable range, and the values of the standard error of the bus_tau and rail_tau were high compared to the coefficient values; however, the values of z and P>|z| , are not directly computed by Stata.com.[9]

For the second experiment, detailed results were determined (see Appendix I) for when a car is available. In this case study there are three levels in the nested structure, as the upper level has both a nest for car and a branch for public transport. The branch of public transport is nested at the middle level, to include both air travel and a branch for rail. HSR and Hyperloop are nested under the branch of rail at the lower level, as shown in Figure 7-3.

[9] https://www.stata.com/manuals13/rnlogit.pdf

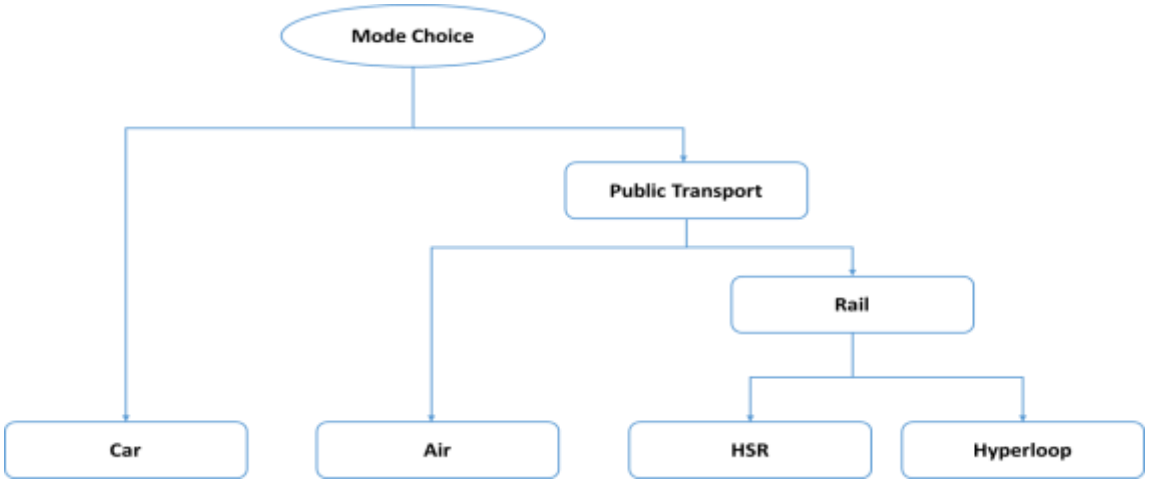


Figure 7-3: Three-level nested structure of second experiment

For the second equation the variable CarAvailable is specified, which identifies the upper-level alternatives with respect to gender_male, using ‘car’ as the baseline category, as in Table 7-19.

| **Non-normalized nested logit regression** | | | | Number of obs = 16,416 | | | |
|---|---|---|---|---|---|---|---|
| Case variable: Observation | | | | Number of cases = 4,104 | | | |
| Alternative variable: Mode | | | | Alts per case: min = 4 | | | |
| | | | | avg = 4.0 | | | |
| | | | | max = 4 | | | |
| | | | | Wald chi2(8) = 202.41 | | | |
| Log-likelihood = -5330.2822 | | | | Prob > chi2 = 0.0000 | | | |
| | **Chosen** | **Coef.** | **Std. err.** | **Z** | **P>\|z\|** | **[95% conf. interval]** | |
| **Mode** | car_asc | -2.12356300 | 0.446774 | -4.75 | 0.000 | -2.999224 | -1.247902 |
| | air_asc | -2.04669600 | 0.437849 | -4.67 | 0.000 | -2.904863 | -1.188528 |
| | hsr_asc | -2.15394800 | 0.459856 | -4.68 | 0.000 | -3.055249 | -1.252648 |
| | hyperloop_asc | -1.99068600 | 0.437428 | -4.55 | 0.000 | -2.848029 | -1.133344 |
| | Time | 0.31457710 | 0.052796 | 5.96 | 0.000 | 0.2110992 | 0.418055 |
| | Cost | -0.00113730 | 0.000397 | -2.86 | 0.004 | -0.0019163 | -0.0003583 |
| **CarAvailable equations** | | | | | | | |
| | Car | 0 (base) | | | | | |
| | Public transport | -0.0342386 | 0.109437 | -0.31 | 0.754 | -0.2487308 | 0.1802536 |
| | Rail | -0.2658203 | 0.090923 | -2.92 | 0.003 | -0.444026 | -0.0876146 |
| **Inclusive-value parameters** | | | | | | | |
| CarAvailable | /Car_tau | 0.6111926 | 0.411412 | | | -0.19516 | 1.417545 |
| | /PublicTransport_tau | 0.1677854 | 0.173527 | | | -0.1723204 | 0.5078911 |
| | /Rail_tau | -0.8756731 | 0.338955 | | | -1.540012 | -0.2113346 |
| LR test for IIA (tau=1): chi2(4) = 411.80 Prob > chi2 = 0.0000 | | | | | | | |

Table 7-19: Outcome of nested analysis for second experiment

From the outcomes of the analysis, the parameters of car_tau and public transport_tau were between 0 and 1, while the coefficient of rail_tau was negative. In any event, none of the results were significantly different from zero at the 95% confidence interval.

The outcome of the first experiment was that most independent variables and alternative-specific constants were insignificant, from the values of the P>|z|. The outcome of the second experiment was that the sign of time is positive while the sign of cost is negative, leading to a negative sign of value of time, which is implausible. In terms of the P>|z| most values are highly significant, yet this does not make the NL model acceptable for this study's model. In short, the data did not support the nested structures that were tested. Also, the coefficient values of car_tau, public transport_tau and rail_tau for the second experiment supported the rejection of the nested logit model.

## 7.5 Demand Forecast

In the case study, the SP survey method was chosen to forecast the demand for Hyperloop in the initial year of proposed operation (2030), and the data collection targeted passengers on the conventional train between Riyadh and Dammam via Hofuf and Bqaiq.

At this point, the impact of introducing a new transport system (e.g. HSR) to existing modes of travel along various routes needs to be reviewed.

### 7.5.1 Impact of HSR on existing transport modes

From the evidence obtained from five existing continental European HSR schemes, around 30% of demand is diverted from classic rail, 30% from air and 15% from car transport, while 25% is newly generated (Preston, 2013). For Phase 1's initial estimates for the United Kingdom's proposed HS2 line, around 57% of journeys were to switch from classic rail, 8% from car and 8% from air travel, and 27% would be generated. In Table 7-20, the highest percentage of demand is of transfers from classic rail to HSR, at 40% on the Paris–Lyons corridor, followed by 29%, 20% and 11% for induced demand, for transfers from air transport and for transfers from road travel, respectively.

| Route | Transferred from road | Transferred from classic rail | Transferred from air | Induced |
|---|---|---|---|---|
| Paris–Lyons | 11 | 40 | 20 | 29 |
| Madrid–Seville | 6 | 20 | 24 | 50 |
| Madrid–Barcelona | 10 | 10 | 60 | 20 |
| Thalys | 34 | 47 | 8 | 11 |
| Eurostar | 19 | 12 | 49 | 20 |

Table 7-20: Diversion factors resulting from introduction of HSR. (Source: Preston, 2013)

For the Mumbai–Ahmedabad project (India), when it opens in 2035 it is expected that the HSR service will have 46% of the demand, car 24%, classic rail 10%, bus 16% and air transport 4%. The current modal share on this corridor is 28% by classic rail, 34% by bus, 10% by air and 28% by car (Preston, 2013). In general, the introduction of an HSR service affects the market share of other modes of transport such as road, conventional rail and air, as shown in Table 7-21, dependent on cost, time and travelling conditions (de Rus, 2009).

| Line | Transport mode | Before HSR (%) | Year | After HSR (%) | Year |
|---|---|---|---|---|---|
| Paris–Lyons | Road | 29 | 1980 | 21 | 1997 |
| | Conventional rail | 40 | | 3 | |
| | HSR | 0 | | 70 | |
| | Air | 31 | | 6 | |
| Madrid–Seville | Road | 44 | 1991 | 30 | 2002 |
| | Conventional rail | 16 | | 1 | |
| | HSR | 0 | | 61 | |
| | Air | 40 | | 8 | |
| Hamburg–Frankfurt | Road | 57 | 1985 | 45 | 2000 |
| | Conventional rail | 23 | | 3 | |
| | HSR | 0 | | 48 | |
| | Air | 10 | | 4 | |

Table 7-21: Modal market share before and after introduction of HSR system. (Source: de Rus, 2009)

In this instance, most of the demand shifted from the Paris–Lyons and Hamburg–Frankfurt conventional lines, and from air for the Madrid–Seville line (de Rus, 2009). To take another example, the change in market share along the Paris–Lyons corridor upon the introduction of HSR line greatly affected conventional rail, and demand fell from 40% to 3% and the classic rail service was essentially withdrawn.

Interestingly, in Taiwan in 2006, private car trips had accounted for the greatest modal share of 30% before the introduction of the HSR, and after the launch the share actually increased by 1%, in contrast to that of other intercity transport modes, as shown in Table 7-22. In this instance, total demand grew by 9% and 6% (2,097,211-1,986,850)/1,986,850) for the Taipei–Kaohsiung and Taipei–Taichung HSR lines for 2006 and 2007, respectively.

| Line | Year | Mode | Monthly trips | Percentage (%) |
|---|---|---|---|---|
| Taipei–Kaohsiung | 2006 | Bus | 302,411 | 34.49 |
| | | Classic rail | 85,108 | 9.71 |
| | | Air | 218,762 | 24.95 |
| | | HSR | 0 | 0.00 |
| | | Car | 270,546 | 30.86 |
| | | **Total** | **876,827** | **100** |
| | 2007 | Bus | 236,433 | 24.76 |
| | | Classic rail | 50,657 | 5.31 |
| | | Air | 124,100 | 13.00 |
| | | HSR | 239,015 | 25.03 |
| | | Car | 304,532 | 31.90 |
| | | **Total** | **954,737** | **100** |
| Taipei–Taichung | 2006 | Bus | 619,514 | 31.18 |
| | | Classic rail | 187,094 | 9.42 |
| | | Air | 3,977 | 0.20 |
| | | HSR | 0 | 0.00 |
| | | Car | 1,176,265 | 59.20 |
| | | **Total** | **1,986,850** | **100** |
| | 2007 | Bus | 602,557 | 28.73 |
| | | Classic rail | 179,619 | 8.56 |
| | | Air | 228 | 0.01 |
| | | HSR | 181,568 | 8.66 |
| | | Car | 1,133,239 | 54.04 |
| | | **Total** | **2,097,211** | **100** |

Table 7-22: Trip distribution for intercity transportation before and after HSR operation in Taiwan. (Source: Cheng, 2010)

In the case of the Japanese Sanyo Shinkansen, 55% of HSR demand was diverted from other rail lines, 23% from air and 16% from bus and car, while 6% was newly

induced: 32% of AVE passengers were from air travel, 25% from car and 17% from conventional rail, while 26% was new generated (Cheng, 2010).

In general, the market shares of air, rail and road travel are dependent on the parameters of national regulations, geographic context, and so on. In most European countries where HSR is in operation, the car is still the main mode of transport, especially for short and medium distances, while air is the most used for long distances. The major factor in the competition between HSR and air transport, been proved in many places worldwide, is the relationship between the door-to-door travel times of each mode (de Angoiti, 2018).

A bus service can compete with HSR travel, as it is cheaper and may serve several stops in a city, reducing passengers' access/egress time. Bus operators are starting to offer better on-board services (e.g. Wi-Fi) at a low cost to achieve economic competitiveness. Car competition for HSR is more complex than that of intercity public modes of transport such as air, classic rail and bus, due to its superior privacy, offering a full door-to-door trip, choice of route, choice of departure time and date and ease of handling luggage; however, over long distances, HSR remains highly efficient (de Angoiti, 2018).

The impact on air transport by introducing HSR appears to be significant. To take the example of China, between some cities it has led to permanent cancellations of air services. Air Express ceased its Chongqing–Chengdu service in 2009 due to competition from intercity HSR, while Hainan Airline cancelled its Guangzhou–Wuhan service upon the introduction of HSR and the Zhengzhou–Xi service ceased in 2010. Road transport (e.g. intercity bus services) has also been massively affected by the introduction of HSR lines, and there have been reductions in services nationwide due to declining demand (Chen *et al.*, 2019).

On the other hand, conventional rail competes strongly with HSR, as passenger demand is expected to vary between the two modes and switching is expected to increase. In an example from China, in the first year of HSR operation between Guangzhou and Wuhan in 2009 the total ridership was over 20 million passengers: 50% had been diverted from conventional rail services and 5% from air transport, together with a small percentage from road services, while 45% comprised newly

induced demand (Chen *et al.*, 2019). This section on the modal split or the shifting of passengers from one mode to another, due to characteristics such as travel time, travel cost, frequency and comfort, represents a vital aspect of this study.

### 7.5.2 Evolution of HSR traffic

Growth in demand varies by country, and some HSR lines are more mature. However, some HSR services have been in operation for long enough to experience positive evolution over these years in terms of passengers-kilometres in countries such as Japan, France, Germany, Italy and Spain. In such cases, it is normally known that the HSR lines between large cities can influence demand growth rates. To take a few examples, in France growth in demand has been intensive for the junction of Paris, connecting TGV Sud-East and TGV Nord-Europe, and Spain's HSR lines saw increases from the 2010s, from 11.7 billion to 16.1 billion passenger-kms when the network grew from 2,102 km to 3,002 km eight years later (Table 7-23) (Pedro, Silva and Abreu, 2014; UIC, 2020b). Germany's HSR growth in demand fell by 2.51% from 2010 to 2011, yet China's rose by 128.51% that year (UIC, 2020b).

| | 2010 | 2011 | 2012 | 2013 | 2014 | 2015 | 2016 | 2017 | 2018 |
|---|---|---|---|---|---|---|---|---|---|
| Italy (billion-PKM) | 8.0 | 8.3 | 9.6 | 11.6 | 11.7 | 13.6 | 14.3 | 15.1 | 15.1 |
| Growth rate | -- | 3.8 | 15.7 | 20.8 | 0.9 | 16.2 | 5.2 | 5.6 | 0.0 |
| Germany (billion-PKM) | 23.9 | 23.3 | 24.8 | 25.2 | 24.3 | 25.3 | 27.2 | 28.5 | 31.1 |
| Growth rate | -- | -2.5 | 6.4 | 1.6 | -3.6 | 4.1 | 7.5 | 4.8 | 9.1 |
| Spain (billion-PKM) | 11.7 | 11.2 | 11.2 | 12.7 | 12.8 | 14.1 | 15.1 | 15.5 | 16.1 |
| Growth rate | -- | -4.3 | 0.0 | 13.4 | 0.8 | 10.2 | 7.1 | 2.7 | 3.9 |
| France (billion-PKM) | 51.9 | 52.0 | 51.1 | 50.8 | 50.7 | 50.0 | 50.5 | 58.3 | 56.8 |
| Growth rate | -- | 0.2 | -1.7 | -0.6 | -0.2 | -1.4 | 1.0 | 15.5 | -2.6 |
| China (billion-PKM) | 46.3 | 105.8 | 144.6 | 214.1 | 282.5 | 386.3 | 464.1 | 577.6 | 680.5 |
| Growth rate | -- | 128.5 | 36.7 | 48.1 | 32.0 | 36.7 | 20.1 | 24.5 | 17.8 |
| Taiwan (billion-PKM) | 7.5 | 8.1 | 8.6 | 8.6 | 8.6 | 9.7 | 10.5 | 11.1 | 11.6 |
| Growth rate | -- | 8.0 | 6.2 | 0.0 | 0.0 | 12.8 | 8.3 | 5.7 | 4.5 |
| Japan (billion-PKM) | 77.4 | 81.4 | 86.0 | 89.2 | 91.0 | 97.4 | 99.6 | 101.4 | 103.6 |
| Growth rate | -- | 5.2 | 5.7 | 3.7 | 2.0 | 7.0 | 2.3 | 1.8 | 2.2 |
| Korea (billion-PKM) | 11.0 | 13.6 | 14.1 | 14.5 | 14.4 | 15.1 | 16.3 | 14.9 | 15.3 |
| Growth rate | -- | 23.6 | 3.7 | 2.8 | -0.7 | 4.9 | 8.0 | -8.6 | 2.7 |

Table 7-23: Evolution of HSR traffic in different countries (2010–2018). (Source: UIC, 2020b)

### 7.5.3 Forecasting Hyperloop demand

To forecast demand for Hyperloop in the case study's Riyadh–Dammam corridor, estimated figures were obtained from Flightradar (2019), SRO, SMoT (Saudi Ministry of Transport) and SAPTCO for the current number of passengers travelling by air, bus, car and classic rail in 2018. The total for the modes of transport being considered is 5.1 million passengers: 1.6 million by air; 0.24 million by bus; and 1.4 million by car. In 2018, more than 1.8 million passengers travelled directly between the two cities on classic rail, as shown in Table 7-24.

| | Air | Bus | Car[10] | Classic rail | Total |
|---|---|---|---|---|---|
| Mean of service per month[11] | 592 | 504 | 48,541 | 328 | |
| Mean of capacity per vehicle | 273 | 49 | 5 | 576 | |
| Mean occupancy factor | 85% | 80% | 48% | 80% | |
| No. of passengers per month | 137,374 | 19,757 | 116,498 | 151,142 | 424,771 |
| No. of passengers per year | 1,648,483 | 237,082 | 1,397,981 | 1,813,709 | 5,097,254 |
| % | 32 | 5 | 27 | 36 | 100 |

Table 7-24: Nos. of passengers travelling on planes, buses, cars and classic rail along Riyadh–Dammam corridor in 2018[12]

The numerical data for the experiments were collected by the study's survey, which was designed to forecast future intercity travel mode choice in the Riyadh–Dammam corridor in order to develop travel demand models. Mean occupancy factors of air, bus, car and classic rail transport were assumed, based on dissimilar reasons for each mode. For example, the load factor of a car was estimated at about 48%, due to household size, assuming an average capacity of five people per car and a mean load of 2.4. For intercity bus services, especially between two large cities, smaller sized buses are generally fully occupied with a load factor of 80% (MMUTIS Study

[10] Computed on the basis of a departure every minute.

[11] This means the number of vehicles per month.

[12] Annual number of passengers travelling between Riyadh and Dammam.

Team, 1999). Occupancy rates for classic rail are commonly up to 80% in Saudi Arabia, through technical improvements to the system or marketing strategies, while the actual size of a train can be adjusted to varying levels of demand (Douglas and Karpouzis, 2006). The load factor of airlines is high and has increased slightly in recent years, as the occupancy of aircraft seats averages 85% due to the limited number of airlines serving the main cities of the country (Houghton, 2013). As a result, along the Riyadh–Dammam corridor in each direction classic rail was found to be the mode with the highest share of trips at 36%, followed by air, car and bus transport at 32%, 27% and 5%, respectively.

Car demand in Saudi Arabia is mainly related to the number of households, yet it has also increased due to the limited intercity public transport services. In this case study, the percentages of passengers with or without access to a car were assumed to be 75% and 25%, respectively (Statista, 2020). This split between those with or without access to a car might change over time due to rising petrol prices and improved intercity public transport, but it is likely that the 25% without cars will decrease due to rising incomes. To determine for the model the number of passengers with access to a car, the total number of passengers along the Riyadh–Dammam corridor was multiplied by the demand for existing modes of transport, as shown in Table 7-25. In this case, the total size of market (TM) = total market of car available (TCA) + Total market of non-car available (TNCA), which is thus fixed and does not change from before to after, as the SP does not include trip generation.

| Type | Nos. of passengers in 2018 | Total percentage (%) | Included mode | Passengers per mode | Total passenger nos |
|---|---|---|---|---|---|
| Access to car | 5,097,255 | 75 | Bus | 177,812 | 3,822,941 |
| | | | Car | 1,048,486 | |
| | | | Air | 1,236,362 | |
| | | | Conventional rail | 1,360,282 | |
| No access to car | | 25 | Bus | 59,271 | 1,274,314 |
| | | | Car | 349,495 | |
| | | | Air | 412,121 | |
| | | | Conventional rail | 453,427 | |

Table 7-25: Nos. of passengers who have access/no access to a car in 2018

In this case, for 2018, the number of passengers with access to a car was found to be 3,822,941 (75%), and the number without 1,274,314 (25%), to give a total demand market of 5,097,254. For example, the number of bus passengers with a car available (177,812) was achieved by multiplying total bus demand (237,082) presented in Table 7-24, by 75% and for no car available by 25% to achieve 59,271. In this case, it assumes that bus passengers are a perfect sample of the total population, as it is likely that some with a car are travelling by bus due to the low fares. Also, in the absence of data to the contrary, the same mode split is assumed for both car available and non-car available, being the only basis to allocate the use of modes between those with and without a car available. Ideally, we would have data on mode split by car availability (cross-tabulation). We could use multinomial logit models to forecast the mode splits for both car available and no car available in the situation without HSGT technologies.

The utility of existing transport modes (bus, classic rail, air and car transport) and new modes (HSR and Hyperloop) for both experiments depends on travel cost, travel time and the ASC. In this case study, the values of attributes of travel cost and travel time for current modes, as shown in Table 7-26, were based on the figures on the websites of SRO, SAPTCO and the Saudi Authority of Civil Aviation (GACA). Values for HSR and Hyperloop were based on the HHSR and the Hyperloop alpha White Paper presented by Musk (2013). In terms of values of ASC, the coefficients of HSR in both experiments were taken in order to achieve a -0.31 for the No car available Hyperloop ASC by multiplying the coefficient of -0.17 (Hyperloop Car available) by the ratio of the coefficients of 0.93 (HSR No car available) and 0.52 (HSR Car available).

| Mode | Travel cost[13] (Riyals) | Travel time (hrs) | No car available | | Car available | |
|---|---|---|---|---|---|---|
| | | | ASC | Utility | ASC | Utility |
| Bus | 68 | 6.25 | 0 | -3.06 | -0.41 | -2.74 |
| HSR | 232 | 2 | 0.93 | -0.66 | 0.52 | -0.61 |
| Classic rail | 79 | 4.33 | 1.40 | -0.82 | 0.78 | -0.89 |
| Hyperloop | 373 | 1 | -0.31 | -1.84 | -0.17 | -1.20 |
| Air | 139 | 1.85 | -0.29 | -1.54 | -0.16 | -1.07 |
| Car | 50 | 4.22 | - | - | 0 | -1.58 |

Table 7-26: Alternative-specific constants and utilities of included transport systems

In a second case, the ASC coefficient of -0.41 for the bus for those with car available was determined by subtracting the coefficients of HSR (0.52-0.93), as the HSR was common in both experiments. Furthermore, the ASC coefficient of air (-0.29) for those with no car available was achieved by multiplying the coefficients of 0.93 (HSR No car available) by the ratio of the -0.16 (Air Car available) and 0.52 (HSR Car available). Lastly, the alternative-specific constant of classic rail (0.78) in the second experiment was calculated by multiplying the coefficient of 0.52 (HSR Car available) by the ratio of the coefficients of 1.40 (Classic rail No car available) and 0.93 (HSR No car available).

From the SP, the probabilities (P) of using each mode before and after the introduction of HSR and Hyperloop for both the car-available (CA) and non-car available (NCA) markets were determined, as the calculations of the probabilities were based on the utilities of the modes of transport. For example, if introducing HSR on its own to the existing transport modes for the no-car available experiment, the HSR gets a 42% share, as shown in Table 7-27.

[13] The travel cost in Riyals for HSR and Hyperloop were determined on the basis of the price of Haramain High-Speed Rail and the expected price by Musk, E. (2013) *Hyperloop alpha*. Available at: http://www.spacex.com/sites/spacex/files/hyperloop_alpha-20130812.pdf.

| Mode | Utility | Probability before HSR and Hyperloop | Probability after HSR only | Probability after Hyperloop only |
|---|---|---|---|---|
| Bus | -3.06 | 0.07 | 0.04 | 0.05 |
| HSR | -0.66 | -- | 0.42 | -- |
| Classic rail | -0.82 | 0.63 | 0.36 | 0.51 |
| Hyperloop | -1.84 | -- | -- | 0.18 |
| Air | -1.54 | 0.31 | 0.18 | 0.25 |
| Car | -- | -- | -- | -- |
| **Total** | | **1.00** | **1.00** | **1.00** |

Table 7-27: Probability of existing transport modes before and after introducing HSR and Hyperloop for no car available

In this case, the total probability of existing transport modes (bus, classic rail and air transport) before introducing the HSR system was equal to one, as classic rail has the highest probability of 63%, compared to 7% and 31% for bus and air transport. In reality, upon the introduction of HSR/Hyperloop classic rail's frequency is expected to fall. On the other hand, Hyperloop achieves a 18% share after its introduction, on its own, to the existing transport modes, while the remaining percentage is split 5%, 51% and 25% between bus, classic rail and air transport, respectively (to total 82%).

For the car available experiment, the HSR total probability of existing transport modes (bus, classic rail, air transport and car) before the introduction of the HSR system is also equal to one, as shown in Table 7-28; however, the HSR achieves a 35% share, while the remaining are split 4%, 26%, 22% and 13% for bus, classic rail, air and car transport, respectively (to total 65%).

| Mode | Utility | Probability before HSR | Probability after HSR only | Probability after Hyperloop only |
|---|---|---|---|---|
| Bus | -2.74 | 0.06 | 0.04 | 0.05 |
| HSR | -0.61 | -- | 0.35 | -- |
| Classic rail | -0.89 | 0.40 | 0.26 | 0.31 |
| Hyperloop | -1.20 | -- | -- | 0.23 |
| Air | -1.07 | 0.33 | 0.22 | 0.26 |
| Car | -1.58 | 0.20 | 0.13 | 0.16 |
| **Total** | | **1.00** | **1.00** | **1.00** |

Table 7-28: Probability of existing transport modes before and after introducing HSR for car available

On the other hand, Hyperloop has a 23% share, while the remaining are split 5%, 31%, 26% and 16% for bus, classic rail, air and car transport, respectively. For

example, the new share for HSR can be determined by multiplying the appropriate P by the appropriate volume in order to compute this size of the market as follows:

$$SPHSR = P(HSR\ NCA) * TNCA + P(HSR\ CA) * TCA \quad \text{Equation 7-15}$$

where

$\mathrm{SPHSR} = \text{total demand for HSR from the SP model}$

$\mathrm{P(HSR\ NCA)} = \text{probability of HSR for non} - \text{car available}$

$\mathrm{TNCA} = \text{total demand of non} - \text{car available market}$

$\mathrm{P(HSR\ CA)} = \text{probability of HSR for car available}$

$\mathrm{TCA} = \text{total demand of car available market.}$

As the total market is 3,822,941 for those with a car available with a 35%[14] share for HSR, the demand for HSR is equal to 1,325,115, as shown in Table 7-29. For the experiment with no car available, the total market is estimated at 1,274,314 with a 42% share of HSR, which gives an HSR demand of 540,503.

| Mode | No car available | | | Car available | | | Total demand[15] |
|---|---|---|---|---|---|---|---|
| | Utility | Probability after HSR only | Demand | Utility | Probability after HSR only | Demand | |
| Bus | -3.06 | 0.04 | 49,033 | -2.74 | 0.04 | 157,473 | 206,506 |
| HSR | -0.66 | 0.42 | 540,503 | -0.61 | 0.35 | 1,325,115 | 1,865,618 |
| Classic rail | -0.82 | 0.36 | 460,586 | -0.89 | 0.26 | 1,001,501 | 1,462,087 |
| Hyperloop | -1.84 | -- | -- | -1.2 | -- | -- | -- |
| Air | -1.54 | 0.18 | 224,191 | -1.07 | 0.22 | 836,524 | 1,060,715 |
| Car | -- | -- | 0 | -1.58 | 0.13 | 502,329 | 502,329 |

Table 7-29: Total demand for transport modes from the SP model after introducing HSR to both experiments

[14] Note: The level of precision and results are based on Excel's computation: in this Word file, figures are rounded to two decimal places.

[15] Demand for classic rail is very resilient – but, in reality, one would expect reductions in frequencies and hence reductions in demand.

In this case, the total demand for HSR from the SP model is equal to 1,865,618. Bus travel has a total demand of 206,506; that is, 49,033 and 157,473 for the no car and car available markets, respectively. In addition, classic rail has a total demand of 1,462,087, computed from 460,586 and 1,001,501 for no car and car available, respectively. Air transport has a total demand of 1,060,715; that is, 224,191 and 836,524 for no car and car available, respectively, while the total demand for car travel was found to be 502,329, from only car available.

On the other hand, the total demand for Hyperloop from the SP model can be determined as follows:

$$SPHL = P(HL\ NCA) * TNCA + P(HL\ CA) * TCA \qquad \text{Equation 7-16}$$

where

$\mathrm{SPHL} = \text{total demand for Hyperloop from the SP model}$

$\mathrm{P(HL\ NCA)} = \text{probability of Hyperloop for non} - \text{car available}$

$\mathrm{TNCA} = \text{total demand of non} - \text{car available market}$

$\mathrm{P(HL\ CA)} = \text{probability of Hyperloop for car available}$

$\mathrm{TCA} = \text{total demand of car available market.}$

The demand for Hyperloop from the SP model is equal to 868,752 for car available, as the total market also is 3,822,941 with a 26% share for Hyperloop. For the no car available experiment, the total market was estimated at 1,274,314 with a 18% share for Hyperloop, which gives a Hyperloop demand of 235,188. As a result, the total demand for Hyperloop from the SP model is 1,103,940 passengers (Table 7-30).

| Mode | No car available | | | Car available | | | Total demand |
|---|---|---|---|---|---|---|---|
| | Utility | Probability after Hyperloop only | Demand | Utility | Probability after Hyperloop only | Demand | |
| Bus | -3.06 | 0.05 | 69,435 | -2.74 | 0.05 | 186,244 | 255,679 |
| HSR | -0.66 | -- | -- | -0.61 | -- | -- | -- |
| Classic rail | -0.82 | 0.51 | 652,221 | -0.89 | 0.31 | 1,184,479 | 1,836,700 |
| Hyperloop | -1.84 | 0.18 | 235,188 | -1.2 | 0.23 | 868,752 | 1,103,940 |
| Air | -1.54 | 0.25 | 317,470 | -1.07 | 0.26 | 989,360 | 1,306,830 |
| Car | -- | -- | -- | -1.58 | 0.16 | 594,106 | 594,106 |

Table 7-30: Total demand for transport modes from the SP model after introducing Hyperloop to both experiments

In this case, bus has a total demand of 255,679; that is, 69,435 and 186,244, while classic rail has a total demand of 1,836,700, computed from 652,221 and 1,184,479 for no car and car available, respectively. Air transport has a total demand of 1,306,830; that is, 317,470 and 989,360 for no car and car available, respectively, while total demand for car travel was found to be 594,106, from only car available.

The probability of adding HSR and taking the classic rail away was also calculated: 0.66 and 0.47 for no car and car available. This gives a total demand of 2,640,939, the sum of 845,239 and 1,795,700, respectively, as in Table 7-31.

| Mode | Probability of no car available | Demand, without access to a car | Probability of car availability | Demand, with access to a car | Total demand |
|---|---|---|---|---|---|
| Add HSR, take away classic rail | 0.66 | 845,239 | 0.47 | 1,795,700 | 2,640,939 |
| Add Hyperloop, take away classic rail | 0.37 | 477,625 | 0.33 | 1,256,493 | 1,734,118 |
| Add HSR and Hyperloop (HSR) | 0.37 | 477,002 | 0.29 | 1,113,292 | 1,590,294 |
| Add HSR and Hyperloop (Hyperloop) | 0.11 | 145,169 | 0.16 | 615,330 | 760,499 |
| Add HSR and Hyperloop (sum) | 0.49 | 622,170 | 0.45 | 1,728,622 | 2,350,792 |
| Add HSR and Hyperloop, take away classic rail (HSR) | 0.55 | 703,274 | 0.37 | 1,425,591 | 2,128,865 |
| Add HSR and Hyperloop, take away classic rail (Hyperloop) | 0.17 | 214,032 | 0.21 | 787,941 | 1,001,973 |
| Add HSR and Hyperloop, take away classic rail (sum) | 0.72 | 917,305 | 0.58 | 2,213,532 | 3,130,837 |

Table 7-31: Estimated result of demand for each included transport mode when car is available or non-available in 2018 (NB Figures have been rounded)

In addition, the probability of adding Hyperloop and taking classic rail away is 0.37 and 0.33 for no car and car available, to give a total demand of 1,734,118, the sum of 477,625 and 1,256,493. The probability of adding both transport modes, using

the HSR as a base, is calculated at 0.37 and 0.29, to give a total demand of 1,590,294, while the probability of adding both modes, using Hyperloop as a base, is equal to 0.11 and 0.16 for no car and car available, respectively, to give a total demand of 760,499 passengers.

To forecast the travel demand for Hyperloop in the initial year of operation (2030), it was necessary to examine growth in demand from 2018 to 2030 due to population increases, GDP per capita increases and the passage of time for classic rail, air, car and bus.

In elasticity analysis, real prices are used with an inflation adjustment, as inflation consists of increasing/decreasing prices since a base year. For example, real prices are constant if nominal prices increase by 10% in that time period yet inflation is also 10%. On the other hand, real prices increase by around 9% if nominal prices rise by 20% in that period yet inflation is running at 10% (Litman, 2013). In this case, GDP per capita and fares are shown in real terms, as GDP is determined by dividing the nominal GDP per capita by the GDP inflation deflator. In the case study, the demand for classic rail was determined for 2030, 2040 and 2050 using the log-linear DDM to obtain values of 2.24 million, 3.10 million and 3.90 million passengers, respectively, as shown in Table 7-32.

| Year | Population | Mean GDP per capita ($) | Mean train service frequency | Mean speed | Mean fare | Total predicted passengers |
|---|---|---|---|---|---|---|
| 2030 | 10,025,000 | 40,963.30 | 9 | 200 | 180 | 2,238,108 |
| 2040 | 11,589,296 | 46,249.70 | 10 | 220 | 190 | 3,055,267 |
| 2050 | 12,397,683 | 52,124.69 | 11 | 230 | 200 | 3,903,981 |

Table 7-32: Estimated demand of classic rail in 2030, 2040 and 2050

Growth in demand for bus, car and air travel also needs to be considered, using income and population elasticities. An increase of 6% in population is projected when GDP per capita increases by 24% between 2018 and 2030. To determine the estimated demand for bus, car and air transport, the elasticity for bus with respect to income is assumed to be -0.5, and at 0.5 and 1.5 for car and air transport, respectively (based on Litman, 2013). Furthermore, the increasing/decreasing percentages of demand with respect to GDP per capita from 2018 to 2030 are -5%,

18% and 46% for bus, car and air, respectively. In this case, there is a projected decrease in demand for bus from 0.24 million (2018) to 0.23 million (2030), then an increase to 0.25 million and 0.263 in 2040 and 2050, respectively, as shown in Table 7-33.

| Year | 2018 | 2030 | 2040 | 2050 |
|---|---|---|---|---|
| Population | 9,453,827 | 10,025,000 | 11,589,296 | 12,397,683 |
| GDP per capita | 33,089.37 | 40,963.30 | 46,249.70 | 52,124.69 |
| Population change | | 1.06 | 1.23 | 1.31 |
| GDP change | | 1.24 | 1.40 | 1.58 |
| Demand of bus (passengers/year) | 237,082 | 225,955 | 245,832 | 247,716 |
| Demand of car (passengers/year) | 1,397,981 | 1,649,420 | 2,026,100 | 2,300,974 |
| Demand of air Transport (passengers/year) | 1,648,483 | 2,407,802 | 3,339,370 | 4,274,151 |
| Demand of classic rail (passengers/year) | 1,813,709 | 2,238,108 | 3,055,267 | 3,903,981 |
| **Total demand (passengers/year)** | **5,097,254** | **6,521,285** | **8,666,568** | **10,726,821** |

Table 7-33: Estimated demand for bus, car and air transport in 2030, 2040 and 2050

Estimated demand for car transport is projected to increase by 18% from 1.4 million in 2018 to 1.6 million in 2030 and by 45% and 65% in 2040 and 2050 to achieve a total demand of 2.0 million and 2.3 million, respectively (see Figure 7-4). For air transport, there is an increase in demand of 46%, 102% and 159%, from 1.6 million in 2018 to 2.4, 3.3 and 4.3 million in 2030, 2040 and 2050, respectively.

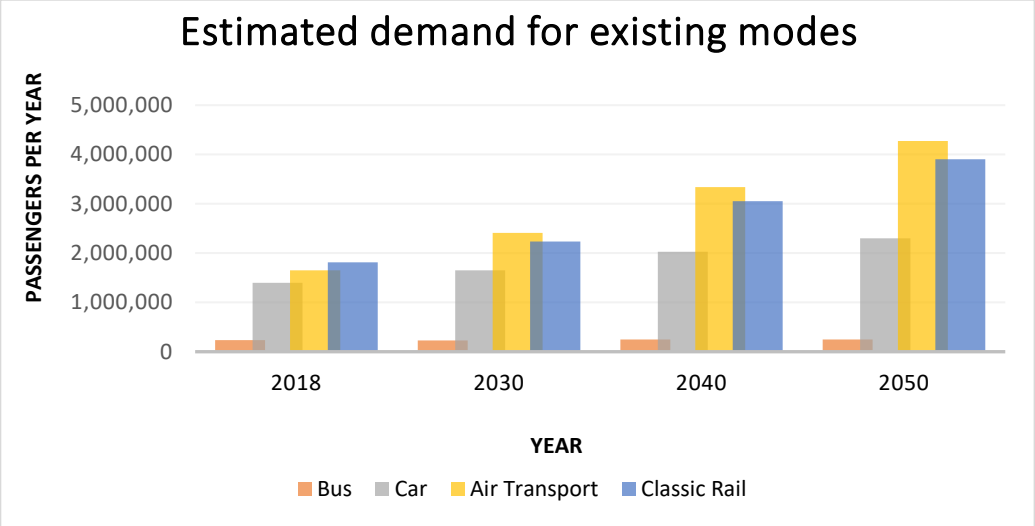


Figure 7-4: Estimated demand for bus, car, air transport and classic rail in 2030, 2040 and 2050

Total demand for existing modes of transport is projected to increase from 5.1 million in 2018 to 6.5 million in 2030, a percentage rise of 27.9%.

Based on the estimated demand for HSR demand of 5,150,256, using the DDM, only about 36% (1,865,618/5,150,256) of demand is abstracted, while the rest is generated (64%). In this case, 5% of demand is abstracted from bus travel, and 28%, 21% and 10% from classic rail, air and car transport, respectively. The demand generated for HSR was found by subtracting the total demand for HSR using SP from the DDM HSR forecast, as follows:

$$HSRGEN = DDMHSR - SPHSR \qquad \text{Equation 7-17}$$

where

HSRGEN = generated demand for HSR
DDMHSR = demand for HSR using the DDM
SPHSR = total demand for HSR from the SPM.

The total generated demand for HSR was found to be 3,284,638 passengers, as shown in Table 7-34, split between those with a car available and those without (0.75:0.25) to give a generated demand of 2,463,478 and 821,159, respectively. In this case, the value of 821,159 was determined by multiplying 0.25 by 3,284,638, while the total generated demand of 3,284,638 was obtained by subtracting 1,865,618 from 5,150,256. In addition, the new demand for those with no car available of 2,095,473 was determined by adding 1,274,314 to 821,159.

| | **Demand, no car available** | **Demand, car available** | **Total demand 2018** |
|---|---|---|---|
| Demand for HSR (DDM) | | | **5,150,256** |
| Demand for existing travel modes | 1,274,314 | 3,822,941 | **5,097,255** |
| Demand for HSR (abstracted) | 540,503 | 1,325,115 | **1,865,618** |
| Generated demand | 821,159 | 2,463,478 | **3,284,638** |
| New demand | 2,095,473 | 6,286,420 | **8,381,893** |

Table 7-34: Total new demand for travel in the corridor in 2018

The total new demand for travel in the corridor then increases to 8,381,623, achieved by adding the total generated demand (3,284,638) to the total demand for existing modes (5,097,255).

In order to check how the introduction of new modes of transport increases the size of the market, the logsum before and after adding the HSR system needed first to be determined for no car and car available, by dividing by the cost parameter value ($\alpha_1$). However, it is calculated using only current transport modes, before the introduction of new modes of HSR and Hyperloop for no car available, including bus, classic rail and air transport, as follows:

$$\text{Log sum before (NCA)} = \frac{1}{\alpha_1} \log(\exp^{U_B} + \exp^{U_{CL}} + \exp^{U_{Air}}) \quad \text{Equation 7-18}$$

The logsum of exponential utility for a car available before introducing the new transport of HSR and Hyperloop system is determined by including bus, classic rail, air and car transport, as follows:

$$\text{Log Sum before (CA)} = \frac{1}{\alpha_2} \log(\exp^{U_B} + \exp^{U_{CL}} + \exp^{U_{Air}} + \exp^{U_{Car}}) \quad \text{Equation 7-19}$$

On the other hand, the logsum of the first experiment when no car is available is calculated by taking the exponential of utility of all transport modes being considered, after introducing HSR and Hyperloop to the existing modes serving the corridor, namely bus, classic rail and air transport.

$$\text{Log Sum after (NCA)} = \frac{1}{\alpha_1} \ln(\exp^{U_B} + \exp^{U_{HSR}} + \exp^{U_{CL}} + \exp^{U_{HL}} + \exp^{U} \quad \text{Equation 7-20}$$

The logsum of exponential utility for a car available after introducing the new transport system of HSR and Hyperloop is presented as follows:

$$\text{Log Sum after (CA)} = \frac{1}{\alpha_2} \log(\exp^{U_B} + \exp^{U_{HSR}} + \exp^{U_{CL}} + \exp^{U_{HL}} + \exp^{U_{Air}} + \exp^{U_{Car}}) \quad \text{Equation 7-21}$$

As a result, the logsum for no car and car available before and after introducing HSR and Hyperloop is determined as shown in Table 7-35.

| Mode | Utility | |
|---|---|---|
| | Non-car available | Car available |
| Bus | -3.06 | -2.75 |
| HSR | -0.66 | -0.61 |
| Classic rail | -0.82 | -0.9 |
| Hyperloop | -1.85 | -1.2 |
| Air | -1.54 | -1.07 |
| Car | -- | -1.58 |
| Cost parameter | -0.0029012 | -0.0018236 |
| Log Sum after adding HSR and HL | -109.9639287 | -341.4886935 |
| Log Sum after adding HSR Only | -68.13149479 | -244.8451216 |
| Log Sum after adding HL Only | 52.41244379 | -152.5242561 |
| Log Sum before | 122.1041892 | -10.58006593 |

Table 7-35: Logsum before and after adding HSR and Hyperloop for car and no car available

For the logsum before adding HSR and Hyperloop, when bus, classic rail and air are the only options to choose from, the disutility of travelling is Riyals122 for those in the no car available experiment, by assuming that the composite cost is equivalent to a disutility. In addition, in the after situation, the traveller is basically willing to pay Riyals110 to travel (there is a positive utility), which will make a benefit of Riyals232 as result of extending the choice, computed to give an equivalent benefit of €51 for each traveller. Among those with a car available, a traveller is willing to pay of Riyals11 to travel before the situation of adding HSR and Hyperloop, when bus, classic rail, air transport and car are the only options to choose from. In this case, after the introduction of HSR and Hyperloop a traveller is prepared to pay Riyals340, with a benefit of Riyals331, an equivalent €72 each. Therefore, the market's increased size is estimated by using the b parameter, based on the division of the differences in total demand before and after the introduction of the HSR system and the composite cost, with and without HSR, as follows:

$$b = \frac{Total\ demand\ in\ 2018\ with\ HSR - Total\ demand\ in\ 2018\ without\ HSR}{Composite\ Cost\ with\ HSR - Composite\ Cost\ without\ HSR}$$ Equation 7-22

where the difference in composite cost is calculated by subtracting the logsum before and after the introduction of the HSR system, as shown in Table 7-36. The values of 1,274,314 and 3,822,941 were calculated by multiplying 5,097,255 by 0.25 and 0.75, respectively.

| | No car available | Car available | Total Demand |
|---|---|---|---|
| Log sum after adding HSR | -68.13 | -244.85 | -- |
| Log sum before adding HSR | 122.10 | -10.58 | -- |
| Demand for existing transport modes | 1,274,314 | 3,822,941 | 5,097,255 |
| Demand for HSR (abstracted) | 540,503 | 1,325,115 | 1,865,618 |
| Generated demand | 821,159 | 2,463,478 | 3,284,637 |
| New demand | 2,095,473 | 6,286,420 | 8,381,893 |
| Difference in composite cost | -190.24 | -234.27 | -- |
| **B** | **-4,316.54** | **-10,515.77** | **--** |

Table 7-36: Determining the increased size of the market

The results of the b parameter indicate that a one-unit increase in composite cost leads to a loss of 4,317 travellers from the 'no car available' market and 10,516 per annum from the 'car available' market. The substantial reductions in composite costs are the result of HSR generating a great deal of demand.

On the other hand, the abstracted demand for Hyperloop for those with no car available in 2018 is 235,188, determined by multiplying the probability of 0.18 by the demand for existing modes of travel for those with no car available: 1,274,314. For those with a car available, it resulted in 868,752, using a probability of 0.23, as shown in Table 7-37.

| | Total demand 2018 | Total demand 2030 | Total demand 2040 | Total demand 2050 |
|---|---|---|---|---|
| Demand for existing modes (no car available) | 1,274,314 | 1,630,321 | 2,166,642 | 2,681,705 |
| Demand for Hyperloop (abstracted no car available) | 235,188 | 691,504 | 918,986 | 1,137,451 |
| Demand for existing modes (car available) | 3,822,941 | 4,890,964 | 6,499,926 | 8,045,116 |
| Demand for Hyperloop (abstracted car available) | 868,752 | 1,695,315 | 2,253,017 | 2,788,614 |
| Total demand for existing travel modes | **5,097,255** | **6,521,285** | **8,666,568** | **10,726,821** |
| Total demand for Hyperloop (abstracted) | **1,103,940** | **2,386,820** | **3,172,003** | **3,926,065** |

Table 7-37: Total abstracted demand for Hyperloop in 2018, 2030, 2040 and 2050

The total abstracted demand for Hyperloop was found to be 1,103,940 in 2018, 2,386,820 in 2030, 3,172,003 in 2040 and 3,926,065 in 2050, based on total

demand for existing modes of travel. The total demand in 2018 without Hyperloop and the difference in composite cost before and after introducing Hyperloop were used in order to calculate the total demand in 2018 with Hyperloop as follows:

$$Total\ demand\ with\ Hyperloop\ in\ 2018 = Total\ demand\ without\ Hyperloop + b * (Composite\ Cost\ with\ Hyperloop - Composite\ Cost\ without\ Hyperloop)$$ Equation 7-23

where b was determined previously in Table 8-38 for both no car and car available; however, the total demand with Hyperloop was calculated at 6,890,735 for 2018, from 1,575,141 for those with no car available and 5,315,594 for those with a car available, as shown in Table 7-38.

| | No car Available | Car available | Total market |
|---|---|---|---|
| Log sum after adding Hyperloop | 52.41244379 | -152.5242561 | |
| Log sum before adding Hyperloop | 122.1041892 | -10.58006593 | |
| Total demand in 2018 without Hyperloop | 1,274,314 | 3,822,941 | **5,097,255** |
| Difference in composite cost | -69.69174544 | -141.9441902 | |
| B | -4,316.54 | -10,515.77 | |
| Generated demand for Hyperloop | 300,827 | 1,492,653 | **1,793,480** |
| Total demand in 2018 with Hyperloop | 1,575,141 | 5,315,594 | **6,890,735** |
| Abstracted Demand for Hyperloop | 235,188 | 868,752 | **1,103,940** |
| Total Hyperloop demand in 2018 | 536,015 | 2,361,405 | **2,897,420** |

Table 7-38: Total Hyperloop demand in 2018[16]

Furthermore, the generated demand for Hyperloop is 1,793,480, achieved by multiplying the difference in composite cost by the value of b, computed from 33,827 and 1,492,653 for non-car and car available, respectively. As a result, the total demand of Hyperloop in 2018 is 2,897,420, computing from the sum of generated and abstracted demand for Hyperloop.

[16] Note that the calculations are different from HSR, as no information from the direct demand model has to be considered.

The forecast demand for Hyperloop for 2030, 2040 and 2050 was determined using the elasticity of Hyperloop with respect to income, which is assumed to be 1.5, and using the total demand for Hyperloop in 2018 of 2,897,420 as a base. In this case, the forecast for Hyperloop demand for 2030 is the result of the multiplication of total demand for Hyperloop in 2018 (2,897,420), population change (1.06) and GDP change (1.24) to the power of 1.5, as shown in Table 7-39.

| **Year** | **2018** | **2030** | **2040** | **2050** |
|---|---|---|---|---|
| Population | 9,453,827 | 10,025,000 | 11,589,296 | 12,397,683 |
| GDP per capita | 33,089.37 | 40,963.30 | 46,249.70 | 52,124.69 |
| Population change | | 1.06 | 1.23 | 1.31 |
| GDP change | | 1.24 | 1.40 | 1.58 |
| **Total demand for Hyperloop** | **2,897,420** | **4,232,021** | **5,869,370** | **7,512,367** |

Table 7-39 Forecast demand for Hyperloop in 2030, 2040 and 2050

It was found that demand for Hyperloop increased from 2,897,420 in 2018 by 46%, 103% and 159%: to 4,232,021 in 2030; to 5,869,370 in 2040; and to 7,512,367 in 2050 respectively.

Induced demand was detected by the logsum calculations and comparisons with the elasticity model. It was assumed that non-rail users have the same characteristics as rail users, the key distinction being whether they have access to a car or not. This permitted different forecasts of modal choice for those with and without an available car for both HSR and Hyperloop, based on the SP experiments (Tables 7.29 and 7.30). Similarly, this permitted different estimates of the change in logsum between travellers with and without a car available (Table 7.35). However, where the forecasts were from aggregate models (such as the DDM), it was not possible to distinguish between these segments (for example, Table 7.34). An assumption was made that the proportion of travel generated was the same across the two segments. Further work might investigate triangulating the results from the disaggregate SPM and the aggregate DDM.

## 7.6 Conclusion

This chapter summarizes the output of the demand models that were constructed to forecast the levels of demand for the HSR, Maglev and Hyperloop systems, namely the direct demand, elasticity and stated preference models respectively.

In the case study, the proposed HSR service was assumed to open to the public in 2018 with a forecast demand of 5.1 million, using the DDM. In addition, the demand for HSR for 2030, 2040 and 2050 was forecast at 7.5 million, 10.4 million and 13.4 million, respectively. These figures are mainly based on the elasticity of HSR demand with respect to income, which is assumed to be 1.5, using the total demand for HSR in 2018 as a base.

The demand for Maglev was forecast using the elasticity demand model, in terms of generalized journey travel time. In this case, the GJT was determined for both HSR and Maglev on the basis of in-vehicle travel time, service frequency and interchange to obtain values of 114 and 85 mins, respectively. Consequently, the forecast change was ascertained using the generalized journey times of both systems with an elasticity of -0.9 to achieve a result of 1.3024. This means that demand for Maglev is higher than for HSR by 30.24%. As a result, demand for Maglev was forecast to reach 9.8 million in the initial year of 2030, increasing by the same percentage as HSR demand due to the elasticity between them to 13.6 million and 17.4 million for 2040 and 2050.

SP was used to forecast the demand level for Hyperloop by testing the nested logit and multinomial logit models. Therefore, the outcome of nested analysis showed that most of the independent variables and alternative-specific constants are insignificant. This led to the elimination of the NL model and the commencement of testing the multinomial logit model, which showed that it is more suited to this study due to the significant results. In order to forecast demand for Hyperloop, total demand for existing modes of travel (car, air, classic rail and bus transport) was calculated, amounting to 5,097,255 passengers. In this case, total demand for Hyperloop was found to be 2.9 million in 2018, and 4.2 million, 5.9 million and 7.5 million for 2030, 2040 and 2050, respectively. This reflects the reduced capacity provided by this system.

# Chapter 8. Comparative Assessment of Total Social Cost Model

## 8.1 Introduction

Previous chapters have described the three models for travel demand – for HSR, the DD function; for Maglev, the EDM; and for Hyperloop, the SP approach – and their outcomes in terms of forecast levels of demand. This chapter describes the process of using comparative assessment at a strategic level to verify the performance of the three HSGT technologies being considered, in terms of average social cost (ASC), applying it to the case study of the Riyadh–Dammam corridor.

First, the social cost model to be used is described in detail, including the unit cost values, the calculation of the operator, user and external costs and the equations for intermediate variables such as the capital recovery factor, frequency and the operation cycle time, as shown in section 8.2.

Section 8.3 presents the results and a discussion of the comparative assessment, with a comparison of the three HSGT systems' forecast travel demand. The total social costs were based on the endogenous demand levels of HSR, Maglev and Hyperloop resulting from the DDM, EDM and SPM, respectively. A list of the key assumptions for each mode about fare levels, frequency, vehicle size, the implied load factors and the (non-)treatment of in-mode congestion is provided. Fare levels and vehicle size were assumed, using the HHSR, the Transrapid Maglev and the article on Hyperloop Alpha for HSR, Maglev and Hyperloop, respectively. The forecasting of travel demand played a major role in determining the frequency for all the HSGT systems included, whilst the implied load was assumed, based on Janić's 2018 study.

## 8.2 Total Social Cost Model

The TSCM is dependent on the total annual volume of passengers, based on three main categories:

$$TSC = TOC + TUC + TEC \qquad \text{Equation 8-1}$$

where TOC represents the operator costs of infrastructure construction, maintenance costs and the acquisition and O&M of rolling stock/capsule.

Regarding acquisition, the price of an HSR train is determined by its technical specification, including its capacity and the unit cost of its acquisition. On the other hand, costs of labour, the energy consumed by running the trains and the number of trains operated on a specific line are operating costs. The costs of maintaining rolling stock relate to fleet size, labour, materials and spare parts, and train usage (total distance covered by each train every year). Total user cost (TUC) represents the user costs, which are based on door-to-door travel time, including access/egress time, waiting time and in-vehicle travel time, converted into monetary terms using the value of time. Finally, TEC represents external environmental costs, accounting for the expense of the external impact of air pollution, noise, climate change and accidents. The characteristics of the basic parameters need to be recognized in order to evaluate the social cost of HSGT attributes such as line length, numbers of stations, average operating speed, vehicle capacity and carriages per train. Several cost categories are assumed, captured by alternative-specific constants such as safety, convenience, comfort and construction/operation complexity.

### 8.2.1 Operator cost

The operator cost (OC) of HSGT involves both the infrastructure cost (IC) of line/tube and rolling stock/capsule cost (RSC):

$$OC = IC + RSC \qquad \text{Equation 8-2}$$

Annual capital recovery costs are considered only for annual infrastructure construction and annual rolling stock/capsule acquisition.

#### 8.2.1.1 Infrastructure cost

The infrastructure costs of an HSGT line/tube are divided into infrastructure construction costs (ICCs) and infrastructure maintenance costs, as both are relatively dependent on the length of corridor and average unit costs.

#### 8.2.1.1.1 Infrastructure construction cost

The total ICC of a line/tube is calculated by using the required length of the route multiplied by the unit construction cost and the proportion of the construction costs spent on planning. In this case, in terms of fare these HSGT technologies are inclusive from the point of view of construction costs, as HSR fares were assumed to be based on the HHSR fare, using the same for Maglev. For Hyperloop, the fare was based on the Alpha paper presented by Elon Musk in 2013.

The ICC is converted to an annual basis by using the equation of capital recovery factor designed by Rogers and Duffy (2012):

$$ICC = L\,[c_c(1+\rho)] * [\frac{i(1+i)^n}{(1+i)^n-1}] \qquad \text{Equation 8-3}$$

where:

ICC = infrastructure construction cost of HSGT line/tube (€/year)

L = length of a given HSGT line (km)

$c_c$ = infrastructure construction unit cost of a given HSGT line (€/km)

ρ = planning costs as a proportion of construction costs

$i$ = discount rate (percentage/year)

$n$ = lifespan of infrastructure element (year).

For fixed-line HSGT technologies, the cost of infrastructure construction involves planning and land costs, infrastructure building costs and superstructure costs. First, the planning and land costs incorporate the result of studies on a project's technical and economic feasibility, land purchase, administrative and legal fees, permits, licences, and so on. These costs often represent 5% to 10% of the total infrastructure construction costs. Second, the construction of IC is related to the preparation of terrain and construction of platforms, and these are dependent on the line's characteristics, such as tunnels, bridges and viaducts. Finally, the superstructure costs are related to specific rail/tube elements such as tracks and sidings, electrification mechanisms and catenaries, signalling systems, safety and communications installations, and so on.

Once the technical and economic feasibility studies had been completed, the total duration of the case study's project was estimated on the basis of Campos, de Rus and Barron's work (2007a) at 40 years: five years for the infrastructure construction and 35 for lifetime operation.

The social discount rate is the financial return anticipated from investing in a project, and this usually depends on the project's lifespan. In Europe, the discount rate ranges between 3% and 6%, while it is generally higher in the three Asian developing countries (India, Pakistan and Philippines), in the range of 12% to 15% (Zhuang *et al.*, 2007). As recommended by the European Commission, for the evaluation of infrastructure projects the social discount rate is 5% in real terms (de Rus, 2009).

The discount rate that was used for the case study, over various periods, is as stated by the UK Department for Transport (2018), so that all costs are on an annual basis, as presented in Table 8-1. This study assumes that the discount rate is the same in Saudi and UK projects.

| **Duration** | **0–30** | **31–75** | **76–125** | **126–200** | **201–300** | **301 and over** |
|---|---|---|---|---|---|---|
| Discount rate (%) | 3.50 | 3.00 | 2.50 | 2.00 | 1.50 | 1.00 |

Table 8-1: Discount rates over different periods. (Source: Department for Transport, 2018)

#### 8.2.1.1.2 Infrastructure maintenance cost

The infrastructure maintenance cost (IMC) of HSGT technology is calculated by using the required length of track/tube multiplied by the unit cost of its maintenance:

$$IMC = L * c_m \qquad \text{Equation 8-4}$$

where:

IMC = infrastructure maintenance cost of HSGT line/tube (€/year)

$c_m$ = infrastructure maintenance unit cost of a given HSGT line (€/year/km).

Infrastructure maintenance costs concern the maintenance of tracks/tubes, electric traction installations and other equipment, such as system of power supply, vacuum (Hyperloop), and so on. As a result of calculation of the IC of HSGT line, it is expressed as follows:

$$IC = L \left\{ \left[ \frac{c_c(1+\rho)*i(1+i)^n}{(1+i)^n-1} \right] + c_m \right\}$$ Equation 8-5

#### 8.2.1.2 Rolling stock/capsule cost

The acquisition and O&M of rolling stocks/capsules are the main categories of this cost of running services on an HSGT route.

##### 8.2.1.2.1 Rolling stock/capsule acquisition cost

The process of contracting, designing, building, delivering and testing in order to purchase new rolling stock usually takes several years, even when the projected demand is known in advance. The cost of HSR rolling stock usually depends on the number of seats, as to keep maintenance down it is best to choose a train with a large capacity, besides the number of departures. Acquisition cost is calculated from the annual value, multiplying the number of trains/capsules by their average capacity and average unit cost of acquiring rolling stock/capsule per seat.

$$RSC_A = [RS_t * c_A * c] * [\frac{i(1+i)^n}{(1+i)^n - 1}]$$ Equation 8-6

where:

$RSC_A$ = acquisition costs of rolling stock/capsule (€/year)

$RS_t$ = total number of acquired trains/capsule

$c_A$ = unit cost of acquiring a rolling stock/capsule (€/seat)

C = average seat capacity of a train/capsule (seat).

Average vehicle capacity for each HSGT technology in the case study was estimated at 417, 500 and 28 seats for HSR, Maglev and Hyperloop, respectively (ArabianBusiness, 2018; Janić, 2018). In this model, the total number of acquired trains/capsule ($RS_t$) is dependent on the operation cycle time of the train/capsule and frequency, as follows:

$$RS_t = (1.5) \times \tau \times F_t$$ Equation 8-7

where:

$\tau$ = operation cycle time of the train/capsule (hour/train or capsule)

$F_t$ = transport service frequency on the corridor (vehicle/hour).

The value of 1.5 is defined as the exogenous contingency factor associated with the risk of failing to provide services, and it relates to the acquisition and O&M cost of an over-sized fleet. It varies from 1.25 to 1.6, depending on the line (Campos, de Rus and Barron, 2007a).

Operation cycle time is defined as the average turnaround time of a train/vehicle along the travel corridor, which is closely based on its length and operating speed, plus the time to turning at the start and end stations. It is calculated as follows:

$$\tau = 2 * (L/v) + (20 + 20)/60\text{min} \qquad \text{Equation 8-8}$$

where:

$\tau$ = operation cycle time of the train/vehicle (hour/train)

$v$ = average commercial speed (km/hour)

$L$ = length of corridor (km).

Frequency is the total number of daily services per direction, obtained from the level of projected demand and the effective occupation capacity of a train/capsule, and it can be calculated by multiplying the train's capacity by the average load factor per service frequency on the line, as follows:

$$F_t = \frac{Q_t}{O_d \times Q_e} \qquad \text{Equation 8-9}$$

where:

$F_t$ = frequency (trains per hour, one direction)

t = t-th year starting from the beginning of the period of (n) years of operation of a given line/tube (year)

$Q_t$ = projections of the (one-way) daily demand (passengers)

$O_d$ = operating daily hours (hour)

$Q_e$ = effective occupation (seats).

The projection of daily demand per direction in years is based on dividing the initial annual demand by the number of directions and days per year, as follows:

$$Q_t = \frac{ID_a}{N * days/year}$$ Equation 8-10

where:

$Q_t$ = projections of the (one-way) daily demand (passenger)

$ID_a$ = initial annual demand (passengers/year)

$N$ = number of directions.

In the case study, the direct DDM was used to forecast the initial annual passenger demand for HSR, based on the population and mean GDP per capita of cities along the proposed line, the number of trains per day, mean speed, mean fare and the dummy variable for the month. For the first year of operation, the EDM and SP models were used for the proposed Maglev and Hyperloop lines, respectively, (2030). It is usual to use two directions when proposing an HSGT line.

To calculate the effective occupation, the load factor and train/capsule capacity had to be estimated. The load factor is generally used to measure how efficiently a transport provider fills seats to derive fare revenue, and how this is estimated depends on the mode. In this case, the effective occupation in the TSCM is calculated as follows:

$$Q_e = l * c$$ Equation 8-11

where:

$l$ = load factor (percentage)

$c$ = train/capsule capacity (seats).

Based on the results of effective occupation and the projections of daily demand, the number of trains/capsules per day-direction (NS) can be determined as follows:

$$NS = \frac{Q_t}{Q_e}$$ Equation 8-12

#### 8.2.1.2.2 Rolling stock/capsule operating cost

Rolling stock/capsule operating cost is a product of frequency, vehicle capacity, line/tube length and average unit cost of operating a rolling stock/capsule. In this case, the value of 2 represents the number of directions:

$$\mathrm{RSC_O} = 2 * \mathrm{c_O} * \mathrm{F_t} * \mathrm{c} * \mathrm{L} \qquad \text{Equation 8-13}$$

where:

$\mathrm{RSC_O}$ = operating costs of rolling stock (€/year)

$\mathrm{c_O}$ = average unit cost of operating a rolling stock (€/seat-km).

#### 8.2.1.2.3 Rolling stock/capsule maintenance cost

The maintenance cost of HSGT rolling stock/capsule is found by multiplying the acquired number of trains, their use during a given period and average seat capacity by the average unit cost of maintaining rolling stock/capsule, as follows:

$$\mathrm{RSC_M} = \mathrm{c_M} * \mathrm{u_t} * \mathrm{c} * \mathrm{RS_t} \qquad \text{Equation 8-14}$$

where:

$\mathrm{RSC_M}$ = maintenance cost of rolling stock/capsule (€/year)

$\mathrm{u_t}$ = annual usage of a train/capsule (km/seat)

$\mathrm{C_M}$ = unit cost of maintaining rolling stock/capsule (€/seat-km).

The annual usage of a train is assumed to be 500,000 km per seat (Janić, 2017).

### 8.2.2 Total operator cost

The TOC is calculated as a sum of the infrastructure costs (construction cost and maintenance cost) and the rolling stock/capsule costs (acquisition cost, operating cost and maintenance cost), as follows:

$$\mathrm{TOC} = \mathrm{ICC} + \mathrm{ICM} + \mathrm{RSC_A} + \mathrm{RSC_O} + \mathrm{RSC_M} \qquad \text{Equation 8-15}$$

where:

$\mathrm{TOC}$ = total annual operator cost (€/year).

### 8.2.3 User cost

To calculate total social cost, user cost is considered, as HSGT passengers experience disutility according to how long they spend on the journey. In this model, user cost includes access/egress time ($T_{AE}$), waiting time ($T_{WT}$) and in-vehicle travel time ($T_{IV}$).

#### 8.2.3.1 Access/egress time

Access time is defined as the total time spent in reaching a train/Hyperloop station (A) from the point of origin, while egress time is the total spent getting from the train/Hyperloop station to the destination. In this model, access/egress travel time per passenger is dependent on average access/egress distance and average travel speed, calculated as follows:

$$T_{AE} = \frac{D_{AE}}{V_{AE}} \qquad \text{Equation 8-16}$$

where:

$T_{AE}$ = average access/egress time per passenger (hours)

$D_{AE}$ = average access/egress distance to/from the train/capsule station (kilometres)

$V_{AE}$ = average travel speed (kilometre/hour).

Total access/egress time is calculated by multiplying the average access/egress time per passenger by the total passengers per year, as total cost is on an annual basis. In this case, the average access/egress time has to be multiplied by a factor of two to account for both access and egress to and from the HSGT station, as follows:

$$TT_{AE} = 2 * Q_t * T_{AE} \qquad \text{Equation 8-17}$$

where:

$TT_{AE}$ = total annual passenger access/egress time (hours)

$Q_t$ = passenger demand in the time period t per direction (passengers/year).

#### 8.2.3.2 Waiting time

Passenger waiting time is considered to be one the most crucial components of TUC for HSGT technologies, and it is calculated by taking half of the headway, as follows:

$$\mathrm{T_{WT}} = \frac{1}{2} * \mathrm{Headway} \qquad \text{Equation 8-18}$$

where:

$\mathrm{T_{WT}}$ = average waiting time per passenger for the time period (hours).

In this case, average waiting time in hours is dependent on the regular arrival of trains and the random arrival of passengers. Headway is based on the transport service's frequency on the line (vehicle/hour), as follows:

$$\mathrm{Headway} = \frac{1}{2 * \mathrm{F_t}} \qquad \text{Equation 8-19}$$

To obtain the TUC to HSGT passengers on an annual basis, total annual waiting time is calculated from annual demand, as follows:

$$\mathrm{TT_{WT}} = \mathrm{Q_t} * \mathrm{T_{WT}} \qquad \text{Equation 8-20}$$

where:

$\mathrm{TT_{WT}}$ = total annual passenger waiting time (hours).

#### 8.2.3.3 In-vehicle time

In-vehicle time for HSGT technologies is dependent on the average length of journey and average operating speed $(\mathrm{v})$. As there are no intermediate stops on the line for the HSGT systems in the case study, dwell time was excluded from the calculation. Average in-vehicle time is calculated simply by dividing the average journey length by the average speed, as follows:

$$\mathrm{T_{IV}} = \frac{\mathrm{L}}{\mathrm{v}} \qquad \text{Equation 8-21}$$

where:

$T_{IV}$ = average in-vehicle time per passenger (hour)

L= average length of a given proposed line (km)

v = average operating speed (km/h).

Annual HSR passengers' in-vehicle time can be calculated from average passenger journey length, the average operating speed of the HSGT system and the annual passenger demand, as follows:

$$TT_{IV} = Q_t * T_{IV} \qquad \text{Equation 8-22}$$

where:

$TT_{IV}$ = total annual passenger in-vehicle time (hours).

### 8.2.4 Total user cost

In order to evaluate the total social cost, the disutility of travelling by HSGT technology needs to be expressed in monetary terms. Hence, VOT is a component in the total of user cost, calculated by multiplying an hourly wage rate by an average ridership component (Daniels, Ellis and Stockton, 1999). In this case, the VOT is taken to be the average hourly wage rate, calculated from the average monthly wage rate and working hours per month, as follows:

$$VOT = \frac{AMWR}{AWH} \qquad \text{Equation 8-23}$$

where:

VOT = value of in-vehicle time for HSR (€/hour)

AMWR = average monthly wage rate (€/month)

AWH = monthly working hours (hours/month).

The case study used the average monthly wage in Saudi Arabia, about €1,395, and working hours per month were estimated at 160 hours. However, VOT is related to the wage rate in terms of costs to employer, accounting for 1.33 and 0.67 of the wage rate per hour for work/business trips and longer commuting trips, respectively, while leisure trips are included in commuting (Gwilliam, 1997; Small, Verhoef and Lindsey, 2007).

TUC is related to GT, including walking time, waiting time and in-vehicle time, and is converted to GC by multiplying by the value of time, as follows:

$$\mathrm{TUC} = [(\mathrm{W_{AE}} \times \mathrm{TT_{AE}}) + (\mathrm{W_{wt}} \times \mathrm{TT_{WT}}) + \mathrm{TT_{IV}}] \times \mathrm{VOT} \qquad \text{Equation 8-24}$$

where:

$\mathrm{TUC}$ = annual total user costs (€/year)

$\mathrm{W_{AE}}$ = factor to represent the weighting perception of access/egress time vs. in-vehicle time (number)

$\mathrm{W_{wt}}$ = factor to represent the weighting perception of waiting time vs. in-vehicle time (number).

The weighting perception of walking time is dependent on the ease of ascertaining one's bearings and the congestion in the pedestrian flows, while comfort, safety, security, type of trips and length of time to wait are its main factors. In this case, the values of weighting perception for access/egress and waiting time are taken as two and three times the in-vehicle time, respectively (Wardman, 2004).

### 8.2.5 External environmental cost

The operation of the HSGT service has an external environmental impact on society, representing another cost. These externalities can be grouped into air pollution, noise pollution, climate change and accidents, which depend on total traffic volume. Each transport system has characteristic levels of air pollutant emissions, noise and other specific environmental impacts. In the case study, the external environmental costs related to construction and operation of the HSGT line involved specific categories in which the impact is especially strong because of the heavily populated areas through which the lines run.

The external environmental cost is determined by multiplying the sum of unit values of external cost by the total traffic volume (passengers-kilometre), as follows:

$$\mathrm{TEC} = (\mathrm{UAP_c} + \mathrm{UNP_c} + \mathrm{UA_c} + \mathrm{UCC_c})\ \mathrm{X}\ \mathrm{PKM} \qquad \text{Equation 8-25}$$

where:

$\mathrm{TEC}$ = annual total external costs (€/year)

$\mathrm{UAP_c}$ = unit air pollution costs per passenger-kilometre (€/pkm)

$\mathrm{UNP_c}$ = unit noise pollution costs per passenger-kilometre (€/pkm)

$\mathrm{UA_c}$ = unit accident costs per passenger-kilometre (€/pkm)

$\mathrm{UCC_c}$ = unit climate change costs per passenger-kilometre (€/pkm)

PKM = total passengers-km.

The unit external cost per passenger-kilometre is identified by using the Purchasing Power Parity (PPP) rate, an economic theory to consider the values of currency rates and the PPP of various countries in a base year. Due to the limitations of data collection in the case-study country of Saudi Arabia, the PPP rate between the United Kingdom and Saudi Arabia was used to calculate the unit cost of the impact of the proposed HSGT system. Additionally, the elasticity (e) of 1 was used to determine the cost rates for particular countries (Maibach *et al.*, 2008).

$$\mathrm{UAP_{c-SA}} = \mathrm{UAP_{c-UK}} * \left[\frac{\mathrm{GDP\ per\ capita}_{SA} * \mathrm{PPP\ Income}_{SA}}{\mathrm{GDP\ per\ capita}_{UK} * \mathrm{PPP\ Income}_{UK}}\right]^{\mathrm{e}} \qquad \text{Equation 8-26}$$

$\mathrm{UAP_{c-SA}}$ = unit air pollution cost of HSGT system in Saudi Arabia (€/1,000 pkm)

$\mathrm{UAP_{c-UK}}$ = unit air pollution cost of HSGT system in United Kingdom (€/1,000 pkm)

$\mathrm{GDP\ per\ capita}_{SA}$ = GDP per capita of Saudi Arabia (€)

$\mathrm{GDP\ per\ capita}_{UK}$ = GDP per capita of United Kingdom (€)

$\mathrm{PPP\ Income}_{SA}$ = PPP income rate of Saudi Arabia (€)

$\mathrm{PPP\ Income}_{SA}$ = PPP income rate of United Kingdom (€).

The worst effects of air pollution on human health are from particulate matter such as $PM_{10}$, $PM_{2.5}$, ozone (O3) and similar (Maibach et al., 2008). The noise generated by HSGT depends on the specific technology, track, moving train/capsule and distance operated (Janić, 2017). The impact on climate change is mainly from emissions of GHGs such as carbon dioxide ($CO_2$), methane ($CH_4$) and nitrous oxide ($N_2O$) (Maibach *et al.*, 2008). The external accident cost relates to traffic accidents

and depends on both the accident rate and the insurance system (Maibach *et al.*, 2008).

In the TSC approach, since they are just a means of transferring the benefit to the operator and the cost to the passenger no fares are included. By contrast, they are indeed included in the cost–benefit analysis: this is determined by the welfare approach, which has some important differences from the TSC approach. One of the differences is that, assuming no externalities, welfare analysis consists of a consumer surplus and a producer surplus. In this case, the greater the demand, the larger the consumer surplus tends to be. However, changes in consumer surplus are difficult to measure when there are multiple modes with multiple changes in generalised costs.

Similar problems apply to measurements of producer surplus. In the TSC approach, producer benefits are determined by reductions in operating costs per passenger km; users' benefits are determined by the reduction in user costs per passenger km; and societal benefits are determined by the reduction in external costs per passenger km. The focus on average social cost per passenger (or passenger km) may be seen as a form of cost-effectiveness analysis that represents a simplification of cost-benefit analysis that is particularly useful for strategic analyses

## 8.3 Results and Discussion

This section explains in detail the results of the comparative assessment of operating HSR, Maglev and Hyperloop, in terms of forecasted endogenous demand levels and average OC, average user cost and average external environmental cost. The results are then summarized and discussed to reveal their benefits and impacts for the case study's Riyadh–Dammam corridor.

After calculating endogenous demand by means of the DD, EDM and SP methods, the total operator cost (TOC), total user cost (TUC), total external cost (TEC) and total social cost (TSC) were obtained by using the TSCM for the options of HSR, Maglev and Hyperloop. The DDM was used to calculate expected demand for the first year of HSR operation (2030) on the proposed line.

Travel demand for HSR was estimated at 7.5 million passengers in the first year (2030), as shown in Table 8-2, using various parameters including population, mean GDP per capita, mean service frequency, mean speed, mean fare and country-specific dummy variables. An ED model was constructed for the proposed HSR and Maglev lines, regarding numbers of trips and GJTs. To determine the demand level for Maglev, GJT was based on in-vehicle time and the SIP. In this case, Maglev demand was forecast at 9.8 million passengers for the initial year of operation while, based on the outcome probability of the SP method, the annual initial demand for Hyperloop was forecast to be 4.2 million.

| | **High-Speed Rail** | **Maglev** | **Hyperloop** |
|---|---|---|---|
| Annual initial demand (2030) | 7,522,552 | 9,797,372 | 4,232,021 |
| Days per year | 365 | 365 | 365 |
| Daily demand (passengers per direction) | 10,305 | 13,421 | 5,797 |

Table 8-2: Final endogenous demand levels for the initial year of operation (2030)

The projected figures for total one-way daily demand for HSR, Maglev and Hyperloop are 10,305, 13,421 and 5,797 passengers. These are based on the total initial demand, determined from the output of the demand-forecasting models and the number of directions. Based on the level of demand for the three HSGT technologies, the results of total social costs of constructing and operating an HSR line worldwide were calculated, grouped into sub-sections.

### 8.3.1 Total operator costs

First are the total operator costs, which include the infrastructure construction and maintenance costs, rolling stock/capsule acquisition and operating and maintenance costs. Descriptions of some input parameters for the three HSGT systems are presented in Table 8-3, as the capacities of the HSR and Maglev, and Hyperloop systems are determined of 604 seats, 449 seats and 28 seats, respectively. For the case study’s proposed HSR, Maglev and Hyperloop lines, the load factors were estimated at 90%, 72% and 87%, based on Janić's 2018 study.

| System | HSR | Maglev | Hyperloop |
|---|---|---|---|
| Line length (km) | 412 | 412 | 412 |
| No. of stations per line | 2 | 2 | 2 |
| Average operating speed (km/h)[b] | 300 | 400 | 1000 |
| Vehicle capacity (seats per train/capsule)[b] | 604 | 449 | 28 |
| Carriages per train [b] | 13 | 5 | 2 |
| Average acceleration/deceleration rate ($m/s^2$)[b] | 0.7 | 0.7 | 1.5 |
| Frontal area ($m^2$/train)[b] | 12.7 | 15.4 | 3.9 |
| Minimum horizontal curve (km)[a] | 7.6 | 9.1 | 4.8 |
| Load factor (%)[b] | 90 | 72 | 87 |

[a] CH2M HILL, 2017.

[b] Janić, 2018.

Table 8-3: Basic input parameters of the characteristics of HSR, Maglev and Hyperloop systems

The main parameters to be included in the calculation are the length of the line (L) in km (412), the estimated project timeline (n) in years (35), the capacity of the train/capsule (c) in seats, the capacity load factor (l), the average commercial speed (s) in km/h and 18 operating hours daily (06:00–24:00).

In order to evaluate the total social costs, some unit cost values from previous studies were incorporated, such as the unit ICC cost, the unit of maintenance cost and the unit costs of acquiring, operating and maintaining vehicles. The unit costs of infrastructure construction and maintenance and the acquisition, maintenance and operating of rolling stocks/vehicle used in calculating the total social cost of the HSR, Maglev and Hyperloop lines are shown in Table 8-4. For the case study, the unit costs presented in Table 8-4 for Maglev and Hyperloop were converted from 2009 and 2015 figures, respectively, to 2017 figures in order to have all values for the same year. The UK Consumer Price Index (CPI) was consulted, as shown in Table 8-5.

| Unit cost | HSR[f] | Maglev[a,b,c,d,e] | Hyperloop[g] |
|---|---|---|---|
| Infrastructure construction unit cost (€/route-km) | 26,600,000 | 35,839,676 | 10,522,275[1] |
| Infrastructure maintenance unit cost (€/year/km) | 35,500 | 14,694 | 17,019[2] |
| Acquisition unit cost of rolling stock/vehicle (€/seat) | 45,000 | 58,816 | 55,456[3] |
| Average operating unit cost of rolling stock/vehicle (€/ct-seat-km) | 0.133 | 0.116 | 0.046[4] |
| Maintenance unit cost per rolling stock/vehicle (€/seat-km) | 0.0124 | 0.0131 | 0.00061 |

Notes:

[1] Estimated cost for Hyperloop's tubes on pillars.

[2] Cost of maintaining the infrastructure of Hyperloop's solid ground.

[3] Cost when a toilet is added.

[4] Annual operation cost for one capsule is €75,000 for line length of 600 km.

Sources:

a) Nassar, 1996.
b) Boardman, 2005.
c) Nuworsoo, 2009.
d) Ziemke, 2010.
e) Retzmann *et al.*, 2011.
f) Janić, 2017.
g) Van Goeverden *et al.*, 2018

Table 8-4: Unit costs of HSR, Maglev and Hyperloop at 2017 prices.

| CPI in 2009 | CPI in 2015 | CPI in 2017 | Index 2009/2017 | Index 2015/2017 |
|---|---|---|---|---|
| 84.878 | 99.258 | 101.4 | 1.19 | 1.02 |

Table 8-5: Conversion between years using consumer price index[17]

IC depends on the HSGT line/tube construction and maintenance costs. In the case study, the annual ICCs of HSR, Maglev and Hyperloop were calculated at €561 million, €756 million and €222 million, as in Table 8-6, using the capital recover factor where r = 0.03 and n = 35. The figures represent the product of the capital recovery factor, length of line, the infrastructure construction unit cost of €26.6 million, 35.8 million and 10.5 million per route-km, respectively, and the estimated

[17] https://tradingeconomics.com/united-kingdom/consumer-price-index-cpi

proportion cost on planning (ρ) of 10%. The capital recovery factor is 5%, dependent on project timeline and a social discount rate (i) of 3%.

For the case study, Table 8-4's unit costs for Maglev and Hyperloop were converted from 2009 and 2015 figures, respectively, to 2017 figures to have all values for the same year. The UK Consumer Price Index (CPI) was consulted, as in Table 8-5.

| **Item** | **HSR** | **Maglev** | **Hyperloop** |
|---|---|---|---|
| Length of line | 412 | 412 | 412 |
| Construction unit cost (€/km) | 26,600,000 | 35,839,676 | 10,522,275 |
| Proportion cost on planning (%) | 10 | 10 | 10 |
| Maintenance unit cost (€/year) | 35,500 | 14,694 | 17,019 |
| Construction period (year) | 5 | 5 | 5 |
| Cycle time (year) | 35 | 35 | 35 |
| Social discount rate (i) (%) | 3 | 3 | 3 |
| Infrastructure construction cost (€) | 12,055,120,000 | 16,242,541,163 | 4,768,695,030 |
| Uniform series present worth factor | 27.08 | 27.08 | 27.08 |
| Capital recovery factor (%) | 0.05 | 0.05 | 0.05 |
| Infrastructure construction cost (€/year) | 561,036,745 | 755,916,359 | 221,931,688 |
| Infrastructure maintenance cost (€/year) | 14,626,000 | 6,053,928 | 7,011,828 |
| Total infrastructure construction and maintenance costs (€/year) | 575,662,745 | 761,970,287 | 228,943,516 |

Table 8-6: Total infrastructure construction and maintenance costs (€/year)

The IMCs of the HSGT systems were calculated at €14.6 million, €6.1 million and €7.0 million per year, respectively, using the product of length of line and the infrastructure maintenance unit cost of €35.5 thousand, €14.7 thousand and €17.01 thousand per year. As a result, the total infrastructure construction and maintenance costs presented in Table 8-6 show values of €576 million, €762 million and €229 million per year, respectively**.**

Effective occupation was based on an estimated load factor of 90%, 72% and 87% for HSR, Maglev and Hyperloop, and a train/capsule capacity of 604, 449 and 28 seats, as in Table 8-7, giving 544, 323 and 24 seats. In addition, the projection of one-way total daily demand was 10.3 thousand, 13.4 thousand and 5.6 thousand passengers, dependent on the initial annual demand of 7.5 million, 9.8 million and 4.2 million passengers, respectively, as determined from the output of the demand

models and the number of directions. The number of services per day-direction (trains/or capsules) for HSR, Maglev and Hyperloop was calculated at 19 trains, 42 trains and 238 capsules, as shown in Table 8-7, based on projected daily demand and effective occupation. The frequency was calculated as one train, two trains and 13 capsules per hour, based on daily passengers per direction, effective occupation and operating hours. This means a train/capsule every hour, 30 mins and 5 mins, respectively, calculated by dividing 60 mins by service frequency per hour, as it will improve with growing demand.

| Item | HSR | Maglev | Hyperloop |
|---|---|---|---|
| Days per year (day) | 365 | 365 | 365 |
| Round trip (direction) | 2 | 2 | 2 |
| Operating hours per day (hour) | 18 | 18 | 18 |
| Load factor (%) | 90 | 72 | 87 |
| Capacity (seat) | 604 | 449 | 28 |
| Effective occupation (seat) | 544 | 323 | 24 |
| Annual demand initial (passenger/year) | 7,522,552 | 9,797,372 | 4,232,021 |
| Per day, initial year (t=5) | 10,305 | 13,421 | 5,797 |
| Number of service per day-direction | 19 | 42 | 238 |
| Service frequency per hour | 1 | 2 | 13 |

Table 8-7: Service frequency per hour

The number of trains/capsules to be acquired for the proposed corridor was calculated at five trains, nine trains and 30 capsules for HSR, Maglev and Hyperloop, respectively, as in Table 8-8. It is based on a train/capsule operation cycle time of 3.41 and 2.73 hour/train and 1.49 hour/capsule, respectively, the value put on the risk of failing, at 1.5, and the service frequency specified in Table 8-7.

| Item | HSR | Maglev | Hyperloop |
|---|---|---|---|
| Length of line | 412 | 412 | 412 |
| Operating speed | 300 | 400 | 1000 |
| Train turnaround time | 3.41 | 2.73 | 1.49 |
| Value to the risk of failing | 1.5 | 1.5 | 1.5 |
| Service frequency per hour | 1 | 2 | 26 |
| Number of acquired trains | 5 | 9 | 58 |

Table 8-8: No. of acquired trains/capsules

The acquisition cost of rolling stock/capsules is achieved by multiplying the number of trains/capsules needed and the average seating capacity of train/capsules by the

unit cost of acquiring a train/capsule of €45 thousand, €58.8 thousand and €55.5 thousand per seat, respectively, as shown in Table 8-9. These values are converted to an annual value by multiplying by the capital recovery factor of 0.05.

| Item | HSR | Maglev | Hyperloop |
|---|---|---|---|
| Train/capsule capacity (seats) | 604 | 449 | 28 |
| No. of acquired trains/capsules (trains/capsules) | 5 | 9 | 30 |
| Unit cost of acquiring train/capsule (€) | 45,000 | 58,816 | 55,456 |
| Rolling stock/capsule acquisition cost (€/year) | 6,820,710 | 11,593,653 | 2,136,355 |

Table 8-9: Rolling stock/capsule acquisition cost (€/year)

In this case, the rolling stock/capsule acquisition costs were found to be €6.8 million, €11.6 million and €2.1 million per year, respectively.

In this case study, the average operating cost of a train/capsule was based on the average unit cost of operating a train/capsule at € 0.133, € 0.116 and € 0.046 per seat-kilometre, the length of the line at 412 km, the train/capsule capacity and the transport service frequency. It amounted to €0.11 million, €0.16 million and €0.22 million, respectively, as in Table 8-10.

| Item | HSR | Maglev | Hyperloop |
|---|---|---|---|
| Average unit cost of operating rolling stock/capsule | 0.133 | 0.116 | 0.046 |
| Service frequency per hour | 1 | 2 | 13 |
| Train/capsule capacity | 604 | 449 | 28 |
| Length of line | 412 | 412 | 412 |
| Rolling stock operating cost (€/year) | 111,539 | 158,375 | 22,451 |

Table 8-10: Rolling stock/capsule operating cost (€/year)

For the rolling stock/capsule maintenance cost, the unit cost of maintaining a train/capsule of €0.0124, 0.0131 and 0.0006 per seat-kilometre is multiplied by the number of acquired trains, train capacity and the annual usage of 500,000 km-seat, as shown in Table 8-11.

| Item | HSR | Maglev | Hyperloop |
|---|---|---|---|
| Unit cost of maintaining rolling stock/ capsule | 0.0124 | 0.0131 | 0.0006 |
| Number of acquired trains | 5 | 9 | 58 |
| Train/capsule capacity | 604 | 449 | 28 |
| Average usage of train/capsule | 500,000 | 500,000 | 500,000 |
| Rolling stock/capsule maintenance cost (€/year) | 20,192,448 | 27,742,548 | 252,467 |

Table 8-11: Rolling stock/capsule maintenance cost (€/year)

Values of €20.2 million, €27.7 million and €0.25 million[18] per year were achieved for HSR, Maglev and Hyperloop, respectively.

### 8.3.2 Total user costs

Second, the TUC of a proposed HSGT line involves the access/egress time, waiting time and in-vehicle travel time from the origin to destination.

The average access/egress times were based on the average travel distance to/from HSGT stations of 24.9 km and an average travel speed of 45 km/h, resulting in 0.55 hour per passenger. The annual total access/egress time were found to be 4.2 million, 5.4 million and 2.3 million hours for the three proposed HSGT modes, as shown in Table 8-12, from multiplying by a factor of two, representing both directions to/from the HSGT station, the annual number of passengers per direction and average access/egress time per passenger.

[18] This small value is due to the low capacity of Hyperloop and the unit cost of maintaining the capsules.

| Item | HSR | | Maglev | | Hyperloop | |
|---|---|---|---|---|---|---|
| | Riyadh | Dammam | Riyadh | Dammam | Riyadh | Dammam |
| First distance | 15.8 | 31.7 | 15.8 | 31.7 | 15.8 | 31.7 |
| Second distance | 23.3 | 28.6 | 23.3 | 28.6 | 23.3 | 28.6 |
| Third distance | 16.7 | 33.1 | 16.7 | 33.1 | 16.7 | 33.1 |
| Average access/egress distance to/from HSR station (km) | 18.6 | 31.1 | 18.6 | 31.1 | 18.6 | 31.1 |
| Average distance for both stations (km) | 24.9 | | 24.9 | | 24.9 | |
| Average travel speed (km/h) | 45 | | 45 | | 45 | |
| Average access/ egress time | 0.55 | | 0.55 | | 0.55 | |
| Factor represents both directions to/from HSR station | 2 | | 2 | | 2 | |
| Annualization factor (days/year) | 365 | | 365 | | 365 | |
| Passenger demand in the time period t (passengers/year) | 3,761,276 | | 4,898,686 | | 2,116,011 | |
| Total annual passenger access/egress time (hours) | 4,156,907 | | 5,388,555 | | 2,327,612 | |

Table 8-12: Total annual passenger access/egress time (hours)

Average passenger waiting time was found to be 0.50, 0.25 and 0.05 hour, respectively, resulting from half of the headway value, as headway is equal to half of the service frequency on the line of about one train and two trains per hour for HSR and Maglev, respectively, and 13 capsules per hour for Hyperloop. The total annual passenger waiting time was found to be 1.9 million, 1.2 million and 0.11 million hours, as shown in Table 8-13**,** resulting from the multiplication of average waiting time per passenger and the annual projected demand of passengers per direction.

| Item | HSR | Maglev | Hyperloop |
|---|---|---|---|
| Annualization factor (days/year) | 365 | 365 | 365 |
| Operating hours per day | 18 | 18 | 18 |
| Projections of the (one-way) daily demand (passenger) | 10,305 | 13,421 | 11,366 |
| Passenger demand in the time period (passengers/hour) | 1,145 | 1,491 | 1,263 |
| Average waiting time (hours) | 0.500 | 0.250 | 0.050 |
| Projection of the yearly demand (passenger/year) | 3,761,276 | 4,898,686 | 2,116,011 |
| **Total annual passenger waiting time (hrs)** | 1,880,638 | 1,224,672 | 105,801 |

Table 8-13: Total annual passenger waiting time (hours)

Average in-vehicle travel time was found to be 1.37, 1.03 and 0.41 hours, from dividing the length of the line by the average operating speed, as in Table 8-14.

| Item | HSR | Maglev | Hyperloop |
|---|---|---|---|
| Length of HSR corridor (km) | 412 | 412 | 412 |
| Average operating speed (km/h) | 300 | 400 | 1,000 |
| Annualization factor (days/year) | 365 | 365 | 365 |
| Projection of annual demand (passenger/direction) | 3,761,276 | 4,898,686 | 2,116,011 |
| Average in-vehicle time (hours) | 1.37 | 1.03 | 0.41 |
| **Total annual passenger in-vehicle time (hrs)** | 5,165,486 | 5,045,647 | 871,796 |

Table 8-14: Total annual passenger in-vehicle time (hours)

In this case, the total annual passenger in-vehicle travel time was found to be 5.1 million hours, 5.0 million hours and 0.87 million hours, resulting from multiplying average in-vehicle time by the annual projection demand per direction.

### 8.3.3 Total external environmental costs

The total external environmental costs of the proposed HSGT line comprise air pollution, noise pollution, climate change and accidents, as shown in Table 8-15. In addition, the total passenger-kilometres were calculated by multiplying the forecast travel demand of 7.5 million, 9.8 million and 4.2 million for HSR, Maglev and Hyperloop, respectively, by the length of corridor (412 km) and dividing by 1,000.

| Item | HSR | Maglev | Hyperloop |
|---|---|---|---|
| Unit air pollution costs per vehicle-km | 0.35916 | 0.00 | 0.00 |
| Total passenger-km | 3,099,291 | 4,036,517 | 1,743,593 |
| **Average air pollution cost (€/year)** | **1,113,145** | **0.00** | **0.00** |
| Unit noise costs per vehicle-km | 0.01760 | 0.00 | 0.00 |
| Total passenger-km | 3,099,291 | 4,036,517 | 1,743,593 |
| **Average noise pollution cost (€/year)** | **54,550** | **0.00** | **0.00** |
| Unit accident costs per vehicle-km | 1.30782 | 1.30782 | 1.30782 |
| Total passengers-km | 3,099,291 | 4,036,517 | 1,743,593 |
| **Average accident cost (€/year)** | **4,053,301** | **5,279,019** | **2,280,297** |
| Unit climate change costs per vehicle-km | 0.80421 | 1.20 | 1.20 |
| Total passenger-km | 3,099,291 | 4,036,517 | 1,743,593 |
| **Average climate change cost (€/year)** | **2,492,477** | **4,843,821** | **2,092,311** |

Table 8-15: Average cost of air pollution, noise pollution, climate change and accidents

In this case study, the average cost of air pollution was calculated at €1.1 million per year for HSR, by multiplying the unit cost of air pollution of €0.359 per vehicle-kilometre by the total annual demand of 3.1 billion passenger-kms then dividing by 1000. It was assumed that no air pollution is generated by the Maglev and Hyperloop systems, and they were assigned a value of €0.00. The cost of noise pollution was determined at €0.54 million per year for HSR, based on the unit noise pollution cost of €0.018 per vehicle-kilometre and the total of 3.1 million passenger-kilometres. Additionally, it was assumed that no noise pollution is generated by Maglev and Hyperloop due to the contactless design of their moving bodies and guideway during journey, as well as insufficient data.

In terms of unit accidents, the same external costs of HSR were used for the Maglev and Hyperloop systems due to a similar expected number of accidents. In this case, the figure was determined to be €1.3 per vehicle-kilometre, from the calculation of the average external accident cost, resulting in €4.1 million, €5.3 million and €2.3 million per year for HSR, Maglev and Hyperloop, respectively.

Regarding the cost of climate change, the unit cost per vehicle-kilometre is €0.80 for HSR, and it was assumed to be €1.20 for both Maglev and Hyperloop. In this

case, the average external climate change cost resulted in €2.5 million**,** €4.8 million and €2.1 million per year, calculated by multiplying the unit cost of climate change by the total of 3.1 million, 4.0 million and 1.7 million passenger-kms, respectively.

## 8.4 Comparative Assessments

The comparative assessment of intercity HSGT systems is based on their ASC, in terms of total operator costs, user costs and external environmental costs. First, the case study's total operator costs for HSR, Maglev and Hyperloop were calculated at €602.8 million, €801.5 million and €231.4 million per year, respectively**,** as in Table 8-16. Maglev can be seen to involve the highest total operator costs due to its greatest ICC, based on its huge infrastructure construction unit cost.

| **Item** | **HSR** | **Maglev** | **Hyperloop** |
|---|---|---|---|
| Infrastructure construction cost | 561,036,745 | 755,916,359 | 221,931,688 |
| Infrastructure maintenance cost | 14,626,000 | 6,053,928 | 7,011,828 |
| **Total infrastructure costs** | **575,662,745** | **761,970,287** | **228,943,516** |
| Rolling stock/capsule acquisition cost | 6,820,710 | 11,593,653 | 2,136,355 |
| Rolling stock/capsule operating cost | 111,539 | 158,375 | 22,451 |
| Rolling stock/capsule maintenance cost | 20,192,448 | 27,742,548 | 252,467 |
| **Total rolling stock/capsule costs** | **27,124,697** | **39,494,576** | **2,411,273** |
| **Total operator cost (€/year)** | **602,787,441** | **801,464,863** | **231,354,789** |

Table 8-16: Rolling stock/capsule total operator costs (€/year)

On the other hand, HSR's infrastructure maintenance cost was found to be higher than that of Maglev and of Hyperloop, which leads to a higher IMC. In terms of total rolling stock/capsule, too, Maglev was found to have higher total costs of €39.5 than Maglev and Hyperloop due to its high acquisition cost. The total cost of Hyperloop's capsule is €2.4 million, which includes the acquisition cost (€2.1 million), operating cost (€0.22 million) and maintenance cost (€0.25 million).

Second, the total user costs were calculated at €166.5 million, €169.7 million and €50.9 million per year for HSR, Maglev and Hyperloop, respectively, as shown in Table 8-17. These figures result from multiplying the sum of total annual passenger access/egress time, waiting time and in-vehicle time by the average value of time. It involved determining the average value of time, multiplying the average hourly rate and the coefficients for business and commuting travellers (1.33 and 0.667), in

section 9.2.4, by the value of time. The average hourly wage rate is €8.72, achieved by dividing the average monthly wage of €1,395 by 160 working hours per week.

In order to compare the value of time reported in this research, estimated values of times were collected by Levinson *et al.* (1996) from a variety of intercity transportation studies, including HSR, air, car, and bus, for both business and non-business trips. For example, the value of time of air transport for business trip of the Ridout-Miller study, in the United States, is between €2.5 and €23, and between €0.8 and €8.3 for rail. The value of time of rail for non-business trips is between €0.04 and €0.4 for the Ridout-Miller line (Levinson *et al.*, 1996).

| **Item** | **HSR** | **Maglev** | **Hyperloop** |
|---|---|---|---|
| Weighting perception of access/egress time regarding in-vehicle time | 2 | 2 | 2 |
| Weighting perception of waiting time WRT in-vehicle time | 3 | 3 | 3 |
| Value of time for business travellers | 11.60 | 11.60 | 11.60 |
| Value of time for commuting travellers | 5.82 | 5.82 | 5.82 |
| Average of value of time | 8.71 | 8.71 | 8.71 |
| Total annual passenger access/egress time (hours) | 4,156,907 | 5,388,555 | 2,327,612 |
| Total annual passenger's waiting time (hours) | 1,880,638 | 1,224,672 | 105,801 |
| Total annual passenger's in-vehicle time (hours) | 5,165,486 | 5,045,647 | 871,796 |
| **Total user costs (€/year)** | 166,463,004 | 169,732,485 | 50,879,615 |

Table 8-17: Rolling stock/capsule total user costs (€/year)

The Maglev system was found to have the highest total annual user costs of €169.7 million, due to its high demand of 9.8 million, compared to 7.5 million and 4.2 million of HSR and Hyperloop, respectively.

Finally, the total external environmental cost was calculated at €7.7 million, €10.1 million and €4.4 million per year for HSR, Maglev and Hyperloop, respectively, as shown in Table 8-18. This results from the sum of average costs of air pollution, noise pollution, climate change and accidents, based on the values for unit costs presented section 9.3.3 on the external environmental cost of HSGT technology.

| Item | HSR | Maglev | Hyperloop |
|---|---|---|---|
| Average air pollution cost (€/year) | 1,113,145 | 0.00 | 0.00 |
| Average noise pollution cost (€/year) | 54,550 | 0.00 | 0.00 |
| Average accident cost (€/year) | 4,053,301 | 5,279,019 | 2,280,297 |
| Average climate change cost (€/year) | 2,492,477 | 4,843,821 | 2,092,311 |
| **Total external costs (€/year)** | **7,713,473** | **10,122,840** | **4,372,609** |

Table 8-18: Total external costs of HSR, Maglev and Hyperloop (€/year)

In the case study, air and noise pollution were excluded from the Maglev and Hyperloop systems calculations due both to insufficient data and because they do not directly generate polluting emissions.

As a result, Maglev system has the highest total social cost of €981.1 million, compared to €776.9 million and €286.6 million for HSR and Hyperloop, respectively, as shown in Table 8-19.

| Item | HSR | Maglev | Hyperloop |
|---|---|---|---|
| Total operator costs (€/year) | 602,787,441 | 801,464,863 | 231,354,789 |
| Total user costs (€/year) | 166,463,004 | 169,732,485 | 50,879,615 |
| Total external costs (€/year) | 7,713,473 | 10,122,840 | 4,372,609 |
| Total social costs (€/year) | 776,963,918 | 981,320,188 | 286,607,013 |
| Average social cost (€/year) | 103.3 | 100.2 | 67.7 |

Table 8-19: Total social costs of HSR, Maglev and Hyperloop (€/year)

In terms of average social cost, HSR is now the most expensive at €103.3, compared to €100.2 and €67.7 for Maglev and Hyperloop, respectively. However, there are several caveats. First, Hyperloop's operator costs need to be confirmed, given that there are currently no operational systems to benchmark against. For example, it is likely that the energy costs are underestimated (and cannot be provided free of charge by solar energy). Second, the user costs need to be confirmed. The capacity of the proposed Hyperloop service is equivalent to 4.9 million passengers per annum (ppa). This suggests an average load factor of 86%, therefore congestion is likely at peak times, manifesting as increased waiting. On

the other hand, the capacity of the proposed Maglev and HSR systems is estimated at 13.8 million and 8.4 million ppa, respectively. Given the usage forecasts of 9.8 million ppa for Maglev and 7.5 million for HSR, this suggests average load factors of 72% and 89%. This indicates that Hyperloop's capacity is somewhere between that of the Maglev and HSR systems, as the level of HSR services is less than Maglev due to its lower speed. Thirdly, if a network is to be operated Hyperloop faces many potential technical issues, such as maintaining the vacuum and (as with Maglev) problems with the switches and crossings.

## 8.5 Conclusion

This chapter applied the modelling framework that has been developed in this project to the Riyadh–Dammam corridor as a case study to demonstrate a comparative assessment upon the introduction of a new HSGT system. The performance of each of the three HSGT systems under consideration was evaluated and compared, and differences in their social cost were quantified.

The calculation of total social cost is based on operator cost, user cost and external environmental cost, determined using the annual demand level of HSR, Maglev and Hyperloop, separately. In the case study, it resulted in €779.9 million, €981.3 million and €286.6 million for HSR, Maglev and Hyperloop, respectively. In this case, the ICC and rolling stock/capsule acquisition cost were converted to an annual basis by using the equation of capital recovery factor, which includes a discount rate of 3% and a life span of 35 years, and resulted in 5%. Based on annual initial demand of 7.5 million, 9.8 million and 4.2 million passengers for HSR, Maglev and Hyperloop in 2030, the TOC was estimated at €602.8 million, €801.5 million and €231.3 million, respectively. Likewise, TUC was €166.5 million, €169.7 million and €50.9 million. Lastly, the TEC was found to be €7.7 million, €10.1 million and €4.4 million. In terms of ASC, Hyperloop cost €67.7, compared to €103.3 and €100.2 for HSR and Maglev, respectively.

# Chapter 9. Conclusions

## 9.1 Introduction

This chapter summarizes this study, reviewing its achievement of the research objectives stipulated in the first chapter and its contribution to knowledge. Discussions and recommendations for future work are presented in section 9.3.

## 9.2 Research Summary

In this research, a comparative assessment aims to serve as a comprehensive means of establishing the most suitable HSGT system for a selected transportation corridor, with the lowest average social and/or operator cost, based on projected levels of demand. The study's methodology can be applied to any new project for a HSGT system worldwide, although some parameters will need to be replaced by local values. The methods could be used by strategic planning bodies in Saudi Arabia (such as the Saudi Transport Authority, Saudi Railway Company and Ministry of Transport-Saudi Arabia) and beyond.

The main activities undertaken during the study were the review of literature on HSGT (Chapter 2), a methodological review (Chapter 3), the development of the total social cost model (Chapter 4), the development of the direct demand model (Chapter 5), the development of SPM (Chapter 6), the application of demand models (Chapter 7) and a comparative assessment of the TSCM (Chapter 8).

In summary, HSR lines have been operating for more than 38 years on networks in excess of 51.6 thousand km in countries such as Japan, France, Germany, Italy, China, Spain and, recently, Saudi Arabia. Maglev transport technology has around 73.3 km of track in countries such as South Korea, Japan and China. Regarding the new transport technology of Hyperloop, over 6.6 thousand km of line have been proposed worldwide, designed by three main companies: HTT; Virgin Hyperloop One; and TransPod.

The total social cost in the case study was calculated on the basis of the projected endogenous demand of 7.5 million, 9.8 million and 4.2 million passengers for HSR, Maglev and Hyperloop, respectively. From the unit costs of constructing and maintaining the HSGT infrastructure, the Maglev system was found to bear the

greatest ICC of €761.9 million, while the HSR had the highest IMC of €14.6 million. The Maglev system had the highest acquisition cost of €11.6 million, compared to €6.8 million and €2.1 million for HSR and Hyperloop, as well as the highest operating costs (€0.158 million) and maintenance costs (€27.7 million).

In terms of total annual passenger access/egress time, the Hyperloop system was found to involve the shortest time, at 2.3 million hours, due to its high frequency (and lower demand), compared to HSR and Maglev of 4.2 million hours and 5.4 million hours. On the other hand, HSR involved the longest total annual passenger waiting time of 1.9 million hours. This is due to its low frequency of only a single train per hour, compared to 1.2 million and 0.11 million hours for Maglev and Hyperloop, respectively. HSR was found to involve the longest total annual passenger in-vehicle time, at 5.2 million hours, due to its low speed of 300 km/h, contrasting with 400 km/h and 1000 km/h for Maglev and Hyperloop. As a result, the Maglev system has the highest total user cost of €169.7 million per year, compared to €166.5 million for HSR and €50.9 million for Hyperloop.

Regarding total air and noise pollution, HSR was calculated to cost €1.1 million and €0.54 million per year, compared to zero for the Maglev and Hyperloop systems due to their manner of operation. On the other hand, the Maglev system had the highest total accident and climate change costs of €5.3 million and €4.8 million per year, as demand was different even though it was assumed that the unit accident cost was the same for all three HSGT systems due to similar numbers of accidents. In calculating a value for average climate change cost, it was assumed that the Maglev and Hyperloop systems have the same unit cost of €1.20 per vehicle-km, due to their similar operation and the energy requirements for providing the vacuum in Hyperloop.

In the case study, the total social cost and ASC were determined for all three HSGT technologies, revealing that they are highly dependent on the level of demand. For example, the total social cost of Hyperloop was calculated at €286.6 million per year as, using the SP model, the low percentage of probability leads to the high forecast of annual demand of 4.2 million by 2030. Hyperloop appears to be the best next-generation high-velocity HSGT since it has the lowest average social cost (ASC) of €67.7 per passenger, compared to €103.30 for HSR and €100.20 for Maglev.

### 9.2.1 Research tasks

This section recalls the research objectives presented in Chapter 1 in order to identify the study's main achievements and examine the tasks accomplished during the research.

**Research Objective 1:** To evaluate the interactions between the existing intercity transport modes and the introduction of the HSGT systems such as HSR, Maglev and Hyperloop in order to find out how the performance of the new transport modes would affect the level of user demand.

1. The forecast travel demand for HSR technology was determined using the log-linear direct demand-forecasting model based on secondary data input (rail demand) in order to achieve base HSR flows. In this model, a number of factors along the Riyadh–Dammam and North–South conventional corridors were included, such as population, GDP per capita, mean service frequency, mean speed, mean fare and monthly dummy variables. The output regression analysis of the HSR demand model was determined using SPSS software.
2. The estimated demand of a Maglev system was also obtained, which is dependent on the elasticity with respect to passenger GJT between HSR and Maglev. In this case, the model calculations were based on passenger in-vehicle travel time, the SIP and the interchange penalties. After that, the forecast change in elasticity was used to calculate increased Maglev demand on the basis of the demand forecast for HSR.
3. The base demand for a Hyperloop system was determined using SPM, which uses primary data gathered from data analysis of a survey. In this case, the data were collected along the Riyadh–Dammam conventional rail corridor in order to understand a traveller's preference for one of various transport mode choices, especially upon the introduction of new HSGT technologies. The mode-choice decisions of travellers were found to be dependent on the attributes of travel cost, travel time, service frequency, and so on.

**Research Objective 2:** To investigate the total social cost, including operator, user and external costs of the intercity HSGT technologies such as HSR, Hyperloop and Maglev at different points in time (2030, 2040 and 2050).

4. A spreadsheet cost model was constructed to evaluate the total social cost of various intercity HSGT technologies operating along the selected corridor. In this case, the total social cost was calculated as the sum of operator cost, user cost and external environmental cost, which are evaluated from the characteristics of the HSGT system and its operating performance along the corridor.

5. The calculation of the OC of intercity HSGT system was developed, including the infrastructure construction and maintenance costs and the acquisition and O&M of rolling stock/capsules. In this case, the TIC of the line/tube was calculated using the required length of the line, the unit construction cost and the proportion of the construction costs spent on planning, as well as the unit cost of maintaining the line/tube. The acquisition and O&M of the rolling stock/capsules were calculated using the number of trains/capsules, average capacity, frequency, line/tube length, usage during a given period and the average unit cost of acquiring, operating and maintaining the rolling stock/capsule per seat. The HSGT's ICC and rolling stock/capsule acquisition cost were converted to an annual basis by means of the capital recovery factor equation.

6. The calculation of the user cost of the HSGT technology was developed by considering the total GJT of passengers, which includes access/egress time, waiting time and in-vehicle time. Access/egress time was computed using average distance and speed to/from the station. Passenger waiting time was determined from the service frequency of the HSGT system, while the in-vehicle time was calculated using average journey length and average speed. Regarding passenger waiting time, there is a possibility that a passenger might find that the first incoming vehicle is full, leading to an increase in waiting time by introducing queuing.

7. The calculation of external environmental cost was developed, including air pollution, noise pollution, climate change and accident costs. The costs were determined by using the unit cost of the HSGT technology and passenger-kilometres to arrive at the external cost of the public transport system and the passenger demand.

**Research Objective 3:** To analyse the benefits of HSGT systems after applying the models to the proposed Riyadh–Dammam corridor as a case study so that it can be applied to corridors worldwide.

8. A comparative assessment was undertaken to assess the total social cost of introducing intercity HSGT systems on the Riyadh–Dammam corridor. In this case, the total social cost was evaluated using the level of endogenous demand and the service performance of HSGT technology.

9. Detailed results of the model were presented to show the costs and benefits of HSGT systems on the Riyadh–Dammam corridor. Recommendations were made, based on the model results, and demonstrations of the comparative assessment's usefulness.

### 9.2.2 Contribution to knowledge

The main contribution of this study to general knowledge is more practical than methodological, yet it has elements of both. It uses a novel combination of existing techniques to develop a total social cost framework that is applied to intercity transport, and this is a relatively new application. While some studies have previously been undertaken, they have not been within the total social cost framework. Traditional assessments are based on ad hoc and bespoke cost–benefit analyses, whereas this study provides a general framework that permits the strategic assessment of various high-speed technologies. In this case, the main contribution of this research is to demonstrate the development of a complete comparative assessment for intercity HSGT.

First, a generic comparative assessment tool was developed for intercity HSGT technologies. This tool comprises three closely interacting demand models to forecast travel demand for the HSGT systems considered, with respect to the TSCM.

Second, an innovative demand modelling forecast was developed that combines a gravity model (to estimate HSR demand), an elasticity model (to endogenize Maglev demand) and SPM (to forecast demand for Hyperloop).

Third, a cost model, the TSCM, was constructed to evaluate the total social costs of various intercity HSGT technologies. This model calculates HSR, Maglev and Hyperloop's total social costs, such as their operator cost, user cost and external costs.

Fourth, the main results of the SP survey were described, using Stata software to calibrate a demand forecasting model for a Hyperloop system, based on the multinomial logit model.

Fifth, the calculation of endogenous demand assessed the impact of change in the performance of HSGT technology on its utility to users, and hence the level of passenger demand. The result for endogenous demand is based on the updated level of passenger demand to include exogenous factors such as rising incomes. Therefore, it is used as a process of feedback to the calculation of total social cost to increase the actual level of passenger demand through enhancing the attraction of the HSGT service.

Overall, the main achievement is the study's development of a comparative assessment model to evaluate the total social cost – the TSCM – incorporating operator cost, user cost and external environmental cost for various intercity HSGT technologies along a stipulated travel corridor. Although there have been several studies of urban markets, there have not been many on total social costs in the inter-urban market. This is the gap that is filled by this thesis. As indicated above, there have been few systematic studies of intercity transport, particularly of the new transport modes such as Maglev and Hyperloop.

## 9.3 Future Work

This study has evaluated various intercity HSGT technologies operating along travel corridors in terms of their total social cost. The usefulness of this comparative assessment is demonstrated through examination of the Riyadh–Dammam corridor, Saudi Arabia. At present, both the existing and proposed HSGT options are remote from their potential passengers in the cities yet. However, by the end of 2021, Riyadh will have a public transit system with six metro lines covering 176 km with 85 stations and 80 bus routes covering 1,900 km with 3,000 stations and stops. A public transit system for Dammam city was approved in 2014 and is expected to

commence operation in 2022, with 50 km of light rail, 110 km of bus rapid transit and 350 km of feeder buses from the outskirts. The implication of such public transport networks is just one aspect of the potential future work identified during the case study, as discussed in the following sections.

### 9.3.1 Combinations of high-speed ground transport services

The comparisons undertaken in terms of the total social cost were between HSGT systems, as travellers were assumed to access these systems only by car. Access/egress time was calculated by using the distance to/from the rail/Hyperloop station and the average speed of a car. However, the introduction of a public transport system or feeder services such as buses and metro into major cities, whether in the case study cities of Riyadh and Dammam or elsewhere, will increase the services' attractiveness so that average user cost might thus be reduced. This represents a direction for further research.

### 9.3.2 Evaluation of passenger demand level

In the comparative assessment of this study, the variation in passenger demand was evaluated using elasticity of demand with respect to passengers' GJT. The evaluation in the comparative assessment did not encompass the total social costs incurred in using other intercity modes of transport along the corridor such as car, air, conventional rail and bus, as the comparisons were between only HSGT technologies. This represents a direction for further research.

### 9.3.3 A substantial database for high-speed ground transport systems

It would be useful to develop substantial database on which to store the information and characteristics of existing public transport technologies across the world to allow users to compare a wider range of HSGT systems.

### 9.3.4 Policy implications of equity issues

The policy implications of this study include the question of HSR systems and equity issues in terms of how people might alter both their activities and chosen residential location. The implications of spatial equity stem from changes to the distribution of access among urban groups and how easily travellers can move between their origin and a given destination via a certain mode of transport. One of the main issues is the cost of fares on HSR systems, which is generally much higher than on classic

rail. Most travellers are students, so it is difficult for them to pay the extra for faster travel. To the extent that fares are considered as transfers between users and operators they are not directly considered in the total social costs' models, but they are considered in the underpinning demand models.

As well as values and concerns, the involvement, identification and incorporation of stakeholders' needs are essential to the transport decision-making process. In Saudi Arabia, the stakeholders will one day see the realization of HSR, Maglev and Hyperloop in their own neighbourhood. For example, they can assume that the introduction of new HSGT transport mode will reduce their travel time, improve their mobility, create more jobs and positively affect both the economy and environment through connecting cities. Recently, by announcing a partnership to conduct a feasibility study on the use of Hyperloop technology to transport passengers and freight, Virgin Hyperloop took the first step towards creating a network of routes across the Kingdom.

### 9.3.5 Limitations of the research

Limitations of this research were identified while undertaking the case study, as follows.

First, there was a lack of secondary data on current transport modes in terms of mean speed, mean fare, number of passengers, and so on, which seems to be an aspect of the relevant organizations'commercial confidentiality. Moreover, as their staff do not regularly check their email accounts, to obtain the required data it was necessary to identify a contact in these organizations, making the secondary data collection challenging.

Second, the dominance of the private car in Saudi Arabia has led to a lack of experience of intercity public transport in terms of participants' attitudes, especially among full-time employees. The low price of petrol is one of the factors behind the use of cars to travel between cities. At September 2020, petrol cost roughly €0.37/litre, compared to the UK price of €1.20/litre (Trading Economics, 2020).

The entire study represents a snapshot in time, as the foundational assumptions prevailing at the time of study may well need to be adjusted markedly in view of major changes to world prices connected with the Covid-19 pandemic, the supply

of oil, world recession, unstable international relations, politics, and so on. In this case study, global economic growth worldwide has been negatively affected by the current pandemic beyond anything experienced for nearly a century.

One of the key limitations of this study is that its estimate of Hyperloop demand was based on the range of frequencies presented in the SP experiment, known as the demand for a high-frequency system. Under this assumption, higher frequencies generate more demand, so service frequency will rise if demand grows, making Hyperloop increasingly attractive. However, the SP models were unable to detect statistically significant frequency effects. Countervailing this, the SP models did not take into account comfort, nor did the modelling framework consider overcrowding. It is likely that the lack of comfort and the overcrowding would reduce the attractiveness of Hyperloop.

In summary, it is strongly recommended that for the Riyadh-Dammam corridor the HSGT options should be Hyperloop, on the grounds of the lowest average social cost. However, this study recognises that Saudi Arabia's HSGT planners may prefer to delay their final decision on transport modes for this corridor until detailed data are available on the new technologies represented by Hyperloop and Maglev, as both are yet to come into their maturity.

## References


Abdelrahman, A.S., Sayeed, J. and Youssef, M.Z. (2018) 'Hyperloop transportation system: Analysis, design, control, and implementation', *IEEE Transactions on Industrial Electronics*, 65(9), 7427-7436.

Abeye, B., Tang, A., Wong, S., Mishra, H. and Van, K. (2012) *Maglev Trains: A look into economic concessions*. Report available at: https://user.eng.umd.edu/~austin/enes489p/projects2011a/MaglevTrains-FinalReport.pdf

Abuhjeeleh, M. (2019) 'Rethinking tourism in Saudi Arabia: Royal Vision 2030 perspective'. *African Journal of Hospitality, Tourism and Leisure*, 8(5)

Akamaihd, A. (2002) The Shanghai Maglev Route. Available at: https://steamcdn-a.akamaihd.net/steam/apps/376933/manuals/Shanghai_Maglev_Manual_English.pdf?t=1460539219

Al-Ahmadi, H.M. (2006) 'Development of intercity mode-choice models for Saudi Arabia.' *Engineering Sciences*, 17(1).

Albalate, D. and Bel, G. (2017) *Evaluating High Speed Rail: Interdisciplinary perspectives.* New York: Routledge.

Aldagheiri, M. (2010) 'The expected role of railways in the economic development of Saudi Arabia.' *WIT Transactions on the Built Environment*, 111, 157-167.

Aldroubi, M. (2018) 'Saudi King inaugurates Kingdom's first high-speed train'. Available at: https://www.thenational.ae/world/mena/saudi-king-inaugurates-kingdom-s-first-high-speed-train-1.773904 (accessed 25 September 2018).

Allard, R.F. and Moura, F. (2013) 'Analysis of accessibility distributions for inter-city travel by public transport'. *Transport Reviews*, 36, 251-277.

Almujibah, H. and Preston, J. (2018) 'The total social costs of constructing and operating a maglev line using a case study of the Riyadh-Dammam corridor, Saudi Arabia.' *Transportation Systems and Technology*, 4(3 suppl. 1), 298-327.

Alsugair, S. (2016) 'SRO orders 238 passenger trips per week.' ArabNews, 20 September 2016. Available at: http://www.arabnews.com/node/986886/saudi-arabia.

American Magline Group. (2002) *Technology Comparison: High Speed Ground Transportation Transrapid Superspeed Maglev and Bombardier JetTrain*. Available at: http://faculty.washington.edu/jbs/itrans/transrapid-jettrain1.pdf.

Amos, P., Bullock, D. and Sondhi, J. (2010) *High-Speed Rail: The fast track to economic development,* p. 28. Beijing: World Bank. Available at: https://openknowledge.worldbank.org/handle/10986/27812

de Angoiti, I.B. (2018) 'High-speed rail-fast track to sustainable mobility'. *Brochure of the International Union of Railways (UIC)*, 3.

Angoori, I.N. (2010) 'High-speed rail-fast track to sustainable mobility.' *Brochure of the International Union of Railways (UIC)*, 3.

Anisimow, V. *et al.* (2004) *Urban Maglev Technology Development Program: Colorado Maglev Project: part 1: Executive summary of final report*.

Anthony, S. (2013) 'Hyperloop: Hypothetical pipe dream, or the most important invention since the car?' Available at: https://www.extremetech.com/extreme/163803-hyperloop-hypothetical-pipe-dream-or-the-most-important-invention-since-the-car (accessed 13 August 2013).

ArabianBusiness (2018) 'Saudi's high-speed Haramain railway to be inaugurated today.' Arabian Business, 25 September. Available at: https://www.arabianbusiness.com/

transport/404957-saudis-high-speed-railway-to-be-inaugurated-today (accessed 25 September 2018).

ArabNews (2017) 'Haramain high-speed train arrives in Jeddah for first time.' *ArabNews* 19 July. Available at: http://www.arabnews.com/node/1131811/saudi-arabia (accessed 19 July 2017).

Arduin, J.-P. and Ni, J. (2005) 'French TGV network development'. *Japan Railway & Transport Review*, 40(3), 22-28.

Argaam (2019) 'Saudi Arabia's Haramain train to resume service in 30 days: minister.' Argaam, 2 October. Available at: https://www.argaam.com/en/article/articledetail/id/1318187 (accessed 2 October 2019).

Asad, F.H. (2015) 'Travel demand forecasting using UK TRICS database', *International Journal*, 3(3), 98-107.

Atkins (2012) *Norway HSR Assessment Study - Phase III: Model Development Report.* Available at: https://www.banenor.no/contentassets/d2b183386b04479b882e9d563f2b0b91/norway-hsr-phase-iii_model-development_final-report_atkins_25-01-12.pdf

Awasthi, G. (2016) 'Hyperloop - A 21st century transportation revolution'. Available at: https://www.slideshare.net/GyanendraAwasthi3/hyperloop-a-21st-century-transportation-revolution (accessed 6 October 2016).

Balcombe, R., Mackett, R., Paulley, N., Preston, J., Shires, J., Titheridge, H., Wardman, M. and White, P. (2004) The demand for public transport: A practical guide. *Transportation Research Laboratory Report* (TRL593). London: Transportation Research Laboratory.

Bansal, K. (2014) Trains at the Speed of Bullets? Available at: http://nopr.niscair.res.in/bitstream/123456789/29490/1/SR%2051%2810%29%2014-21.pdf (accessed 1 October 2014).

Barrow, K. (2016) 'Changsha airport maglev line opens.' International Railway Journal, 4 April. Available at: http://www.railjournal.com/index.php/asia/changsha-airport-maglev-line-opens.html (accessed 4 April 2016).

BBC News (1999) 'The magnetic attraction of trains'. Available at: http://news.bbc.co.uk/1/hi/sci/tech/488394.stm (accessed 9 November 1999).

BBC News (2003) 'Train smashes London-Paris record'. Available at: http://newsimg.bbc.co.uk/1/hi/uk/3145396.stm (accessed 27 November 2003).

Beaton, P., Chen, C. and Meghdir, H. (1997) 'Stated choice for transportation demand management models: Using a disaggregate truth set to study predictive validity', *Transportation Research Record: Journal of the Transportation Research Board*, 1598, 1-8.

Ben-Akiva, M. (2010) 'Planning and action in a model of choice'. In S. Hess and A. Daly (eds), *Choice Modelling: The state-of-the-art and the state-of-practice: Proceedings from the Inaugural International Choice Modelling Conference,* pp. 19-34. Emerald.

Benson, A.R., Kumar, R. and Tomkins, A. (2016) 'On the relevance of irrelevant alternatives'. Proceedings of the 25th International Conference on World Wide Web, pp. 963–973. https://doi.org/10.1145/2872427.2883025

Bonsor, K. and Chandler, N. (2019) 'How Maglev trains work.' Available at: https://science.howstuffworks.com/transport/engines-equipment/maglev-train1.htm#

Borjesson, M. (2014) 'Forecasting demand for high speed rail'. *Transportation Research Part A: Policy and Practice*, 70, 81-92.

Boslaugh, S.E. (2020) 'Maglev.' *Encyclopedia Brittanica* online. Available at: https://www.britannica.com/technology/maglev-train (accessed 15 December 2020).

Brand, C. and Preston, J. (2003) ' Which technology for urban public transport? A review of system performance, costs and impacts'. *Proceedings of the Institution of Civil Engineers-Transport,* 156(4), 201-210, ISBN: 0965-092X

Brand, D. *et al.* (1992) 'Forecasting high-speed rail ridership'. *Transportation Research Record*, 1341.

Brown, M. (2017) 'TransPod wants to develop a Hyperloop for Canada by 2020'. Available at: https://www.inverse.com/article/29088-transpod-hyperloop-system-canada-italy-france-offices (accessed 15 March 2017).

Brunello, L.R. (2011) 'Investigation to enhance high speed rail accessibility'. PhD thesis, Queensland University of Technology.

Businesswire (2020) Hyperloop Transportation Technologies Receives Official Classification Under United States Department of Transportation. Available at: https://www.businesswire.com/news/home/20200723005965/en/Hyperloop-Transportation-Technologies-Receives-Official-Classification-Under-United-States-Department-of-Transportation (accessed July 23, 2020).

Cabral, T.D.F. and Chavarette, F.R. (2015) 'Dynamics and control design via LQR and SDRE Methods for a maglev system'. *International Journal of Pure and Applied Mathematics*, 101(2), 289-300.

Cambridge Systematics *et al.* (2012) *Travel Demand Forecasting: Parameters and techniques*. Transportation Research Board.

Campos, J., de Rus, G. and Barron, I. (2006) 'Some stylized facts about high speed rail. A review of HSR experiences around the world. *Proceedings of the 11th World Conference on Transport Research,* Berkeley, CA, USA.

Campos, J., de Rus, G. and Barron, I. (2007a) 'The cost of building and operating a new high speed rail line'. In: G. de Rus (ed.), *Economic Analysis of High Speed Rail in Europe,* chap. 2. BBVA Foundation.

Campos, J., de Rus, G. and Barron, I. (2007b) 'A review of HSR experiences around the world'. In: G. de Rus (ed.), *Economic Analysis of High Speed Rail in Europe,* chap. 1. BBVA Foundation.

Cao Qingqing, G.Y. (2020) 'China's 600 km/h high-speed maglev prototype completes successful trial run.' CGTN News, 21 June. Available at: https://news.cgtn.com/news/2020-06-21/China-s-600-km-h-high-speed-maglev-completes-trial-run-RvueeEECTm/index.html.

Carballo-Cruz, F. (2007) 'The economics of high-speed railway'. Introduction: An analysis of HSR introduction in the Lisbon-to-Porto corridor.' University of Oxford.

Cascetta, E. and Coppola, P. (2011) 'High speed rail demand: Empirical and modelling evidences from Italy'. Proceedings of the European Transport Conference (ETC.), Glasgow, UK.

Cascetta, E. and Coppola, P. (2014) 'High Speed Rail (HSR) induced demand models'. *Procedia-Social and Behavioral Sciences*, 111, 147-156.

Cassat, A. and Bourquin, V. (2011) MAGLEV – Worldwide status and technical review. *Electrotechnique du Futur 2011 conference,* December, Belfort.

Cassat, A. and Bourquin, V. (2011) *MAGLEV – Worldwide Status and Technical Review*. *Electrotechnique du Futur 2011 conference,* December, Belfort.

Central Japan Railway Company (2017) 'Superconducting Maglev (SCMaglev)'. Available at: http://english.jr-central.co.jp/company/company/others/_pdf/superconducting_maglev.pdf

CH2M HILL, I. (2017) Ultra High-Speed Ground Transportation Study for Washington State Department of Transportation. Available at: https://app.leg.wa.gov/ReportsToTheLegislature/Home/GetPDF?fileName=UltraHighSpeedGroundTransportation_98119447-d3df-4488-97dd-fffb675edba5.pdf

Chadha, A. Ballani, A., Bhavnani, A., Vishnani, B., Jain, A. and Malkalni A. (2009) 'Maglev'. *Report for Humanities section, Thadomal Shahani Engineering College, University of Mu*mbai. Mumbai: TSEC.

Charles River Associates Incorporated (2000) *Independent Ridership and Passenger Revenue Projections for High Speed Rail Alternatives in California.* Boston: Charles River Associates.

Chen, M., Tang, H.-L. and Zhang, K. (2014) 'Some critical issues in the development of Chinese high-speed rail: Challenges and coping strategies'. *Journal of Transportation Technologies*, 4(2), 164-174.

Chen, X. *et al.* (2007) 'High-speed maglev noise impacts on residents: A case study in Shanghai'. *Transportation Research Part D: Transport and Environment*, 12(6), 437-448.

Chen, Z. *et al.* (2019) *High Speed Rail and China's New Economic Geography: Impact assessment from the regional science perspective*. Cheltenham: Edward Elgar.

Cheng, Y.-H. (2010) 'High-speed rail in Taiwan: New experience and issues for future development'. *Transport Policy*, 17(2), 51-63.

Chin, J.C., Gray, J.S., Jones, S. and Berton, G. (2015) 'Open-source conceptual sizing models for the hyperloop passenger pod'. 56th AIAA/ASCE/AHS/ASC Structures, Structural Dynamics, and Materials Conference.

Chinowsky, P., Helman, J., Gulati, S., Neumann, J. and Martinich, J. (2017) 'Impacts of climate change on operation of the US rail network'. *Transport Policy*, 75, 183-191.

Chopade, S. (2017a) 'Magnetically Levitated Trains (Maglev)'. *International Research Journal of Engineering and Technology*, 4(4).

Chopade, S.S. (2017b) 'Dedicated to Ministry of Railways/CRR/ITT Kharagpur/RDSO Hyperloop trains'. *International Journal of Modern Trends in Engineering and Research* (IJMTER), 4(4). DOI: 10.21884/IJMTER.2017.4134.7CCP1

Chopade, S.S. and Sharma, P.K. (2013) 'High Speed trains', *International Journal of Modern Engineering Research* 3(2), 1161-1166.

Choudhury, S. and Chetty, P. (2018) 'How to perform point forecasting in STATA'. Available at: https://www.projectguru.in/point-forecasting-stata/ (accessed 22 November 2018).

Coelho, T.M.S. (2016) *Hyperloop Alpha-Conceptual study.* University of Lisbon.

Cooke, B. (2016) 'Hyperloop Transportation Technologies, Inc. Reveals Hyperloop™ Levitation System.' PRN Newswire, 9 May. Available at: https://www.prnewswire.com/news-releases/hyperloop-transportation-technologies-inc-reveals-hyperloop-levitation-system-300264946.html (accessed 9 May 2016).

Daly, A., Fox, J., Patruni, B. and Milthorpe, F. (2011) 'Pivoting in travel demand models'. *Australasian Transport Research Forum 2012 Proceedings,* September, Perth. Available at: http://www.patrec.org/atrf.aspx

Daniels, G., Ellis, D.R. and Stockton, W.R. (1999) *Techniques for Manually Estimating Road User Costs Associated with Construction Projects*. Texas Transportation Institute Texas, USA.

DaTian, Z. Wei, X. Ali, H. Wang and Han, W. (2015) Study on model based hazard Identification for the Hyperloop system. *International Seminar on Computation,*

*Communication and Control (IS3C-15)*, March, Sydney. https://doi.org/10.2991/is3c-15.2015.6

Davies, A. (2015) 'So Elon Musk's Hyperloop is actually getting kinda serious.' Available at: https://www.wired.com/2015/08/elon-musk-hyperloop-project-is-getting-kinda-serious/ (accessed 20 August 2015).

Decker, K. *et al*. (2017) 'Conceptual feasibility study of the Hyperloop vehicle for next-generation transport'. *55th American Institute of Aeronautics and Astronautics Meeting, SciTech Forum.* January, Grapevine, Texas. Available at: https://ntrs.nasa.gov/api/citations/20170001624/ downloads/20170001624.pdf

DeNicola, E. *et al*. (2016) 'Road traffic injury as a major public health issue in the Kingdom of Saudi Arabia: A review'. *Frontiers in Public Health*, 4, 215.

Department for Transport (2018) 'Historical and reference information on all the appraisal and modelling values referred to in the transport analysis guidance (TAG)'. Available at: https://www.gov.uk/government/publications/tag-data-book (accessed 29 November 2018).

de Dios Ortuzar, J. and Willumsen, L.G. (2011) *Modelling Transport*. Chichester: John Wiley & Sons.

Dona, S. and Singh, A. (2017) 'The workings of Maglev: A new way to travel'. Research Report UHM/CE/2017-01, Hawaii. Available at: http://www.cee.hawaii.edu/ wp-content/uploads/2016/05/UHM-CEE-17-01.pdf

Dorciak, M. (2015) 'Cost-benefit analysis of the German high speed rail network', *Undergraduate Economic Review*, 12(1), p. 4.

Douglas, N. and Karpouzis, G. (2006) 'Valuing rail service quality attributes through rating surveys'. *29th Australasian Transport Research Forum*, Gold Coast, Australia.

DW.com (2016) 'China masters German train technology, will cut costs'. Available at: https://www.dw.com/en/china-masters-german-train-technology-will-cut-costs/a-1982476

Ebeling, K. (2005) 'High-speed railways in Germany'. *Japan Railway & Transport Review*, 40, 36-45.

Eckert, F. *et al.* (2018) 'Energy consumption of track-based high-speed trains: maglev systems in comparison with wheel-rail systems'. *Russian Journal of Logistics & Transport Management*, 4(3 S1).

Edwards, N. (2012) 'High speed rail: Benefits that add up. A report for the Australian Greens'. Available at: https://adam-bandt.greensmps.org.au/sites/default/ files/hsrbenefitsreport.pdf

Edwin, F. (2015) 'A train as fast as an aeroplane – Maglev train'. Kinooze website. Available at: http://kinooze.com/a-train-as-fast-as-an-aeroplane-maglev-train/

Einstein, N. (2007) *Locator map of Mecca, in western Saudi Arabia*. Available at: https://commons.wikimedia.org/wiki/File:Mecca,_Saudi_Arabia_locator_map.png.

Esmail, H. (2018) 'Economic growth of Saudi Arabia between present and future according to 2030 vision'. *Asian Social Science*, 14(12), 192.

ESTECO Academy (2018) 'Optimizing a levitating rail-free pod design for SpaceX Hyperloop design'. Winning competition entry information. ESTECO Academy. Available at: https://www.esteco.com/academy/optimizing-levitation-propulsion-system-spacex-hyperloop-design-competition

European Court of Auditors (2018) *A European High-speed Rail Network: Not a reality but an ineffective patchwork*. Special report no. 19/2018: Available at: https://op.europa.eu/webpub/eca/special-reports/high-speed-rail-19-2018/en/

Ferran, T. (2017) 'Haramain high-speed crawls towards the start of operations.' International Railway Journal. Available at: https://www.railjournal.com/in_depth/haramain-high-speed-crawls-towards-the-start-of-operations.

Fibich, G., Gavious, A. and Lowengart, O. (2005) 'The dynamics of price elasticity of demand in the presence of reference price effects'. *Journal of the Academy of Marketing Science*, 33(1), 66-78.

Fiske, O.J. *et al.* (2010) 'Track switching for a magnetically levitated transportation system and method', LAUNCHPOINT Tech Inc, U.S. Patent 7,757,609.

Flightradar (2019) Riyadh King Khalid International Airport. Available at: https://www.flightradar24.com/data/airports/ruh/routes (accessed 22 August, 2019).

Flyvbjerg, B. (2005) 'Measuring inaccuracy in travel demand forecasting: Methodological considerations regarding ramp up and sampling', *Transportation Research Part A: Policy and Practice*, 39(6), 522-530.

Follett, A. (2016) 'Scientist lays out 5 huge problems with Elon Musk's Hyperloop'. Daily Calller, 26 July. Available at: https://dailycaller.com/2016/07/26/scientist-lays-out-5-huge-problems-with-elon-musks-hyperloop-video/.

Frost, J. (2017) 'Multicollinearity in regression analysis: problems, detection, and solutions'. Available at: https://statisticsbyjim.com/regression/ multicollinearity-in-regression-analysis/ (accessed 20 September 2017).

Garavaglia, S. and Sharma, A. (1998) ' A smart guide to dummy variables: four applications and a macro'. *Proceedings of the Northeast SAS Users Group Conference.*

Garcia, R.C. *et al.* (2016) 'Development of a feasibility model for a High Speed Rail (HSR) line project'. *Journal of Transport Literature*, 10(2), 20-24.

General Authority for Statistics, Saudi Arabia (2012) Population distribution. Available at: http://www.data.gov.sa/en/dataset/al-riyad-region.

General Authority of Civil Aviation, Saudi Arabia. (2016) Annual Report. General Authority of Civil Aviation. Available at: https://gaca.gov.sa/web/en-gb/page/publications.

Givoni, M. (2006) 'Development and Impact of the Modern High-speed Train: A Review'. *Transport Review*, 26(5), 593-611.

Gizmo Highway (2011) Japan's Maglev Train. Available at: http://www.gizmohighway.com/transport/japan_maglev_train.htm.

GMI (2020) 'Saudi Arabia's population statistics of 2020.' Available at: https://www.globalmediainsight.com/blog/saudi-arabia-population-statistics/ (accessed 6 July 2020).

Gorham, R. (2009) *Demystifying induced travel demand*. Sustainable Urban Transport Technical Document 1. Federal Ministry for Economic Cooperation and Development

Gorlewski, B. (2011) 'Travel cost reduction as a factor of economic appraisal of high speed-rail project'. *Logist. Sci. J. Trans. Logist.* 2: 16–26.

Gould, W., Pitblado, J. and Sribney, W. (2006) *Maximum Likelihood Estimation with Stata*. College Station: Stata Press.

Grigolon, A., Kemperman, A. and Timmermans, H. (2010) 'Estimation strategy to complex multi-dimensional stated portfolio choice models'. *Proceedings of the International Conference on Design & Decision Support Systems in Architecture and Urban Planning,* July, Eindhoven, The Netherlands.

'Guidance note' (2019) 'Guidance note on passenger demand forecast third party funded local rail schemes'. UK Government. Available at: https://assets.publishing.service.gov.uk/government/uploads/system/uploads/attachment_data/file/3978/guidance-note.pdf

Guzzo, R. and Mazzulla, G. (2004) 'Modal choice models estimation using mixed revealed and stated preferences data'. *WIT Transactions on the Built Environment*, 75.

Gwilliam, K.M. (1997) *The Value of Time in Economic Evaluation of Transport Projects: Lessons from recent research*. Washington DC: World Bank.

Hart, C. (2019) 'Saudi Arabia's hyperloop a step closer to reality.' Available at: https://www.cips.org/en-GB/supply-management/news/2019/august/saudi-to-build-first-long-range-hyperloop-track/.

Hawkins, A. (2016) *Hyperloop startup selects Vibranium for pods because it's good enough for Captain America*. Available at: https://www.theverge.com/2016/5/24/11750666/hyperloop-transportation-vibranium-carbon-fiber-marvel-comics.

He, N. *et al.* (2017) 'Rail-induced traffic in China'. *Promet - Traffic & Transportation*, 29(5), 511-520.

Heath, N. (2018) *Hyperloop: A cheat sheet*. Available at: https://www.techrepublic.com/article/hyperloop-the-smart-persons-guide/.

Heiss, F. (2002) 'Structural choice analysis with nested logit models'. *Stata Journal*, 2(3), 227-252.

Hensher, D.A. (1994) 'Stated preference analysis of travel choices: The state of practice', *Transportation*, 21(2), 107-133.

Hensher, D.A., Rose, J.M. and Greene, W.H. (2005) *Applied Choice Analysis: A primer*. Cambridge: Cambridge University Press.

Hodaib, A.E. and Fattah, S.F.A. (2016) 'Conceptional design of a hyperloop capsule with linear induction propulsion system', *International Journal of Mechanical, Aerospace, Industrial, Mechatronic and Manufacturing Engineering*, 10(5), 997-1005.

Holmer, P. (2003) 'China is throttling up a 430-km/h magnetically levitated train to link Shanghai and its airport.' Available at: https://spectrum.ieee.org/transportation/mass-transit/faster-than-a-speeding-bullet-train.

Holmer, P. (2011) Maglev enables higher average speed. Available at: https://web.archive.org/web/20120724152619/http://namti.org/wp-content/uploads/2010/11/HSR-Maglev-Compare-Acceleration.jpg.

Houghton, R. (2013) 'Why HS2 is not needed to solve capacity issues on UK's railways.' Available at: https://www.hs2actionalliance.org/wp-content/uploads/2013/11/130909-HS2AA-Capacity-Report.pdf

Hume Regional Development, A. (2014) 'High speed rail: Economic and social benefits for the Hume region'. Available at: https://www.rdv.vic.gov.au/__data/assets/pdf.file/0010/1166428/Hume-HSR-Final-Report-Dec-14-r1.pdf.

Hunt, H.E. and Hussein, M.F. (2007) 'Ground-borne vibration transmission from road and rail systems: Prediction and control'. *Handbook of Noise and Vibration Control*, 1458-1469.

Igor, J. and Howaida, K. (2014) 'Methods for estimation of external costs of transport', *Zbornik Radova Građevinskog Fakulteta*, 26, 149-158.

Ilonidis, S. (2010) 'Maglev energy budget'. Available at: http://large.stanford.edu/courses/2010/ph240/ilonidis2/ (accessed 28 November 2010).

Jain, M. (2016) 'A seminar report on Hyperloop High Speed Transportation'.

Janić, M. (2016) 'A multidimensional examination of performances of HSR (High-Speed Rail) systems'. *Journal of Modern Transportation*, 24(1), 1-21.

Janić, M. (2017) *Transport Systems: Modelling, planning, and evaluation*. Boca Raton, FL: CRC Press.

Janić, M. (2018) 'Multicriteria evaluation of the high speed rail: Transrapid maglev and hyperloop systems'. *Transportation Systems and Technology*, 4(4), 5-31.

Janić, M. (2020) 'Estimation of direct energy consumption and CO2 emission by high speed rail, Transrapid maglev and hyperloop passenger transport systems', *International Journal of Sustainable Transportation*, pp. 1-22.

Jansson, J.O. (1984) *Transport System Optimization and Pricing*. Chichester: Wiley.

Jansson, J.O., Holmgren, J. and Ljungberg, A. (2015) 'Pricing public transport services'. In *Handbook of Research Methods and Applications in Transport Economics and Policy,* pp. 260–308. Cheltenham: Edward Elgar.

Janzen, R. (2016) 'The future of mobility: Driving sustainable productivity with tomorrow's transportation systems'. Available at: http://www.apo-tokyo.org/news/wp-content/uploads/sites/4/2018/07/ Future_of_Transportation_APO_Sustainable_Productivity_Summit-2018_Mr.-R.-Janzen.pdf

Jingfang, D., Zhiqiang, L. and Xin, Y. (2017) 'Robotics and Automation Engineering (ICRAE)'. *2nd International Conference on IEEE*.

Jithendra, P. (2015) 'Hyperloop transportation system: A new mode of transportation'. *International Journal of Science and Research*, 7(3), 769-771.

Johnson, L.R. *et al.* (1989) *Maglev vehicles and superconductor technology: Integration of high-speed ground transportation into the air travel system*. DOI:10.2172/6303324

JR-Central (2017) *Central Japan Railway Company Guide.* Available at: http://english.jr-central.co.jp/company/company/others/data-book/_pdf/2016.pdf.

Kale, S., Laghane, Y.N, Kharade, K.A. and. Kadus, S.B. (2019) 'Hyperloop: Advance mode of transportation system and optimize solution on traffic congestion'. *International Journal for Research in Applied Science & Engineering Technology (IJRASET)*, 7(7): 539-552.

Kemp, R. and Smith, R. (2007) 'Technical issues raised by the proposal to introduce a 500 km/h magnetically-levitated transport system in the UK'. Report on Imperial College London and Lancaster University

Kenton, W. (2019) Durbin-Watson Statistic Definition. Available at: https://www.investopedia.com/terms/d/durbin-watson-statistic.asp (accessed 18 July 2019).

Khan, O.A. (2007) 'Modelling passenger mode-choice behaviour using computer aided stated preference data'. PhD thesis, Queensland University of Technology.

Knaub, J. (2017) *Essential Heteroscedasticity*. Insights from K.R.W. Brewer (2002) *Combined Survey Sampling Inference: Weighing Basu's elephants* (Arnold: London and Oxford University Press) (2002). Available at: https://www.researchgate.net/profile/James_Knaub/publication/320853387_Essential_Heteroscedasticity/links/5ea151e0299bf14389401640/Essential-Heteroscedasticity.pdf

Krausz, S. (2016) 'The Hyperloop: A new frontier of travel'. Essay. Available at: http://docshare01.docshare.tips/files/27040/270408438.pdf

Kremers, H., Nijkamp, P. and Rietveld, P. (2002) 'A meta-analysis of price elasticities of transport demand in a general equilibrium framework'. *Economic Modelling*, 19(3), 463-485.

Kumar, A. and Khan, A.B. (2017) 'Hyperloop high speed of transportation'. *International Conference on Emerging Trends in Engineering, Technology, Science and Management*, April, Greater Noida, India. Available at: http://data.conferenceworld.in/IIMT2017/P430-439.pdf

Latino, F. and Yokobri, T. (2009) 'Urban Magnetic Levitation (MAGLEV) transit - Japanese HSST system'. Available at: https://faculty.washington.edu/ jbs/itrans/hsstpage.htm

Lavars, N. (2018) 'Virgin Hyperloop One shows off shiny new passenger pod for Saudi Arabia'. Available at: https://newatlas.com/virgin-hyperloop-one-pod-saudi-arabia/54082/ (accessed 5 April 2018).

Le, T.V. *et al.* (2018) 'Influence of introducing high speed railways on intercity travel behavior in Vietnam'. *arXiv preprint arXiv:*1810.00155.

Lee, H.-W., Kim, K.-C. and Lee, J. (2006) 'Review of maglev train technologies'. *IEEE Transactions on Magnetics*, 42(7), 1917-1925.

Levinson, D. *et al.* (1996) 'The full cost of intercity transportation: A comparison of high speed rail, air and highway transportation in California'.

Levinson, D. *et al.* (1997) 'The full cost of high-speed rail: An engineering approach'. *Annals of Regional Science*, 31(2), 189-215.

Levinson, D., Kanafani, A. and Gillen, D. (1999) 'Air, high-speed rail, or highway: A cost comparison in the California Corridor', *Transportation Quarterly*, 53, 123-131.

Li, X. (2015) 'A comparative assessment for innovative public transport technologies'. PhD thesis, University of Southampton.

Li, X. and Preston, J. (2015) 'Assessing the financial and social costs of public transport in differing operating environments and with endogenous demand', *Transportation Planning and Technology*, 38(1), 28-43.

Litman, T. (2013) Understanding Transport Demands and Elasticities: How prices and other factors affect travel behavior. Litnam: Victoria Transport Policy Institute. Available at http://www.vtpi.org/elasticities.pdf (accessed 22 November 2013).

Looveren, Y. (2017) 'Amazon considers hyperloop for same-day delivery'. Available at: https://www.retaildetail.eu/en/news/m-tail/amazon-considers-hyperloop-same-day-delivery

Loukaitou-Sideris, A. and Peters, D. (2015) 'Promoting connectivity at HSR stations: Lessons from Germany and Spain'. University of California report. Available at: https://www.its.ucla.edu/wp-content/uploads/sites/6/2015/12/JPT_ Loukaitou-Sideris_Peters.pdf

Louviere, J.J., Hensher, D.A. and Swait, J.D. (2000) *Stated Choice Methods: analysis and applications*. Cambridge University Press.

Luguang, Y. (2002) 'Progress of high-speed Maglev in China'. *IEEE Transactions on Applied Superconductivity*, 12(1), 944-947.

Lusvter (2015) 'The disadvantages of HSR (High-Speed Rail)'. Available at: https://zhangjin881001.wordpress.com/2015/03/07/the-disadvantages-of-hsr-high-speed-rail-going-to-a-wrong-way/

Luu, T. and Nguyen, D. (2005) 'MagLev: The train of the future'. *5th Annual Freshman Conference,* Tesla Society, April.

Ma, S., Kockelman, K.M. and Fagnant, D.J. (2015) 'Welfare analysis using logsum differences vs. rule of half: A series of case studies 2'. *Transportation Research Record: Journal of the Transportation Research Board*, 16(2), 147–166.

Maddala, G.S. and Lahiri, K. (1992) *Introduction to Econometrics*. New York: Macmillan.

Maeyer, J. and Pauwels, T. (2003) 'A literature review on the role of quality of service attributes and their monetary valuation in freight demand models. '.

Maglev Board (2018) Chuo Maglev Shinkansen. Available at: https://www.maglevboard.net/en/facts/systems-overview/chuo-maglev-shinkansen.

Maibach, M. *et al.* (2008) *Handbook on Estimation of External Costs in the Transport Sector*. CE Delft. Available at: https://ec.europa.eu/transport/sites/transport/files/themes/sustainable/doc/2008_costs_handbook.pdf

Maout, E.L. and Kato, H. (2016) 'Life cycle cost-estimation model for building, operating, and maintaining high-speed rail systems'. *Asian Transport Studies*, 4(1), 245-260.

Markvica, K. *et al*. (2018) 'On the development of a sustainable and fit-for-the-future transportation network'. *Infrastructures*, 3(3), 23.

Mathur, A. (2017) 'Proposing a fifth mode of transportation: The Hyperloop'. Available at: https://www.slideshare.net/ayushmathur2009/hyperloop-75351014

McCourt, D. (2019) Perfect on paper, so where are all the maglev trains? Available at: https://www.androidpit.com/where-are-all-the-maglev-trains (accessed 1 July, 2019).

Meyer, J., Kain, J. and Wohl, M. (1965) *The Urban Transportation Problem.* Cambridge, MA: Harvard University Press.

Meyer, M.D. and Miller, E.J. (2001) *Urban Transportation Planning: A decision-oriented approach*. New York: McGraw Hill.

Ministry of Municipal and Rural Affairs, SA (2016) The National Report for 3rd UN Conference on Housing and Sustainable Urban Development (HABITAT III) for the Kingdom of Saudi Arabia Available at: http://habitat3.org/wp-content/uploads/Saudi-Arabia-National-Report.pdf.

Ministry of Transport, Saudi Arabia (2017) 'The daily traffic rate on the Kingdom's road network'. Available at: https://www.mot.gov.sa/Ar/MediaCenter/News/Pages/news780.aspx

MIT Hyperloop Team (2017) *MIT Hyperloop Final Report: An overview of the design, build, and testing process for MIT's entry in the SpaceX Hyperloop Competition 2015-2017*. Available at: http://web.mit.edu/mopg/www/papers/MITHyperloop_FinalReport_2017_public.pdf

MMUTIS Study Team (1999) *Metro Manila Urban Transportation Integration Study: Final report.* Department of Transportation and Communication, Republic of the Philippines.

Mokhim, M. (2015a) 'Maglev train'. Available at: https://www.slideshare.net/mokhim/maglev-46528538 (accessed 1 April 2015).

Mokhim, M. (2015b) Maglev Train (Train that floats in the air). Available at: https://www.slideshare.net/mokhim/maglev-train-train-that-floats-in-the-air.

Musk, E. (2013) 'Hyperloop alpha'. Available at: http://www.spacex.com/sites/spacex/files/hyperloop_alpha-20130812.pdf

Mustapha, B. and Bababe, A. (2017) 'Propulsion of magnetic levitation train'. *International Journal of Enhanced Research in Science, Technology & Engineering*, 5(12): 44-47.

MVA Consultancy (2009) *High-Speed Rail Development Programme 2008/9.* Final Report for Workstream 1. Available at: http://www.greengauge21.net/wp-content/uploads/PC_Workstream_1.pdf

Nalam, S., Medepalli, V. and Motukuri, R.S. (2018) 'Overview of Hyperloop: Transportation 5.0'. *Ultra High-Speed Ground Transportation Study*. Washington State Department of Transportation. Available at: https://wsdot.wa.gov/planning/studies/ultra-high-speed-travel/ground-transportation-study

Nash, C. (2010) 'Enhancing the cost benefit analysis of high speed rail'. In B.L. Pérez Henríquez and E. Deakin (eds), *High-Speed Rail and Sustainability: Decision-making and the political economy of investment*, chap. 11, pp. 163-184. New York: Routledge.

Nath, T. (2018) 'Hyperloop vs. high speed train: What's best for California?' Available at: https://www.investopedia.com/articles/investing/050815/elon-musks-hyperloop-economically-feasible.asp

Naufal, D.A.M. (2008) 'Maglev suspension systems'. Available at: http://emt18.blogspot.co.uk/2008/10/maglev-suspension-systems.html

Nuworsoo, C. (2009) 'Preliminaries to a feasibility analysis of the Maglev proposal of the Southern California Association of Governments for the region'. *Seed Grant Study*, California Polytechnic State University. San Bernardino, CA: Leonard Transportation Center.

OECD (2018) GDP long-term forecast. OECD Data online. Available at: https://data.oecd.org/gdp/gdp-long-term-forecast.htm

Office of National Statistics. (2018) *Regional Labour Market Statistics in the UK: February 2018.* Office of National Statistics.

Ogunbodede, E. and Ale, A. (2015) 'The regression model in the forecast of travel demand in Akure, Nigeria.' *Annals of the University of Oradea, Geography Series/Analele Universitatii din Oradea, Seria Geografie*, 25(2).

Opgenoord, M.M. and Caplan, P. (2017) 'On the Aerodynamic Design of the Hyperloop Concept'. *35th AIAA Applied Aerodynamics Conference,* June, Denver, CO.

Ortega-Hortelano, A.O. *et al.* (2016) 'Price elasticity of demand on the high-speed rail lines of Spain: Impact of the new pricing scheme'. *Transportation Research Record: Journal of the Transportation Research Board*, 2597, 90-98.

Ortega-Hortelano, A., Almujibah, H. and Preston, J. (2018) 'High speed railway in Saudi Arabia: Lessons to be learnt from the Spanish experience'. *International Congress on High-speed Rail: Technologies and Long Term Impacts,* pp. 511-529. June, Ciudad Real, Spain. Available at: http://eprints.soton.ac.uk/id/eprint/427162

Oum, T.H., Waters, W.G. and Yong, J.-S. (1992) 'Concepts of price elasticities of transport demand and recent empirical estimates: An interpretative survey'. *Journal of Transport Economics and Policy*, 26(2): 139-154.

Ozonder, G. and Miller, E.J. (2019) 'Analysis of activity location and trip mode choice: A study on hierarchical ordering.' *Procedia Computer Science*, 151, 739-744.

Pagliara, F. and Preston, J. (2013) 'An induced demand model for High Speed 1 in UK'. *Journal of Transportation Technologies*, 3(1), 44.

Pagliara, F. *et al.* (2016) 'An analysis of spatial equity concerning investments in high-speed rail systems: The case study of Italy', *Transport Problems*, 11(3), 55--68.

Pagliara, F., Hayashi, Y. and Ram, K.S. (2018) *Deriving Policies from Land Use-Transport interactions for Sustainable High-Speed Rail Development in Asia*. ADBI Institute. Available at: https://www.adb.org/sites/default/files/event/639626/files/adbi-pn-policies-land-use-transport-interactions-high-speed-rail-development-asia.pdf

Pagliara, F., Vassallo, J. and Román, C. (2012) 'High-speed rail versus air transportation: Case study of Madrid–Barcelona, Spain', *Transportation Research Record: Journal of the Transportation Research Board*, 2289, 10-17.

Palacin, R. *et al.* (2014) 'High speed rail trends, technologies and operational patterns: A comparison of established and emerging networks'. *Transport Problems*, 9(spec. issue), 123-129.

Pandey, N., Kumar, M. and Tiwari, P. (2016) 'Analysis of magnetic levitation and Maglev trains'. *IJISET - International Journal of Innovative Science, Engineering & Technology*, 3(12): 108-112.

Pandey, V. and Pallissery, S. (2017) 'Hyperloop, train of future*'. International Journal of Scientific & Engineering Research*, 8(2), 1-8. ISSN 2229-5518)

Park, C.-B., Lee, H.-W. and Lee, J. (2012) 'Performance analysis of the linear induction motor for the deep-underground high-speed GTX', *Journal of Electrical Engineering and Technology*, 7(2), 200-206.

Paulley, N. *et al.* (2006) 'The demand for public transport: The effects of fares, quality of service, income and car ownership'. *Transport Policy*, 13(4), 295-306.

Pearce, D., Ozdemiroglu, E. and Britain, G. (2002) *Economic valuation with stated preference techniques: summary guide*. Department for Transport, Local Government and the Regions London.

Pedro, M., Silva, J. and Abreu, D. (2014) 'A contextual analysis of the impacts of high speed rail on regional development and mobility'. *13th World Conference on Transport Research,* July, Lisbon.

Peers, J.B. and Bevilacqua, M., Alan M. Voorhees and Associates, Inc (1976) 'Structural travel demand models: An intercity application', *Transportation Research Record*, 569, 124-135.

Petrik, O., Silva, J.D.A.E. and Moura, F. (2016) 'Stated preference surveys in transport demand modeling: Disengagement of respondents'. *Transportation Letters*, 8(1), 13-25.

Pourreza, S. (2011) 'Economic analysis of high speed rail'. Trondheim: Norwegian University of Science and Technology.

PR Newswire (2016) Hyperloop transportation technologies reaches agreement with Slovakia. Available at: https://www.prnewswire.com/news-releases/hyperloop-transportation-technologies-reaches-agreement-with-slovakia-300234762.html (accessed 11 March 2016).

Preston, J. (2009) 'The case for high speed rail: A review of recent evidence', *Paper*, 9, p. 129. *RAC Foundation*. Available at: https://www.racfoundation.org/wp-content/uploads/2017/11/high-speed-rail-preston-301009-report.pdf

Preston, J. (2013) *The Economics of Investment in High-Speed Rail.* International Transport Forum, Discussion papers no. 30. Paris: OECD.

Preston, J. (2010) *The Case for High Speed Rail*. London: RAC Foundation.

Preston, J. (2015) 'Public transport demand'. In C. Nash (ed.), *Handbook of Research Methods and Applications in Transport Economics and Policy*, pp. 192–211. Cheltenham: Edward Elgar. doi:10.4337/9780857937933.00018

Preston, J. (2021) 'The total social cost (TSC) of public transport modes', in G. Currie (ed.), *Handbook of Public Transport Research*. Edward Elgar Publishing.

Profillidis, V.A. (2014) *Railway Management and Engineering*. Farnham, Surrey: Ashgate.

Rail Delivery Group (2011) *Passenger Demand Forecasting Handbook*. London: RDG. Available at: https://www.raildeliverygroup.com/pdfc.html

Railway Pro (2017) CRRC delivers new maglev trains for Changsha. *Railway Pro.* Available at: https://www.railwaypro.com/wp/crrc-delivers-new-maglev-trains-changsha/

Rail Travel Station (2019) 'Incheon Airport Maglev Line: Incheon International Airport Terminal 1 to Yongyu by Hyundai Rotem Ecobee Urban Maglev Train'.

Railway Technology (2019) 'CAF secures train maintenance contracts in Spain and Saudi Arabia'. Available at: https://www.railway-technology.com/news/caf-secures-train-maintenance-contracts-in-spain-and-saudi-arabia/

Railway Technology, Saudi Arabia (2008) ‘Haramain High-Speed Rail Project’. Available at: https://www.railway-technology.com/projects/haramain-high-speed/.

Ramachandran, V. (2013) 'Elon Musk reveals hyperloop transport system Alpha Design'. Available at: https://mashable.com/2013/08/12/elon-musk-hyperloop-reveal/?europe=true#Dv0W3ZPB0OqI

Ranger, S. (2018) 'Hyperloop technologies could revolutionise travel: Here's everything you need to know about the technology and the companies involved'. Available at: https://www.zdnet.com/article/what-is-hyperloop-everything-you-need-to-know-about-the-future-of-transport/

Rastogi, R. (2000) 'Stated preference survey: Experience from developing country'. Unpublished report, Department of Civil Engineering, Engineering College, KOTA Mumbai, India.

Ren, X. *et al.* (2020) 'Impact of high-speed rail on social equity in China: Evidence from a mode choice survey'. *Transportation Research Part A: Policy and Practice*, 138, 422-441.

Retzmann, M., Eiler, K., Klühspies, J. and Wiegand, D. (2011) 'The Moscow–Warsaw–Berlin project: A high-speed Maglev for long distance transport'. *21st International Conference on Magnetically Levitated Systems and Linear Drives*, October, Daejeon, Korea.

RF Wireless World (2015) *Advantages of Hyperloop Technology | Disadvantages of Hyperloop technology*. Available at: http://www.rfwireless-world.com/ Terminology/Advantages-and-Disadvantages-of-Hyperloop-Technology.html.

Richard, W. (2020) 'Heteroskedasticity', Lecture notes (sociology), pp. 2-3. University of Notre Dame, Notre Dame, IN.

Ristea, V. (2016) 'Global demand for high-speed rail'. BEng project, June, University of Southampton.

Rogers, M. and Duffy, A. (2012) *Engineering Project Appraisal*. John Wiley & Sons.

Roman, C., Espino, R. and Martín, J.C. (2010) 'Analyzing competition between the high speed train and alternative modes: The case of the Madrid-Zaragoza-Barcelona Corridor'. *Journal of Choice Modelling*, 3(1), 84-108.

Rose, C.R., Peterson, D.E. and Leung, E.M. (2008) 'Implementation of cargo MagLev in the United States'. *Maglev 2008: 20th International Conference on Maglev Systems and Drives*, December, San Diego, CA.

de Rus, G. (ed.) (2009) *Economic Analysis of High Speed Rail in Europe.* Bilbao: Fundacion BBVA.

de Rus, G. (2011) 'The BCA of HSR: Should the government invest in high speed rail infrastructure?' *Journal of Benefit-Cost Analysis*, 2(1), 1-28.

de Rus, G. (2012) *Economic analysis of high speed rail in Europe*. Fundacion BBVA.

de Rus, G. (2012a) *Economic Analysis of High Speed Rail in Europe.* Fundación BBVA.

de Rus, G. (2012b) 'Economic evaluation of the high speed rail', revised edition. *Expertgruppen för studier i offentlig ekonomi*. Available at: http://www.ems.expertgrupp.se/Uploads/Documents/HSR%20Sweden.pdf

de Rus, G. and Nombela, G. (2007) 'Is investment in high speed rail socially profitable?', *Journal of Transport Economics and Policy (JTEP)*, 41(1), 3-23.

Rutzen, B. and Walton, C.M. (2011) *High Speed Rail: A study of international best practices and identification of opportunities in the US*. Report no. SWUTC/11/476660-00071-1. Austin, TX: Center for Transportation Research.

Saat, M.R. and Barkan, C.P. (2019) 'Hazards associated with HSR operations adjacent to conventional tracks: Enhanced literature review part II: Draft Guidance Document'.

Sagar, Y. (2016) 'What are the advantages and disadvantages of Maglev trains?' Available at: https://www.quora.com/What-are-the-advantages-and-disadvantages-of-Maglev-trains

SANDAG (2006) *SANDAG Maglev Study Phase 1*. Available at: https://www.sandag.org/programs/transportation/comprehensive_transportation_projects/Maglev/2006_maglev_reduced.pdf.

Sanko, N. (2001) 'Guidelines for stated preference experiment design', Master of Business Administration dissertation., Ecole Nationale des Ponts et Chaussées.

Sato, Y. (2014) 'JR-Central's Chuo Maglev project approved'. Available at: https://www.railjournal.com/passenger/high-speed/jr-centrals-chuo-maglev-project-approved/.

Schonig, M. (2019) 'Maglev and Hyperloop – 5 years on.' Available at: https://skedgo.com/maglev-and-hyperloop-5-years-on/ (accessed 11 June 2019).

Sekhar, C. (2014) 'Mode choice analysis: The data, the models and future ahead', *International Journal for Traffic & Transport Engineering*, 4(3).

Seltman, H. (2012) 'Approximations for mean and variance of a ratio'. Unpublished note.

Seminarsonly (2009) Transrapid claims to use a quarter less power at 200 km/h than the InterCityExpress (7 September 2009). Available at: http://www.123seminarsonly.com/Seminar-Reports/025/33400940-Maglev.pdf.

Sergeroux (2016) Hyperloop Passenger Station. Available at: http://dev.sergeroux.com/portfolio/hyperloop-passenger-station/.

Shaik, A. (2018) Magnetic Train. Available at: http://www.physics-and-radio-electronics.com/blog/magnetictrain-maglevtrain/.

Sharma, R.C. *et al.* (2014) 'Magnetically levitated vehicles: Suspension, propulsion and guidance'. *International Journal of Engineering Research & Technology*, 3(11), 5-8.

Simon, M. and Choi, S. (2017) Hyperloop One Announces 10 Winners for Hyperloop One Global Challenge. Available at: https://hyperloop-one.com/sites/default/files/press-releases/2017-09/H1GC%20Winners%20Press%20Release.pdf

Small, K.A., Verhoef, E.T. and Lindsey, R. (2007) *The Economics of Urban Transportat*ion. Abingdon: Routledge.

Smith, R. (2017) 'Shanghai's 430kph train benefits wider economy.' Available at: https://www.thenational.ae/business/shanghai-s-430kph-train-benefits-wider-economy-1.10451.

Stansfield, A. (2018) 'HSGT Systems: HSR, Maglev and Hyperloop'. Permanent Way Institution. *The Journal,* October(136) Pt 4.

Stata Software (2019) Asclogit - Alternative-specific conditional logit (McFadden's choice) model. Available at: https://www.stata.com/manuals13/rasclogit.pdf.

Statista (2020) 'Saudi Arabia: Do you have access to a car?' Available at: https://www.statista.com/statistics/915013/saudi-arabia-access-to-cars/.

Statistics Bureau (2016) *Statistical Handbook of Japan 2016*. Tokyo: Statistics Bureau.

Stiles, D.C. (1998) *High-Speed Ground Transportation: Federal and State role in research, development and deployment.* Washington: American Society of Civil Engineers. Available at: http://www.wise-intern.org/journal98/ STILES.PDF

Tabeta, S. (2020) 'China looks to build new maglev rail line to boost economy'. Available at: https://asia.nikkei.com/Business/Transportation/China-looks-to-build-new-maglev-rail-line-to-boost-economy (accessed 17 April 2020).

Tang, S., Boyles, S.D. and Jiang, N. (2015) 'High-speed rail cost recovery time based on an integer optimization model'. *Journal of Advanced Transportation*, 49(5), 634-647.

Taylor, C.L., Hyde, D.J. and Barr, L.C. (2016) *Hyperloop Commercial Feasibility Analysis: High level overview*. Cleveland, OH: John A. Volpe National Transportation System Center.

Taylor, M. (2014) 'California economic activity'. Available at: http://www.lao.ca.gov/reports/2014/calfacts/calfacts-2014.pdf

Temple-ERM (2013) *High Speed Rail: Consultation on the route from the West Midlands to Manchester, Leeds and beyond Sustainability Statement*

Thorstrand, A. (2020) 'Maglev deployment in winter climate'.

Toumi, H. (2018) 'New speed limits on Saudi highways.' *Gulf News,* 18 February. Available at: https://gulfnews.com/world/gulf/saudi/new-speed-limits-on-saudi-highways-1.2175248 (accessed 18 February 2018).

Tracy, A. (2020) China completes test run of self-developed maglev train prototype that can travel at 372 miles per hour (the equivalent of London to Paris in 49 minutes). Daily Mail Available at: https://www.dailymail.co.uk/news/article-8455279/China-completes-test-run-self-developed-maglev-train-travel-372-miles-hour.html.

Trading Economics, Saudi Arabia. (2020) Gasoline prices. Available at: https://tradingeconomics.com/country-list/gasoline-prices

Train. (2011) 'Propulsion system', in *Maglev Train technical paper*. Available at: www.newtechpapers.com.

Transrapid International (2002) *High-Tech for Flying on the Ground : Maglev System Transrapid*. Presentation by Transrapid. Available at: https://www.ncl.ac.uk/media/wwwnclacuk/pressoffice/files/pressreleaseslegacy/TRI_Flug_Hoehe_e_5_021.pdf

Tsai, C.-H.P., Mulley, C. and Clifton, G. (2014) 'Forecasting public transport demand for the Sydney Greater Metropolitan Area: A comparison of univariate and multivariate methods', *Road & Transport Research: A Journal of Australian and New Zealand Research and Practice*, 23(1), 51.

Tsekeris, T. and Tsekeris, C. (2011) 'Demand forecasting in transport: Overview and modeling advances'. *Economic Research-Ekonomska istraživanja*, 24(1), 82-94.

Twaddle, H. (2011) 'Stated preference survey design and pre-test for valuing influencing factors for bicycle use'. Master's dissertation, Institute of Transportation, Munich.

Tweeten, L. (2019) *Agricultural Policy Analysis Tools for Economic Development.* New York: Routledge.

UIC, HSR. (2010a) International system summary: China. Available at: https://ftp.dot.state.tx.us/pub/txdot-info/rail/high_speed/system-summaries/china.pdf.

UIC, HSR. (2010b) 'International system summary: France'. Available at: https://ftp.dot.state.tx.us/pub/txdot-info/rail/high_speed/system-summaries/france.pdf.

UIC, HSR. (2010c) International system summary: Germany. Available at: https://ftp.dot.state.tx.us/pub/txdot-info/rail/high_speed/system-summaries/germany.pdf.

UIC, HSR. (2010d) 'International system summary: Italy'. Available at: https://ftp.txdot.gov/pub/txdot-info/rail/high_speed/system-summaries/italy.pdf

UIC, HSR. (2010e) International system summary: Saudi Arabia. Available at: https://ftp.txdot.gov/pub/txdot-info/rail/high_speed/system-summaries/saudi-arabia.pdf.

UIC, HSR. (2010f) International system summary: Spain. Available at: https://ftp.dot.state.tx.us/pub/txdot-info/rail/high_speed/system-summaries/spain.pdf.

UIC, HSR. (2010g) International system summary: United Kingdom. Available at: https://ftp.dot.state.tx.us/pub/txdot-info/rail/high_speed/system-summaries/united-kingdom.pdf.

UIC, HSR. (2017) International system summary: Japan. Available at: https://ftp.dot.state.tx.us/pub/txdot-info/rail/high_speed/system-summaries/japan.pdf.

UIC, HSR. (2020a) 'High speed lines in the world'. Available at: https://uic.org/IMG/pdf/20171101_high_speed_lines_in_the_world.pdf

UIC, HSR. (2020b) 'High speed traffic in the world'. Available at: https://uic.org/IMG/pdf/20200127_high_speed_passenger_km.pdf.

UIC, HSR. (2020c) Map of HSR lines, available at. https://uic.org/passenger/highspeed/article/high-speed-database-maps

Upbin, B. (2016) What advantages does a hyperloop offer over a high-speed rail? Available at: https://www.quora.com/What-advantages-does-a-hyperloop-offer-over-a-high-speed-rail.

de Ureña, J.M. (2016) *Territorial Implications of High Speed Rail: A Spanish perspective.* Aldershot: Routledge.

US Commercial Service. (2015) *Doing Business in Saudi Arabia: 2015 Country Commercial Guide for US Companies* Available at: https://photos.state.gov/libraries/saudi-arabia/231771/public/2015%20CCG%20Saudi%20Arabia.pdf

Van Goeverden, K. *et al.* (2018) 'Analysis and modelling of performances of the HL (Hyperloop) transport system'. *European Transport Research Review*, 10(2), 41.

Vansteenwegen, P. and Vanoudheusden, D. (2007) 'Decreasing the passenger waiting time for an intercity rail network'. *Transportation Research Part B: Methodological*, 41(4), 478-492.

Vikannanda, M. (2018) 'Economic feasibility analysis of Indonesia high speed rail'. Master dissertation, University of Southampton.

Virgin Hyperloop One (2018) Estimating Travel Times for Los Angeles–San Francisco Route, USA. Available at: https://hyperloop-one.com/route-estimator/los-angeles-us/san-francisco-us/travel-times.

Vuchic, V.R. (2005) *Urban Transit: Operations, Planning, and Economics 2005.* Hoboken, NJ: Wiley.

Vuchic, V.R. and Casello, J.M. (2002) 'An evaluation of maglev technology and its comparison with high speed rail'. *Transportation Quarterly*, 56(2), 33.

Vyas, A.D. and Rote, D.M. (1993) 'Market and energy demand analysis of a US maglev system'. *12th International Conferencguidancee on Magnetically Levitated Systems and Linear Drives*, April, Argonne, IL, US.

Walker, R. (2018) 'Hyperloop: Cutting through the Hype'. Wokingham: TRL. ISBN: 9781912433438 Available at: https://trl.co.uk/uploads/trl/documents/ACA003-Hyperloop.pdf

Wallis, I. (2003) *Review of Passenger Transport Demand Elasticities.* Transfund report no. 248. Wellington, NZ: Booz Allen Hamilton Ltd. https://www.nzta.govt.nz/assets/resources/research/reports/248/248-Review-of-passenger-transport-demand-elasticities.pdf

Walsh, N. (2018) 'The world's first commercial hyperloop is coming to Abu Dhabi in 2020.' Available at: https://www.archdaily.com/893006/the-worlds-first-commercial-hyperloop-is-coming-to-abu-dhabi-in-2020.

Wang, Y. *et al.* (2014) 'Modeling traveler mode choice behavior of a new high-speed rail corridor in China.' *Transportation Planning and Technology*, 37(5), 466-483.

Wardman, M. (2004) 'Public transport values of time', *Transport Policy*, 11(4), 363-377.

Wayson, R. and Bowlby, W. (1989) 'Noise and air pollution of high-speed rail systems'. *Journal of Transportation Engineering*, 115(1), 20-36.

Westin, J. and Kågeson, P. (2012) 'Can high speed rail offset its embedded emissions?', *Transportation Research Part D: Transport and Environment*, 17(1), 1-7.

White, P.R. (2016) *Public Transport: Its planning, management and operation.* Natural and Built Environment Series. London: Taylor & Francis.

Wilson, C. (2015) *Maglev: Magnetic Levitating Trains.* Available at: https://sites.tufts.edu/eeseniordesignhandbook/2015/maglev-magnetic-levitating-trains/.

Wong, M. (2018) 'Hyperloop, the superfast "vacuum train," is coming to China'. Available at: https://edition.cnn.com/travel/article/first-hyperloop-in-guizhou-china/index.html.

World Bank (2020a) 'International tourism, number of arrivals - Saudi Arabia'. Available at: https://data.worldbank.org/indicator/ST.INT.ARVL?locations=SA.

World Bank (2020b) 'Saudi Arabia'. World Bank. Available at: https://data.worldbank.org/country/saudi-arabia

WSDOT (2019) Ultra-High-Speed Ground Transportation business case analysis. Available at: https://wsdot.wa.gov/sites/default/files/2019/07/12/Ultra-High-Speed-Ground-Transportation-Study-Business-Case-Analysis-Executive-Summary-2019.pdf.

Wu, H.-S. (2011) Categorical Data Analysis. Available at: https://www.bgsu.edu/content/dam/BGSU/college-of-arts-and-sciences/center-for-family-and-demographic-research/documents/Workshops/2011-workshop-Categorical-Data-Analysis-Using-SAS-and-Stata.pdf (accessed 7 November 2011).

Xinhua (2006) 'Flawed battery likely cause of Shanghai Maglev fire'. Available at: http://www.chinadaily.com.cn/china/2006-08/21/content_669554.htm (accessed 21 August 2006).

Yadav, M. *et al.* (2013) 'Review of magnetic levitation (maglev): A technology to propel vehicles with magnets'. *Global Journal of Research in Engineering*.

Yadav, M., Mehta, N., Gupta, A., Chaudhary, A. and Mahindru, D.V. (2013) 'Review of magnetic levitation (maglev): A technology to propel vehicles with magnets.' *Global Journal of Research in Engineering*, 13(7).

Yaghoubi, H., Barazi, N. and Aoliaei, M.R. (2012) 'Maglev'. In X. Perpinya (ed.), *Infrastructure Design, Signalling and Security in Railway*. InTech. DOI: 10.5772/35339. Available from: https://www.intechopen.com/books/ infrastructure-design-signalling-and-security-in-railway/maglev

Yao, E. and Morikawa, T. (2005) 'A study of an integrated intercity travel demand model'. *Transportation Research part A: Policy and Practice*, 39(4), 367-381.

Yao, E., Yang, Q., Zhang, .and Sun, X. (2013) 'A study on high-speed rail pricing strategy in the context of modes competition'. *Discrete Dynamics in Nature and Society*, online. Available at: https://doi.org/10.1155/2013/715256

Yasuda, Y. *et al.* (2004) 'The first HSST maglev commercial train in Japan'. *Proceedings of 18th International Conference on Magnetically Levitated Systems and Linear Drives (MAGLEV 2004)*. Citeseer.

Zhou, D. *et al.* (2010) 'Review of coupled vibration problems in EMS maglev vehicles', *International Journal of Acoustics and Vibration*, 15(1), 10.

Zhang, D. *et al.* (2019) 'Induced travel demand modeling for high-speed intercity transportation', *Transportation Research Record*, 2673(3), 189-198.

Zhuang, J. *et al.* (2007) 'Theory and practice in the choice of social discount rate for cost-benefit analysis: A survey'.

Zhuang, J., Liang, Z., Lin, T. and de Guzman, F. (2007) 'Theory and practice in the choice of social discount rate for cost-benefit analysis: A survey'. *ERD Working Paper,* series 94. Asian Development Bank. Available at: https://www.adb.org/sites/default/files/publication/28360/wp094.pdf

Ziemke, D. (2010) Comparison of high-speed rail systems of the United States. Georgia Institute of Technology. Doctoral dissertation, Georgia Institute of Technology. Available at: https://smartech.gatech.edu/bitstream/handle/1853/37286/ziemke_dominik 201012_ mast.pdf.

Zschoche, F., Bente, H. and Schilling, M. (2013) 'Further development of the European High Speed Rail Network'. Available at: https://civity.de/asset/en/sites/2/2018/05/civity_dev_eu_hsr_network_012014.pdf

# APPENDICES

Appendix A: Spreadsheet Cost Model Interface

The Spreadsheet Cost Model developed in this thesis aims to evaluate the total and average social cost of various public transport technologies (HSR, Maglev and Hyperloop). It is considered as a mathematical model, and it was created in Microsoft Excel. A screenshot of the model for years 2030, 2040 and 2050 is shown below:

| | 2030 | | |
|---|---|---|---|
| | **HSR** | **Maglev** | **Hyperloop** |
| Days per year | 365 | 365 | 365 |
| Round trip | 2 | 2 | 2 |
| Operating hours per day | 18 | 18 | 18 |
| Load factor | 90% | 72% | 87% |
| Train capacity | 604 | 449 | 28 |
| Effective occupation | 544 | 323 | 24 |
| Annual demand initial | 7,522,552 | 9,797,372 | 4,232,021 |
| Per day, Initial Year (t=5) | 10,305 | 13,421 | 5,797 |
| Number of service per day-direction | 19 | 42 | 238 |
| Service frequency per hour | 1.05 | 2.31 | **13.22** |
| Length of line | 412 | 412 | 412 |
| Operating speed | 300 | 400 | 1000 |
| Train turn around time | 3.41 | 2.73 | 1.49 |
| Value to the risk of failing | 1.5 | 1.5 | 1.5 |
| Number of acquired trains | 5 | 9 | **30** |
| Construction unit cost | 26,600,000 | 35,839,676 | 10,522,275 |
| Proportion cost on planning | 10% | 10% | 10% |
| Maintenance unit cost | 35,500 | 14,694 | 17,019 |
| Construction period | 5 | 5 | 5 |
| Cycle time | 35 | 35 | 35 |
| The social distant rate | 3.0% | 3.0% | 3.0% |
| Infrastructure Construction Cost | 12,055,120,000 | 16,242,541,163 | 4,768,695,030 |
| capital recovery factor | 0.05 | 0.05 | 0.05 |
| Annual Infrastructure construction cost | 561,036,745 | 755,916,359 | 221,931,688 |
| Infrastructure maintenance cost | 14,626,000 | 6,053,928 | 7,011,828 |
| Total infrastructure construction and maintenance costs | 575,662,745 | 761,970,287 | 228,943,516 |
| Unit cost of acquiring a train | 45,000 | 58,816 | 55,456 |
| Rolling Stock Acquisition Cost | 6,820,710 | 11,593,653 | **2,136,355** |
| Average unit cost of operating a rolling stock | 0.133 | 0.116 | 0.046 |
| Rolling stock operating cost | 111,539 | 158,375 | **22,451** |
| Unit cost of maintaining a rolling stock | 0.0124 | 0.0131 | 0.0006 |
| Average utilization of a train | 500,000 | 500,000 | 500,000 |
| Rolling Stock maintenance cost | 20,192,448 | 27,742,548 | **252,467** |
| **Total Operator Costs (€/year)** | **602,787,441** | **801,464,863** | **231,354,789** |
| Average access/egress distance for both statios (km) | 24.9 | 24.9 | 24.9 |
| Average access/egress travel speed (km/h) | 45 | 45 | 45 |
| Passenger demand in the time period t (passenger / year-direction) | 3,761,276 | 4,898,686 | 4,148,611 |
| Averge Access/Egress Time | 0.55 | 0.55 | 0.55 |
| The total annual passenger access/egress time (hours) | 4,156,907 | 5,388,555 | 4,563,472 |
| In-vehicle time (hour) | 1.37 | 1.03 | 0.41 |
| The total annual passenger's in-vehicle time (hours) | 5,165,486 | 5,045,647 | 1,709,228 |
| Average waiting time (hour) | 0.500 | 0.250 | 0.010 |
| The total annual passenger's waiting time (hours) | 1,880,638 | 1,224,672 | 105,801 |
| Average monthly wage rate | 1,395 | 1,395 | 1,395 |
| Working hours per week | 40 | 40 | 40 |
| Working hours per month | 160 | 160 | 160 |
| Average hourly wage rate | 8.72 | 8.72 | 8.72 |
| Value of time for business travellers | 11.60 | 11.60 | 11.60 |
| Value of time for commuting travellers | 5.82 | 5.82 | 5.82 |
| Weighting perception of aacess/egress time WRT in-vehicle time | 2 | 2 | 2 |
| Weighting perception of waiting time WRT in-vehicle time | 3 | 3 | 3 |
| Average of value of time | 8.71 | 8.71 | 8.71 |
| **Total User Costs (€/year)** | **166,463,004** | **169,732,485** | **50,879,615** |
| Unit air pollution costs per vehicle-kilometre (UK) | 0.368 | 0.00 | 0.00 |
| Unit air pollution costs per vehicle-kilometre (Saudi Arabia) | 0.35916 | 0.00 | 0.00 |
| Total passenger-kilomtre | 3,099,291 | 4,036,517 | 1,743,593 |
| Average air pollution cost (€/year) | 1,113,145 | 0.00 | 0.00 |
| Unit noise costs per vehicle-kilometre (UK) | 0.01803 | 0.00 | 0.00 |
| Unit noise costs per vehicle-kilometre (Saudi Arabia) | 0.01760 | 0.00 | 0.00 |
| Average noise pollution cost (€/year) | 54,550 | 0.00 | 0.00 |
| Unit accident costs per vehicle-kilometre (UK) | 1.34 | 1.34 | 1.34 |
| Unit accident costs per vehicle-kilometre (Saudi Arabia) | 1.30782 | 1.30782 | 1.30782 |
| Average accident cost (€/year) | 4,053,301 | 5,279,019 | **2,280,297** |
| Unit climate change costs per vehicle-kilometre (UK) | 0.824 | 0.000011 | 0.000011 |
| Unit climate change costs per vehicle-kilometre (Saudi Arabia) | 0.80421 | 1.20 | 1.20 |
| Average climate change cost (€/year) | 2,492,477 | 4,843,821 | **2,092,311** |
| **Total External costs (€/year)** | **7,713,473** | **10,122,840** | **4,372,609** |
| **Total social costs (€/year)** | **776,963,918** | **981,320,187** | **286,607,012** |
| **Average social costs (€/year)** | **103.3** | **100.2** | **67.7** |

| | 2040 | | |
|---|---|---|---|
| | **HSR** | **Maglev** | **Hyperloop** |
| Days per year | 365 | 365 | 365 |
| Round trip | 2 | 2 | 2 |
| Operating hours per day | 18 | 18 | 18 |
| Load factor | 90% | 72% | 87% |
| Train capacity | 604 | 449 | 28 |
| Effective occupation | 544 | 323 | 24 |
| Annual demand initial | 10,432,991 | 13,587,928 | 5,869,370 |
| Per day, Initial Year (t=5) | 14,292 | 18,614 | 8,040 |
| Number of service per day-direction | 26 | 58 | 330 |
| Service frequency per hour | 1.46 | 3.20 | **18.34** |
| Length of line | 412 | 412 | 412 |
| Operating speed | 300 | 400 | 1000 |
| Train turn around time | 3.41 | 2.73 | 1.49 |
| Value to the risk of failing | 1.5 | 1.5 | 1.5 |
| Number of acquired trains | 7 | 13 | **41** |
| Construction unit cost | 26,600,000 | 35,839,676 | 10,522,275 |
| Proportion cost on planning | 10% | 10% | 10% |
| Maintenance unit cost | 35,500 | 14,694 | 17,019 |
| Construction period | 5 | 5 | 5 |
| Cycle time | 35 | 35 | 35 |
| The social distant rate | 3.0% | 3.0% | 3.0% |
| Infrastructure Construction Cost | 12,055,120,000 | 16,242,541,163 | 4,768,695,030 |
| capital recovery factor | 0.05 | 0.05 | 0.05 |
| Annual Infrastructure construction cost | 561,036,745 | 755,916,359 | 221,931,688 |
| Infrastructure maintenance cost | 14,626,000 | 6,053,928 | 7,011,828 |
| Total infrastructure construction and maintenance costs | 575,662,745 | 761,970,287 | 228,943,516 |
| Unit cost of acquiring a train | 45,000 | 58,816 | 55,456 |
| Rolling Stock Acquisition Cost | 9,459,609 | **15,947,081** | **2,962,900** |
| Average unit cost of operating a rolling stock | 0.133 | 0.116 | 0.046 |
| Rolling stock operating cost | 154,693 | **217,845** | **31,137** |
| Unit cost of maintaining a rolling stock | 0.0124 | 0.0131 | 0.0006 |
| Average utilization of a train | 500,000 | 500,000 | 500,000 |
| Rolling Stock maintenance cost | 28,004,809 | 38,476,006 | **350,145** |
| **Total Operator Costs (€/year)** | **639,733,840** | **816,745,124** | **232,287,699** |
| Average access/egress distance for both statios (km) | 24.9 | 24.9 | 24.9 |
| Average access/egress travel speed (km/h) | 45 | 45 | 45 |
| Passenger demand in the time period t (passenger / year-direction) | 5,216,496 | 6,738,148 | 9,767,695 |
| Averge Access/Egress Time | 0.55 | 0.55 | 0.55 |
| The total annual passenger access/egress time (hours) | 5,765,194 | 7,411,962 | 10,744,464 |
| In-vehicle time (hour) | 1.37 | 1.03 | 0.41 |
| The total annual passenger's in-vehicle time (hours) | 7,163,987 | 6,940,292 | 4,024,290 |
| Average waiting time (hour) | 0.250 | 0.100 | 0.010 |
| The total annual passenger's waiting time (hours) | 1,304,124 | 673,815 | 29,347 |
| Average monthly wage rate | 1,395 | 1,395 | 1,395 |
| Working hours per week | 40 | 40 | 40 |
| Working hours per month | 160 | 160 | 160 |
| Average hourly wage rate | 8.72 | 8.72 | 8.72 |
| Value of time for business travellers | 11.60 | 11.60 | 11.60 |
| Value of time for commuting travellers | 5.82 | 5.82 | 5.82 |
| Weighting perception of aacess/egress time WRT in-vehicle time | 2 | 2 | 2 |
| Weighting perception of waiting time WRT in-vehicle time | 3 | 3 | 3 |
| Average of value of time | 8.71 | 8.71 | 8.71 |
| **Total User Costs (€/year)** | **196,806,912** | **207,070,157** | **67,498,886** |
| Unit air pollution costs per vehicle-kilometre (UK) | 0.368 | 0.00 | 0.00 |
| Unit air pollution costs per vehicle-kilometre (Saudi Arabia) | 0.35916 | 0.00 | 0.00 |
| Total passenger-kilomtre | 4,298,392 | 5,552,234 | 2,418,180 |
| Average air pollution cost (€/year) | **1,543,816** | **0.00** | **0.00** |
| Unit noise costs per vehicle-kilometre (UK) | 0.01803 | 0.00 | 0.00 |
| Unit noise costs per vehicle-kilometre (Saudi Arabia) | 0.01760 | 0.00 | 0.00 |
| Average noise pollution cost (€/year) | **75,655** | **0.00** | **0.00** |
| Unit accident costs per vehicle-kilometre (UK) | 1.34 | 1.34 | 1.34 |
| Unit accident costs per vehicle-kilometre (Saudi Arabia) | 1.30782 | 1.30782 | 1.30782 |
| Average accident cost (€/year) | **5,621,503** | **7,261,296** | **3,162,533** |
| Unit climate change costs per vehicle-kilometre (UK) | 0.824 | 0.00 | 0 |
| Unit climate change costs per vehicle-kilometre (Saudi Arabia) | 0.80421 | 1.20 | 1.20 |
| Average climate change cost (€/year) | **3,456,805** | **6,662,680** | **2,901,817** |
| **Total External costs (€/year)** | **10,697,779** | **13,923,976** | **6,064,350** |
| **Total social costs (€/year)** | **847,238,531** | **1,037,739,257** | **305,850,934** |
| **Average social costs (€/year)** | **81.2** | **76.4** | **52.1** |

| | 2050 | | |
|---|---|---|---|
| | **HSR** | **Maglev** | **Hyperloop** |
| Days per year | 365 | 365 | 365 |
| Round trip | 2 | 2 | 2 |
| Operating hours per day | 18 | 18 | 18 |
| Load factor | 90% | 72% | 87% |
| Train capacity | 604 | 449 | 28 |
| Effective occupation | 544 | 323 | 24 |
| Annual demand initial | 13,353,471 | 17,391,561 | 7,512,367 |
| Per day, Initial Year (t=5) | 18,292 | 23,824 | 10,291 |
| Number of service per day-direction | 34 | 73 | 422 |
| Service frequency per hour | 1.87 | **4.06** | **23.47** |
| Length of line | 412 | 412 | 412 |
| Operating speed | 300 | 400 | 1000 |
| Train turn around time | 3.41 | 2.73 | 1.49 |
| Value to the risk of failing | 1.5 | 1.5 | 1.5 |
| Number of acquired trains | 10 | 17 | **52** |
| Construction unit cost | 26,600,000 | 35,839,676 | 10,522,275 |
| Proportion cost on planning | 10% | 10% | 10% |
| Maintenance unit cost | 35,500 | 14,694 | 17,019 |
| Construction period | 5 | 5 | 5 |
| Cycle time | 35 | 35 | 35 |
| The social distant rate | 3.0% | 3.0% | 3.0% |
| Infrastructure Construction Cost | 12,055,120,000 | 16,242,541,163 | 4,768,695,030 |
| capital recovery factor | 0.05 | 0.05 | 0.05 |
| Annual Infrastructure construction cost | 561,036,745 | 755,916,359 | 221,931,688 |
| Infrastructure maintenance cost | 14,626,000 | 6,053,928 | 7,011,828 |
| Total infrastructure construction and maintenance costs | 575,662,745 | 761,970,287 | 228,943,516 |
| Unit cost of acquiring a train | 45,000 | 58,816 | 55,456 |
| Rolling Stock Acquisition Cost | 12,107,613 | 20,580,185 | **3,792,297** |
| Average unit cost of operating a rolling stock | 0.133 | 0.116 | 0.046 |
| Rolling stock operating cost | 197,995 | **278,826** | **39,854** |
| Unit cost of maintaining a rolling stock | 0.0124 | 0.0131 | 0.0006 |
| Average utilization of a train | 500,000 | 500,000 | 500,000 |
| Rolling Stock maintenance cost | 35,844,122 | **48,841,904** | **448,161** |
| **Total Operator Costs (€/year)** | **657,106,129** | **831,502,123** | **233,223,827** |
| Average access/egress distance for both statios (km) | 24.9 | 24.9 | 24.9 |
| Average access/egress travel speed (km/h) | 45 | 45 | 45 |
| Passenger demand in the time period t (passenger / year-direction) | 6,676,736 | 8,624,340 | 3,756,184 |
| Averge Access/Egress Time | 0.55 | 0.55 | 0.55 |
| The total annual passenger access/egress time (hours) | 7,379,029 | 9,486,773 | 4,131,802 |
| In-vehicle time (hour) | 1.37 | 1.03 | 0.41 |
| The total annual passenger's in-vehicle time (hours) | 9,169,383 | 8,883,070 | 1,547,548 |
| Average waiting time (hour) | 0.500 | 0.075 | 0.025 |
| The total annual passenger's waiting time (hours) | 3,338,368 | 646,825 | 93,905 |
| Average monthly wage rate | 1,395 | 1,395 | 1,395 |
| Working hours per week | 40 | 40 | 40 |
| Working hours per month | 160 | 160 | 160 |
| Average hourly wage rate | 8.72 | 8.72 | 8.72 |
| Value of time for business travellers | 11.60 | 11.60 | 11.60 |
| Value of time for commuting travellers | 5.82 | 5.82 | 5.82 |
| Weighting perception of aacess/egress time WRT in-vehicle time | 2 | 2 | 2 |
| Weighting perception of waiting time WRT in-vehicle time | 3 | 3 | 3 |
| Average of value of time | 8.71 | 8.71 | 8.71 |
| **Total User Costs (€/year)** | **295,492,659** | **259,403,714** | **87,865,174** |
| Unit air pollution costs per vehicle-kilometre (UK) | 0.368 | 0.00 | 0.00 |
| Unit air pollution costs per vehicle-kilometre (Saudi Arabia) | 0.35916 | 0.00 | 0.00 |
| Total passenger-kilomtre | 5,501,630 | 7,106,456 | 3,095,095 |
| Average air pollution cost (€/year) | **1,975,972** | **0.00** | **0.00** |
| Unit noise costs per vehicle-kilometre (UK) | 0.01803 | 0.00 | 0.00 |
| Unit noise costs per vehicle-kilometre (Saudi Arabia) | 0.01760 | 0.00 | 0.00 |
| Average noise pollution cost (€/year) | **96,833** | **0.00** | **0.00** |
| Unit accident costs per vehicle-kilometre (UK) | 1.34 | 1.34 | 1.34 |
| Unit accident costs per vehicle-kilometre (Saudi Arabia) | 1.30782 | 1.30782 | 1.30782 |
| Average accident cost (€/year) | **7,195,116** | **9,293,931** | **4,047,813** |
| Unit climate change costs per vehicle-kilometre (UK) | 0.824 | 0.00 | 0 |
| Unit climate change costs per vehicle-kilometre (Saudi Arabia) | 0.80421 | 1.20 | 1.20 |
| Average climate change cost (€/year) | **4,424,459** | **8,527,747** | **3,714,114** |
| **Total External costs (€/year)** | **13,692,380** | **17,821,678** | **7,761,927** |
| **Total social costs (€/year)** | **966,291,169** | **1,108,727,516** | **328,850,929** |
| **Average social costs (€/year)** | **72.4** | **63.8** | **43.8** |

Appendix B: Public Transport Authority's Approval letter


هيئة النقل العام
PUBLIC TRANSPORT AUTHORITY
مكتب الرئيس
٢١٧

**To: Ethics Committee at University of Southampton,**

**Name of student:** Hamad Raja Almujibah

**Thesis title:** A Comparative Assessment for Intercity Transport Technologies: A Saudi Arabian Case Study.

The Saudi Arabian Transport Authority reports that it is pleased to support the application of the PhD student named above to carry out a field study of Saudi Arabian railways. This research will be undertaken as part of the student's doctoral studies at the University of Southampton, UK.

He will be given permission to collect data through questionnaires with railway passengers, involving surveys at stations and on-trains and interviews at the Authority's offices. It is understood that the information he will obtain will be kept as highly confidential and used purely for academic purpose and that his research protocols have been through the University of Southampton's ethics processes.

The Authority will also collaborate with the research in terms of providing relevant technical documents and data.

Please feel free to contact me if you require any further information

Yours sincerely,

**DR. Rumaih M . Al-Rumaih**

**President**

**Public Transport Authority**

Kingdom of Saudi Arabia P.O.Box 87078 Riyadh 11642
Head Office : +966 11 826 1111 Fax: +966 11 826 1199

المملكة العربية السعودية ص.ب ٨٧٠٧٨ الرياض ١١٦٤٢
هاتف : ٩٦٦١١٨٢٦١١١١+ فاكس: ٩٦٦١١٨٢٦١١٩٩+

www.pta.gov.sa

Appendix C: Approval Letter by Faculty Ethics Committee

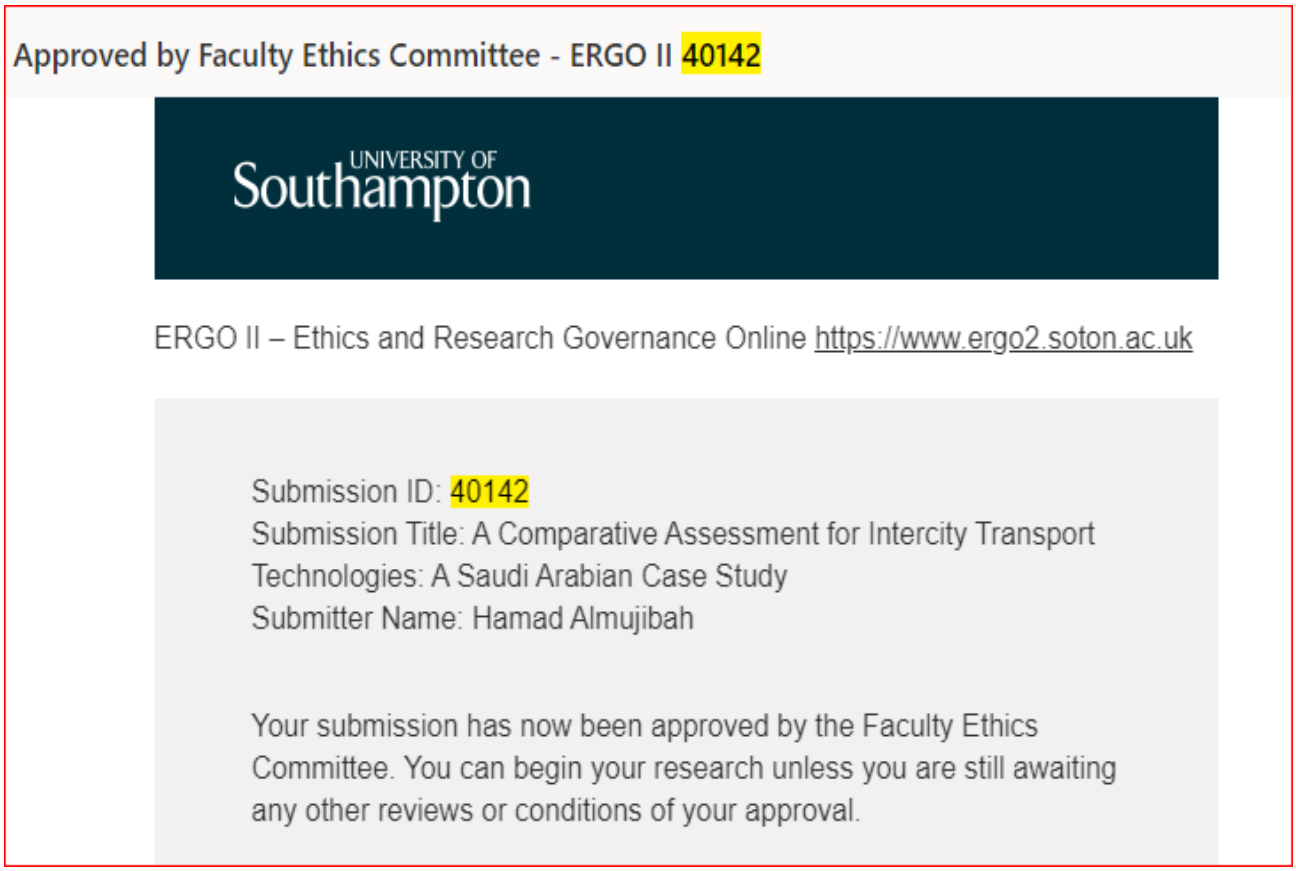

Approved by Faculty Ethics Committee - ERGO II 40142

University of Southampton

ERGO II – Ethics and Research Governance Online https://www.ergo2.soton.ac.uk

Submission ID: 40142
Submission Title: A Comparative Assessment for Intercity Transport Technologies: A Saudi Arabian Case Study
Submitter Name: Hamad Almujibah

Your submission has now been approved by the Faculty Ethics Committee. You can begin your research unless you are still awaiting any other reviews or conditions of your approval.

Appendix D: Questionnaires of Experiment 1

## Questionnaire 1 (Experiment 1)

Part 1: Your Journey

Firstly, we would like to know about the journey you are making today

**1-** Where are you traveling from and to on this journey?

From:

- □ Riyadh
- □ Dammam
- □ Other, Please specify_____

To:

- □ Riyadh
- □ Dammam
- □ Other, Please specify_____

**2-** What is the main purpose of your journey? (Please tick one box only)

- □ Commuting to/from work
- □ Commuting for education (to/from college/school/university)
- □ Visiting friends or relatives
- □ On company business (or own if self-employed)
- □ On personal business (e.g. job interview, hospital's appointment, etc.)
- □ Shopping trip
- □ Travel to/from holiday
- □ Other, Please specify_____

**3-** How many other people are traveling with you?

- □ None
- □ Number of Adults_____
- □ Number of Children_____

**4-** How often do you make this journey?

- □ 3 or more times a week
- □ Once or twice a week
- □ Once or twice a month
- □ Once every 2-3 months
- □ Once every 6 months
- □ Less often

**5-** Is this your first time making this journey?

- □ Yes
- □ No

For Public Transport Users only

**6-** What type of ticket are you traveling on for this journey?

- First class ticket
- Standard class ticket
- Other, Please specify_____

**7-** Was your ticket an Advanced Purchased Ticket?

- Yes
- No

**8-** Did you qualify for a discount?

- Yes - Student Discount
- Yes - Disabled Discount
- Yes – Other, Please Specify_____
- No

**9-** How much did your ticket cost?

Par 2: Personal Details

**10-** Gender (Please tick one box only)

- Male
- Female

**11-** Age (years) (Please tick one box only)

- 16-24
- 25-34
- 35-44
- 45-54
- 55-64
- 65-74
- 75 years or over
- Prefer not to say

**12-** Which of the following describes you best? (Please tick one box only)

- In full time education
- Full time employed
- Part time employed
- Self-employed
- Unemployed
- Fully retired from work
- Looking after the home
- Other, Please specify_____
- Prefer not to say

Part 3: Mode Choices

We would like you to imagine that you are making a journey, sometime in the future within Riyadh-Dammam Corridor (for the same purpose as your journey today). In this case, there are three options of transport modes (Bus, High Speed Rail (HSR), and Classic Rail) and each option will be described in terms of the following:

- Total travel time
- Service frequency
- Total travel cost or Fare

In the following exercises, please look at the three available options (Bus, High Speed Rail (HSR), and Classic Rail) and state which one you would prefer for this future journey.

**13-** Please consider the following three options and tick your preferred preference.

| Attributes \ Alternatives | Bus | HSR | Classic Rail |
|---|---|---|---|
| Total Travel Time | 6 hrs 00 mins | One hr 30 mins | 4 hrs 15 mins |
| Service Frequency | Every 20 mins | Every 15 mins | Every 10 mins |
| Total Travel Cost or Fare (SR) | 68 | 170 | 79 |
| Which would you use for your journey? | | | |

**14-** Please consider the following three options and tick your preferred preference.

| Attributes \ Alternatives | Bus | HSR | Classic Rail |
|---|---|---|---|
| Total Travel Time | 6 hrs 00 mins | One hr 30 mins | 4 hrs 20 mins |
| Service Frequency | Every 30 mins | Every 45 mins | Every 35 mins |
| Total Travel Cost or Fare (SR) | 104 | 226 | 137 |
| Which would you use for your journey? | | | |

**15-** Please consider the following three options and tick your preferred preference.

| Attributes \ Alternatives | Bus | HSR | Classic Rail |
|---|---|---|---|
| Total Travel Time | 6 hrs 00 mins | One hr 30 mins | 4 hrs 35 mins |
| Service Frequency | Every 50 mins | Every 25 mins | Every hour |
| Total Travel Cost or Fare (SR) | 94 | 300 | 110 |
| Which would you use for your journey? | | | |

**16-** Please consider the following three options and tick your preferred preference.

| Attributes \ Alternatives | Bus | HSR | Classic Rail |
|---|---|---|---|
| Total Travel Time | 6 hrs 00 mins | 2 hrs 00 mins | 4 hrs 15 mins |
| Service Frequency | Every 20 mins | Every 15 mins | Every 35 mins |
| Total Travel Cost or Fare (SR) | 94 | 300 | 137 |
| Which would you use for your journey? | | | |

**17-** Please consider the following three options and tick your preferred preference.

| Attributes \ Alternatives | Bus | HSR | Classic Rail |
|---|---|---|---|
| Total Travel Time | 6 hrs 00 mins | 2 hrs 00 mins | 4 hrs 20 mins |
| Service Frequency | Every 30 mins | Every 45 mins | Every hour |
| Total Travel Cost or Fare (SR) | 68 | 170 | 110 |
| Which would you use for your journey? | | | |

**18-** Please consider the following three options and tick your preferred preference.

| Attributes \ Alternatives | Bus | HSR | Classic Rail |
|---|---|---|---|
| Total Travel Time | 6 hrs 00 mins | 2 hrs 00 mins | 4 hrs 35 mins |
| Service Frequency | Every 50 mins | Every 25 mins | Every 10 mins |
| Total Travel Cost or Fare (SR) | 104 | 226 | 79 |
| Which would you use for your journey? | | | |

**19-** Please consider the following three options and tick your preferred preference.

| Attributes \ Alternatives | Bus | HSR | Classic Rail |
|---|---|---|---|
| Total Travel Time | 6 hrs 00 mins | 2 hrs 30 mins | 4 hrs 15 mins |
| Service Frequency | Every 20 mins | Every 15 mins | Every hour |
| Total Travel Cost or Fare (SR) | 104 | 226 | 110 |
| Which would you use for your journey? | | | |

**20-** Please consider the following three options and tick your preferred preference.

| Attributes \ Alternatives | Bus | HSR | Classic Rail |
|---|---|---|---|
| Total Travel Time | 6 hrs 00 mins | 2 hrs 30 mins | 4 hrs 20 mins |
| Service Frequency | Every 30 mins | Every 25 mins | Every 10 mins |
| Total Travel Cost or Fare (SR) | 94 | 300 | 79 |
| Which would you use for your journey? | | | |

**21-** Please consider the following three options and tick your preferred preference.

| Attributes \ Alternatives | Bus | HSR | Classic Rail |
|---|---|---|---|
| Total Travel Time | 6 hrs 00 mins | 2 hrs 30 mins | 4 hrs 35 mins |
| Service Frequency | Every 50 mins | Every 25 mins | Every 35 mins |
| Total Travel Cost or Fare (SR) | 68 | 170 | 137 |
| Which would you use for your journey? | | | |

**Questionnaire 2 (Experiment 1)**

**1-** Please consider the following three options and tick your preferred preference.

| Attributes \ Alternatives | Bus | HSR | Classic Rail |
|---|---|---|---|
| Total Travel Time | 6 hrs 15 mins | One hr 30 mins | 4 hrs 15 mins |
| Service Frequency | Every 30 mins | Every 25 mins | Every 35 mins |
| Total Travel Cost or Fare (SR) | 94 | 226 | 110 |
| Which would you use for your journey? | | | |

**2-** Please consider the following three options and tick your preferred preference.

| Attributes \ Alternatives | Bus | HSR | Classic Rail |
|---|---|---|---|
| Total Travel Time | 6 hrs 15 mins | One hr 30 mins | 4 hrs 20 mins |
| Service Frequency | Every 50 mins | Every 15 mins | Every hour |
| Total Travel Cost or Fare (SR) | 68 | 300 | 79 |
| Which would you use for your journey? | | | |

**3-** Please consider the following three options and tick your preferred preference.

| Attributes \ Alternatives | Bus | HSR | Classic Rail |
|---|---|---|---|
| Total Travel Time | 6 hrs 15 mins | One hr 30 mins | 4 hrs 35 mins |
| Service Frequency | Every 20 mins | Every 45 mins | Every 10 mins |
| Total Travel Cost or Fare (SR) | 104 | 170 | 137 |
| Which would you use for your journey? | | | |

**4-** Please consider the following three options and tick your preferred preference.

| Attributes \ Alternatives | Bus | HSR | Classic Rail |
|---|---|---|---|
| Total Travel Time | 6 hrs 15 mins | 2 hrs 00 mins | 4 hrs 15 mins |
| Service Frequency | Every 30 mins | Every 25 mins | Every hour |
| Total Travel Cost or Fare (SR) | 104 | 170 | 79 |
| Which would you use for your journey? | | | |

**5-** Please consider the following three options and tick your preferred preference.

| Attributes \ Alternatives | Bus | HSR | Classic Rail |
|---|---|---|---|
| Total Travel Time | 6 hrs 15 mins | 2 hrs 00 mins | 4 hrs 20 mins |
| Service Frequency | Every 50 mins | Every 15 mins | Every 210 mins |
| Total Travel Cost or Fare (SR) | 94 | 226 | 137 |
| Which would you use for your journey? | | | |

**6-** Please consider the following three options and tick your preferred preference.

| Attributes \ Alternatives | Bus | HSR | Classic Rail |
|---|---|---|---|
| Total Travel Time | 6 hrs 15 mins | 2 hrs 00 mins | 4 hrs 35 mins |
| Service Frequency | Every 20 mins | Every 45 mins | Every 35 mins |
| Total Travel Cost or Fare (SR) | 68 | 300 | 110 |
| Which would you use for your journey? | | | |

**7-** Please consider the following three options and tick your preferred preference.

| Attributes \ Alternatives | Bus | HSR | Classic Rail |
|---|---|---|---|
| Total Travel Time | 6 hrs 15 mins | 2 hrs 30 mins | 4 hrs 15 mins |
| Service Frequency | Every 30 mins | Every 25 mins | Every 10 mins |
| Total Travel Cost or Fare (SR) | 68 | 300 | 137 |
| Which would you use for your journey? | | | |

**8-** Please consider the following three options and tick your preferred preference.

| Attributes \ Alternatives | Bus | HSR | Classic Rail |
|---|---|---|---|
| Total Travel Time | 6 hrs 15 mins | 2 hrs 30 mins | 4 hrs 20 mins |
| Service Frequency | Every 50 mins | Every 15 mins | Every 35 mins |
| Total Travel Cost or Fare (SR) | 104 | 170 | 110 |
| Which would you use for your journey? | | | |

**9-** Please consider the following three options and tick your preferred preference.

| Attributes \ Alternatives | Bus | HSR | Classic Rail |
|---|---|---|---|
| Total Travel Time | 6 hrs 15 mins | 2 hrs 30 mins | 4 hrs 35 mins |
| Service Frequency | Every 30 mins | Every 45 mins | Every hour |
| Total Travel Cost or Fare (SR) | 94 | 226 | 79 |
| Which would you use for your journey? | | | |

**Questionnaire 3 (Experiment 1)**

**1-** Please consider the following three options and tick your preferred preference.

| Attributes \ Alternatives | Bus | HSR | Classic Rail |
|---|---|---|---|
| Total Travel Time | 6 hrs 25 mins | One hr 30 mins | 4 hrs 15 mins |
| Service Frequency | Every 50 mins | Every 45 mins | Every hour |
| Total Travel Cost or Fare (SR) | 104 | 300 | 137 |
| Which would you use for your journey? | | | |

**2-** Please consider the following three options and tick your preferred preference.

| Attributes \ Alternatives | Bus | HSR | Classic Rail |
|---|---|---|---|
| Total Travel Time | 6 hrs 25 mins | One hr 30 mins | 4 hrs 20 mins |
| Service Frequency | Every 20 mins | Every 25 mins | Every 10 mins |
| Total Travel Cost or Fare (SR) | 94 | 170 | 110 |
| Which would you use for your journey? | | | |

**3-** Please consider the following three options and tick your preferred preference

| Attributes \ Alternatives | Bus | HSR | Classic Rail |
|---|---|---|---|
| Total Travel Time | 6 hrs 25 mins | One hr 30 mins | 4 hrs 35 mins |
| Service Frequency | Every 30 mins | Every 15 mins | Every 35 mins |
| Total Travel Cost or Fare (SR) | 68 | 226 | 79 |
| Which would you use for your journey? | | | |

**4-** Please consider the following three options and tick your preferred preference.

| Attributes \ Alternatives | Bus | HSR | Classic Rail |
|---|---|---|---|
| Total Travel Time | 6 hrs 25 mins | 2 hrs 00 mins | 4 hrs 15 mins |
| Service Frequency | Every 50 mins | Every 45 mins | Every 10 mins |
| Total Travel Cost or Fare (SR) | 68 | 226 | 110 |
| Which would you use for your journey? | | | |

**5-** Please consider the following three options and tick your preferred preference.

| Attributes \ Alternatives | Bus | HSR | Classic Rail |
|---|---|---|---|
| Total Travel Time | 6 hrs 25 mins | 2 hrs 00 mins | 4 hrs 20 mins |
| Service Frequency | Every 20 mins | Every 25 mins | Every 35 mins |
| Total Travel Cost or Fare (SR) | 104 | 300 | 79 |
| Which would you use for your journey? | | | |

**6-** Please consider the following three options and tick your preferred preference.

| Attributes \ Alternatives | Bus | HSR | Classic Rail |
|---|---|---|---|
| Total Travel Time | 6 hrs 25 mins | 2 hrs 00 mins | 4 hrs 35 mins |
| Service Frequency | Every 30 mins | Every 15 mins | Every hour |
| Total Travel Cost or Fare (SR) | 94 | 170 | 137 |
| Which would you use for your journey? | | | |

**7-** Please consider the following three options and tick your preferred preference.

| Attributes \ Alternatives | Bus | HSR | Classic Rail |
|---|---|---|---|
| Total Travel Time | 6 hrs 25 mins | 2 hrs 30 mins | 4 hrs 15 mins |
| Service Frequency | Every 50 mins | Every 45 mins | Every 35 mins |
| Total Travel Cost or Fare (SR) | 94 | 170 | 79 |
| Which would you use for your journey? | | | |

**8-** Please consider the following three options and tick your preferred preference.

| Attributes \ Alternatives | Bus | HSR | Classic Rail |
|---|---|---|---|
| Total Travel Time | 6 hrs 25 mins | 2 hrs 30 mins | 4 hrs 20 mins |
| Service Frequency | Every 20 mins | Every 25 mins | Every hour |
| Total Travel Cost or Fare (SR) | 68 | 226 | 137 |
| Which would you use for your journey? | | | |

**9-** Please consider the following three options and tick your preferred preference.

| Attributes \ Alternatives | Bus | HSR | Classic Rail |
|---|---|---|---|
| Total Travel Time | 6 hrs 25 mins | 2 hrs 30 mins | 4 hrs 35 mins |
| Service Frequency | Every 30 mins | Every 15 mins | Every 10 mins |
| Total Travel Cost or Fare (SR) | 104 | 300 | 110 |
| Which would you use for your journey? | | | |

Thank you for completing this questionnaire and your participation is highly appreciated

Appendix E: Questionnaires of Experiment 2

## Questionnaire 1 (Experiment 2)

Part 1: Your Journey

Firstly, we would like to know about the journey you are making today

1- Where are you traveling from and to on this journey?

From:

- ☐ Riyadh
- ☐ Dammam
- ☐ Other, Please specify_____

To:

- ☐ Riyadh
- ☐ Dammam
- ☐ Other, Please specify_____

2- What is the main purpose of your journey? (Please tick one box only)

- ☐ Commuting to/from work
- ☐ Commuting for education (to/from college/school/university)
- ☐ Visiting friends or relatives
- ☐ On company business (or own if self-employed)
- ☐ On personal business (e.g. job interview, hospital's appointment, etc.)
- ☐ Shopping trip
- ☐ Travel to/from holiday
- ☐ Other, Please specify_____

3- How many other people are traveling with you?

- ☐ None
- ☐ Number of Adults_____
- ☐ Number of Children_____

4- How often do you make this journey?

- ☐ 3 or more times a week
- ☐ Once or twice a week
- ☐ Once or twice a month
- ☐ Once every 2-3 months
- ☐ Once every 6 months
- ☐ Less often

5- Is this your first time making this journey?

- ☐ Yes
- ☐ No

For Public Transport Users only

6- What type of ticket are you traveling on for this journey?

- First class ticket
- Standard class ticket
- Other, Please specify_____

7- Was your ticket an Advanced Purchased Ticket?

- Yes
- No

8- Did you qualify for a discount?

- Yes - Student Discount
- Yes - Disabled Discount
- Yes – Other, Please Specify_____
- No

9- How much did your ticket cost?

Par 2: Personal Details

10- Gender (Please tick one box only)

- Male
- Female

11- Age (years) (Please tick one box only)

- 16-24
- 25-34
- 35-44
- 45-54
- 55-64
- 65-74
- 75 years or over
- Prefer not to say

12- Which of the following describes you best? (Please tick one box only)

- In full time education
- Full time employed
- Part time employed
- Self-employed
- Unemployed
- Fully retired from work
- Looking after the home
- Other, Please specify_____
- Prefer not to say

Part 3: Mode Choices

We would like you to imagine that you are making a journey, sometime in the future within Riyadh-Dammam Corridor (for the same purpose as your journey today). In this case, there

are four options of transport modes (Car, Air, High Speed Rail (HSR), and Hyperloop) and each option will be described in terms of the following:

- Total travel time
- Service frequency
- Total travel cost or Fare

In the following exercises, please look at the four available options (Car, Air, High Speed Rail (HSR), and Hyperloop) and state which one you would prefer for this future journey.

13- Please consider the following three options and tick your preferred preference.

| Attributes \ Alternatives | Car | Air | HSR | Hyperloop |
|---|---|---|---|---|
| Total Travel Time | 3 hrs 30 mins | One hr 50 mins | One hr 30 mins | 50 mins |
| Service Frequency | --- | Every hour | Every 15 mins | Every 20 secs |
| Total Travel Cost or Fare (SR) | 76 | 278 | 170 | 300 |
| Which would you use for your journey? | | | | |

14- Please consider the following three options and tick your preferred preference.

| Attributes \ Alternatives | Car | Air | HSR | Hyperloop |
|---|---|---|---|---|
| Total Travel Time | 3 hrs 30 mins | One hr 50 mins | One hr 30 mins | One hour |
| Service Frequency | --- | Every hour | Every 30 mins | Every 30 secs |
| Total Travel Cost or Fare (SR) | 128 | 278 | 226 | 450 |
| Which would you use for your journey? | | | | |

15- Please consider the following three options and tick your preferred preference.

| Attributes \ Alternatives | Car | Air | HSR | Hyperloop |
|---|---|---|---|---|
| Total Travel Time | 3 hrs 30 mins | One hr 50 mins | One hr 30 mins | One hr 10 mins |
| Service Frequency | --- | Every hour | Every 45 mins | Every 40 secs |
| Total Travel Cost or Fare (SR) | 96 | 278 | 300 | 370 |
| Which would you use for your journey? | | | | |

16- Please consider the following three options and tick your preferred preference.

| Attributes \ Alternatives | Car | Air | HSR | Hyperloop |
|---|---|---|---|---|
| Total Travel Time | 3 hrs 30 mins | One hr 50 mins | 2 hrs 00 mins | 50 mins |
| Service Frequency | --- | Every hour | Every 15 mins | Every 30 secs |
| Total Travel Cost or Fare (SR) | 96 | 278 | 300 | 450 |
| Which would you use for your journey? | | | | |

17- Please consider the following three options and tick your preferred preference.

| Attributes \ Alternatives | Car | Air | HSR | Hyperloop |
|---|---|---|---|---|
| Total Travel Time | 3 hrs 30 mins | One hr 50 mins | 2 hrs 00 mins | One hour |
| Service Frequency | --- | Every hour | Every 30 mins | Every 40 secs |
| Total Travel Cost or Fare (SR) | 76 | 278 | 170 | 370 |
| Which would you use for your journey? | | | | |

18- Please consider the following three options and tick your preferred preference.

| Attributes \ Alternatives | Car | Air | HSR | Hyperloop |
|---|---|---|---|---|
| Total Travel Time | 3 hrs 30 mins | One hr 50 mins | 2 hrs 00 mins | One hr 10 mins |
| Service Frequency | --- | Every hour | Every 45 mins | Every 20 secs |
| Total Travel Cost or Fare (SR) | 128 | 278 | 226 | 300 |
| Which would you use for your journey? | | | | |

19- Please consider the following three options and tick your preferred preference.

| Attributes \ Alternatives | Car | Air | HSR | Hyperloop |
|---|---|---|---|---|
| Total Travel Time | 3 hrs 30 mins | One hr 50 mins | 2 hrs 30 mins | 50 mins |
| Service Frequency | --- | Every hour | Every 15 mins | Every 40 secs |
| Total Travel Cost or Fare (SR) | 128 | 278 | 226 | 370 |
| Which would you use for your journey? | | | | |

20- Please consider the following three options and tick your preferred preference.

| Attributes \ Alternatives | Car | Air | HSR | Hyperloop |
|---|---|---|---|---|
| Total Travel Time | 3 hrs 30 mins | One hr 50 mins | 2 hrs 30 mins | One hour |
| Service Frequency | --- | Every hour | Every 30 mins | Every 20 secs |
| Total Travel Cost or Fare (SR) | 96 | 278 | 300 | 300 |
| Which would you use for your journey? | | | | |

21- Please consider the following three options and tick your preferred preference.

| Attributes \ Alternatives | Car | Air | HSR | Hyperloop |
|---|---|---|---|---|
| Total Travel Time | 3 hrs 30 mins | One hr 50 mins | 2 hrs 30 mins | One hr 10 mins |
| Service Frequency | --- | Every hour | Every 45 mins | Every 30 secs |
| Total Travel Cost or Fare (SR) | 76 | 278 | 170 | 450 |
| Which would you use for your journey? | | | | |

**Questionnaire 2 (Experiment 2)**

In the following exercises, please look at the four available options (Car, Air, High Speed Rail (HSR), and Hyperloop) and state which one you would prefer for this future journey.

**1-** Please consider the following three options and tick your preferred preference.

| Attributes \ Alternatives | Car | Air | HSR | Hyperloop |
|---|---|---|---|---|
| Total Travel Time | 3 hrs 50 mins | One hr 50 mins | One hr 30 mins | 50 mins |
| Service Frequency | --- | Every hour | Every 30 mins | Every 30 secs |
| Total Travel Cost or Fare (SR) | 96 | 278 | 226 | 370 |
| Which would you use for your journey? | | | | |

**2-** Please consider the following three options and tick your preferred preference.

| Attributes \ Alternatives | Car | Air | HSR | Hyperloop |
|---|---|---|---|---|
| Total Travel Time | 3 hrs 50 mins | One hr 50 mins | One hr 30 mins | One hour |
| Service Frequency | --- | Every hour | Every 45 mins | Every 40 secs |
| Total Travel Cost or Fare (SR) | 76 | 278 | 300 | 300 |
| Which would you use for your journey? | | | | |

**3-** Please consider the following three options and tick your preferred preference.

| Attributes \ Alternatives | Car | Air | HSR | Hyperloop |
|---|---|---|---|---|
| Total Travel Time | 3 hrs 50 mins | One hr 50 mins | One hr 30 mins | One hour |
| Service Frequency | --- | Every hour | Every 15 mins | Every 20 secs |
| Total Travel Cost or Fare (SR) | 128 | 278 | 170 | 450 |
| Which would you use for your journey? | | | | |

**4-** Please consider the following three options and tick your preferred preference.

| Attributes \ Alternatives | Car | Air | HSR | Hyperloop |
|---|---|---|---|---|
| Total Travel Time | 3 hrs 50 mins | One hr 50 mins | 2 hrs 00 mins | 50 mins |
| Service Frequency | --- | Every hour | Every 30 mins | Every 40 secs |
| Total Travel Cost or Fare (SR) | 128 | 278 | 170 | 300 |
| Which would you use for your journey? | | | | |

**5-** Please consider the following three options and tick your preferred preference.

| Attributes \ Alternatives | Car | Air | HSR | Hyperloop |
|---|---|---|---|---|
| Total Travel Time | 3 hrs 50 mins | One hr 50 mins | 2 hrs 00 mins | One hour |
| Service Frequency | --- | Every hour | Every 45 mins | Every 20 secs |
| Total Travel Cost or Fare (SR) | 96 | 278 | 226 | 450 |
| Which would you use for your journey? | | | | |

**6-** Please consider the following three options and tick your preferred preference.

| Attributes \ Alternatives | Car | Air | HSR | Hyperloop |
|---|---|---|---|---|
| Total Travel Time | 3 hrs 50 mins | One hr 50 mins | 2 hrs 00 mins | One hr 10 mins |
| Service Frequency | --- | Every hour | Every 15 mins | Every 30 secs |
| Total Travel Cost or Fare (SR) | 76 | 278 | 300 | 370 |
| Which would you use for your journey? | | | | |

**7-** Please consider the following three options and tick your preferred preference.

| Attributes \ Alternatives | Car | Air | HSR | Hyperloop |
|---|---|---|---|---|
| Total Travel Time | 3 hrs 50 mins | One hr 50 mins | 2 hrs 30 mins | 50 mins |
| Service Frequency | --- | Every hour | Every 30 mins | Every 20 secs |
| Total Travel Cost or Fare (SR) | 76 | 278 | 300 | 450 |
| Which would you use for your journey? | | | | |

**8-** Please consider the following three options and tick your preferred preference.

| Attributes \ Alternatives | Car | Air | HSR | Hyperloop |
|---|---|---|---|---|
| Total Travel Time | 3 hrs 50 mins | One hr 50 mins | 2 hrs 30 mins | One hour |
| Service Frequency | --- | Every hour | Every 45 mins | Every 30 secs |
| Total Travel Cost or Fare (SR) | 128 | 278 | 170 | 370 |
| Which would you use for your journey? | | | | |

**9-** Please consider the following three options and tick your preferred preference.

| Attributes \ Alternatives | Car | Air | HSR | Hyperloop |
|---|---|---|---|---|
| Total Travel Time | 3 hrs 50 mins | One hr 50 mins | 2 hrs 30 mins | One hr 10 mins |
| Service Frequency | --- | Every hour | Every 15 mins | Every 40 secs |
| Total Travel Cost or Fare (SR) | 96 | 278 | 226 | 300 |
| Which would you use for your journey? | | | | |

**Questionnaire 3 (Experiment 2)**

In the following exercises, please look at the four available options (Car, Air, High Speed Rail (HSR), and Hyperloop) and state which one you would prefer for this future journey.

**1-** Please consider the following three options and tick your preferred preference.

| Attributes \ Alternatives | Car | Air | HSR | Hyperloop |
|---|---|---|---|---|
| Total Travel Time | 4 hrs 15 mins | One hr 50 mins | One hr 30 mins | 50 mins |
| Service Frequency | --- | Every hour | Every 45 mins | Every 40 secs |
| Total Travel Cost or Fare (SR) | 128 | 278 | 300 | 450 |
| Which would you use for your journey? | | | | |

**2-** Please consider the following three options and tick your preferred preference.

| Attributes \ Alternatives | Car | Air | HSR | Hyperloop |
|---|---|---|---|---|
| Total Travel Time | 4 hrs 15 mins | One hr 50 mins | One hr 30 mins | One hour |
| Service Frequency | --- | Every hour | Every 15 mins | Every 20 secs |
| Total Travel Cost or Fare (SR) | 96 | 278 | 170 | 370 |
| Which would you use for your journey? | | | | |

**3-** Please consider the following three options and tick your preferred preference.

| Attributes \ Alternatives | Car | Air | HSR | Hyperloop |
|---|---|---|---|---|
| Total Travel Time | 4 hrs 15 mins | One hr 50 mins | One hr 30 mins | One hour |
| Service Frequency | --- | Every hour | Every 30 mins | Every 30 secs |
| Total Travel Cost or Fare (SR) | 76 | 278 | 226 | 300 |
| Which would you use for your journey? | | | | |

**4-** Please consider the following three options and tick your preferred preference.

| Attributes \ Alternatives | Car | Air | HSR | Hyperloop |
|---|---|---|---|---|
| Total Travel Time | 4 hrs 15 mins | One hr 50 mins | 2 hrs 00 mins | 50 mins |
| Service Frequency | --- | Every hour | Every 45 mins | Every 20 secs |
| Total Travel Cost or Fare (SR) | 76 | 278 | 226 | 370 |
| Which would you use for your journey? | | | | |

**5-** Please consider the following three options and tick your preferred preference.

| Attributes \ Alternatives | Car | Air | HSR | Hyperloop |
|---|---|---|---|---|
| Total Travel Time | 4 hrs 15 mins | One hr 50 mins | 2 hrs 00 mins | One hour |
| Service Frequency | --- | Every hour | Every 15 mins | Every 30 secs |
| Total Travel Cost or Fare (SR) | 128 | 278 | 300 | 300 |
| Which would you use for your journey? | | | | |

**6-** Please consider the following three options and tick your preferred preference.

| Attributes \ Alternatives | Car | Air | HSR | Hyperloop |
|---|---|---|---|---|
| Total Travel Time | 4 hrs 15 mins | One hr 50 mins | 2 hrs 00 mins | One hr 10 mins |
| Service Frequency | --- | Every hour | Every 30 mins | Every 40 secs |
| Total Travel Cost or Fare (SR) | 96 | 278 | 170 | 450 |
| Which would you use for your journey? | | | | |

**7-** Please consider the following three options and tick your preferred preference.

| Attributes \ Alternatives | Car | Air | HSR | Hyperloop |
|---|---|---|---|---|
| Total Travel Time | 4 hrs 15 mins | One hr 50 mins | 2 hrs 30 mins | 50 mins |
| Service Frequency | --- | Every hour | Every 45 mins | Every 30 secs |
| Total Travel Cost or Fare (SR) | 96 | 278 | 170 | 300 |
| Which would you use for your journey? | | | | |

**8-** Please consider the following three options and tick your preferred preference.

| Attributes \ Alternatives | Car | Air | HSR | Hyperloop |
|---|---|---|---|---|
| Total Travel Time | 4 hrs 15 mins | One hr 50 mins | 2 hrs 30 mins | One hour |
| Service Frequency | --- | Every hour | Every 15 mins | Every 40 secs |
| Total Travel Cost or Fare (SR) | 76 | 278 | 226 | 450 |
| Which would you use for your journey? | | | | |

**9-** Please consider the following three options and tick your preferred preference.

| Attributes \ Alternatives | Car | Air | HSR | Hyperloop |
|---|---|---|---|---|
| Total Travel Time | 4 hrs 15 mins | One hr 50 mins | 2 hrs 30 mins | One hr 10 mins |
| Service Frequency | --- | Every hour | Every 30 mins | Every 20 secs |
| Total Travel Cost or Fare (SR) | 128 | 278 | 300 | 370 |
| Which would you use for your journey? | | | | |

Thank you for completing this questionnaire and your participation is highly appreciated

Appendix F: Stata Outcomes with Service Frequency for Experiment 1

```
2 . asclogit Chosen Cost Freq Time, case (Observation) alternatives (Alternative) casevars (gender_male)

Iteration 0:   log likelihood =  -3805.4817
Iteration 1:   log likelihood =   -3649.535
Iteration 2:   log likelihood =  -3636.0943
Iteration 3:   log likelihood =    -3636.06
Iteration 4:   log likelihood =    -3636.06

Alternative-specific conditional logit          Number of obs      =        12,312
Case variable: Observation                      Number of cases    =          4104

Alternative variable: Alternative               Alts per case: min =             3
                                                               avg =           3.0
                                                               max =             3

                                                Wald chi2(    5)   =       1162.40
Log likelihood =    -3636.06                    Prob > chi2        =        0.0000
```

| Chosen | Coef. | Std. Err. | z | P>\|z\| | [95% Conf. | Interval] |
|---|---|---|---|---|---|---|
| **Alternative** | | | | | | |
| Cost | -.0029012 | .0004828 | -6.01 | 0.000 | -.0038476 | -.0019549 |
| Freq | .0007351 | .0013623 | 0.54 | 0.589 | -.0019349 | .0034051 |
| Time | -.4585835 | .0231098 | -19.84 | 0.000 | -.5038779 | -.4132892 |
| **A** | (base alternative) | | | | | |
| **B** | | | | | | |
| gender_male | .9328235 | .1273342 | 7.33 | 0.000 | .6832531 | 1.182394 |
| **C** | | | | | | |
| gender_male | 1.400621 | .1203329 | 11.64 | 0.000 | 1.164773 | 1.636469 |

Appendix G: Stata Outcomes with Service Frequency for Experiment 2

```
3 . asclogit Chosen Cost Freq Time, case (Observation) alternatives (Alternative) casevars (gender_male)

  Iteration 0:   log likelihood =   -5529.7379
  Iteration 1:   log likelihood =   -5507.1825
  Iteration 2:   log likelihood =   -5507.1656
  Iteration 3:   log likelihood =   -5507.1656

  Alternative-specific conditional logit          Number of obs      =         16,416
  Case variable: Observation                      Number of cases    =           4104

  Alternative variable: Alternative               Alts per case: min =              4
                                                                 avg =            4.0
                                                                 max =              4

                                                  Wald chi2(    6)   =         362.83
  Log likelihood =  -5507.1656                       Prob > chi2     =         0.0000
```

| Chosen | Coef. | Std. Err. | z | P>\|z\| | [95% Conf. Interval] | |
|---|---|---|---|---|---|---|
| **Alternative** | | | | | | |
| Cost | -.0018188 | .0003509 | -5.18 | 0.000 | -.0025066 | -.0011311 |
| Freq | .000107 | .0008134 | 0.13 | 0.895 | -.0014873 | .0017014 |
| Time | -.353541 | .0370503 | -9.54 | 0.000 | -.4261582 | -.2809238 |
| **A** | (base alternative) | | | | | |
| **B** | | | | | | |
| gender_male | -.1630512 | .1002173 | -1.63 | 0.104 | -.3594735 | .0333711 |
| **C** | | | | | | |
| gender_male | .5181852 | .0828315 | 6.26 | 0.000 | .3558385 | .6805319 |
| **D** | | | | | | |
| gender_male | -.1709886 | .0980741 | -1.74 | 0.081 | -.3632103 | .0212331 |

Various commands are used to estimate the NL model in Stata. First, 'NLOGITGEN' creates a variable to define the structure of the decision tree. In the first experiment, the 1, 2 and 3 represent bus, classic rail and HSR, respectively, so the command is:

nlogitgen NonCarAvailable = Mode (Bus: 1, Rail: 2|3)

This creates the variable **NonCarAvailable** that defines the structure of the decision tree, as there are two branches in the upper level: bus and rail. The transport options of classic rail and HSR are available in the rail branch. As a result, the output of **nlogitgen** command was as follows:

new variable NonCarAvailable is generated with two groups

label list lb_NonCarAvailable

lb_NonCarAvailable:

1 Bus

2 Rail

This outcome revealed only two groups, which are bus and rail (classic rail and HSR). To view the structure of tree, the command is:

nlogittree Mode NonCarAvailable, choice(Chosen)

where 'chosen' is the dependent variable and the output of the nlogittree command is as shown in Table 1:

| | **Mode** | **N** | **Mode** | **N** | **K** |
|---|---|---|---|---|---|
| NonCarAvailable | Bus | 4,104 | 1 | 4,104 | 240 |
| | Rail | 8,208 | 2 | 4,104 | 1,648 |
| | | | 3 | 4,104 | 2,216 |
| | **Total** | | | 12,312 | 4,104 |
| | k=no. of times alternative is chosen | | | | |
| | N=no. of observations at each level | | | | |

Table 1: Tree structure specified for the nested logit model of first experiment.

In this case, only 5.8% chose the bus, making it a minority mode. HSR had the majority percentage of 54% and classic rail 40%. Next, the alternative-specific constant was considered as a part of the outcomes for the transport modes of bus, classic rail and HSR, determined as follows:

gen bus_asc=mod(_n, 3)==1

gen classic_asc=mod(_n, 3)==2

gen hsr_asc=mod(_n,3)==3

In this case, the values of 1, 2 and 3 represent the alternative-specific constant (asc) of bus, classic rail and HSR, respectively, while the n represents the number of alternatives. The NL model can involves the following command:

nlogit Chosen bus_asc classic_asc hsr_asc Time Cost || NonCarAvailable: gender_male, base(Bus) || Mode:, case(Observation) nonnormalized nolog noconstant notree

where || are simply delimiters to separate the equations.

The first equation specifies the dependent variable ‘chosen’ and three alternative-specific variables Bus_asc, Classic_asc and HSR_asc, as well as the independent variables of time and cost. For the second equation, the variable NonCarAvailable is specified, which identifies the upper-level alternatives with respect to gender_male in order to assess the strength of the use of transport modes by men, using bus as the baseline category. In the third equation, the variable of mode identifies the bottom-level alternatives after the second equation delimiter, while ‘case ( )’ is required to specify an identification variable for each participant. Non-normalized is there to request unscaled parameterization, while nolog suppresses an iteration log of the log-likelihood, noconstant suppresses the constant terms for the bottom-level alternatives and notree suppresses the display of the tree-structure output.

The incorporation of the commands non-normalized, nlog, nonconstant and notree into the model follows the method developed by Wu (2011).

Appendix I: Nested Logit Mode Using Stata for Experiment 2

In this second experiment, the command **NLOGITGEN** creates a variable that defines the structure of the decision tree, as 1, 2, 3 and 4 represent car, air, HSR and Hyperloop travel, respectively:

nlogitgen CarAvailable = Mode (Car: 1, PublicTransport: 2|3|4, Rail: 3|4)

This creates the variable CarAvailable that defines the structure of the decision tree, as there are two branches in the upper level: car and public transport. The transport options of air and rail appear lower, in the public transport branch, while the options of HSR and Hyperloop appear lower again, in the rail branch. As a result, the output of the **nlogitgen** command was as follows:

new variable CarAvailable is generated with three groups

label list lb_CarAvailable

lb_CarAvailable:

1 Car

2 PublicTransport

3 Rail

In this case, the values of 1, 2 and 3 represent the groups of car, public transport and rail (HSR and Hyperloop), respectively. To see the structure of tree, the command is:

nlogittree Mode CarAvailable, choice(Chosen)

where ‘chosen’ is the dependent variable and the output is as in Table 2:

| | Mode | | | N | | Mode | N | k |
|---|---|---|---|---|---|---|---|---|
| CarAvailable | Car | | | 4,104 | 4,104 | 1 | 4,104 | 594 |
| | PublicTransport | Air | | 4,104 | 12,312 | 2 | 4,104 | 768 |
| | | Rail | HSR | 8,208 | | 3 | 4,104 | 1,761 |
| | | | Hyperloop | | | 4 | 4,104 | 981 |
| | | **Total** | | | | | 16,416 | 4,104 |
| | | k=number of times alternative is chosen | | | | | | |
| | | N=number of observations at each level | | | | | | |

Table 2: Three-level structure specified for the nested logit model of second experiment

In this case, only 14.5% of participants were found to opt for car travel, making it a minority mode, followed by air travel and Hyperloop at 18.7% and 24%, respectively, while most would choose HSR (43%). The alternative-specific constant is considered to be a part of the outcomes for the transport modes of car, air, HSR and Hyperloop, determined as follows:

```
gen car_asc=mod(_n, 4)==1

gen air_asc=mod(_n, 4)==2

gen hsr_asc=mod(_n, 4)==3

gen hyperloop_asc=mod(_n, 4)==4
```

Next, the NL model was applied by the following command:

```
nlogit Chosen car_asc air_asc hsr_asc hyperloop_asc Time Cost || CarAvailable: gender_male, base(Car) || Mode:, case(Observation) nonnormalized nolog noconstant notree
```

where the first equation specifies the dependent variable ‘chosen’ and four alternative-specific variables Car_asc, Air_asc, HSR_asc and Hyperloop_asc, as well as the independent variables of time and cost.